Characterisation of Proendothelin-1 Derived Peptides and Evaluation of Their Utility as Biomarkers of Vascular and Renal Pathologies

Jale Yuzugulen

A thesis submitted for the degree of Doctor of Philosophy (Ph.D) in the Barts and the London School of Medicine and Dentistry of the Queen Mary, University of London 2014

Centre for Translational Medicine & Therapeutics,

William Harvey Research Institute,

John Vane Science Centre

Charterhouse Square

London

UK

Statement of originality

I, Jale Yuzugulen, confirm that the research included within this thesis is my own work or that where it has been carried out in collaboration with, or supported by others, that this is duly acknowledged below and my contribution indicated. Previously published material is also acknowledged below.

I attest that I have exercised reasonable care to ensure that the work is original, and does not to the best of my knowledge break any UK law, infringe any third party's copyright or other Intellectual Property Right, or contain any confidential material.

I accept that the College has the right to use plagiarism detection software to check the electronic version of the thesis.

I confirm that this thesis has not been previously submitted for the award of a degree by this or any other university.

Signature: [ ]

Date: 10/03/2014

List of publications and abstracts arising from this thesis:

1. Yuzugulen J, Wood EG, Douthwaite JA, Villar IC, Patel NS, Jegard J, Montoya A, Cutillas P, Hartley O, Ahluwalia A, Corder R. (2012) Characterization of Proendothelin-1 Derived Peptides Identifies a Co-secreted Modulator of ET-1 Vasoconstriction, and Provides Insights for Biomarker Measurements. *Circulation.* 126: A18898 (Poster presentation; AHA meeting; Core 7: Vascular Disease: Biology and Clinical Science).
2. Dhaun N, Yuzugulen J, Kimmitt RA, Wood EG, Lilitkarntakul P, MacIntyre IM, Goddard J, Webb DJ, Corder R. Plasma proendothelin-1 peptide concentrations rise in CKD and following selective endothelin-A receptor antagonism. Manuscript in preparation.
3. Yuzugulen J, Wood EG, Villar IC, Douthwaite JA, Patel NSA, Jegard J, Montoya A, Cutillas P, Gaertner H, Rossitto-Borlat I, Rose K, Hartley O, Ahluwalia A, Corder R. (2013). Characterisation Of the "Endothelin-Like Domain Peptide" (ELDP) Co-synthesised With Endothelin-1 from the *EDN1* gene. Life Sciences: Vol 93 Issues 25-26, 18 Dec 2013, page e2 [Oral presentation; Special Section of Thirteenth International Conference on Endothelin (ET-13), Tokyo, September 8-11, 2013].
4. Yuzugulen J, Kimmitt R, Dhaun N, Wood EG, Goddard J, Webb DJ, Corder R. (2013). Effect of sitaxentanon plasma biomarkers of proendothelin-1 synthesis in patients with chronic kidney disease. Life Sciences: Vol 93 Issues 25-26, 18 Dec 2013, page e66 [Poster presentation; Special Section of Thirteenth International Conference on Endothelin (ET-13), Tokyo, September 8-11, 2013].
5. Yuzugulen J, Lilitkarntakul P, Wood EG, Kimmitt RA, Dhaun N, Goddard J, Webb DJ, Corder R. (2013). Evaluation Of Urinary and Plasma Endothelin-Like Domain Peptide (ELDP) in Chronic Kidney Disease. Life Sciences: Vol 93 Issues 25-26, 18 Dec 2013, page e14 [Poster presentation; Special Section of Thirteenth International Conference on Endothelin (ET-13), Tokyo, September 8-11, 2013].
6. Yuzugulen J, Villar IC, Wood EG, Douthwaite JA, Patel NSA, Jegard J, Montoya A, Cutillas P, Gaertner H, Rossitto-Borlat I, Rose K, Hartley O, Ahluwalia A, Corder R. (2012). The Endothelin-Like Domain Peptide (ELDP) co-synthesised with endothelin-1 from the *EDN1* gene modulates ET-1 induced vasoconstriction and has potential for biomarker measurements. Proceedings of the British

Pharmacological Society at http://www.pA2online.org/abstracts/Vol10Issue4abst186P.pdf. [Poster presentation, BPS Winter Meeting. London].

Abstract

Endothelin-1 (ET-1), the potent vasoconstrictor peptide, is synthesised from the 212 amino acid precursor preproendothelin-1 (ppET-1). ET-1 is strongly implicated in cardiac and renal pathologies. However, ET receptor antagonists demonstrated only limited efficacy in clinical trials of chronic heart failure (HF) and hypertension. ET-1 has a short circulating half-life and its plasma measurements have been inaccurate. Thus, alternative ppET-1 derived peptides may be more stable and could serve as better biomarkers of ET-1 synthesis. Moreover, alternative ppET-1 derived peptides may contribute to the biological effects resulting from *EDN1* gene expression and may be interacting with the vasoconstrictor responses of ET-1 or other mediators. The aims of these investigations were to characterise ppET-1 derived peptide products and to evaluate their potential as biomarkers of ET-1 synthesis.

A combination of specific immunoassays and HPLC were used to characterise ppET-1 processing in human endothelial (EA.hy 926) and epithelial (A549) cells in culture. NT-proET-1 (ppET-$1_{[18-50]}$), endothelin-like domain peptide (ELDP, ppET-$1_{[93-166]}$) and CT-proET-1 (ppET-$1_{[169-212]}$) were identified in conditioned media samples as the main ppET-1 derived peptide products. The identities of ELDP and CT-proET-1 were confirmed by LC-MS/MS mass spectrometry.

The three ppET-1 peptides were chemically synthesised and their *in vivo* clearance was investigated in male Wistar rats. Arterial plasma levels after intravenous administration of proET-1 peptides showed rapid clearance (<5 min) of NT-proET-1, while CT-proET-1 had the slowest clearance rate. Studies of proET-1 peptide stability in blood samples also showed NT-proET-1 had lower stability. Specific double-recognition site sandwich ELISAs optimised for plasma measurements were used to evaluate plasma concentrations of ELDP and CT-proET-1 in patients with chronic HF and chronic kidney disease (CKD).

In conclusion, the results described in this thesis provide further evidence linking ET-1 to cardiac and renal disease processes. But the small differences between healthy individuals and patients with cardiovascular or renal disease indicate only a limited potential for proET-1 peptides as diagnostic biomarkers of *EDN1*-linked pathologies.

Table of Contents

List of Figures

List of Tables

Chapter 1

Chapter 2

Chapter 3

Chapter 4

Chapter 5

Chapter 6

Chapter 7

No tables

Abbreviations

A549	Human lung adenocarcinoma epithelial cell line
AA	Arachidonic acid
ACE	Angiotensin converting enzyme
ACh	Acetylcholine
ADM	Adrenomedullin
ANG II	Angiotensin II
ANOVA	Analysis of variance
ANP	Atrial natriuretic peptide
AVP	Vasopressin
BAECs	Bovine aortic endothelial cells
BP	Blood pressure
BPAECs	Bovine pulmonary artery endothelial cells
BPASM	Bovine pulmonary artery smooth muscle cells
BSA	Bovine serum albumin
BW	Body weight
CAC	Coronary artery calcium
CAD	Coronary artery disease
cAMP	Cyclic adenosine monophosphate
CD	Collecting duct
CH_3CN	Acetonitrile
CID	Collision-induced dissociation
cIMT	Carotid intima-medial thickness
CKD	Chronic kidney disease
CM	Carboxymethyl
CO	Cardiac output
COX	Cyclooxygenase
CTF	C-terminal fragment of big ET-1
CTGF	Connective tissue growth factor

CT-proET-1	C-terminal pro-endothelin-1
DBP	Diastolic blood pressure
DM	Diabetes mellitus
DMEM	Dulbecco's modified Eagle's medium
DMSO	Dimethyl sulfoxide
EA.hy 926	Hybrid human cell line that results from the fusion of primary HUVEC with A549 cells
ECE	Endothelin converting enzyme
ECM	Extracellular matrix
ECs	Endothelial cells
EDCF	Endothelium-dependent contracting factor
EDD	Endothelium-dependent vasodilatation
EDN1	Preproendothelin-1 gene
EDTA	Ethylenediaminetetraacetic acid
ELDP	Endothelin-like domain peptide
ELISA	Enzyme-linked immunosorbent assay
ENaC	Epithelial sodium channel
ER	Endoplasmic reticulum
ERAs	Endothelin receptor antagonist(s)
ESI	Electrospray ionization
ET-1	Endothelin-1
ET_A	Endothelin receptor type-A
ET_B	Endothelin receptor type-B
FBF	Forearm blood flow
FCS	Foetal calf serum
FF	Filtration fraction
FMD	Flow mediated dilatation
FRS	Framingham Risk Score
FT-ICR	Fourier transform ion cyclotron resonance

GFR	Glomerular filtration rate
G-HCl	Guanidine hydrochloride
HCl	Hydrochloric acid
HCM	Human cardiomyocytes
HEPES	4-(2-hydroxyethyl)-1-piperazineethanesulfonic acid
HF	Heart failure
HIC	Hydrophobic interaction chromatography
HMEC-1	Human microvascular endothelial cell line
HPLC	High performance liquid chromatography
HR	Heart rate
HUVEC	Human umbilical vein endothelial cells
HUVSMC	Human umbilical vein vascular smooth muscle cells
i.p.	Intraperitoneal route
i.v.	Intravenous route
IEC	Ion-exchange chromatography
IFN-γ	Interferon-gamma
IMCD	Inner medullary collecting duct
ir	Immunoreactive
KLF2	Krüppel-like factor 2
KO	Knockout
LPS	Lipopolysaccharide
LTQ	Linear triple quadrupole
LV	Left ventricular
MAP	Mean arterial blood pressure
MeS	Methionine sulphone
MetSO	Methionine sulphoxide
MR-proADM	Mid-regional pro-adrenomedullin
MS	Mass spectrometer
MTT	3-(4,5-Dimethylthiazol-2-yl)-2,5-diphenyltetrazolium bromide

N_2	Nitrogen
Na^+	Sodium ion
NaCl	Sodium chloride
NADPH	Nicotinamide adenine dinucleotide phosphate-oxidase
NEP-24.11	Neutral endopeptidase-24.11
N-HRP	Neutravidin-horeradish peroxidase
NO	Nitric oxide
NT-proBNP	N-terminal pro-brain natriuretic peptide
NT-proET-1	N-terminal pro-endothelin-1
NYHA	New York Heart Association
$O_2^{\cdot -}$	Superoxide anion
ODN	Oligodeoxynucleotide
$ONOO^-$	Peroxynitrite
ox-LDL	Oxidised-LDL
PAH	Pulmonary artery hypertension
PASMCs	Pulmonary arterial smooth muscle cells
PBS	Phosphate buffered saline
PCs	Pro-hormone/pro-protein convertases
PGI_2	Prostacyclin
pI	Isoelectric point
PKC	Protein kinase C
PLA_2	Phospholipase A_2
PMF	Peptide mass fingerprinting
ppET-1	Preproendothelin-1
Pre-H	Mild/pre-hypentension
proET-1	Proendothelin-1
PTMs	Post-translational modifications
RAAS	Renin-angiotensin-aldosterone system
RBF	Renal blood flow

RIA	Radioimmunoassay
ROS	Reactive oxygen species
RPF	Renal plasma flow
SAB	Sandwich assay buffer
SBP	Systolic blood pressure
SMC	Smooth muscle cells
SNP	Sodium nitroprusside
SPE	Solid phase extraction
TFA	Trifluoroacetic acid
TG	Transgenic
TNF-α	Tumour necrosis factor-alpha
UPLC	Ultrahigh pressure liquid chromatography
VR	Vascular resistance
VSMC	Vascular smooth muscle cells
vWF	von Willebrand factor

Measurements and Units

amu	Atomic mass unit
CI	Confidence interval
Da	Daltons, mass unit
EC_{50}	Median effective concentration to induce a 50% effect
fmol/ml	Fentomole per millilitre
h	Hour(s)
kD	Kilo Daltons
kg	Kilogram
M	Molar concentration
m/z	Mass-to-charge ratio
mmu	Milli-mass unit
MWt	Molecular weight

n	Number of observations
P	Probability
pmol/ml	Picomole per millilitre
ppm	Parts-per-million
rpm	Revolutions per minute
s.e.m	Standard error of the mean
U	Units
v/v	Volume/volume
w/v	Weight per volume
µg	Micrograms
µl	Microliters

Acknowledgements

First, I would like to give my immense gratitude to Prof. Roger Corder for giving me the opportunity to work for, and learn from him. As a supervisor, his spark for new ideas, technical excellence and expert knowledge of the Endothelin field has been crucial in the progression of this work. Roger has been a great teacher and I could not have made it this far without his support and encouragement.

Members of Roger`s group, Liz Wood and Noorafza Khan, I am indebted to both, for their continued support and useful advice. Liz played a major role during development of immunoassays used in this thesis. She also taught me how to get started on this project guiding me on the assay studies and providing cultured cells for use during experiments. Her enthusiasm made working fun. Noorafza`s excellent organisation has made everything run smoothly in the lab. It has been always nice to have both of you around.

I am grateful to Dr. Pedro Cutillas for his expert knowledge on mass spectrometry. I am also indebted to Alex Montoya and Vinothini Rajeeve for their technical assistance with operating the mass spectrometry system. I would like to thank Prof. David Webb at University of Edinburgh for providing CKD plasma and urine samples, and for the interaction with members of his group; in particular, Dr. Bean Dhaun and Robert Kimmitt for undertaking the statistical analyses of the proET-1 assay results from CKD patients. I am also grateful to our collaborators at the University of Geneva who chemically synthesised the proET-1 peptides used in this project.

I would like to express my great appreciation to all my teachers, members of William Harvey Research Institute and friends for their encouragements and filling life with great memories. It has been a privilege to have known such great people and to work at WHRI.

Finally, I would like to thank the three most special people in my life: my parents and my sister, for their unconditional love, belief, and continued support throughout my years at school and university. I am a lucky person to have such great family.

This project was supported by the Medical Research Council, grant number G0801509.

CHAPTER 1

Introduction

1 INTRODUCTION

1.1 Identification of endothelin-1

Endothelium-dependent contracting factor (EDCF) was first described in 1985 (Hickey *et al.*, 1985). This peptidic EDCF was isolated, purified, sequenced and cloned by Yanagisawa and colleagues in 1988 from the conditioned medium of porcine aortic endothelial cells, and named as endothelin-1 (ET-1) (Yanagisawa *et al.,* 1988). The human preproendothelin-1 (ppET-1) messenger RNA (mRNA) was cloned and complete nucleotide sequence was determined by Inoue *et al.,* 1989. The human ET-1 gene (*EDN1*) encodes a 212 amino acid precursor, ppET-1 (Bloch *et al.,* 1989).

Endothelin (ET) occurs as three isoforms ET-1, ET-2 and ET-3 that are generated from three distinct human genes encoding ppET-1, ppET-2, and ppET-3, respectively (Inoue *et al.,* 1989). All ET peptides are 21 amino acids long, differ only in their N-terminal sequence, contain four cysteine residues forming two intra-chain disulphide bridges at Cys^{1} – Cys^{15} and Cys^{3} – Cys^{11} (Yanagisawa *et al.,* 1988; Inoue *et al.,* 1989) and share a common hydrophobic C-terminal with Trp^{21}, which is essential for biological activity (Bouallegue *et al.,* 2007) (Table 1.1).

ET-1 is the principal cardiovascular isoform and the most potent vasoconstrictor peptide described yet (Yanagisawa *et al.,* 1988). ET-1 contributes to the maintenance of vascular tone in healthy humans (Haynes & Webb, 1994). Nevertheless, ET-1 is also implicated in the pathophysiology of cardiovascular diseases including atherosclerosis (Lerman *et al.,* 1991) where it has enhanced expression (Winkles *et al.,* 1993) and contributes to increased constriction in atherosclerotic human coronary arteries (Kinlay *et al.,* 2001).

Table 1.1: ***Comparison of the amino acid sequences of three human ET isoforms: ET-1, ET-2 and ET-3.*** *Homologous residues to ET-1 are represented as hyphens (-). Cysteine residues at positions 1 – 15 and 3 – 11 form disulphide bridges and are conserved in all peptides. The C-terminal hydrophobic region is also highly conserved across the three ET peptides.*

ET peptide	**1**	**2**	**3**	**4**	**5**	**6**	**7**	**8**	**9**	**10**	**11**	**12**	**13**	**14**	**15**	**16**	**17**	**18**	**19**	**20**	**21**
ET-1	C	S	C	S	S	L	M	D	K	E	C	V	Y	F	C	H	L	D	I	I	W
ET-2	-	-	-	-	-	W	L	-	-	-	-	-	-	-	-	-	-	-	-	-	-
ET-3	-	T	-	F	T	Y	K	-	-	-	-	-	-	Y	-	-	-	-	-	-	-

1.2 Processing of proendothelin-1

Human ET-1 is derived from a 212 amino acid precursor ppET-1 (Bloch *et al.,* 1989). The initial step in processing of the ET-1 precursor involves removal of the amino (N)-terminal signal sequence of ppET-1 by a signal peptidase. This occurs in the endoplasmic reticulum (ER) on entry of the nascent protein into the secretory pathway (Steiner, 1982). This generates proendothelin-1 (proET-1), which is condensed and packed in the trans-Golgi network and then transported to the cell surface by the constitutive secretory pathway. Intracellular proteolytic processing of proET-1 occurs in secretory vesicles in endothelial cells (ECs) (Harrison *et al.,* 1995). ProET-1 undergoes further proteolytic processing by pro-hormone/pro-protein convertases (PCs) at carboxyl (C)-terminal of pairs of basic residues (Rockwell & Thornier, 2004). This proteolytic processing generates the inactive intermediate big ET-1 (38 amino acid residues) following Lys^{51}-Arg^{52} and Lys^{91}-Arg^{92} (Kido *et al.,* 1997). In ECs big ET-1 is generated from proET-1 via furin (Denault *et al.,* 1995; Blais *et al.,* 2002). The final step of ET-1 biosynthesis involves a novel endopeptidase, which is called endothelin-converting enzyme (ECE) (Yanagisawa *et al.,* 1988).

ECE cleaves big ET-1 to the biologically active ET-1 and a C-terminal fragment (CTF) of big ET-1 (big $ET\text{-}1_{[22-38]}$) by selective hydrolysis of the peptide bond at Trp^{21} – Val^{22} residues (Figure 1.1) (Emori *et al.,* 1989; Ikegawa *et al.,* 1990). These studies were also performed using pulmonary aortic endothelial cells (PAEC)/bovine aortic endothelial cells (BAEC) (Harrison *et al.,* 1995) and this was subsequently confirmed in human umbilical vein endothelial cells (HUVEC) (Corder *et al.,* 1995b).

ProET-1 contains six potential cleavage sites by PCs that are beyond the sequence of big ET-1. Based on the human sequence, these potential cleavage sites are at C-terminal of Lys-Arg (KR) at 92/93; or Lys-Lys (KK) at 118/119, 144/145, and 154/155; or Arg-Lys (RK) at 165/166; or Arg-Arg (RR) at 168/169 (Figure 1.1). However, only two of these processing sites (Lys-Arg or Arg-Arg) occur frequently. Cleavage at these residues could generate potential proET-1 peptide fragments. This results in the co-secretion of the biologically active peptide ET-1 with other peptide fragments, which are generally considered to be biologically inert (Struck *et al.,* 2005). However, these peptide fragments can act as markers for the release of the active vasoconstrictor ET-1 (Struck *et al.,* 2005; Papassotiriou *et al.,* 2006).

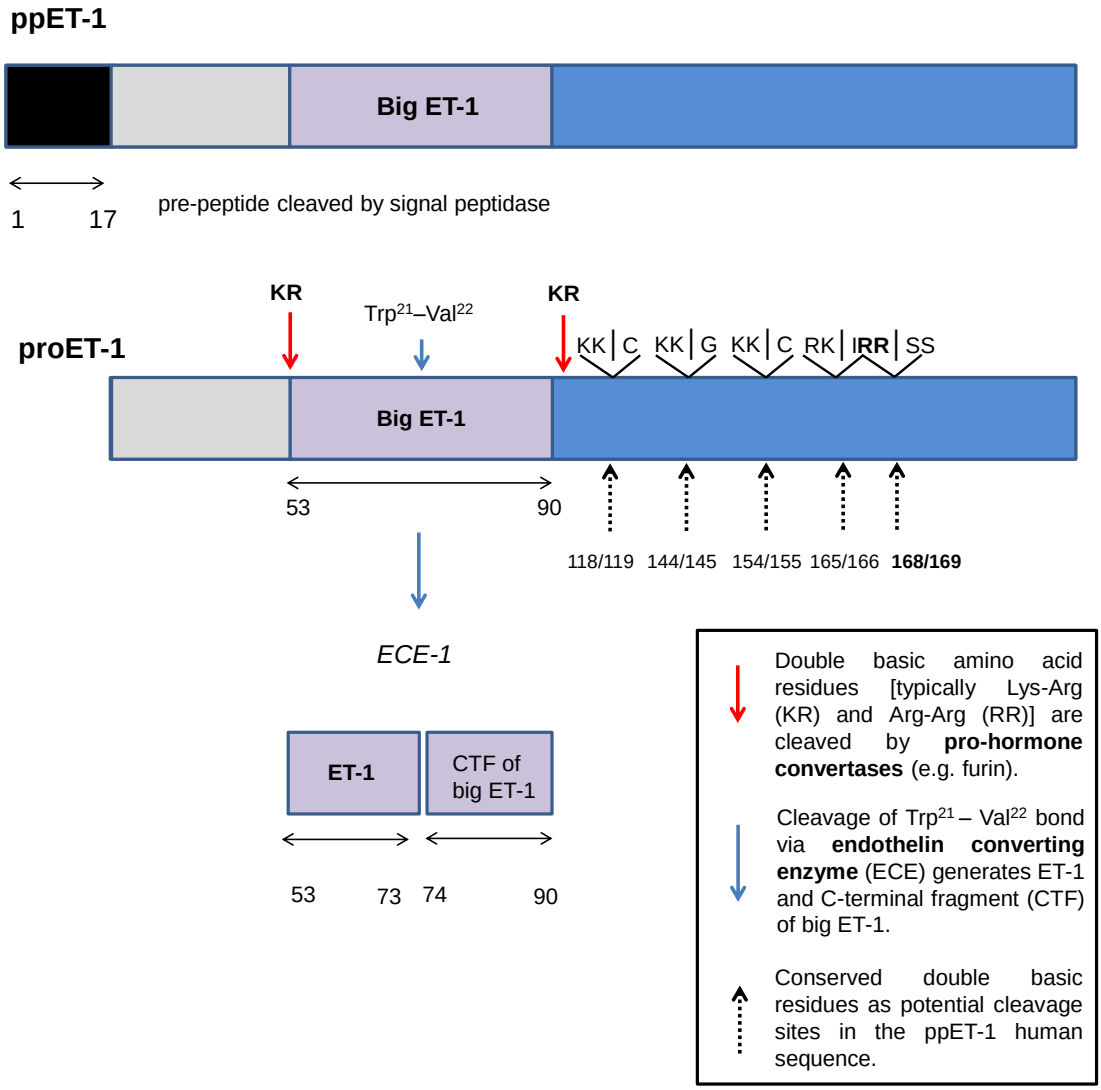

Figure 1.1: ***Biosynthesis of human preproendothelin-1.*** *The signal sequence (position 1 – 17) of ppET-1 is cleaved by a signal peptidase. ProET-1 is then proteolytically processed by PCs at double basic residues (typically Lys-Arg or Arg-Arg). These sites are marked with arrows and indicate cleavage possibly via furin-like convertase. This generates the inactive intermediate big ET-1, which is cleaved at a Trp^{21}–Val^{22} bond (Trp^{73} – Val^{74}amino acid residue numbers based on human ppET-1) by the proposed endopeptidase ECE. This generates the vasoactive peptide ET-1 and a C-terminal fragment (CTF) of big ET-1. Potential cleavage sites at conserved double basic residues are marked with dotted arrows. Cleavage at these sites could generate potential proET-1 peptide fragments.*

Two distinct pathways are involved in ET-1 release at the cell surface. Firstly, ET-1 is released by the constitutive pathway from vesicles originating from the trans-Golgi network as described. Secondly, ET-1 is also released from endothelial cell-specific storage granules, called Weibel-Palade bodies by a regulated pathway (Russell & Davenport, 1999). This occurs through the regulated pathway in response to an external physiological or pathophysiological stimulus including thrombin, hypoxia, and shear stress (Lowenstein *et al.*, 2005). Weibel-Palade bodies also store von Willebrand factor (vWF), which plays a key role in thrombus formation by facilitating platelet adhesion (Turritto *et al.*, 1985).

1.3 The role of pro-hormone/pro-protein convertases (PCs)

There are seven members of PCs identified in humans and other mammals. Furin is the best characterised member with Kex2/kexin being its homologous counterpart in yeast *Saccharomyces cerevisiae* (Fuller & Thorner, 1989). Other mammalian relatives are PC1/PC3, PC2, PACE4, PC4, PC5/PC6 and PC7/PC8/LPC/SPC7 (Rockwell & Thorner, 2004). PCs are calcium-dependent serine proteases. All PCs contain an N-terminal signal sequence for directing entry into the secretory pathway, a pro-domain which has a role in protein folding and it is essential for activity, a subtilisin-related catalytic domain and a variable domain, which in furin and PACE4 includes a cysteine-rich domain (Henrich *et al.,* 2003). Furin, PACE 4 and PC5/PC6 enzymes are more ubiquitously distributed while PC2, PC1/PC3 and PC4 enzymes are localised to endocrine/neuroendocrine cells and testicular spermatids (PC4).

Full-length furin, the PC6 isoform, PC7 and kexin also contain an additional C-terminal transmembrane domain and a short cytoplasmic sequence (Henrich *et al.,* 2003). Furin and kexin family of proteases recognise dibasic amino acid motifs typically Lys-Arg and Arg-Arg and less frequently Lys-Lys, Arg-Lys or Arg-X-X-Arg (Rockwell & Thornier, 2004; Bergeron *et al.,* 2000). A cleavage site followed by an Arg represented with a P_1 at the first residue on the N-terminal side of the cleaved peptide bond. In addition, furin is also specific for Arg at the -4 position relative to the scissile bond (P_4-Arg) (Kido *et al.,* 1997; Rockwell & Thornier, 2004). Both furin and kexin require an Arg at P_1 and P_4 for cleavage.

Furin and PC7 cleave proET-1 to big ET-1 in ECs (Blais *et al.,* 2002). Similar to furin, PC7 requires Arg at P_1 and P_4 but, in addition, a P_2 basic residue is also essential (Blais *et al.,* 2002). The processing of proET-1 is not fully characterised *in vivo* and requires further investigation.

1.4 Endothelin Converting Enzyme (ECE)

ET-1 biosynthesis is dependent on the hydrolysis of the intermediate big ET-1 by an endopeptidase designated as endothelin converting enzyme (ECE) (Yanagisawa *et al.*, 1988). ECE was initially proposed by Yanagisawa *et al.*, 1988, with the first clear evidence being provided by studies showing the inhibitory effect of phosphoramidon on cultured porcine aortic endothelial cells (Ikegawa *et al*., 1990). ET-1 synthesis was markedly suppressed by the metalloprotease inhibitor phosphoramidon due to inhibition of ECE resulting in the accumulation of the inactive intermediate big ET-1 in cell culture conditioned medium (Sawamura *et al.,* 1991; Ikegawa *et al*., 1991; Corder *et al.,* 1995b; Isaka *et al*., 2003). This led to the understanding that ECE is a phosphoramidon-sensitive neutral metalloproteinase.

The conformation of human big ET-1 is important for its hydrolysis by ECE (Corder, 1996). This was confirmed by decreased specificity/interaction of ECE to hydrolyse the modified big ET-1 [incorporated with N-hydroxysuccinimide esters of 3-(p-hydroxyphenyl)propionic acid (HPP) or S-acetylthioglycolic acid (ATG) groups, or removal of disulphide bridges] (Corder, 1996).

Two ECE genes have been cloned and they are referred to as ECE-1 (Shimada *et al.,* 1995; Xu *et al.,* 1994) and ECE-2 (Emoto & Yanagisawa, 1995). ECE-2 is expressed in the trans-Golgi network and shares 59% identity with the amino acid sequence of ECE-1 (Emoto & Yanagisawa, 1995). ECE-3 was later described and purified from bovine iris microsomes and is specific for big ET-3 (Hasegawa *et al.,* 1998). All ECE isoforms cleave big ET-1 with the same efficiency (D'Orléans-Juste *et al.,* 2003). The cleavage of big ET-2 occurs at the Trp^{21} – Val^{22} bond, as in big ET-1, whereas big ET-3 is cleaved at the Trp^{21} – Ile^{22} bond to produce ET-3. ECE-2 is more selective for big ET-1 than for big ET-2 and big ET-3. Immunohistochemical studies shown highest ECE-1 expression in cardiovascular endothelium (Whyteside & Turner, 2013). ECE-1 is the most abundant isoform and it is widely expressed in many cells and human tissues (Rossi *et al.,* 1995; Valdenaire *et al.,* 1995; Schweizer *et al.,* 1997).

1.4.1 Structural features of ECE-1

ECE-1 is a type II integral membrane-bound neutral metalloproteinase. ECE-1 has structural similarity to neutral endopeptidase 24.11 or neprilysin (NEP-24.11) (Malfroy *et al.,* 1988) and Kell blood group protein (Lee *et al.,* 1991) and both ECE-1 and NEP-24.11 are localised on the plasma membrane of human ECs (Waxman *et al.,* 1994; Corder *et al.,* 1995b) (Table 1.2, page 11).

ECE-1 consists of **(1)** a short N-terminal cytoplasmic domain, **(2)** a single transmembrane helix, and **(3)** a large extracellular domain that includes the active catalytic site (comprising the C-terminal end) and a HEXXH (His^{591}, Glu^{592}, X, X, His^{595}) zinc-binding motif (Sansom *et al.,* 1995; Whyteside & Turner, 2013). This suggested that ECE-1 has similar topology and cellular location and possibly exist as an ectoenzyme converting big ET-l to ET-1 at the extracellular face of the plasma membrane (Turner & Tanzawa, 1997). Mutational studies of ECE have established a conserved NAYY (Asn^{566}, Ala^{567}, Tyr^{568}, Tyr^{569}) motif to be important for substrate binding and unique to ECE (Sansom *et al.,* 1998).

In contrast to NEP-24.11, ECE-1 is highly glycosylated (ten N-linked glycosylation sites) and has ten highly conserved Cys residues. Under reducing conditions ECE-1 was estimated to exist with a molecular weight (MWt) of 120 – 130 kD (SDS-PAGE) (Xu *et al.,* 1994; Turner & Murphy, 1996). Human ECE-1 was estimated to be ~250 kD (gel filtration chromatography) (Corder *et al.,* 1995b). This suggested that ECE-1 has two disulphide-linked subunits (Takahashi *et al.,* 1995; Shimada *et al.,* 1996).

Four human ECE-1 isoforms (ECE-1a – d) are expressed in ECs. These are derived from the same gene through alternative splicing of mRNA. They differ from each other in their N-terminal cytoplasmic tails (Valdenaire *et al.,* 1995). These tails play a role in enzyme targeting and turnover with di-leucine and tyrosine-based motifs affecting localisation (Valdenaire *et al.,* 1995). While ECE-1a (758 amino acid residues) and ECE-1c (754 amino acid residues) are found on the plasma membrane as ectoenzymes (Schweizer *et al.,* 1997), ECE-1b (770 amino acid residues) is located intracellularly (Takahashi *et al.,* 1995). Later, Muller *et al.,* 2003 demonstrated in transfected AtT-20 neuroendocrine cells that both ECE-1b and ECE-1d are located intracellularly in the endosomal system. ECE-1b mRNA is widely expressed in a variety of tissues, but ECE-1a is more abundantly expressed than ECE-1b in ECs (Shimada *et al.,* 1995) and human

tissue (Mockridge *et al.,* 1998) but not in primary cultures of smooth muscle cells (SMC) (Valdenaire *et al.,* 1999). In contrast, Schweizer *et al.,* 1997 showed ECE-1c mRNA as the main isoform expressed in most human tissues while confirming ECE-1a as the predominant isoform in ECs. Subsequent studies showed ECE-1c and ECE-1d expression in vascular smooth muscle cells (VSMC) (Barker *et al.,* 2001) while all isoforms were expressed in ECs. In general, ECE-1 is localised to the luminal surface on ECs rather than VSMC (Russell *et al.,* 1998). Even though there is difference in their tissue distribution ECE-1a – c isoforms cleave big ET-1 with comparable efficiencies (Schweizer *et al.,* 1997).

Both ECE-1 and ECE-2 catalyse the conversion of big ET-1 to ET-1 with a neutral (pH 6.8) and acidic (pH 5.6) pH optimum, respectively (Emato & Yanagisawa, 1995). ECE-2 is localised in secretion vesicles and ECs but not expressed on plasma membrane (Emato & Yanagisawa, 1995).

The association between specific ECE-1 isoforms to ET-1 synthesis and factors regulating cell-specific expression of ECE-1 isoforms have been unclear (Corder *et al.,* 1998). In BAEC, Corder & Barker, 1999 found no relation between the level of ET-1 synthesis or ppET-1 expression with the level of ECE-1 expression (ECE-1a, ECE-1c, or all the ECE-1 isoforms).

ECE-1 activity is increased in isolated endothelium-denuded human atherosclerotic coronary arteries (Maguire & Davenport, 1998) as well as in rat balloon-injured arteries. In rat balloon-injured arteries, in contrast to EC localisation in uninjured vessels, immunohistochemical staining located ECE-1 in neointimal SMC in injured arteries (Minamino *et al.,* 1997; Dashwood *et al.,* 1999). Furthermore, ECE-1 was detected in the intimal and medial VSMC and localised in macrophages and fibrous cap of atherosclerotic lesions (Ihling *et al.,* 2001). Upregulation of the ECE-1/ET-1 system was also shown to be associated with chronic inflammation and to be present in the early stages of atherosclerotic plaque development (Ihling *et al.,* 2001). Together these data suggest a possible role of ECE-1 in the vascular remodelling process. Increased ECE-1 activity may also contribute to increased big ET-1 conversion to ET-1 (Böhm *et al.,* 2002) that is evident with increased ET-1 levels observed in atherosclerosis (Zeiher *et al.,* 1995).

Table 1.2: ***Distinguishing features of ECE-1 and NEP-24.11.***

	ECE-1	**NEP-24.11**
Structure	● ECE-1 (120 – 130 kD) forms covalent disulphide-linked dimers (as shown by site-directed mutagenesis of Cys^{412} in rat ECE-1 (Cys^{428} in human).	● NEP-24.11 (90 – 100 kD) forms a non-covalent monomeric structure (Shimada *et al*., 1996).
Substrate specificity	● ECE-1 cleaves Trp^{21} – Val^{22} bond of big ET-1 but also cleaves bradykinin (Hoang & Turner, 1997) substance P, and hydrolyses insulin B chain at multiple sites with similar efficiency to that of big ET-1 (Johnson *et al.,* 1999).	● NEP-24.11 has broader substrate specificity. Cleaves peptide bonds on the N-terminal of hydrophobic amino acids (Turner & Tanzawa, 1997). Atrial natriuretic peptide (ANP) and oxytocin are also substrates of NEP-24.11.
Sensitivity to inhibitors	● Phosphoramidon inhibits both ECE-1 and NEP-24.11 but has a greater potency (lower Ki) for NEP-24.11. ● Thiorphan is a potent inhibitor of NEP-24.11 but not ECE-1 (Turner & Murphy, 1996).	
Metabolism of ET peptides	● At lower concentrations (1 µM), NEP-24.11 rapidly degrades ET peptides.	

1.4.2 Analysing the physiological role of ECE-1 in ET-1 biosynthesis

1.4.2.1 *Inhibitor studies with protease inhibitors*

In anaesthetised rats, the conversion of exogenously administered big ET-1 to ET-1 was observed with increased blood pressure (BP) and airway contractile responses (Fukuroda *et al.,* 1990). Phosphoramidon inhibited the BP response of systemically administered big ET-1 but not to ET-1 (Fukuroda *et al.,* 1990; Matsumura *et al.,* 1990; Corder & Vane, 1995). In contrast, incubation of tissues from guinea pig gallbladder with protease inhibitors such as thiorphan inhibitor NEP-24.11 (3×10^{-4} M); or metalloprotease inhibitor 1,10-phenanthroline (10^{-4} M); an angiotensin converting enzyme (ACE) inhibitor captopril (10^{-4} M); an inhibitor of aspartic proteases pepstatin A (10^{-5} M); an irreversible inhibitor of serine proteases PMSF (10^{-3} M); a serine protease inhibitor E-64; a trypsin-like serine protease inhibitor leupeptin (10^{-4} M); a chymotrypsin-like serine protease inhibitor chymostatin (10^{-4} M); aprotinin (10^{-6} M); and an inhibitor of aminopeptidases bestatin (10^{-5} M) before the addition of big ET-1 were all insufficient to prevent the conversion to ET-1 (Battistini *et al.,* 1995).

Likewise neither captopril nor kelatorphan was able to block the pressor activity of big ET-1 in the anaesthetised rats (McMahon *et al.,* 1991). However, thiorpan dose-dependently inhibited the pressor response to big ET-1, but this inhibition was less potent than phosphoramidon (McMahon *et al.,* 1991). These metalloprotease inhibitors (phosphoramidon, kelatorphan, and thiorphan) have equal potency for NEP-24.11 and since kelatorphan and thiorphan were unable to inhibit ECE activity, it confirmed that ECE and NEP-24.11 are distinct members of the metalloprotease family. These results collectively showed evidence that ECE-1 is a phosphoramidon-sensitive metalloprotease.

1.4.2.2 *Inhibitor studies in endothelial cells*

Incubation of big ET-1 with cultured ECs in the presence of phosphoramidon inhibited ET-1 production (Ikegewa *et al.,* 1990; Corder *et al.,* 1995b). Similarly, in cultured vascular ECs and VSMC phosphoramidon inhibited the conversion of exogenous big ET-1 to ET-1 (Ikegewa *et al.,* 1991). Higher concentrations of phosphoramidon were required to inhibit endogenous sysnthesis of ET-1 in comparison to those required to inhibit exogenous big ET-1 (Corder *et al.,* 1995b). Consistent with intracellular synthesis of ET-1 in the secretory vesicles, this was indicative of intracellular hydrolysis of the endogenous peptide, which is relatively inaccessible to phosphoramidon (Corder, 2001).

Phosphoramidon and thiorphan are zinc metallopeptidase inhibitors. While NEP-24.11 is inhibited by both (at nM concentrations), ECE-1 is only sensitive to phosphoramidon (at µM concentrations). Phosphoramidon inhibits other metallopeptidases such as bacterial metalloendopeptidase thermolysin, which has similar substrate specificity as NEP-24.11.

1.4.2.3 *Functional studies*

Although, ECE-1 has been proposed to be the physiological ECE that hydrolyses the Trp^{21} – Val^{22} bond in big ET-1 to generate vasoactive ET-1 (Yanagisawa *et al.,* 1988; Turner & Murphy, 1996) it is still not known whether or not ECE-1 is the only enzyme involved in this process. Yanagisawa *et al.,* 1998 reported developmental defects in cardiac- and neural crest-derived tissues in a targeted null mutation of ECE-1 gene in mouse (ECE-$1^{-/-}$) that was virtually identical to the defects seen in ET-1 and ET_A-deficient embryos (Yanagisawa *et al.,* 1998). In order to further investigate the role of ECE-2 in cardiovascular development Yanagisawa *et al.,* 2000 generated a null mutation in ECE-2 by homologous recombination. ECE-$2^{-/-}$ knockout (KO) mice were healthy into adulthood and fertile in both sexes (Yanagisawa *et al.,* 2000). However, when they were bred into an ECE-1 null background, defects in cardiac outflow structures became more severe than those in ECE-$1^{-/-}$ single KO embryos. More interestingly, tissue levels of ET-1/ET-2 measured in whole-embryo extracts from ECE-$1^{-/-}$ and ECE-$2^{-/-}$ mutant embryos were similar to those from ECE-1 (48% reduction in ET-1 levels when compared to controls) without increases in big ET-1 levels (Yanagisawa *et al.,* 2000). This indicated that protease(s) distinct from ECE-1 and ECE-2 can activate mature ET-1/ET-2 *in vivo* (Yanagisawa *et al.,* 2000).

Furthermore, Barker *et al*., 2001 characterised ECE-1 isoforms in bovine pulmonary artery smooth muscle cells (BPSMC), and used an antisense oligodeoxynucleotide (ODN) for ECE-1c (the predominant isoform in BPSMC) to test the effect of ECE-1 depletion on ET-1 synthesis. Treatment with ECE-1c antisense ODN specifically reduced ECE-1c mRNA levels and ECE-1 protein, but had a negligible effect on ET-1 synthesis (Barker *et al*., 2001). This suggested that the physiological role of ECE-1 in ET-1 biosynthesis is not clear and still needs to be further elucidated.

1.5 Alternative processing pathways of ET-1 synthesis

As well as metalloproteinases (Okada *et al.*, 1990), serine and aspartic proteases (Ikegawa *et al.*, 1990) can also cleave big ET-1 to produce ET-1. These include matrix metalloproteases (MMPs) and human chymase, which produce the vasoactive peptide ET-$1_{[1-32]}$ and ET-$1_{[1-31]}$, respectively.

1.5.1 Matrix metalloproteinase-2

Matrix metalloproteinase-2 (MMP-2, gelatinase A) is a zinc-dependent proteinase secreted from vascular endothelial and SMC (Li *et al.*, 1999). MMP-2 cleaves human big ET-1 at Gly^{32} – Leu^{33} bond (Fernandez-Patron *et al.*, 1999). TIMP-2 is an endogenous inhibitor of MMPs with preferred effects on MMP-2 (Woessner, 1998) inhibited MMP-2–dependent conversion of big ET-1 (Fernandez-Patron *et al.*, 1999).

1.5.2 Chymase

Incubation of big ET-1 with purified human connective tissue mast cell chymase (a chymotrypsin-like serine protease) produced ET-$1_{[1-31]}$ by cleaving at the Tyr^{31} – Gly^{32} bond of big ET-1 (Nakano *et al.*, 1997). In endothelium-denuded human umbilical venous smooth muscle, ET-$1_{[1-31]}$ does not bind to ET receptors at physiological concentrations but is converted by enzymatic activity to ET-1 (Maguire & Davenport, 2004; Davenport & Maguire, 2006). In human bronchial smooth muscle cells ET-$1_{[1-31]}$ is hydrolysed by ECE-1 and NEP-24.11 and is a trachea and vascular smooth muscle constricting peptide.

1.6 Factors regulating ET-1 biosynthesis in endothelial cells

ET-1 biosynthesis is dependent on regulation and transcription of ET-1 mRNA (Rubanyi & Polokoff, 1994). Transcriptional factors that are involved in the regulation of ET-1 gene expression with relevance to atherosclerosis and diabetes include activator protein-1 (AP-1), hypoxia inducible factor-1 (HIF-1), nuclear factor κB (NFκB), vascular endothelial zinc finger 1 (Vezf1), GATA binding protein-2 (GATA-2) and GATA-4, and nuclear factor of activated T-cells (NFAT) (Stow *et al.,* 2011). Moreover, DNA methylation and histone modifications as well as post-transcriptional modifications that affect mRNA stability also modulate *EDN1* expression (Stow *et al.,* 2011).

Transcriptional factors can be activated by stimuli such as thrombin (Yanagisawa *et al.,* 1988; Marsen *et al.,* 1995), angiotensin II (Ang II) (Emori *et al.,* 1991; Imai *et al.,* 1992), growth factors [transforming growth factor-β (TGF-β)] (Lee *et al.,* 2000; Rodríguez-Pascual *et al.,* 2003), cytokines [tumour necrosis factor-α (TNF-α)], insulin (Oliver *et al.,* 1991; Hattori *et al.,* 1991; Hu *et al.,* 1993), hypoxia (Kourembanas *et al.,* 1991; Kang *et al.,* 2011), reactive oxygen species (ROS) (Kahler *et al.,* 2001; Ruef *et al.,* 2001), low density lipoprotein (LDL) (Boulanger *et al.,* 1992), epinephrine, and phorbol ester enhances the secretion of ET-1. By contrast, mediators like calcium ionophore (Corder *et al.,* 1993b; Brunner *et al.,* 1994), nitric oxide (NO) (Boulanger & Lüscher, 1990), cyclic guanosine monophosphate (cGMP) (Wort *et al.,* 2000), ANP (Hu *et al.,* 1992), and prostacyclin (PGI_2) (Prins *et al.,* 1994) reduce the release of endogenous ET-1. Consensus sequences for these regulators (including shear stress, TGF-β, insulin, thrombin, epinephrine, interleukin-1, and Ang II,) are also found in the human ECE-1 gene (Valdenaire *et al.,* 1995).

1.6.1 Fluid shear stress

Fluid shear stress regulates ET-1 mRNA in a biphasic manner (Yoshizumi *et al.,* 1989; Malek *et al.,* 1999). ET-1 gene expression is stimulated at low shear stress (4 – 5 dyn/cm^2) (Harrison *et al.,* 1998). In contrast, fluid shear stress at physiological magnitude (6 h, 20 dyn/cm^2) suppressed ET-1 mRNA expression by 5 – 10-fold in cultured BAEC (Malek *et al.,* 1993) and HUVEC (Sharefkin *et al.,* 1991). Exposing primary cultures of HUVEC to laminar shear stress transiently upregulated ppET-1 mRNA, reaching its maximum after 30 min. When HUVEC were exposed to long-term laminar shear stress (24 h), ppET-1 mRNA and ECE-1a mRNA levels (most abundant ECE-1 isoform in HUVEC) were downregulated (Morawietz *et al.,* 2000). Downregulation of ppET-1 mRNA and ET-1 release occurs in a shear stress magnitude dependent manner (Morawietz *et al.,* 2000). Protein kinase C (PKC) inhibitor calphostin C (1 µM) did not hinder shear-induced downregulation of ET-1 and forskolin (10 µM) an activator of adenylate cyclase (AC) had no significant effect on cyclic adenosine monophosphate (cAMP) levels in response to shear stress of up to 60 min (20 dynes/cm^2) and resulted in significant downregulation of ET-1 mRNA (Malek *et al.,* 1993). These data suggest that the regulation of ET-1 by shear stress (of magnitude 20 dynes/cm^2) in aortic endothelium is independent of PKC and cAMP (Malek *et al.,* 1993). HUVEC were not affected by PKC, cAMP or tyrosine kinase inhibition (Morawietz *et al.,* 2000). Steady laminar shear stress (20 dyn/cm^2) increased endothelial nitric oxide synthase (eNOS) mRNA levels (Malek *et al.,* 1999). The mechanism of this effect could result from shear stress induced activation of Ca^{2+} dependent eNOS, which inhibits ET-1 (Malek *et al.,* 1999). Inhibition of eNOS (by L-NAME, 500 µM) prevented the downregulation of ppET-1 mRNA by shear stress (Morawietz *et al.,* 2000).

Increase in ET-1 release following short periods of mechanical stretch was demonstrated in ECs (Macarthur *et al.,* 1994; Hishikawa *et al.,* 1995) and in human atherosclerotic coronary arteries *in vivo* (Hasdai *et al.,* 1997).

1.6.2 Krüppel-like factor 2 (KLF2)

The most important mechanism regulating ET-1 gene expression in ECs in response to fluid shear stress is through the activation of a transcription factor, Krüppel-like factor 2 (KLF2). Expression of KLF2 is specific for ECs where it mediates the effect of fluid shears on ET-1 expression. This response is blocked by siRNA for KLF2 (Parmar *et al.*, 2006). Inhibition of flow-induced upregulation of KLF2 in ECs caused significant decrease of the regulation of upregulated genes such as eNOS (Parmar *et al.*, 2006). Downregulation of interleukin-8 (IL-8), Ang-II, and ET-1 was abolished at the mRNA level (Parmar *et al.*, 2006). Overexpression of KLF2 in HUVEC potently induces eNOS and inhibits the induction of key adhesion molecules such as vascular cell adhesion molecule 1 (VCAM-1) and E-selectin (through NFκB-dependent pathway), but not intracellular adhesion molecule-1 (Feinberg *et al.*, 2004).

KLF2 inhibits activation of pro-inflammatory cytokines including TNF-α, LPS, and thrombin (Atkins & Jain, 2007). KLF2 inhibits protease-activated receptor-1 (PAR-1), which is the principal receptor of thrombin. Therefore, KLF2 inhibits thrombin-induced activation of cytokine/chemokine such as IL-6, IL-8, and monocyte chemoattractant protein-1 (MCP-1) (Atkins & Jain, 2007).

1.6.3 Calcium (Ca^{2+}) ionophores

Stimulation of ECs with Ca^{2+} ionophores for short periods increase ppET-1 mRNA expression (Tasaka & Kitazumi, 1994) while longer stimulation suppress ET-1 synthesis (Corder *et al.*, 1993b). Calcium ionophore, A23187, inhibited ET-1 release from cultured HUVEC (Russell *et al.*, 1998). The inhibitory effect of A23187 was unaffected by NOS inhibitor NG-monomethyl-L-arginine (0.2 mM) or COX inhibitor indomethacin (10 μM). Therefore, inhibition of ET-1 release by A23187 was independent from NO or prostacyclin synthesis in BAEC and EA.hy 926 cells (Corder *et al.*, 1993b). Calphostin (PKC inhibitor) suppressed basal ppET-1 expression in ECs (Malek *et al.*, 1993), indicating a role of specific PKC isoforms in the regulation of ET-1 gene expression.

1.6.4 Thrombin

Thrombin stimulates ppET-1 gene expression and ET-1 release in macrovascular [HUVEC and bovine pulmonary artery endothelial cells (BPAEC)] and microvascular cells [human endothelial cell line (HMEC-1)] with highest induction occurring at 4 U/ml after 2 h (Marsen *et al.*, 1995). Thrombin stimulated ppET-1 mRNA and ET-1 peptide induction was mediated by phosphorylation and activation of protein tyrosine kinase (PTK) through PKA and PKC-independent pathway (Marsen *et al.*, 1995). This conclusion was reached using selective PTK inhibitors herbimycin A (1 μmol/L for 6 h) and genistein (6 μg/ml for 30 min) before thrombin stimulation, which reduced ppET-1 mRNA expression and thrombin-stimulated ET-1 peptide synthesis to control levels in HUVEC and HMEC-1, and below control levels in BPAEC (Marsen *et al.*, 1995). Phorbol ester (an activator of PKC) transiently induced ppET-1 mRNA but had no effect on ET-1 peptide synthesis. Thrombin stimulated ppET-1 mRNA was unaffected by inhibition of PKC using sangivamycin (0.1 μmol/L for 30 min) and calphostin C (0.1 μmol/L for 30 min). Forskolin (20 μmol/L for 2 h) had no effect on thrombin stimulated ppET-1 mRNA levels and ET-1 peptide synthesis.

In contrast, thrombin stimulated ppET-1 mRNA in porcine aortic ECs can be mediated by PKC (Kitazumi & Tasaka, 1993) and immunoreactive (ir) ET-1 release was inhibited by PKC inhibitors H7 [91-(5-isoquinolinesulphonyl)-2-methylpiperazine)] and staurosporin (Kohno *et al.*, 1992).

1.6.5 Bacterial lipopolysaccharide (LPS)

Treatment of BAEC with bacterial lipopolysaccharide (LPS) (10 μg/ml) resulted in a concentration-dependent increase in ET-1 release and increased ppET-1 mRNA expression (Douthwaite *et al.*, 2003). Increase in ppET-1 mRNA transcription was relatively small in comparison to increase in ppET-1 mRNA levels and the degree of induction of ET-1 release (Douthwaite *et al.*, 2003). Therefore, decreased mRNA degradation and increased stability were more likely to be the key contributing factors to the increased mRNA levels. LPS increased ppET-1 mRNA stability by approximately 2-fold (Douthwaite *et al.*, 2003). Jersmann *et al.*, 2001 also stated that TNF-α and LPS act synergistically to upregulate expression of endothelial cell adhesion molecules such

as intercellular adhesion molecule-1 (ICAM-1), E-selectin and VCAM-1, which are important mediators in the regulation of leukocyte trafficking from the blood to the site of inflammation.

1.6.6 Insulin

Insulin stimulated ET-1 levels (2-fold) in the conditioned medium from BAEC (Potenza *et al.,* 2005). Pre-treatment with a PI3K inhibitor, wortmannin, had no significant effect on insulin-stimulated ET-1 secretion while MAPK (MEK1/MEK2) inhibitor PD-98059 abolished this effect of insulin. Therefore, suggesting MAPK-dependent pathways (but not PI3-kinase-dependent pathways) are involved in insulin mediated ET-1 secretion in BAEC.

The mRNA expression of ppET-1 and ET receptors was increased in diabetic rats (STZ-induced diabetic rats) when compared to age-matched controls (Matsumoto *et al.,* 2004).

1.7 Regulation of ET-1 synthesis in other cell types: vascular smooth muscle cells, cardiomyocytes, airway epithelial cells and expression in cancer cells

Although ECs are the primary source of vascular ET-1 production, other cell types such as VSMC, cardiomyocytes, macrophages (Ehrenreich *et al.*, 1990), leukocytes, and fibroblasts can also synthesise ET-1 (Nunez *et al*., 1990). In addition to cardiovascular system, tubular epithelial cells, mesangial cells and podocytes of the kidney also synthesise ET-1 (Kohan, 1997). In non-ECs, ET-1 synthesis is low, if any, but in pathological conditions, it can be induced by several stimuli (as described in the previous section 1.6 for ECs).

1.7.1 Vascular smooth muscle cells

In contrast to ECs, ppET-1 mRNA was not constitutively expressed in quiescent cultures of rat aortic VSMC. Nevertheless, vasoconstrictor peptides [Ang II, arginine-vasopressin (AVP) and ET-1 itself], growth factors [TGF-β, platelet derived growth factor AA (PDGF-AA) and epidermal growth factor (EGF)] induced ppET-1 mRNA expression in rat (Hahn *et al.,* 1990) and human VSMC (Resink *et al.*, 1990). This was rapid but with transient kinetics (peak at 3 – 5 h and return to basal within 7 h) (Resink *et al.*, 1990). Thrombin induced ppET-1 mRNA expression in rat aortic SMC with maximal effects at 4 U/ml after 80 min incubation (Lepailleur-Enouf *et al.*, 2000). In addition, glucocorticosteroids can also increase ET-1 secretion in VSMC. A pure glucocorticoid agonist, RU 28362 at 100 nM increased ET-1 secretion by 3.3-fold after 1 h (Morin *et al.*, 1998).

In healthy saphenous and mesenteric veins, and mesenteric and internal mammary arteries, ET staining in medial SMC was undetectable (Howard *et al.*, 1992). This suggested that in VSMC, there is very low ET-1 synthesis, if any. However, cultures of VSMC explanted from diseased human coronary artery, thoracic aorta, left internal mammary artery, saphenous vein, and HUVSMC (human umbilical vein vascular smooth muscle cells) secreted ET-1 (Yu & Davenport, 1995). In HUVSMC, the level of release was lower than ECs (Yu & Davenport, 1995).

TNF-α (maximal stimulation with 10 ng/ml) and interferon-γ (IFN-γ) (fixed concentration at 1000 U/ml) incubated in combination over 48 h significantly increased ppET-1 mRNA and the expression of ET-1 in human VSMC derived from internal mammary artery and saphenous vein (Woods *et al.,* 1999). IL-1β, (up to 10 ng/ml), IL-6 (up to 10 ng/ml), and bacterial endotoxin (up to 10 ng/ml) did not produce an additional increase in ET-1 production (Woods *et al.,* 1999).

1.7.2 Pulmonary arterial smooth muscle cells (PASMC)

ET-1 is synthesised from pulmonary arterial smooth muscle cells (PASMC) and plays a key role in the pathology of vascular remodelling in pulmonary artery hypertension (PAH) (Tchekneva *et al.,* 2000; Wort *et al.,* 2001). ET-1 upregulates proliferation of human primary PASMC only in the presence of stimuli such as serum (Lambers *et al.,* 2013) through an ET_A receptor-mediated mechanism (Panettieri *et al.,* 1996). Davie *et al.,* 2002 showed increased ir-ET-1 with 10% foetal bovine serum (FBS) or TGF-β1 (10 ng/ml), while cicaprost (10^{-10} – 10^{-7} mol/L for 24 h), a PGI_2 analogue, inhibited the proliferation of PASMC. TGF-β1 (10 ng/ml), as well as increasing ir-ET-1, it also increased PASMC proliferation (Davie *et al.,* 2002). In this study, ET-1 reduced the inhibitory effects of cicaprost and forskolin on DNA synthesis (Davie *et al.,* 2002). In contrast to TGF-β1 (1 – 10 ng/well for 24 h), hypoxia (exposure to 0% O_2 for 24 h) did not increase ppET-1 mRNA or ET-1 production in PASMCs (Markewitz *et al.,* 2001).

ET-1 also increased the *de novo* synthesis and deposition of extracellular matrix (ECM) components; collagen type-I and fibronectin, which involved TGF- β 1 and connective tissue growth factor (CTGF), respectively (Lambers *et al.,* 2013). Inhibition of ET_A receptor (with BQ-123) or ET-1 synthesis using phosphoramidon decreased serum induced proliferation of human PASMC, confirming an autocrine role for ET-1 (Wort *et al.,* 2001).

1.7.3 Cardiomyocytes

Cultured neonatal rat cardiomyocytes incubated with ET-1 (10^{-7} M) over 6 h induced muscle-specific gene expression [myosin light chain 2 (2.6-fold), α-actin (1.6-fold) and troponin I (3.6-fold)], in a dose dependent manner and the actions lasted up to 24 h (Ito *et al.,* 1991). ET-1 transiently induced transcriptional activation of proto-oncogene c-fos, however the levels were undetectable after 6 h. These results supported the notion that ET-1 may function as a hypertrophic factor for cardiomyocytes.

Ang II (10^{-6} M) upregulated ppET-I mRNA by 3-fold over control levels as early as 30 min (Ito *et al.,* 1993). After 2 h, ppET-1 gene expression had returned to basal levels and remained constant during 24 h (Ito *et al.,* 1993). Ang II incuded ET-1 release was both concentration- and time-dependent.

Phorbol ester, tetradecanoylphorbol-acetate (TPA) (10^{-7}), which is a PKC activator, and a Ca^{2+} ionophore, ionomycin similarly induced the expression of muscle specific genes (Ito *et al.,* 1991). Both TPA and ionomycin mimicked the effects of Ang II and ET-1 (Ito *et al.,* 1993). Ang II-induced ppET-1 gene expression was completely inhibited by a PKC inhibitor, H-7 (10^{-5} M). An antisense oligonucleotide used against the coding region of ppET-1 mRNA inhibited the Ang II-stimulated ppET-l mRNA and protein synthesis (Ito *et al.,* 1993). This supported the role of endogenous ET-1 to Ang II-induced cardiac hypertrophy.

1.7.4 Airway epithelial cells

Human bronchial epithelial cells stimulated with LPS and various inflammatory mediators, such as IL-1 (IL-1r3, IL-Iα) and TNF-α, increased ppET-I mRNA expression and ET-I release (Nakano *et al.,* 1994; Michael & Markewitz, 1996). After a 24 h incubation of cultured guinea pig tracheal epithelial cells LPS (1, 5, 10 μg/ml), TNF-α (5, 10 ng/ml), and IL-1β (1, 5 ng/ml) enhanced basal ET-1 release (Yang *et al.,* 1997). Pre-treatment with dexamethasone (100 nM, over 24 h), a corticosteroid that is commonly used in the treatment of asthmatic patients, reduced LPS- (10 μg/ml), TNF-α- (10 ng/ml) and IL-1β- (1 ng/ml) mediated ET-1 release by 48%, 31%, and 38%, respectively (Yang *et al.,* 1997). Dexamethasone (100 nM) also reduced FBS (10%) and

IL-2-stimulated and basal ET-1 release in adenocarcinomic human alveolar epithelial cells (A549) (Calderón *et al.*, 1994).

Human bronchial epithelial cells derived from asthmatic patients express higher ET-1 levels, while ppET-1 mRNA expression (determined by *in situ* hybridisation) was undetectable and low in healthy controls and chronic bronchitis, respectively (Vittori *et al.*, 1992). Hydrocortisone (10^{-6} M) treatment of asthmatic bronchial epithelial cells for 48 h reduced ET-1 release (Vittori *et al.*, 1992).

1.7.5 Cancer cells

Human cervix (HeLa) and larynx (Hep-2) derived epithelial carcinoma cell lines express ppET-1 mRNA under basal conditions in which LPS (10%) stimulated ET-1 release by 62 and 8.5-fold, respectively (Shichiri *et al.*, 1991). ET-1 stimulated (10^{-3}–10^{-9} M, 72 h) proliferation of HeLa and Hep-2 cells was inhibited by nicardipine (10^{-7} M), a dihydropyridine calcium-channel blocker (Shichiri *et al.*, 1991).

Androgens downregulate ET-1 synthesis in androgen-sensitive prostate adenocarcinoma cells (LNCaP), while TGF-β-1, IL-1α and EGF upregulated ET-1 gene expression in androgen-insensitive PC-3 and DU145 cells (Granchi *et al.*, 2001). In contrast, neither of factors had an effect on ECE-1 gene expression (Granchi *et al.*, 2001). These suggest that ET-1 might have a role in the progression of prostate cancer. Higher ET-1 and ET_A receptor expression but lower ET_B receptor expression detected in advanced prostate cancer further supports this role (Nelson *et al.*, 1996).

1.8 Endothelin receptors

Two ET receptor subtypes, ET_A and ET_B, have been identified, cloned and sequenced (Arai *et al.,* 1990; Sakurai *et al.,* 1990; Saito *et al.,* 1991). Both receptors belong to the seven-transmembrane domain, G protein-coupled rhodopsin-type receptor superfamily. ET-1 has similar affinity for both ET_A and ET_B receptors. ET-1 and ET-2 have equal binding affinity and efficacy at the ET_A receptors while ET-3 is less potent (Arai *et al.,* 1990; Sakurai *et al.,* 1990; Davenport, 2002) (Table 1.3). All ET isoforms have equal affinity for ET_B receptors (de Nucci *et al.,* 1988; Rubanyi & Polokoff, 1994; Love *et al.,* 2000).

Table 1.3: ***Affinity of ET peptides for ET_A and ET_B receptors.***

ET receptor	ET peptide selectivity
ET_A	ET-1 = ET-2 ≫ ET-3
ET_B	ET-1 = ET-2 = ET-3

ET_A receptors predominate on VSMC mediating vasoconstriction (pressor response) (Davenport *et al.,* 1995; Maguire & Davenport, 1995; Love *et al.,* 2000). A small density (<15%) of ET_B receptors are also expressed on VSMC, where their activation contributes to vasoconstriction (Clozel *et al.,* 1992; Maguire & Davenport, 1995). ET_B receptors are mainly expressed on the vascular ECs (Summer *et al.,* 1992), where their activation results in vasodilatation (depressor response). This is mediated by the release of endothelium-derived vasodilators NO and PGI_2 (de Nucci *et al.,* 1988; Verhaar *et al.,* 1998) (Figure 1.2, page 36). ET_B receptors mediate anti-proliferative and anti-inflammatory actions by releasing NO. They were also shown to stimulate apoptosis in rat aortic VSMC (Cattaruzza *et al.,* 2000).

Distribution of ET receptors shows species, regional, and developmental differences (Fukuroda *et al.,* 1994b). Thereby, based on this difference, vasoconstrictor responses mediated by ET receptors vary depending on the vascular bed (Davenport & Maguire, 1994). Contractile activities of ET isoforms were in the order of ET-1 > ET-2 = ET-3 in human isolated bronchus (Advenier *et al.,* 1990). In human arteries and veins ET-2 as a vasoconstrictor was equipotent with ET-1 (Maguire & Davenport, 1995).

In contrast to ET_A receptors being more prevalent in cardiovascular system, ET_B receptors are expressed at high densities particularly in the lung, kidney and liver (Kuc *et al.,* 1995; Johnström *et al.,* 2002) where they mediate clearance of ET-1 from the circulation (Fukuroda *et al.,* 1994a). In the kidney, ET_B receptors comprise 70% of the receptors present in both cortex and medulla (Neuhofer & Pittrow, 2009). Collecting duct (CD) is the main renal site of ET-1 production and a CD-specific epithelial cell KO of ET_B receptor gene (CD ET_B KO) caused sodium (Na^+) retention and thereby salt-sensitive hypertension (Ge *et al.,* 2006). In contrast, endothelial cell specific ET_B receptor KO (with preserved CD ET_B expression) had impaired endothelium-dependent vasodilatation (EDD) without altering BP, even with increased plasma ET-1 concentrations (Bagnall *et al.,* 2006). Thus, these investigations suggested that ET_B receptors in the CD are important in the control of BP and mediate natriuretic effects of ET-1. More recently the epithelial sodium channel (ENaC), which is the main regulator of Na^+ reabsorption in the CD, has been shown to be regulated mainly via the ET_B receptors (Bugaj *et al.,* 2012).

The effects of blocking ET_B receptor system was investigated in wild-type and ET_B receptor KO using a mouse model of vascular remodelling (induced by blood flow cessation in the carotid artery). This demonstrated worsening of vascular remodelling in ET_B receptor KO mice after injury (Murakoshi *et al.,* 2002).

In disease states, expression of ET receptors shows regional differences. Some of these findings are as follows: in a rabbit model of diabetes mellitus (DM), kidneys had increased ET_A receptor binding sites, but not ET_B in the cortex and medulla (Khan *et al.,* 1999). In chronic HF patients, ET_A receptors were upregulated in hearts (Pönicke *et al.,* 1998), while ET_B receptors can be downregulated (Zolk *et al.,* 1999). This in turn results in reduced clearance of ET-1 and increased circulating levels, which together with increased ET_A receptor sites contributes to pathological changes. In pulmonary arteries of patients with PAH, the expression of both ET receptors were upregulated (Davie *et al.,* 2002). Both receptors can mediate vasoconstrictor action of ET-1 (McCulloch *et al.,* 1998). In atherosclerotic arteries Bacon *et al.,* 1996 reported increased expression of ET-1 without altered expression of ET receptors in ischaemic heart disease.

1.8.1 ET receptor antagonists and clinical trials

Although there is strong evidence that ET-1 expression is increased and likely plays a pivotal role in vascular pathologies, ET receptor antagonists (ERAs) have been disappointing in clinical trials of HF and hypertension (Packer *et al.,* 2005). However, a non-selective ERA bosentan (Tracleer, Actelion Pharmaceuticals) (Rubin *et al.,* 2002), and an ET_A selective antagonist ambrisentan (Letairis, Volibris, GlaxoSmithKline) (Vatter & Seifert, 2006) have been approved for the treatment of pulmonary arterial hypertension (PAH).

There are four structural classes of ERAs. These are peptides, sulphonamides, carboxylic and myceric acids (Palmer, 2009). Sitaxentan (highly ET_A selective) and bosentan (non-selective) both belong to a sulphonamide group of ERAs and sitaxentan due to hepatotoxicity was withdrawn from the market (Galiè *et al.,* 2011) after receiving regulatory approval for PAH in Europe in 2007.

In human clinical trials of hypertension and HF, ERAs had little or no benefit. Instead they were associated with adverse effects including fluid retention (Weber *et al.,* 2009; Battistini *et al.,* 2006; Mann *et al.,* 2010) and liver toxicity (Galiè *et al.,* 2011). Fluid retention was indicated by weight gain, reduction in haemoglobin and increased incidence of oedema, which occurred in spite of diuretic use. Hypotension, renal dysfunction and reduction in arterial oxygen saturation were other important side effects observed in acute HF (Coletta *et al.,* 2002).

Table 1.4 summarises clinical trials of ERAs in patients with HF. In the REACH-1 trial, long-term effects of bosentan were investigated in patients with chronic HF for improvement in clinical symptoms. Patients treated with a higher dose of bosentan had dose-dependent worsening of chronic HF and renal insufficiency (Packer *et al.,* 2005) (Table 1.4, a). Short term administration of bosentan (1 g, twice daily) to 36 patients with symptomatic HF over 2 weeks improved systemic and pulmonary haemodynamic (decreased mean arterial pressure and vascular resistance, increased cardiac output but heart rate was unchanged) (Sütsch *et al.,* 1998). After bosentan treatment, plasma levels of ET-1 were increased while baseline levels of other hormones (norepinephrine, plasma renin activity, and Ang II) were unchanged. Increase in plasma ET-1 levels was a consequence of blocking clearance of ET-1 via ET_B receptors (Kelland *et al.,* 2010). This effect of bosentan was a common feature of dual $ET_{A/B}$ antagonism and it was

observed in other studies including in patients with PAH (Hiramoto *et al.,* 2009). Moreover, ET_B gene mutations were also associated with an increase in ET-1 concentration (Gariepy *et al.,* 2000). A lower dose of bosentan evaluated in ENABLE-1 and -2 trials (Table 1.4, b), and darusentan investigated in HEAT and EARTH trials (Table 1.4, c and d) were all associated with side effects. Darusentan (50, 100 and 300 mg/day) (DORADO-AC trial) administered over 14 weeks in patients (n = 734) with resistant hypertension, with existing co-morbidities [type-2 DM and chronic kidney disease (CKD)] produced greater decreases in SBP and DBP but the treatment was unable to achieve the target BP goal (change from baseline to week 14) (Weber *et al.,* 2009; Bakris *et al.,* 2010).

ET antagonists have also been evaluated in cancer. Zibotentan, an ET_A selective antagonist (10 and 15 mg/day) was used in 312 patients with metastatic castration-resistant prostate cancer over ~4 months. Time to progression (165 progression events) was evaluated as the primary end-point. There was an improvement in overall survival time. However, the primary outcome was unchanged and peripheral oedema (placebo *vs.* zibotentan; 11% *vs.* 45%), dyspnoea, and cardiac failure were reported as adverse effects (James *et al.,* 2010).

A possible limitation of these trials could be evaluation criteria of treatment outcomes/primary end-points. As such, achieving a target BP may be difficult due to compensatory mechanisms. A more reliable measurement criterion is required to investigate the effects of these treatments, as well as monitoring adverse effects. Moreover, whether ERAs add further benefit to those already achieved with commonly used ACE inhibitors or whether beneficial effects can be sustained, have not been evaluated fully due to incomplete investigations. In general, clinical investigations suggested that selective ET_A receptor antagonists in which beneficial effects of ET_B can be preserved, may be superior to non-selective $ET_{A/B}$ antagonists.

Table 1.4: ***Failed clinical trials of ERAs investigating clinical outcomes in patients with heart failure.*** *Modified from Kohan et al., 2012.*

Study & Disease	ERA & Dose	Receptor	Number of patients	Duration	Primary end-point	Observations
(a) REACH-1 Chronic HF	Bosentan 500 mg b.i.d	$ET_{A/B}$	369	~6 m	Change in clinical symptoms (NYHA class or worsening of HF)	- No clinical benefit with bosentan - Higher risk of worsening in the placebo group - Increase in hepatotoxicity and decrease in haemoglobin with bosentan
(b) ENABLE 1 & 2 Chronic HF	Bosentan 125 mg b.d	$ET_{A/B}$	1611	18 m	Death and chronic HF hospitalisation	- Fluid retention. Weight gain (approx. 0.6 kg) and reduction in haemoglobin - Increase in liver enzymes
(c) HEAT Chronic HF	Darusentan 10, 25, 50, 100, or 300 mg/day	ET_A	157	3 w	Change in cardiac index and wedge pressure at the end of treatment	- More adverse events (including death and worsening of HF) at higher doses without further improvements on haemodynamics in comparison to lower doses.
(d) EARTH Chronic HF	Darusentan 10, 25, 50, 100, or 300 mg/day	ET_A	642	24 w	Change in LV end-systolic volume at 24 w from baseline	- Cardiac remodelling, clinical symptoms or outcomes were not improved - Worsened HF in 11% and death of 5% of patients
(e) RITZ-1 Acute HF	Tezosentan 24 – 72 h, 50 mg/h (*i.v.*)	$ET_{A/B}$	669	~1 m	Symptoms of dyspnoea, death or worsening HF	- No improvement of symptoms of dyspnoea - Worsening of HF

Table 1.4 cont:

Study & Disease	ERA & Dose	Receptor	Number of patients	Duration	Primary end-point	Observations
[f] RITZ-2 Severe chronic HF	Tezosentan 24 h, 50 – 100 mg/h (*i.v.*)	$ET_{A/B}$	285	~1 m	Haemodynamics	- Improved dyspnoea score at 24 h - Fewer worsening HF events with 50 mg dose but clinical outcomes unchanged - Adverse hypotensive events - Renal function
[g] VERITAS-1 & -2 Acute HF	Tezosentan 5 mg/h for 30 m, then 1 mg/h for 24 – 72 h)	$ET_{A/B}$	1760	1 m	Change in dyspnea over the first 24 h of treatment death or worsening of HF at 7 days	- Improved haemodynamics without a change in mortality
[h] ASCEND Type-2 DM	Avosentan 25 or 50 mg	ET_A	1329	~4 m	Serum creatinine, ESRD, or death	- Fluid retention and plasma volume expansion. Increased risk of developing HF and worsening renal function - Reduced BP and mirco-albuminuria
[i] LV systolic dysfunction	Enrasentan 60 – 90 mg/day	$ET_{A/B}$	72	6 m	Change in left ventricular end diastolic volume index	- Adverse ventricular remodelling despite an increase in the resting cardiac index

Abbreviations: *[a] Packer et al., 2005; [b] Coletta et al., 2002; [c] Lüscher et al.,2002; [d]Anand et al., 2004; [e]Coletta & Cleland, 2001; [f]Louis et al., 2001; [g] Teerlink et al., 2005; [h] Mann et al., 2010; [i] Prasad et al., 2006,* ***m*** *= months,* ***w*** *= weeks,* ***ERA*** *= endothelin receptor antagonist,* ***NYHA*** *= New York Heart Association,* ***b.d/b.i.d*** *= twice daily, i.v.= intra-venous,* ***SDP*** *= systolic blood pressure,* ***DBP*** *= diastolic blood pressure,* ***ESRD*** *= End-stage renal disease,* ***DM*** *= Diabetes mellitus.*

Despite the fact that ET receptor antagonists have been mainly disappointing in human clinical trials of HF, upregulation of ET-1 in the renal system is also evident (Benigni *et al.*, 1991; Orisio *et al.*, 1993; Sørensen *et al.*, 1994), as demonstrated with increasing ET-1 levels and reductions in urinary Na^+ excretion. Generally, cortical vasoconstrictor actions of ET-1 are mediated by the ET_A, while medullary vasodilatation is mediated by the ET_B receptors (Rubinstein *et al.*, 1995). Hence, selective ET_A antagonism was suggested to be superior to ET_B and $ET_{A/B}$ (Neuhofer & Pittrow, 2009). Indeed, CD was also shown to be of major importance for regulation of BP (Ge *et al.*, 2006). ET_A blockade using sitaxentan improved cardiovascular risk factors (e.g. proteinuria, BP, and arterial stiffness) in patients with CKD (Dhaun *et al.*, 2011, 2013). Therefore, CKD was proposed to be a promising target for ERAs (Dhaun *et al.*, 2006). A summary of pre-clinical and clinical studies showing reductions in proteinuria is provided by Barton, 2008.

1.9 Evolutionary perspective of ET-1 and ET receptors

Sequence conservation of human ET family genes is restricted to the ET-1 sequence (80% homology) and the endothelin-like domain (Arinami *et al.*, 1991). Interestingly, the positions of four cysteine residues are completely conserved in the endothelin-like domain. The homology between human ET-1 and endothelin-like domain is ~38%. Endothelin-like domain is likely to result from exon duplication in an ancestral ET gene (Bloch *et al.*, 1989). The sequence of each peptide is highly conserved throughout evolution (Table 1.5 and 1.6). Endothelin-like domain therefore, might have an important physiological function. However, previous attempts failed to show biological activity for $ppET\text{-}1_{[110-130]}$ when tested at concentrations of 10^{-10} – 10^{-5} M (Cade *et al.*, 1990).

ET peptides also share a striking sequence homology with sarafotoxins (S6a, S6b, S6c, and S6d) (Table 1.5), a snake venom toxin from *Atractaspis engaddensis* (Kloog *et al.*, 1988; Landan *et al.*, 1991; Takasaki *et al.*, 1992). Sarafotoxins, like ET peptides, are 21 amino acids long, contain two disulphide bridges and have a hydrophobic C-terminal sequence. In sarafotoxins, the disulphide bridges are essential for binding to ET receptors (Rubanyi & Polokoff, 1994), where they mediate vasoconstrictor activities. S6b has similar potency for both ET receptors while S6c is a highly selective ET_B agonist

(Sokolovsky, 1994). Different amino acid residues are substituted with closely related residues with the exception of Lys (K) at position 4 and Glu (E) at position 9. S6c differs from S6a and S6b as it is the least toxic and has the lowest vasoconstrictor activity. At the end of its C-terminal, S6c lacks the characteristic cleavage site of ECE. Furthermore, the characteristic dibasic amino acid pair upstream of the first residue in all ET peptides was not conserved in the sarafotoxins (Rubanyi & Polokoff, 1994). Therefore, although the presence of high sequence homology (60%) led to suggestions of a common evolutionary origin (Kloog *et al.,* 1988), sarafotoxins are more likely the result of convergent evolution.

Two ET receptors, ET_A and ET_B, are found only in vertebrates (Hyndman & Evans, 2007) and are distantly related to G-protein coupled receptor 37 (Hyndman *et al.*, 2009). The cDNA sequences show considerable homology (>90%) between human, bovine and rat ET_A receptor whereas ET_B receptors share ~88% homology between human and rat (Arai *et al.*, 1993). Despite the high homology in species, they have differences in their ligand binding characteristics. As such, S6c, which is more selective for ET_B than it is for ET_A, showed differences in its affinity in human and rat left ventricle (Russell & Davenport, 1996). ET_A and ET_B receptors share ~55% homology in human and other species. In human, amino acid sequences of ET_A and ET_B display only 59% similarity (Davenport, 2002). A third ET receptor gene encodes an amphibian-specific receptor ET_C, expressed in *Xenopus* (Karne *et al.*, 1990). Evolution of vertebrate ET genes and their receptors is illustrated in detail in Braasch *et al.*, 2009.

Table 1.5: ***Comparison of the amino acid sequences of human ET-1 and the sarafotoxins.*** *Homologous residues to human ET-1 are represented as hyphens (-). Cysteine residues at positions 1 – 15 and 3 – 11 form disulphide bridges and are completely conserved in evolution. The C-terminal hydrophobic region is also highly conserved across species. Data from Ensemble (http://www.ensembl.org/index.html).*

ET-1 peptide	**1**	**2**	**3**	**4**	**5**	**6**	**7**	**8**	**9**	**10**	**11**	**12**	**13**	**14**	**15**	**16**	**17**	**18**	**19**	**20**	**21**
Human	**C**	**S**	**C**	**S**	**S**	**L**	**M**	**D**	**K**	**E**	**C**	**V**	**Y**	**F**	**C**	**H**	**L**	**D**	**I**	**I**	**W**
Mouse	-	-	-	-	-	-	-	-	-	-	-	-	-	-	-	-	-	-	-	-	-
Opossum	-	-	-	-	-	-	L	-	-	-	-	-	-	-	-	-	-	-	-	-	-
Platypus	-	-	-	-	-	-	L	-	-	-	-	-	-	-	-	-	-	-	-	-	-
Chicken	-	-	-	-	-	-	L	-	E	-	-	-	-	-	-	-	-	-	-	-	-
Lizard	-	-	-	-	-	-	-	-	-	-	-	-	-	-	-	-	-	-	-	-	-
Frog	-	-	-	-	-	-	-	-	-	-	-	-	-	-	-	-	-	-	-	-	-
Zebrafish	-	-	-	-	-	-	-	-	-	-	-	-	-	-	-	-	-	-	-	-	-

S6A	-	-	-	K	D	M	T	-	-	-	-	L	N	-	-	-	Q	-	V	-	-
S6B	-	-	-	K	D	M	T	-	-	-	-	L	-	-	-	-	Q	-	V	-	-
S6C	-	T	-	N	D	M	T	-	E	-	-	L	N	-	-	-	Q	-	V	-	-
S6D	-	T	-	K	D	M	T	-	-	-	-	L	-	-	-	-	Q	-	-	-	-

Table 1.6: ***Comparison of the EDN1 gene derived endothelin-like domain during evolution.*** *Homologous residues to human endothelin-like domain are represented as hyphens (-). Similar to ET-1, cysteine residues at positions 1, 3 and11, 15 are completely conserved in evolution.*

Endothelin-like domain	**1**	**2**	**3**	**4**	**5**	**6**	**7**	**8**	**9**	**10**	**11**	**12**	**13**	**14**	**15**	**16**	**17**	**18**	**19**	**20**	**21**	**22**
Human	**C**	Q	**C**	A	S	Q	K	D	K	K	**C**	W	N	F	**C**	Q	A	G	K	E	L	R
Mouse	-	-	-	-	H	-	-	-	-	-	-	-	-	-	-	-	-	-	-	-	-	-
Opossum	-	-	-	-	-	R	-	-	-	-	-	-	V	-	-	-	-	-	-	-	-	-
Platypus	-	-	-	-	N	-	-	-	-	-	-	-	D	-	-	-	-	-	-	-	-	-
Chicken	-	-	-	-	-	-	R	-	-	-	-	L	-	-	-	-	-	-	-	-	-	-
Lizard	-	-	-	T	N	L	-	-	-	-	-	A	-	-	-	K	-	E	-	-	I	W
Frog	-	-	-	-	-	-	-	-	-	-	-	-	-	-	-	-	-	-	-	-	-	-
Zebrafish	-	K	-	-	D	S	Q	-	-	T	-	S	S	-	-	Q	D	S	A	-	-	Q

1.10 Vascular actions of ET-1

1.10.1 Signal transduction and downstream effectors

ET-1 binding to ET_A and ET_B receptors stimulates a calcium influx through activation of phospholipase C (PLC)-mediated membrane-bound diacylglycerol (DAG) and cytosolic inositol triphosphate (IP_3) production (Figure 1.2). IP_3 initiates the release of Ca^{2+} from intracellular stores (iCa^{2+}) of sarcoplasmic reticulum (SR) and membrane Ca^{2+} channels [$_L$-type voltage dependent Ca^{2+} (VOC)] to stimulate Ca^{2+} flux from extracellular space (Hirata *et al.,* 1988). DAG activates PKC, which along with increased iCa^{2+} phosphorylates and activates calmodulin-dependent myosin light chain (MLC) and mediates ET-1 induced vasoconstriction (Figure 1.2, a).

Vasodilatation mediated by activation of ET_B receptors on ECs involve eNOS-derived NO release. Activation of eNOS is Ca^{2+}-calmodulin-dependent. Once produced, NO diffuses to the underlying SMC, it activates cytosolic soluble guanylate cylase (sGC), which leads to the formation of cyclic guanosine monophosphate (cGMP) (Figure 1.2, b). This in turn inhibits the contractile process (Vanhoutte, 2004).

Increases in iCa^{2+} activate phospholipase-A_2 (PLA_2) to produce arachidonic acid (AA), which activates the main cyclooxygenase (COX) product PGI_2 in ECs (Moncada & Vane, 1979). Diffusion of PGI_2 to SMC activates adenylate cyclase (AC), which produces cAMP and activation of voltage-dependent potassium (K^+) channels (Tirapelli *et al.,* 2005) result in vasodilatation (Figure 1.2, c). ET_A receptors can lead to activation of phospholipase D (PLD), facilitating PKC activation and cellular contraction (Goto *et al.,* 1996) and PLA_2 releasing AA and prostaglandins such as prostaglandin E2 (PGE_2), which can contribute to vasoconstrictor responses.

ET-1 mediated activation of signalling cascades involving MAPK and PI3K activate transcriptional factors that are involved in regulation of growth/proliferation and hypertrophy.

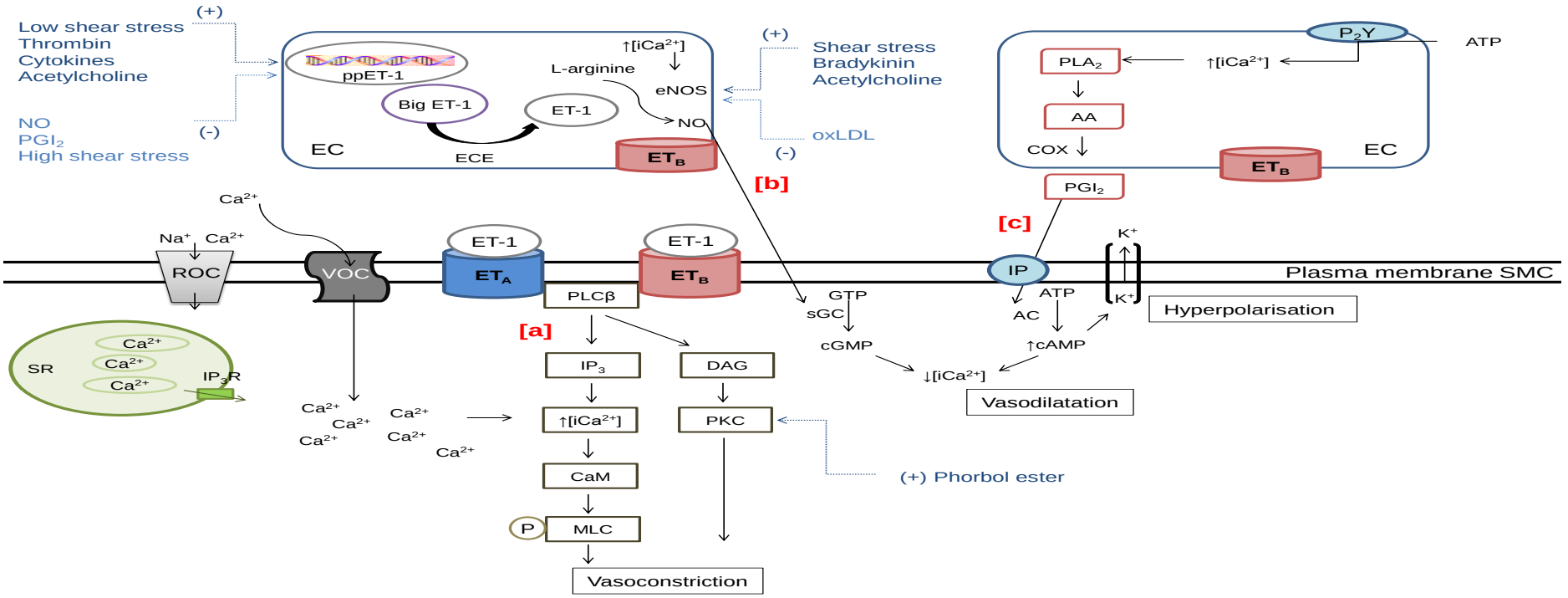

Figure 1.2: ***ET-1 mediated signal transduction pathways. cGMP*** *= cyclic guanosine monophosphate,* ***cAMP =*** *cyclic adenosine monophosphate,* ***CaM =*** *calmodulin,* ***GTP =*** *guanosine triphosphate,* ***ATP =*** *adenosine triphosphate,* ***sGC*** *= soluble guanylyl cyclase,* ***AC =*** *adenyl cyslase,* ***PLC*** *= phospholipase C,* ***DAG*** *= diacylglycerol,* ***IP_3*** *= inositol triphosphate,* ***ROC =*** *receptor operated Ca^{2+} channel,* ***VOC =*** *L-type-voltage operated Ca^{2+} channel,* ***Ca^{2+}*** *= calcium,* ***iCa^{2+} =*** *intracellular calcium,* ***eNOS*** *= endothelial nitric oxide synthase,* ***NO·*** *= nitric oxide,* ***AA =*** *arachidonic acid,* ***COX*** *= cyclooxygenase 1 and 2,* ***PGI_2*** *= prostacyclin,* ***PKC =*** *protein kinase C,* ***SR =*** *sarcoplasmic reticulum,* ***MAPK =*** *mitogen activated protein kinases.* ***MLC =*** *myosin light chain,* ***IP****= prostacyclin receptor, and* ***IP_3R =*** *inositol trisphosphate receptors.*

1.10.2 Mitogenic actions

On VSMC, ET-1 stimulates c-fos and c-myc expression and has proliferating effects in response to stimuli such as Ang II, TGF-β, and PDGF (Komuro *et al.*, 1988). It can also act as a mitogen for VSMC by potentiating the actions of other mitogens including EGF (Battistini *et al.*, 1993). Moreover, low concentrations of ET-1 (10^{-9} M), potentiated the effects of other vasoconstrictor such as serotonin and norepinephrine, in mammary and in coronary arteries (Yang *et al.*, 1990). In general, the mitogenic action of ET-1 is mediated by the ET_A receptors (Eguchi *et al.*, 1992; Yang *et al.*, 1999).

Infusion of Ang II (200 ng/kg/min) stimulated both vascular and renal ET-1 expression, and increased ECE activity *in vivo*. Haemodynamic and proliferative effects were completely blocked by ET_A receptor antagonism (LU135252, 50 mg/kg/day) (Barton *et al.*, 1997b). Thus, ET-1 acting mainly by the ET_A receptors mediates vascular remodelling. All these studies supported the notion that ET-1 could have a significant role in the initiation and development of atherosclerosis.

1.10.3 Inflammatory effects

Increases in ET-1 levels are associated with elevations in plasma concentrations of pro-inflammatory cytokines (TNF-α, IFN-γ, IL-1β) (Warner & Klemm, 1996). In turn, inflammatory and pro-thrombotic mechanisms stimulate ET-1 synthesis (Corder *et al.*, 1995a; Corder, 2001). In cultured macrophages ET-1 stimulated the synthesis of TNF-α and this was blocked by ET_A receptor antagonists BQ-123 or BQ-485. Thus indicating an ET_A mediated mechanism of action (Ruetten & Thiemermann, 1997).

Intravenous (*i.v.*) administration of TNF-α (4 μg/kg) to anesthetised rats resulted in a rapid increase in arterial ET-1 levels, reaching maximum levels within 15 min (Klemm *et al.*, 1995). Hearts were isolated after treatment with TNF-α (4 μg/kg) and perfused *in vitro* by the Langendorff technique. This was associated with a remarkable coronary vasoconstriction (Klemm *et al.*, 1995). Similarly, infusion of TNF-α to healthy volunteers increased plasma levels of ET-1 (Patel *et al.*, 2002). These have strongly suggested that activation of vascular ET-1 is associated with growth and pro-inflammatory effects and therefore contribute to the progression of vascular pathologies.

1.10.4 Endothelial function

Transgenic (TG) mice overexpressing human ppET-1 specifically in the endothelium (generated using promoter/enhancer regions of the endothelium-specific tyrosine kinase receptor Tie-2) showed hypertrophic remodelling, endothelial dysfunction, increased vascular NADPH oxidase activity (measured as p67phox and gp91phoxexpression) and inflammation in mesenteric small arteries in comparison to non-TG wild-type littermates (Amiri *et al.*, 2004). TG mice also had a 3-fold increase in aortic ppET-1 mRNA and a 7-fold increase in plasma ET-1 levels. This study demonstrated the first *in vivo* evidence for overexpression of endothelial-specific ET-1 with altered vascular structure (increased media thickness of mesenteric resistance arteries in TG mice) and function (impaired vasoconstrictor responses to ET-1 and impaired vasodilatation of resistance arteries in TG mice) without any significant changes in BP. This model had increased ET_B mRNA and protein levels in TG mice while ET_A mRNA and protein levels were unaltered.

Endothelium-dependent vasodilatation in human internal mammary arteries was improved following acute ET receptor antagonism. As such, a mixed antagonist bosentan (3 μM for 20 min) showed the greatest beneficial effect on endothelial function [assessed using Acetylcholine (ACh)-induced vasodilatation] while both ET_A [BQ-123 (1 μM for 20 min)] and ET_B [BQ-788 (1 μM for 20 min)] receptor antagonists had similar, but slightly reduced, effects on maximum relaxation (Verma *et al.*, 2001).

Acute ET_A blockade with BQ-123 produced a modest vasodilatation of the coronary microcirculation and improved endothelial dysfunction in coronary artery disease (CAD) (Halcox *et al.*, 2001). This study measured epicardial diameter and Doppler flow velocity (measured coronary blood flow) and calculated coronary vascular resistance (CVR) (arterial pressure ÷ coronary blood flow) as parameters to assess endothelial dysfunction. In patients with early atherosclerosis, long-term administration (6 months) of ET_A antagonist atrasentan (10 mg) improved endothelial function (Reriani *et al.*, 2010a). Furthermore, non-selective blockade of ET receptors in patients with essential hypertension increased forearm blood flow (FBF), which was unaffected in controls (Cardillo *et al.*, 2002). All studies supported the role of ET-1 in the regulation of endothelial function both in early coronary atherosclerosis and in essential hypertension.

1.11 The role of ET-1 in the pathophysiology of cardiovascular disease

ET-1 is highly implicated in various cardiovascular pathologies including atherosclerosis, hypertension, PAH, chronic HF as well as CKD. Endogenous ET-1 production contributes to the maintenance of basal vascular tone and BP (Haynes & Webb, 1994; Haynes, 1995). The precise role of ET-1 in the pathogenesis of cardiovascular disease was evaluated following treatments with ERAs. The effects of ET-1 have been discussed in previous sections but here, existing evidence for the upregulation of ET system and the role of ET-1 in the pathogenesis of atherosclerosis, hypertension, and chronic HF is briefly highlighted.

1.11.1 Atherosclerosis

The role of ET-1 in the pathogenesis of atherosclerosis became evident after detection of ir-ET-1 (using immunohistochemistry) in VSMC as well as in ECs (Lerman *et al.,* 1991). Jones *et al.,* 1996 have shown localisation specifically to ECs overlying atherosclerotic plaques and fatty streaks without detectable ET-1 in VSMC. A number of observations further supported the role of ET-1 in atherosclerosis. These include the findings of increased expression of ET-1, big ET-1 and ECE-1 in atherosclerotic arteries (Lerman *et al.,* 1991; Zeiher *et al.,* 1995; Bacon *et al.,* 1996; Maguire & Davenport, 1998); and detection of ET receptors in vasa vasorum of normal blood vessels and at regions of neovascularisation of atheromatous vessels (Dashwood *et al.,* 1993). Inflammatory and prothrombotic mechanisms elevate ET-1 synthesis (Corder, 2001) and consistent with mitogenic actions, these further contribute to ET-1 mediated atheroma formation. Such evidence for remodelling after angioplasty was shown by Haynes & Webb, 1998. Mechanical pressure and stretch increased ET-1 levels in atherosclerotic coronary arteries with the levels correlating with the extent of mechanical stress (Hasdai *et al.,* 1997). Macrophages and fibroblasts (Martin-Nizard *et al.,* 1991; Ihling *et al.,* 1996; Zeballos *et al.,* 1991), which are abundant in atheromatous plaques, also secrete ET-1. In addition to increased ET-1 synthesis, ET receptor density is also increased in SMC during remodelling (Dashwood *et al.,* 1998).

1.11.2 Hypertension

In experimental models of hypertension [deoxycorticosterone acetate (DOCA) and Dahl salt-sensitive rats], ET-1 induced vascular hypertrophy and increased BP (Larivière *et al.*, 1993; Deng *et al.*, 1996), which were reversed by $ET_{A/B}$ antagonist bosentan (Li *et al.*, 1994). However, the role of ET-1 in spontaneously hypertensive rats (SHR) has been controversial. Interestingly, hypertensive patients have either normal (Davenport *et al.*, 1995) or low ET-1 levels with the exception of black Africans (Ergul *et al.*, 1996). In contrast, patients with pulmonary hypertension had increased ET-1 gene expression with an inverse relation with eNOS and the degree of ir-ET-1 in the lungs (Giaid & Saleh, 1995).

Mice with CD-specific KO of the ET-1 gene (CD ET-1 KO) are hypertensive on a normal-Na^+ diet and this is exacerbated by high Na^+ intake (Ahn *et al.*, 2004). Further gene targeting studies that investigated the physiological role of ET-1 and ET receptors are described in more detail in Chapter 6, section 6.1.2.

1.11.3 Chronic heart failure

Plasma levels of ET-1 are elevated in HF (Stewart *et al.*, 1992). Chronic treatment with an ET_A antagonist BQ-123 (Sakai *et al.*, 1996) or $ET_{A/B}$ antagonist bosentan (Muller *et al.*, 1997) improved the survival and haemodynamic parameters in rats with chronic HF. However, the beneficial effects were not extrapolated to patients (see Table 1.4, page 29).

Cardiomyocyte-specific *EDN1* overexpressing mice [generated as α-myosin heavy chain promoter-dependent cardiac-specific tetracycline-regulated gene expression system (Tet-OFF)] featured activated inflammatory pathway (e.g. NFκB activation and IL-6 expression) that was associated with cardiac hypertrophy and premature death (Yang *et al.*, 2004). However, combination of ET_A and $ET_{A/B}$ receptor antagonists were unable to prevent the lethal HF caused in this model (Yang *et al.*, 2004). As a result, the role of ET-1 in HF has been controversial.

1.12 The area of unmet clinical need and requirement of biomarkers

1.12.1 Endothelial dysfunction

Endothelial dysfunction is a general term referring to the disruption of normal function of the vascular endothelium by impaired production of endothelium-derived relaxing factors (EDRF) (NO and PGI_2) and increased synthesis of endothelium-dependent contracting factors (EDCF) (ET-1) (Vanhouette *et al.,* 2009).

Dyslipidaemia/hypercholesterolemia, diabetes, hypertension and smoking are cardiovascular risk factors that contribute to endothelial dysfunction. It is also closely linked to vascular aging with a loss of endothelium-dependent vasodilatation (EDD) from middle age to the elderly. Endothelial dysfunction is a key mediator and implicated in early stages of progression to atherosclerosis. It is independently associated with increased cardiovascular risk (Suwaidi *et al.,* 2000; Endemann & Schiffrin, 2004).

The mechanism of endothelial dysfunction is characterised by reduced NO bioavailability, which could be resulting from either reduced production of NO by eNOS or increased breakdown by ROS (Versari *et al.,* 2009). NO is the best described vasodilator, which increases its protective role also by inhibiting platelet aggregation, adhesion and penetration of macrophages, SMC migration and proliferation, and suppression ofET-1 synthesis. Impaired NO production and elevated ET-1 are early features of endothelial dysfunction. Greater dysfunction leads to activation of pro-coagulant and pro-inflammatory mechanisms that initiate a sequence of reactions that predispose to atherosclerosis and CAD (Vanhoutte *et al.,* 2009).

Under physiological conditions, NO is produced by the enzymatic conversion of eNOS in presence of substrate L-arginine and the co-factor, tetrahydrobiopterin (BH_4) (Ghafourifar *et al.,* 2005). Under pathological conditions, reduced bioavailability of BH_4 and a deficiency in L-arginine result in uncoupling of eNOS (Touyz & Schiffrin, 2004), and this contributes to the generation of ROS [e.g. superoxide anion ($O_2^{\cdot -}$) and hydrogen peroxide (H_2O_2)] (Vásquez-Vivar *et al.,* 2003). Elevated $O_2^{\cdot -}$ can reduce NO bioavailability by reacting with NO to form peroxynitrite ($ONOO^-$), a strong oxidant which can damage cell membranes. $ONOO^-$ oxidises the essential co-factor of eNOS, BH_4 to its inactive form (Vásquez-Vivar *et al.,* 2001), which together result in a further decline in NO production and increased $O_2^{\cdot -}$ formation by eNOS. In addition, increases

in endogenous competitive inhibitor of eNOS, N^G N^G-dimethyl-L-arginine (ADMA) (Vallance *et al.*, 1992) and arginase activity (which converts L-arginine to urea and ornithine) also cause eNOS uncoupling.

There are other factors that modulate NO release by the endothelium. Shear stress activates Ca^{2+}-dependent eNOS via increased iCa^{2+} and activated protein kinases (PKs) (Vanhoutte *et al.*, 2009). Also in ECs, elevated iCa^{2+} and PKs activate PLA_2, which releases AA from membrane-bound phospholipids and then becomes available for metabolism by COX. Peroxidase activity on COX transforms AA into endoperoxides, which are converted into PGI_2, thromboxane A_2, prostaglandin D_2, prostaglandin E_2 and/or prostaglandin F_2a by their selective synthases (Vanhoutte *et al.*, 2009).

The release of NO can be increased by oestrogen, vasopressin, substance P, bradykinin, histamine, thrombin and products formed during platelet aggregation [serotonin, adenosine diphosphate (ADP)] (Vanhoutte, 2004). Hypercholesterolemia is a major risk factor for human atherosclerosis and increased LDL, especially oxidised-LDL (ox-LDL), reduces the production of NO, by decreasing the gene expression of eNOS and may enhance ET-1 secretion (Ridker *et al.*, 2004).

1.12.2 Changes in vascular function with age, predictive of cardiovascular disease risk

Aging is associated with increased vascular stiffness (increased elastase and collagen production by VSMC), vascular wall intimal thickness (Virmani *et al.,* 1991) and impaired endothelial function (Celermajer *et al.,* 1994). These factors may be the result of **(1)** increased formation of ROS ($O_2^{\cdot -}$), **(2)** alteration in the expression and/or activity of eNOS, **(3)** decrease in L-arginine/NO bioavailability (Boulanger & Lüscher, 1990), due to increased production of $O_2^{\cdot -}$ and **(4)** impaired EDD due to reduced endothelium-mediated relaxation and increased production of vasoconstrictors such as ET-1 (Goettsch *et al.,* 2001) and COX-2 derived prostanoids (Vessières *et al.,* 2013). These have all been suggested as potential mechanisms underlying the impaired endothelium-dependent vasodilator responses that occur with aging (Küng & Lüscher, 1995; Barton *et al.,* 1997a), but the precise triggers have yet to be defined. Other vasoactive factors that are affected during ageing also regulate *EDN1* gene expression and together could contribute to age-dependent changes in vascular function. These include Ang II (Imai *et al.,* 1992), TGF-β1 (Hahn *et al.,* 1990) and oestrogen (Morey *et al.,* 1998).

In response to ACh and Ca^{2+} ionophore A23187, endothelium-dependent relaxations were reduced in the aorta of old rats, with reduced basal release of NO and lower expression of eNOS mRNA (Barton *et al.,* 1997a). In the aortas of old rats, contractions to norepinephrine were increased while ET-1-mediated contractions were reduced (Barton *et al.,* 1997a). Neither endothelium-dependent relaxations nor contractions were affected by aging in the femoral artery (Barton *et al.,* 1997a). Age-related impairment in ACh-mediated EDD (analysed by FBF) was also reported in man by Westby *et al.,* 2011. Co-infusion of ACh with an ET_A selective antagonist, BQ-123, improved ACh-mediated EDD in older men and this suggested that impairment in age-related vasodilatation is partly due to increased vasoconstrictor tone, which is mediated by increased ET-1 levels with age.

1.12.3 Current methodologies measuring endothelial function

Endothelial dysfunction affects resistance and conduit vessels in the forearm and in the coronary circulation. The forearm vascular bed is commonly accepted as a surrogate for assessing endothelial function in the coronary arteries (Wilkinson & Webb, 2001). Endothelium-dependent vasodilatation is evaluated with use of pharmacological stimuli (including ACh, bradykinin, substance P, and 5-hydroxytryptamine) or mechanical stimuli by inducing a shear stress response. Flow-mediated dilatation (FMD) uses increased shear stress to stimulate the release of NO and induce EDD of the brachial artery (Behrendt & Ganz, 2002).

Alternatively, the functional integrity of the vascular endothelium can be assessed with FBF responses to intra-arterial agonists such as ACh (Heitzer *et al.*, 2001). ACh stimulates a receptor-mediated increase in NO synthesis and release from the vascular endothelium and as a result, can be used to monitor EDD responses (Versari *et al.*, 2009). Both FMD and FBF responses to ACh are assessed using a strain-gauge plethysmography (mainly mercury-in-rubber, but alternatively indium-gallium gauges can also be used).

Endothelial dysfunction in the microcirculation can be evaluated by the assessment of the change in epicardial coronary artery diameter in response to ACh concentrations using quantitative coronary angiography and in the microcirculation intravascular ultrasound is used to monitor changes in flow (Versari *et al.*, 2009). Additionally, Doppler flow velocity measurements in response to ACh can be used to evaluate endothelial function. Non-invasive techniques include positron emission tomography (PET), which can be used to assess myocardial blood flow in response to vasodilator agents such as adenosine, and adenosine triphosphate (Reriani *et al.*, 2010b).

The advantages and disadvantages of some techniques used for the assessment of endothelial function are summarised in Table 1.7. A methodology of an ideal test should be non-invasive, reproducible, repeatable, and cheap and it should be specific, provide prognosis of subclinical disease processes and risk stratification.

Table 1.7: ***Methods used in the assessment of vascular endothelial function.*** *Data from Coretti et al., 2002, Deanfield et al., 2007 and Reriani et al., 2010b.*

Test	Vascular bed	Outcome measured (e.g. change in diameter or blood flow)	Equipment	Advantages	Disadvantages
Coronary endothelial function testing	Coronary arteries.	Diameter and BF in response to ACh.	Quantitative coronary angiography and coronary Doppler flow.	"Gold standard" Reproducible.	Invasive Expensive Procedural risks.
Venous occlusion plethysmography	Forearm resistance vessels.	Forearm circumference indicative of forearm BF Can be coupled with brachial artery administration of vasoactive peptides and drugs (e.g. ET-1).	Strain-gauge plethysmography.	Accurate. Reproducible.	Invasive (requires arterial cannulation). Unrepeatable. Difficult to standardise results. Procedural risks.
FMD	Mainly brachial, but radial and femoral arteries can also be used.	Diameter of a conduit artery in response to shear stress.	Ultrasound with Doppler and electrocardiogram (ECG) monitor.	Non-invasive.	Require technical expertise. May not be reproducible. Expensive equipment. Limited for risk stratification.

Table 1.7 cont:

Test	Vascular bed	Outcome measured [e.g. change in diameter or blood flow (BF)]	Equipment	Advantages	Disadvantages
Brachial artery reactivity test	Brachial artery.	Diameter of brachial artery in response to shear stress. Measures FMD.	Ultrasound with Doppler and electrocardiogram (ECG) monitor.	Non-invasive. Easy to use.	Operator variability. Difficulty to standardise results.
Peripheral arterial tonometry (PAT)	Peripheral arteries.	Post-occlusion pulse wave amplitude in relation to the baseline.	Tonometer.	Non-invasive. Automated/easy to use, automatic analysis, reliable and reproducible.	Expense of disposable finger probes.
Positron emission tomography (PET)	Coronary microcirculatory vasculature.	Myocardial BF in response to adenosine/dipyridamole.	Tomography.	Non-invasive. High sensitivity.	Limited specificity for endothelial function. Use of isotopes.
Pulse-wave	Radial, brachial, and femoral artery.	Changes in peripheral pressure waveform in response to β-2 receptor agonist (inhaled albuterol/salbutamol).	Tonometry used for measurements and augmentation index (AIx) for quantification.	Non-invasive. Simple and portable instrumentation can be adapted to large studies.	Unpredictable of outcome.

1.13 Proposed Biomarker(s)

1.13.1 ET-1 as a biomarker of cardiovascular disease risk

Plasma levels of ET-1 are elevated in various pathological conditions (McMurray *et al.,* 1992; Pousset *et al.,* 1997; Goddard & Webb, 2000; Selvais *et al.,* 2000) with the levels correlating with disease progression. Despite the strong evidence that shows a role of ET-1 in disease development/progression and all the factors that increase ET-1 synthesis in disease states, plasma concentrations of ET-1 in healthy subjects are low, ranging between <0.3 pg/ml and 3 pg/ml in most studies (Battistini *et al.,* 1993).

ET-1 is unstable, and due to its short half-life in plasma (Gasic *et al.,* 1992; Corder & Vane, 1994) the significance in diagnosis has been controversial. Studies of cultured ECs indicate that ET-1 is mainly released abluminally and mediates its actions as a paracrine/autocrine factor on smooth muscle cells (Wagner *et al.,* 1992). This likely targets ET-1 to ET_A receptors on the underlying VSMC, which further decreases the amount of ET-1 escaping into the circulation. Particularly in the pulmonary vascular bed, ET binding to ET_B receptors results in clearance, which further decreases the circulating levels of ET-1 (Wagner *et al.,* 1992; Dupuis *et al.,* 1996b). Moreover, ET-1 is degraded by endopeptidases such as NEP-24.11, which is highly expressed on venous ECs (Llorens-Cortes *et al.,* 1992; Abassi *et al.,* 1992).

All immunoassays for ET-1 required a solid-phase extraction step prior to immunoassay. This could result in variations of ET-1 measurements due to differences in recovery, type of immunoassay employed and the specificity of the antisera (Davenport & Kuc, 2002). As a result of the above factors ET-1 is a poor biomarker of vascular ET-1 production. The levels are likely to reflect a spillover that has not bound to ET receptors.

1.13.2 Plasma measurements of big ET-1 and C-Terminal fragment

Proteolytic processing of big ET-1 produces ET-1 and CTF of big ET-1 in equimolar amounts. Slower clearance of big ET-1 (Hemsén *et al.*, 1995; Burkhardt *et al.*, 2000) and the inactive CTF were assessed as alternative markers for estimation of ET-1 release. Plasma levels of big ET-1 were strongly correlated with prediction of 1 year mortality in patients with severe HF to a greater degree than ANP (Pacher *et al.*, 1996). The radioimmunoassay (RIA) for CTF of big ET-$1_{[1 - 38]}$ was based on an extraction methodology and had cross-reactivity of around 82% between the CTF and big ET-$1_{[22 - 38]}$ and <1% with ET isopeptides (Pacher *et al.*, 1996).

Cross-reactivity of big ET-1 in RIA often resulted from recognition of the $ET_{[1 - 15]}$ loop region (Corder, 1996). At high concentrations there was less cross-reactivity, which could suggest equilibrium between an unfolded conformation recognised by antibodies specific for ET-1 and a folded conformation where the C-terminal sequence of big ET-1 folds over ET-$1_{[1 - 15]}$ thereby inhibiting antibody detection. CTF could not be measured with sandwich-ELISA due to the presence of only one of the two epitopes necessary to generate a signal (Plumpton *et al.*, 1995).

Changes in plasma big ET-1 levels may not reflect alterations in ET-1 synthesis because big ET-1 is cleaved at the tissue level not only into active ET-1, but also into ET-$1_{[1 - 31]}$ by the action of chymase (Nakano *et al.*, 1997). These factors limit the use of big ET-1 and CTF of big ET-1 as sensitive biomarkers of ET-1 synthesis.

1.13.3 ProET-1 derived peptides as alternative markers of ET-1 synthesis

Sandwich immunoassays were developed covering six positions of the ppET-1 (18 – 53, 32 – 109, 32 – 181, 94 – 148, 136 – 181 and 168 – 212) and only three ir-proET-1 regions (18 – 53, 94 – 148 and 168 – 212) were detected in control subjects and septic patients (Struck *et al.*, 2005). As a result, CT-proET-1 was proposed as an alternative to indirectly assess ET-1 release (Struck *et al.*, 2005; Papassotiriou *et al.*, 2006).

1.13.4 Other biomarkers of vascular function and risk

Clinical parameters of cardiovascular disease risk include Framingham Risk Score (FRS), New York Heart Association (NYHA) and high-sensitivity C-reactive protein (hsCRP). However, classifications are imprecise and limited. In order to contribute to a better classification, a biomarker should exhibit independent prediction of disease risk from conventional parameters and, at the same time, it should provide sensitivity and specificity for the underlying disease.

Two commonly used imaging techniques coronary artery calcium (CAC) score, measured using computed tomography (CT) and carotid intima-medial thickness (cIMT), measured using B-mode ultrasound can discriminate between risk groups and are used as subclinical disease biomarkers for CAD risk stratification. Although CAC is simple, fast, and accurate for identification of CAD stenosis severity, extent, and distribution, it is associated with low but tolerable radiation exposure. Measuring thickening of the intima-media as an early feature of atherosclerosis with cIMT is also non-invasive and simple. Nevertheless, there is a need for reclassification improvement where circulating biomarkers may provide better risk stratification of cardiovascular disease. Biomarkers of vascular disease can be grouped into six main categories as listed in Figure 1.3 (Ridker *et al.,* 2004; Cohn *et al.,* 2004; Iqbal *et al.,* 2012).An overview of these biomarkers in relation to disease and associated methodological issues is provided in a review by Vasan, 2006.

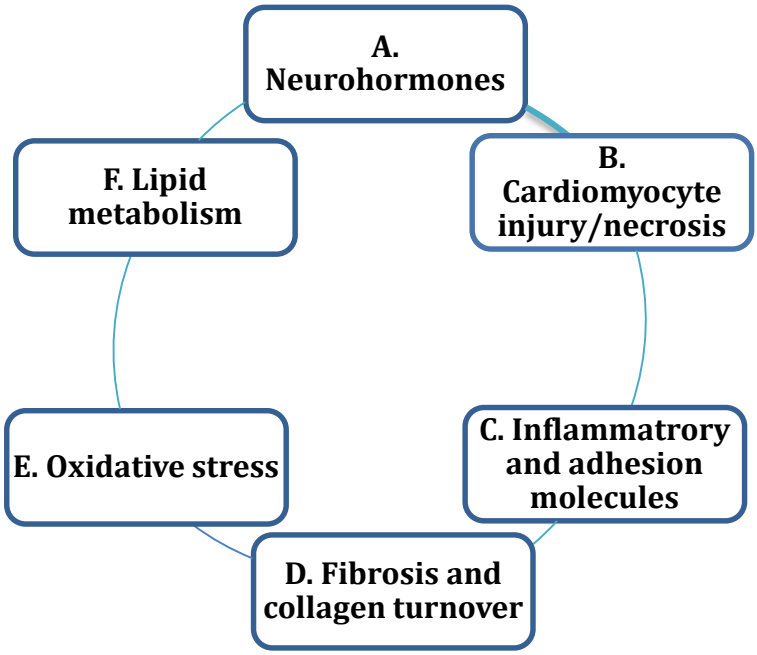

Figure 1.3: ***Main categories of key cardiovascular biomarkers.***

A. **Neurohormones:** N-terminal-pro B-type natriuretic peptide (NT-proBNP) and midregional pro-adrenomedullin (MR-proADM)]; provasopressin or copeptin (CT-proAVP); and midregional pro-atrial natriuretic peptide (MP-proANP). These neurohormones are released in response to strain on cardiomyocytes, haemodynamical stress and to volume expansion, respectively.

B. **Tissue markers of cardiomyocyte injury/necrosis:** Troponins (cTnT and cTnI).

C. **Inflammatrory and adhesion molecules:** hsCRP, IL-6, E-selectin, P-selectin, MCP-1, growth differentiation factor 15 (GDF-15), galectin-3, ICAM-1, and VCAM-1.

D. **Fibrosis and collagen turnover:** CTGF, collagen as an important compartment of myocardial ECM and MMPs (particularly MMP-9), which degrade collagen are markers of fibrosis and collagen turnover. In addition, vWF, tissue plasminogen activator (t-PA), fibrinogen, and D-dimer are possible markers of thrombosis.

E. **Oxidative stress related biomarkers:** oxLDL.

F. **Lipid metabolism:** Apolipoprotein B100 (Apo-B100), Apo-AI.

Although these biomarkers may reflect active disease, they are not sufficiently sensitive or specific to identify cardiovascular disease in asympomatic patients (Ridker *et al.*, 2004; Vasan, 2006). Currently the stable fragment of brain natriuretic peptide (BNP), NT-proBNP is the strongest predictor and it is used for the diagnosis and risk stratification of patients with HF (Maisel *et al.*, 2002; Masson *et al.*, 2006; McMurray *et al.*, 2012). Similarly, in asympomatic patients with HF, high sensitivity cTnT was associatied with cardiovascular mortality risk (deFilippi *et al.*, 2010). However, the prognostic utility of BNP and troponin measurements in the diagnosis of asymptomatic HF patients has yet to be fully evaluated. The ability of NT-proBNP, adhesion and inflammatory markers (CRP, soluble ICAM-1, sVCAM-1 sUL-1Ra, IL-6 and fibrinogen) in predicting cardiovascular events was evaluated previously and as a result, only NT-proBNP provided incremental value for cardiovascular risk prediction over traditional markers such as FRS (Blankenberg *et al.*, 2006). Another study compared the relationship between neurohormonal markers (MR-proADM, MR-proANP, NT-proBNP, CT-proET-1, copeptin, neopterin) and vascular function parameters [FMD and PAT] in 5,000 individuals (Gutenberg Health Study). Baseline vascular function showed strong associations for MR-proANP and baseline pulse amplitude; as well as MR-proANP and NT-proBNP with brachial artery diameter. For hyperaemic response variables, CT-proET-1, MR-proADM, and MR-proANP were related to PAT ratio, which is a representative measure of microvascular circulation (Schmabel *et al.*, 2012). A number of comparative studies investigated the ability of CT-proET-$1_{[168 - 212]}$ and these are summarised in Table 1.8. In general, CT-proET-1 was an independent biomarker, as such in acute myocardial infarction (MI), both NT-proBNP and CT-proET-1 were independent predictors of death and HF (Khan *et al.*, 2007). In diabetic patients, Maier *et al.*, 2009 showed a correlation between endothelial markers MR-proADM, CT-proAVP, CT-proET-1, and MR-proADM and cardiovascular events with MR-proANP being the strongest predictor in this patient group. Boyer *et al.*, 2012 investigated the changes in MR-proADM, MR-proANP and CT-proET-1 during the first 2 – 4, and 12 – 24 h after therapy in 48 patients with acute decompensated heart failure (ADHF). Changes in MR-proANP levels occurred more commonly at 2 – 4 after therapy. Changes in CT-proET-1 showed a relation with ejection fraction, heart rate and BNP. CT-proET-1 over 2 – 4 h after therapy also positively correlated with Na^+ concentration.

Table 1.8: ***The prognostic significance of CT-proET-1 in comparison to other cardiovascular biomarkers.***

Study & Reference	Patients	Biomarkers	Results	Conclusion
Struck *et al.*, 2005	**Sepsis**	Sandwich immunoassays for ppET-1 peptide sequences 18 – 53, 32 – 109, 32 – 181, 94 – 148, 136 – 181 and 168 – 212	Only ppET-1 sequences 18 – 53, 94 – 148 and 168 – 212 showed strongly elevated ir-proET-1 in sepsis. These proET-1 peptides were also detected in normal subjects.	Immunoreactivities of 3 ppET-1epitopes suggest 3 proET-1 derived peptides.
Papassotiriou *et al.*, 2006	**Chronic HF** (n = 77), **sepsis** (n = 116) and healthy (n = 326)	CT-proET-1 Big ET-1	CT-proET-1 significantly correlated with age. Elevated CT-proET-1 levels in chronic HF and sepsis patients. CT-proET-1 correlated with bigET-1 measurements.	The CT-proET-1 assay without extraction and lack of cross-reactivity may be a useful biomarker.
LAMP study Khan *et al.*, 2007	**Acute MI** (n = 983)	CT-proET-1 NT-proBNP	Both NT-proBNP and CT-proET-1 were independent predictors of death and HF. AUC was 0.76 for both NT-proBNP and CT-proET-1.	CT-proET-1 is a strong predictor of adverse outcomes.

Table 1.8 cont:

Study & Reference	Patients	Biomarkers	Results	Conclusion
Behnes *et al.*, 2008	**Acute ST elevation MI or non-ST elevation MI** (n = 30)	MR-proADM CT-proET-1	3 days after MI median CT-proET-1 in event vs. no-event group was significantly higher (72.9 *vs*. 54.4 pmol/L). MR-proADM levels were 0.69 *vs.* 0.59 nmol/L. AUC for MR-proADM and CT-proET-1 was 0.71 and 0.76.	Both MR-proADM and CT-proET-1 may predict acute phase of MI.
Adlbrecht *et al.*, 2009	**Chronic HF** (n = 786)	CT-proET-1 MR-proADM BNP	MR-proADM better predictor of mild to moderate HF. ADM is not superior to NT-proBNP in predicting outcome.	BNP can be a better biomarker of prognosis at a later disease stages.
Dieplinger *et al.*, 2009	**Acute destabilised HF** (n = 137)	CgA CT-proET-1 NT-proBNP	Decedents (n = 41) had higher median plasma concentrations of CgA (9.7 *vs.* 6.0 nmol/L), CT-proET-1 (120 *vs.* 72 pmol/L), and NT-proBNP (5112 *vs.* 2610 ng/L) at baseline than survivors.	CT-proET-1 added independent prognostic information in addition to NT-proBNP measurement.
Maier *et al.*, 2009	**Type 2-DM** (n = 781) Median follow up of 15 months	MR-proADM, CT-proET-1 CT-proAVP MR-proANP Creatinine GFR	All biomarkers increased in future CV events, independently correlated to serum creatinine. MR-proANP was the strongest predictor of CV events (AUC 0.80), while CT-proET-1 (AUC 0.65) was the weakest. MR-proADM and CT-proET-1 also correlated with GFR and serum creatinine.	CT-proET-1 unable to add additional value to predict future CV events. All 4 neurohormonal biomarkers were related to both kidney function and CV events.

Table 1.8 cont:

Study & Reference	Patients	Biomarkers	Results	Conclusion
GISSI-HF Masson *et al.*, 2010	**Chronic and stable HF** (n = 1,237) Median follow-up of 3.9 years	MR-proANP, MR-proADM, CT-proET-1 and CT-proAVP or copeptin	All markers were higher in elderly, in patients with more severe HF symptoms and reduced eGFR. MR-proANP was unable to improve reclassification based on clinical risk factors AUC for MP-proANP, NT-proBNP, and CT-proproET-1 was 0.74, 0.73, and 0.71, respectively.	Although all markers had significance independent of NT-proBNP, the most powerful predictor of outcome was MR-proANP.
GENOA study Habib *et al.*, 2010	**Hypertensive** African Americans (n = 981) and non-Hispanic whites (n = 812)	CT-proET-1 urinary ACR	Higher CT-proET-1 levels in African Americans in comparison to non-Hispanic whites. African Americans had a higher prevalence of diabetes, lower use of statins, and higher eGFR, SBP, and DBP, and greater urinary ACR.	CT-proET-1 independently associated with lower target-organ damage measures (urinary ACR).
Jankowska *et al.*, 2011	**Systolic chronic HF** (91% men) (n = 491)	CT-proET-1 NT-proBNP	Higer CT-proET-1 levels in patients with chronic HF when compared to healthy controls. CT-proET-1 levels were positively associated with age and the disease severity (NYHA class).	CT-proET-1 increased prognostic value of CHF and added value to 12-month CV mortality in patients with CHF.

Table 1.8 cont:

Study & Reference	Patients	Biomarkers	Results	Conclusion
GISSI-AF Lattini *et al.*, 2011	**Hypertensive** (84.8%, 59.7% AF) (n = 382) 1 year follow-up	MR-proANP MR-proADM CT-proET-1 Copeptin/CT-proAVP NT-proBNP hsTnT	Baseline NT-proBNP, MR-proANP and hsTnT were higher in patients older than 70 years, in those with HF or LVEF, and those with CAD. Highest correlation was between NT-proBNP and MR-proANP, which also showed an inverse relationship with recurrence of AF. CT-proET-1 was also associated with the risk of first recurrence of AF.	hsTnT, MR-proANP, NT-proBNP and CT-proET-1 had a modest but statistically significant predictive power for recurrence of AF.
KORA F4 study Seissler *et al.*, 2012	**Type 2-DM and MetS** (n = 1,590)	CT-proET-1 MR-proADM	CT-proET-1 and MR-proADM significantly elevated in patients with MetS.	
PEACE trial Sabatine *et al.*, 2012	**Stable CAD** and preserved LVEF (n = 3,717)	MR-proANP MR-proADM CT-proET-1 Copeptin	MR-proANP, MR-proADM, and CT-proET-1 were independently associated with the risk of CV death or HF.	Increased levels of biomarkers may be useful to identify patients at higher risk of CV death and HF and aid selection of responsive patients to therapy.

Table 1.8 cont:

Study & Reference	Patients	Biomarkers	Results	Conclusion
Drion *et al.*, 2012	**Type 2-DM** (n = 1,225) Median follow-up of 3 or 10 years	CT-proET-1 Albuminuria	CT-proET-1 was associated with fatal cardiovascular events, all-cause mortality, and new-onset albuminuria	CT-proET-1 improved prediction of fatal cardiovascular events.

Abbreviations: ***IR*** *= immunoreactivity,* ***AF*** *= atrial fibrillation,* ***CAD*** = coronary artery disease, ***MI*** *= myocardial infarction,* ***Type 2-DM*** *= Type 2-diabetes mellitus,* ***MetS*** *= metabolic syndrome,* ***LVEF*** = left ventricular ejection fraction, ***LLD*** *= lower limit of detection,* ***NYHA*** *= New York Heart Association Class,* ***CV*** *= Cardiovascular,* ***GFR*** *= glomerular filtration rate,* ***CgA*** *= Chromogranin A,* ***CT-proET-1*** *= C-terminal-proendothelin-1,* ***HsTnT*** *= high sensitivity troponin T,* ***MR-proADM*** *= midregional proadrenomedullin,* ***NT-proBNP*** *= N-terminal-pro* ***B-type*** *natriuretic peptide.* **ACR** = albumin:creatinine ratio. *MR-proANP, MR-proADM, CT-proET-1, Copeptin/CT-proAVP were all measured using chemiluminescence immunoassays (CIA) (BHRAMS), NT-proBNP and HsTnT were measured using electrochemiluminescence immunoassay (Elecys), and big ET-1 was measured using ELISA.*

Cardiovascular disease occurs frequently in patients with renal disease (e.g. CKD) (Foley *et al.,* 2005). Similarly, CKD is an independent risk factor for cardiovascular morbidity and mortality (Jones *et al.,* 2004). Renal function is assessed using estimated glomerular filtration rate (eGFR) but cystatin C and proteinuria are other renal markers. Serum creatinine is used to estimate eGFR. However, it is a poor biomarker of early CKD. This is because detection of renal dysfunction occurs after extensive tissue damage (Hewitt *et al.,* 2004). Thus, there is an unmet clinical need for more sensitive biomarkers that will provide earlier detection of renal impairment and potentially reflect effectiveness of therapy. Since there is interplay between cardiovascular and renal dysfunction, biomarkers investigated in predicting cardiovascular disease risk have also been evaluated in renal disease. As such, cardiovascular biomarkers (NT-proBNP, hsTnT, proANP, copeptin and proADM) were associated with renal function in patients with systolic HF (Bosselmann *et al.,* 2013).

Increased ET-1 production in patients with renal disease and its relation to impaired renal function (as a measure of eGFR), through which contributes to the progression and maintenance of hypertension and arterial stiffness, has been evident (Dhaun *et al.,* 2006; Goddard *et al.,* 2007). Urinary ET-1 excretion is well correlated with renal ET-1 production (Benigni *et al.,* 1991) and thus it was suggested as a potential biomarker for renal injury (Ohta *et al.,* 1991). The diagnostic or prognostic utility of CT-proET-1 in patients with CKD has yet to be described.

1.14 Hypothesis and aims of this thesis

1.14.1 Hypothesis

There is a clinical need for sensitive markers for early diagnosis in both cardiovascular and renal pathologies that would reflect changes in progression and treatment outcomes. Current methods measuring EDD and the effects of treatments in BP have limited diagnostic value. ET-1 is an early contributor to endothelial dysfunction and plays a vital role in regulation of BP. However, ET-1 has a short circulating half-life and its measurement has limitations.

The work described in this thesis investigated the hypothesis that other ppET-1-derived peptides co-released with ET-1 are more stable in circulation and thus could serve as alternative biomarkers of elevated ET-1 synthesis in cardiovascular and renal pathologies. ProET-1-derived peptides may be clinically useful as diagnostic biomarkers and may provide improved risk assessment. Moreover, their measurement could be beneficial for monitoring treatment outcomes of ET receptor antagonists.

1.14.2 Aims

The general aim of this thesis was to characterise ppET-1 synthesis and to develop specific immunoassays for the measurement of proET-1 peptide fragments. Specific aspects of the research were:

(1) To evaluate the release of ET-1 and proET-1 peptides from endothelial (EA.hy 926) and epithelial (A549) cell lines **(Chapter 3)**, which were identified using immunoassays optimised in **Chapter 2**. The aim of this investigation was to define whether proET-1 peptide fragments released into the condition media were stable and whether inhibiting ET-1 synthesis using an ECE inhibitor phosphoramidon and/or protease inhibitors had an effect on the release of proET-1 peptides.

(2) These investigations were also required to find optimal conditions for collection of conditioned media samples from EA.hy 926 and A549 cells for pursuing the purification and characterisation of proET-1 peptides **(Chapter 4)**.

(3) To provide sequence identities of the endogenous proET-1 peptides using mass spectrometry **(Chapter 5)**. This chapter provides evidence for the

identity of a novel ppET-1 derived peptide, which contains an endothelin-like domain.

(4) **(A)** Evaluate the clearance rates of identified proET-1 peptide fragments in the circulation of rats and study their metabolism in whole blood and plasma. **(B)** Using patient samples assess whether stable proET-1 peptides may be potential biomarkers of vascular and renal pathologies **(Chapter 6).**

CHAPTER 2

General materials and methods

2.1 MATERIALS

2.1.1 Reagents and Solutions

1. 0.2 µm filter paper (Whatman, UK).

2. 24-well plates cell culture (VWR, UK).

3. 25G needle (BD Microlance^{TM}, USA).

4. Acetic acid, glacial (CH_3COOH) (Analar grade: BDH Laboratory supplies, UK).

5. Acetonitrile (CH_3CN) HPLC grade (Rathburn Chemicals Ltd., Scotland).

6. Ammonium bicarbonate (NH_4HCO_3) (Analar grade: BDH Laboratory supplies).

7. Ammonium sulphate $(NH_4)_2SO_4$ (Merck, Germany).

8. Anhydrous sodium sulphate (Analar grade: BDH Laboratory supplies, UK).

9. Bacitracin, prepared fresh in DMEM (10 mM) and 0.2 µm filter sterilised before use (Sigma, UK).

10. Benzamidine HCl (anhydrous basis) (MWt = 156.61). A reversible inhibitor of trypsin, trypsin-like enzymes, and serine proteases (Sigma, UK).

11. Bio Gel P-30, 100 g fine 45 – 90 µm (wet) (Bio-Rad, Germany).

12. Bovine serum albumin (BSA) (Sigma, UK).

13. Carboxymethyl Fractogel, EMD COO^- 650 (M) (500 ml) (Merck, Germany).

14. Centrifugal filter devices Amicon Ultra (MWt cut-off 100 kD) (Millipore, Ireland).

15. Clear 96-well plate (Sterlin, UK).

16. CNBr activated Sepharose (1 g makes ~3.5 ml) (Amersham-Pharmacia, UK).

17. Dimethyl formamide (DMF) (Sigma, UK).

18. Dimethyl sulfoxide (DMSO) (Sigma, UK).

19. Dulbecco's Modified Eagle's Medium - high glucose (DMEM) with 4500 mg/L glucose, L-glutamine, sodium pyruvate, and sodium bicarbonate (D6429, Sigma, UK). For use 500 ml DMEM is supplemented with 5 ml antibiotics (100 Units/ml Penicillin and 100 µg/ml streptomycin) and 12.5 ml HEPES (25 mM) (DMEM+).

20. Dulbecco's Phosphate Buffered Saline (without $CaCl_2$ and $MgCl_2$) (Sigma, UK).

21. Endopeptidase Inhibitors: leupeptin, chymostatin and pepstatin A (Sigma, UK). Inhibitor stock solutions chymostatin 100 mM (MWt = 600, 25 mg dissolved in 417 µl of DMSO, stored at -20°C); 10 mM pepstatin A (MWt = 685.9, 5 mg dissolved in 729 µl of DMSO, stored at -20°C); 100 mM leupeptin (MWt = 426.5, 100 mg dissolved in 2.344 µl of H_2O, stored at -20°C). Peptide inhibitor mix was

prepared in DMEM diluting chymostatin and leupeptin at 10 µM, and pepstatin A at 10 µM.

22. Ethanolamine (Analar grade: BDH Laboratory supplies, UK).

23. EDTA (Ethylenediaminetetraacetic acid) (Sigma, UK).

24. EDTA solution, 0.5 M (pH 8.0) (Promega, USA).

25. Ethanolamine-hydrochloride (Sigma, UK).

26. EZ-Link Iodoacetyl-PEG-Biotin, 50 mg (Pierce reagent 21334, USA).

27. EZ-Link NHS-LC-LC-Biotin (Pierce reagent 21343, USA).

28. Falcon tubes, 15 and 50 ml (Beckman, UK).

29. Float A-Lyser G2 (MWt cut-off 8 – 10 kD) (Spectrum, USA).

30. Foetal calf serum (FCS) (Sigma, UK).

31. Formic acid (BDH Laboratory supplies, UK).

32. Freund`s adjuvant (complete, F5881; incomplete, F5506; Sigma, UK).

33. Gamma globulins from bovine blood (Sigma, UK).

34. Glutaraldehyde, 25% (G6257, Sigma, UK).

35. Guanidine hydrochloride (G-HCl) (Sigma, UK).

36. HAT Media Supplement (50×) (H0262, Sigma, UK).

37. Heparin sodium (5,000 Units/ml) (Wockhardt, UK).

38. HEPES 1M (N-2-Hydroxyethylpiperazine-N′-2-ethanesulfonic Acid), free acid (H3375, Sigma, UK).

39. High-binding, flat bottom 96-well plates, black clear bottom polystyrene (Costar, Corning, USA).

40. High-binding, flat bottom 96-well plates, white solid bottom polystyrene (Costar, Corning, USA).

41. Hydrochloric acid (HCl) 10 M stock (Analar grade: BDH Prolabo, UK).

42. Imject Mariculture Keyhole limpet Hemocyanin (mcKLH; 2 x 20 mg vials Pierce product# 77600, USA).

43. Lo-Binding ultracentrifugation tubes (Eppendorf, USA).

44. Low nonspecific binding dialysis membranes (MWt cut-off 10,000, Spectra/Por Biotech Cellulose Ester, 8 mm width; 131261, Spectrum, Perbio Science, UK).

45. Luminex® 100/200 Calibration Kit LX200-CAL (Luminex Corporation, USA).

46. Luminex® 100/200 Performance verification kit LX200-CON (Luminex Corporation, USA).

47. Luminex® 100/200 Sheath fluid (Luminex Corporation, USA).

48. Magnetic beads for NT-proET-1, ELDP, CT-proET-1 immunoassays (Luminex Corporation, USA).

49. Mercaptoethanol (BDH Laboratory supplies, UK).

50. Methanol (HPLC grade: BDH Prolabo, France).

51. MTT [1-(4,5-Dimethylthiazol-2-yl)-3,5-diphenylformazan Thiazolyl blue formazan] powder dissolved in DMEM (0.4 mg/ml) (M2003, Sigma, UK).

52. Natural slick-seal tubes 0.2 ml, 1.5 ml (Bioquote, USA).

53. Neutravidin-horeradish peroxidase (N-HRP) (Pierce, USA).

54. Penicillin/Streptomycin: 10,000 Units/ml Penicillin and 10,000 µg/ml streptomycin (Gibco®, Invitrogen, USA).

55. Peptide mix solution: Prepared at 1 nmol/ml as a mixture of the three peptides, NT-proET-1, ELDP and CT-proET-1, in 0.2 µm filtered 0.9% NaCl/0.1% BSA. The interim dilution was prepared from a fresh stock in freshly prepared 0.9% NaCl/0.1% BSA.

56. pH indicator strips (non-bleeding), pH 0 – 6 and pH 7.5 – 14 (BDH Laboratory supplies, UK).

57. Phosphate buffered saline (PBS) tablets (P4417-100TAB, Sigma, UK).

58. Phosphate-buffered saline (PBS): dissolve 1 PBS tablet (Sigma, UK) in 200 ml uhq-H_2O. 0.01 M phosphate buffer: 0.0027 M KCl, 0.137 M NaCl, pH 7.4, at 25°C.

59. Phosphoramidon 100 mM (Peptide Institute, Japan) (MWt = 543.5): 25 mg dissolved in 460 µl of sterile PBS, 100 µl aliquots stored at -20°C). Diluted in DMEM on the day of experiments.

60. Polyethylene catheters (PE-50) (BD Microlance^{TM}, USA).

61. Polypep bovine protein digest low viscosity (Sigma, UK).

62. Polypropylene tubes (5 ml, 75 x 13 mm) (Sarstedt, Germany).

63. ProClin 300 (SuperCo Analytical, USA).

64. PTFE porous membrane filter, 40 µm pore size (Alltech, Fisher Scientific).

65. Q-Sepharose Fast Flow (300 ml) (GE Healthcare Bio-Sciences AB, Sweden).

66. Rabbit anti-sheep IgG (H+L)-HRP labelled (Immunopure, Pierce Lot# 1D1062475, USA).

67. Sep-Pak® 3cc (500 mg) C2 cartridges (Waters, USA).

68. Sintered glass funnel.

69. Sodium azide (BDH/Merck, UK).

70. Sodium bicarbonate (Analar grade: BDH Laboratory supplies).

71. Sodium carbonate anhydrous (Sigma, UK).

72. Sodium chloride (NaCl) (Sigma-Aldrich Chemical Company, UK).

73. Sodium thiopentone: The anaesthetic was purchased fresh from the supplier and made up at the time of surgery (Intraval Sodium, 120 mg/kg i.p.; Merial Animal Health Ltd., UK).

74. Streptavidin (5 mg) (Immunopure, Thermo Science, USA).

75. Streptavidin-R-Phycoerythrin (Steptavidin-RPE) (Invitrogen, Life Technologies, UK).

76. Succinimidyl 4-[p-maleimidophenyl]butyrate (SMPB) (10 mg, MWt = 356) (Thermo Scientific, Pierce, USA).

77. SulfoLink Coupling Resin (Thermo Scientific, Pierce, USA) (Iodoacetyl-activated crosslinked 6% beaded agarose, slurry in 50% glycerol, 10 mM EDTA with sodium azide).

78. Sulfo-succinimidyl 4-(N-maleimidomethyl) (Thermo Scientific/Pierce, USA).

79. Supersignal ELISA Pico chemiluminescence substrate 250 ml kit (Pierce, USA).

80. Syringes, sterile, 10 ml (Sherwood medical, UK).

81. Tissue culture T25 and T175 cm^2 flasks (VWR, UK).

82. TopTip Carbon+ (Graphite) C18 spintips (10 – 200 µl) (Glygen Corp, USA).

83. Trifluoroacetic acid (TFA) (Rathburn Chemicals Ltd., Scotland).

84. Tris (base) molecular biology grade (Calbiochem, Germany).

85. Tris (hydroxymethyl) methylamine (BDH Laboratory supplies, UK).

86. Triton X-100 (Sigma, UK).

87. Trypsin, Sequencing Grade Modified (20 µg) (Promega, PRV5111). Trypsin Resuspension Buffer (V542A) (supplied with V5111): is composed of 50 mM acetic acid.

88. Trypsin-EDTA Solution (10x) 5.0 g porcine trypsin and 2.0 g EDTA•4Na/L in 0.9% NaCl (Sigma, UK).

89. Tween-20 (Sigma, UK).

90. Urea (VWR, UK).

91. Vectaspin Micro Anopore 0.2 µm centrifugation tubes, 1.5 ml (Whatman, USA).

92. White clear bottom Costar 96-well plates (Costar, Corning, USA).

93. Wistar male rats (Charles River Limited, UK).

2.1.2 Equipment

1. 96-well plate liquid scintillation counter and luminometer (Wallac 1450 MicroBeta Trilux).

2. Alltech 24-port vacuum manifold (Grace Davison Discovery Sciences, USA).

3. Berthold microplate luminometer (Berthold Technologies, GmbH & Co. KG*).*

4. ELx405™ Microplate Washer (BioTek).

5. High-performance liquid chromatography system (HPLC): MERCK Hitachi L-6200 Intelligent Pump with 2 ml injection loop, with gradient elution capability, Shimadzu SPD-6A UV detector that measured absorbance at A_{280} or $A_{215,}$ and Pharmacia LKB Helifrac fraction collector. HPLC columns: ACE C4 (Part number: ACE-223-2546); ACE C18 (Part number: ACE-221-2546) with 5 µm particle size, 300 Å pore size and 4.6 x 250 mm dimensions; and Jupiter C4 (Phenomenex, Part Number: 00G-4169-N0) with 15 µm particle size, 300 Å pore size and 1 x 25 cm dimensions.

6. Infinite 200 PRO series (TECAN plate reader).

7. LTQ Orbitrap XL mass spectrophotometer (Thermo Fisher Scientific).

8. Luminex 100/200 system (Luminex Corporation, USA).

9. Techne sample concentrator (Bibby Scientific Limited, UK).

10. Ultracentrifuge (Beckman Coulter).

2.1.3 Preproendothelin-1 peptides

ProET-1 peptide fragments NT-proET-1 (ppET-$1_{[18 - 50]}$), ELDP (ppET-$1_{[93 - 166]}$) and CT-proET-1 (ppET-$1_{[169 - 212]}$) were chemically synthesised by the University of Geneva. Each peptide was initially dissolved in uhq-H_2O at a nominal concentration of 100 nmol/ml. The purity of each peptide was confirmed by HPLC (ACE C4 column, with absorbance measured at 280 nm). The concentration of each peptide was determined from peak area on HPLC (at A_{280}), and quantified using standard concentrations of tyrosine and tryptophan as reference depending on the relative number of tyrosine and tryptophan residues in the peptide. Peptide sequences of proET-1 peptides are shown in Table 2.2.

2.1.3.1 Direct infusion of proET-1 peptides on Orbitrap

Stock concentrations of synthetic NT-proET-1, ELDP and CT-proET-1 at 70, 85 and 59 nmol/ml, respectively were diluted in 25% acetonitrile containing 0.1% formic acid at 1 pmol/µl prior to LC-MS analysis on Orbitrap XL mass spectrophotometer (MS) (Thermo Fisher Scientific). NT-proET-1 was injected at a flow rate of 2 µl/min while ELDP and CT-proET-1 were injected at a flow rate of 1 µl/min over 5 min.

Comparison of average masses (monoisotopic) of each proET-1 peptide obtained from Orbitrap [NT-proET-1 (3,429.797); ELDP (8,637.348); and CT-proET-1 (5,289.660)] (Table 2.1) with the monoisotopic masses calculated from ProteinProspector [NT-proET-1 (3,429.787); ELDP (8,637.367) and CT-proET-1 (5,289.670)] (see Table 2.2 for amino acid composition), showed mass errors of <0.02 Da. Therefore, the masses of synthetic proET-1 peptides were in agreement with the calculated monoisotopic masses. This indicated that amino acid sequences of proET-1 peptides corresponded correctly with the synthetic peptides.

Table 2.1: ***Characterisation of proET-1 synthetic standards by direct infusion onto Orbitrap.*** *The monoisotopic mass is calculated from the formula: [(m/z) x z] n-1 x H^+, where* ***m/z*** *= mass-to-charge ratio, (m is the ion mass in atomic mass units in Daltons (Da) and z is the number of elemental charge units),* ***n*** *= number of charges,* ***H^+*** *= mass of a proton (1.008 Da).*

ProET-1 peptide	Observed ion (MH^+) mass, m/z	Charge	Monoisotopic Mass
NT-proET-1 (ppET-$1_{[18-50]}$)	1,143.938	3	3,429.798
	858.205	4	3,429.798
	686.766	5	3,429.800
ELDP (ppET-$1_{[93-166]}$)	720.704	12	8,637.360
	665.340	13	8,637.326
	617.890	14	8,637.358
CT-proET-1 (ppET-$1_{[169-212]}$)	882.450	6	5,289.662
	756.528	7	5,289.651
	662.090	8	5,289.667

2.1.4 Preproendothelin-1 antibodies

Preparation of antibodies for ET-1 and big ET-1 immunoassay were described previously (Corder, 2002). Antibodies for proET-1 peptides were also produced following described methodologies (Corder, 2002). Details of the proET-1 peptide antibodies used in immunoassays are shown in Table 2.1. For assay use all antibodies were prepared as affinity purified IgG (Corder, 2002). Synthetic peptide antigens used for raising proET-1 antisera and for the affinity purification of IgG were purchased from Bachem GmbH (Germany).

Underlined sequences in Table 2.2 indicate peptides used as antigens to raise specific antisera for the development of capture and detection antibodies. Specific IgG were purified from antisera using the same antigen coupled to SulfoLink Coupling Resin or CNBr-Sepharose; except for ET-1/big ET-1 where the detection antibody IgG was purified using ppET-$1_{[54-63]}$ coupled to Sulfolink Coupling Resin (Corder, 2002). To enable maleimide conjugation of ppET-$1_{[18-30]}$ and ppET-$1_{[169-186]}$ a C-terminal Cys-NH_2 residue was included in the synthetic peptide used for these antigens.

Table 2.2: ***Antibodies used for proendothelin-1 immunoassays.*** *Amino acid numbering is based on the 212 amino acid sequence for preproendothelin-1 (ppET-1) (Bloch et al., 1989). Underlined sequences indicate peptides used as antigens to raise specific antisera for the development of capture and detection antibodies.*

ProET-1 peptide sequences	Capture Antibody/ Protein Conjugate	Species	Detection Antibody/ Protein Conjugate	Species
ET-1 (ppET-1$_{[53-73]}$): CSCSSLMDKECVYFCHLDIIW	ppET-1$_{[68-73]}$/ Glutaraldehyde	Sheep	ppET-1$_{[54-63]}$/ Carbodiimide	Rabbit
Big ET-1 (ppET-1$_{[53-90]}$): CSCSSLMDKECVYFCHLDIIWVNTPEHVVPYGLGSPRS	ppET-1$_{[74-90]}$/ Glutaraldehyde	Rabbit	ppET-1$_{[54-63]}$/ Carbodiimide	Rabbit
NT-proET-1 (ppET-1$_{[18-50]}$): APETAVLGAELSAVGENGGEKPTPSPPWRLRRS	ppET-1$_{[18-30]}$/ Maleimide	Rabbit	ppET-1$_{[42-50]}$/ Glutaraldehyde	Rabbit
ELDP (ppET-1$_{[93-166]}$): ALENLLPTKATDRENRCQCASQKDKKCWNFCQAGKEL RAEDIMEKDWNNHKKGKDCSKLGKKCIYQQLVRGRKI	ppET-1$_{[93-109]}$/ Maleimide	Sheep	ppET-1$_{[155-166]}$/ Maleimide	Sheep
CT-proET-1 (ppET-1$_{[169-212]}$): SSEEHLRQTRSETMRNSVKSSFHDPKLKGKPSRERYVTH NRAHW	ppET-1$_{[169-186]}$/ Maleimide	Sheep	ppET-1$_{[204-212]}$/ Glutaraldehyde	Rabbit

2.2 METHODS

2.2.1 Cell culture

EA.hy 926 is a hybridoma cell line generated by fusing A549 cells (human adenocarcinoma-derived alveolar epithelial cells) with primary human umbilical vein endothelial cells (HUVEC), which has characteristics of cultured endothelial cells (ECs) (Edgell *et al.,* 1983). Previous studies have shown this is a suitable cell line for studying ET-1 synthesis (Saijonmaa *et al.,* 1991; Corder *et al.,* 1993a; Waxman *et al.,* 1994). Conditioned media released from EA.hy 926 and A549 cells were used to study the effects of protease inhibitors on ET-1 and proET-1 peptide release (Chapters 3) and as source of proET-1 peptides for purification and characterisation of proET-1 peptides (Chapter 4).

2.2.2 Chemiluminescence immunoassays

2.2.2.1 Assay buffers

A. IgG Coating buffer: 50 mM bicarbonate buffer, pH 9.5 (85 mg Na_2CO_3, 143 mg $NaHCO_3$ in 50 ml uhq-H_2O).

B. Blocking buffer (10x): IgG coating buffer containing 0.5% BSA and 0.05% polypep.

C. Neutralisation-buffer for cell culture media (N-SAB 6.9x conc): 363 mg Tris base (0.05 mM), 944 mg HEPES free acid (0.02 mM), 690 mg BSA (0.03 mM), 276 mg IgG (0.07 mM), 276 mg polypep (0.07 mM), 69 µl Triton X-100 in 19.5 ml uhq-H_2O with phenol red. 5 ml aliquots were stored at -20^oC.

D. Sandwich assay buffer (SAB, pH 7.5): 1 PBS tablet, 1 g BSA (0.5%), 0.4 g IgG (bovine gamma globulin) (0.2%), 0.4 g polypep (0.2%), 100 µl Triton X-100, 0.05 g sodium azide in 200 ml uhq-H_2O. Filter sterilised (0.2 µm) and 50 ml aliquots were stored at -20^oC.

E. Sandwich assay buffer for plasma samples (nSAB, pH 7.5): 0.6 g $NaH_2PO_4.2H_2O$, 5.76 g $Na_2HPO_4.12H_2O$, 1.17 g NaCl, 1 g BSA, 0.4 g IgG, 0.05 g sodium azide, 0.01 g heparin sodium salt, 0.1 ml ProClin, 6 ml 0.5 M pH 8.0 EDTA, 0.4 ml Triton X-100 in 193.5 ml uhq-H_2O.

F. SAB with ProClin: 0.1 ml ProClin in 200 ml SAB.

G. Wash buffer (PBS with 0.05% Tween-20): 1 PBS tablet and 100 µl Tween-20 in 200 ml uhq-H_2O.

2.2.2.2 Immunoassays for ET-1 and big ET-1

Step 1: Black clear bottom and high-binding Costar 96-well plates were coated with capture antibodies: 100 µl/well of sheep anti-ET-$1_{[16-21]}$ IgG (ppET-$1_{[68-73]}$) at 3 µg/ml in coating buffer, or rabbit anti-human big ET-$1_{[22-38]}$ (ppET-$1_{[74-90]}$) at 2 µg/ml for big ET-1. Plates were incubated overnight at 4°C.

Step 2: Next day, coating buffer was decanted and plates were blocked by adding 250 µl/well blocking buffer (1x) and incubating for a further 2 h at room temperature.

Step 3: ET-1 standards were prepared at 2000 fmol/ml in sandwich assay buffer (SAB) followed by 1 in 4 serial dilutions over the range 1.9 – 2000 fmol/ml. Human big ET-1 standards were diluted to 300 fmol/ml followed by 1 in 3 serial dilutions over the range 1.2 – 300 fmol/ml.

Step 4: After blocking, plates were washed 3 times with wash buffer and 50 µl of biotinylated antibody rabbit anti ET-$1_{[2-11]}$ IgG (ppET-$1_{[54-64]}$) was added to all wells. 100 µl of each ET-1 or big ET-1 standard or samples were added to corresponding wells. 100 µl of SAB was also added for non-specific binding and 0 fmol/ml wells. Plates were then incubated overnight at 4°C.

Step 5: End-point detection was then carried out after washing plates 3 times with wash buffer followed by addition of 100 µl of neutravidin-HRP diluted in wash buffer containing 0.5% BSA and incubated for 1 h at room temperature. Plates were then washed 4 times with wash buffer and 100 µl of supersignal ELISA Pico chemiluminescence substrate mixed at 1:1 ratio was added to all wells. The plates were covered and mixed for 1 min on a plate mixer and read using a scintillation/luminescence counter (protocol: Isoplate Tropix- reads 1 sec/well).

Both ET-1 and big ET-1 immunoassays are highly specific with a negligible cross-reactivity (<0.01%) in each assay (Corder, 2002).

2.2.2.3 Immunoassays of NT-proET-1, ELDP and CT-proET-1

Chemiluminescent double-recognition site sandwich ELISAs for NT-proET-1, ELDP and CT-proET-1 were performed as described above for ET-1 and big ET-1 using antibodies indicated in Table 2.1. Affinity purification and biotinylation of IgG were prepared following well-established methods (Corder, 2002).

Plates were coated with 100 µl of capture antibody at a concentration of 1 µg/ml. ProET-1 standards were prepared at 1000 fmol/ml in SAB followed by 1 in 3 serial dilutions over the range 1.4 – 1000 fmol/ml. After blocking (as in step 2), 25 µl of SAB was added to all wells. After adding 50 µl of standard or samples plates were mixed at room temperature for 30 min. 25 µl of biotinylated antibody was added before an overnight incubation at 4°C. End-point detection was then carried out in the same way as described above for ET-1 and big ET-1 immunoassays (step 5).

2.2.2.4 Immunoassay of ELDP and CT-proET-1 for plasma and urine measurements

White solid bottom and high-binding Costar 96-well plates were coated with the capture antibodies (1 µg/ml) specific for ELDP and CT-proET-1. After an overnight incubation, plates were blocked (as in step 2) and 25 µl of plasma samples or 100 µl of urine samples were added in wells containing 75 µl of nSAB or 50 µl of 3 times concentrated nSAB. Standards were prepared in the range 0.09 – 200 fmol/ml in nSAB and 50 µl or 100 µl per well was added for plasma or urine measurements, respectively. Following an overnight incubation detection of bound peptide was achieved with biotinylated IgG for ELDP (ppET-$1_{[155 - 166]}$) or CT-proET-1 (ppET-$1_{[204 - 212]}$), respectively. This was in conjunction with neutravidin-HRP and chemiluminescent substrate detection as described above (step 5). The plate was read using Berthold microplate luminometer (1 s/well). The lower limit of detection for ELDP was 0.09 fmol/ml in urine and 0.30 fmol/ml in plasma. The detection limit for CT-proET-1 in plasma was 0.60 fmol/ml.

2.2.3 Magnetic bead-based multiplex assays for proET-1 peptides

Magnetic beads (Bio-Rad) were coated with corresponding capture antibodies for NT-proET-1, ELDP and CT-proET-1 (see Table 2.2, page 68) following standard protocols (Luminex Corporation).

(1) White clear bottom Costar 96-well plates were washed with a microplate washer (ELx405, BioTek). Magnetic beads for NT-proET-1, ELDP and CT-proET-1 were prepared as a combination (and protected from light) by diluting stock solutions in wash buffer at 1 in 50 for NT-proET-1 and 1 in 100 for ELDP and CT-proET-1. A 10 µl volume of the diluted bead combination was added to each well (and protected from light).

(2) 135 µl nSAB was added to the sample wells and to the nSAB standard curve, while for the plasma standard curve 120 µl nSAB and 15 µl rat plasma was added and mixed on an orbital plate mixer. Standards were prepared in the range 2.1 – 1500 fmol/ml. 15 µl of standards or plasma samples were added (total volume per well 150 µl) and the plate was incubated overnight at 4°C on an orbital plate mixer.

(3) On the next day, after washing plates on the ring magnet plate washer, 25 µl of combined biotinylated antibodies were added to all wells and incubated for 2 h at room temperature mixing on the orbital plate shaker.

(4) After washing three times on the plate washer end-point detection was carried out by incubating 25 µl/well of 1 in 10 diluted Streptavidin-RPE (Invitrogen) for 30 min at room temperature on orbital plate shaker. After washing plate 3 times on the ring magnet 100 µl/well sheath fluid was added and mixed before reading on a Luminex 200 System, which was set to analyse magnetic beads at regions 45 (NT-proET-1), 36 (ELDP) and 27 (CT-proET-1) in a volume of 50 µl/well and to count 50 beads/region.

2.2.4 Production of new capture and detection antibodies for CT-proET-1 immunoassay

Initially, the N-terminal sequence SSEEHLRQTRSETMRNSV corresponding to ppET-$1_{[169-186]}$ was used to raise specific antisera for CT-proET-1 immunoassay. The human sequence has four homologous residues with the sheep sequence (Table 2.3). This may result in some cross-reactivity of sheep CT-proET-1 with the sheep antibodies resulting in increased non-specific binding. Therefore, the non-homologous region SSEEHLRQTRS (ppET-$1_{[169-179]}$) was used as the new antigen sequence to raise specific antisera with the aim of increasing assay sensitivity and specificity.

Table 2.3: ***Comparison of human and sheep N-terminal sequence of CT-proET-1 peptide.*** *Bold indicates CT-proET-1 sequence used to raise antisera/purify IgG, hyphens (-) represents missing residues where there is no corresponding amino acid residue in the sequence for these residues and italics indicates non-homologous residues in the sheep sequence.*

	169										179							186
Human	**S**	**S**	**E**	**E**	**H**	**L**	**R**	**Q**	**T**	**R**	**S**	E	T	M	R	N	S	V
Sheep	-	-	-	-	-	-	-	-	-	-	*L*	E	T	*I*	*S*	N	S	*I*

2.2.4.1 Reagents and solutions

2.2.4.1.1 *Custom synthesised CT-proET-1 peptides*

N-terminal CT-proET-1 (ppET-1$_{[169 - 179]}$)-Cys: H-Ser-Ser-Glu-Glu-His-Leu-Arg-Gln-Thr-Arg-Ser-Cys-NH_2 (SSEEHLRQTRSC) trifluoroacetate salt, MWt = 1431.55 (>95% pure, 75% peptide content) (Bachem lot# 3008326, UK).

Cysteine-amide is added to the C-terminus of the N-terminal sequence to facilitate coupling of this peptide to KLH carrier protein (using the maleimide method) and for biotinylation of this peptide-antigen with EZ-Link Iodoacetyl-PEG-Biotin.

C-terminal CT-proET-1 (Lys$_{203}$-ppET-1$_{[204 - 212]}$): H-Lys-Tyr-Val-Thr-His-Asn-Arg-Ala-His-Trp-OH (KYVTHNRAHW) trifluoroacetate salt, MWt = 1311.47 (>97% pure, 71.8% peptide content) (Bachem lot# 3008325, UK).

Lysine at the N-terminal of the C-terminal CT-proET-1 sequence is added to improve coupling efficiency of the peptide sequence to KLH carrier protein using glutaraldehyde and for biotinylation of this peptide-antigen with EZ-Link NHS-LC-LC-Biotin.

2.2.4.1.2 *Conjugation buffers*

1. Phosphate Buffer (0.1 M, pH 7.2): 0.19 g KH_2PO_4 and 0.64 g Na_2HPO_4 in 50 ml uhq-H_2O.
2. Phosphate Buffer with EDTA (0.2 M, pH 7.2/10 mM EDTA): 0.39 g KH_2PO_4, 1.27 g Na_2HPO_4 and 0.19 g Na_2EDTA in 50 ml uhq-H_2O.
3. Reaction buffer for CNBr Sepharose: 0.2 M $NaHCO_3$ and 0.5 M NaCl, pH 8.0.
4. Coupling buffer: 0.5 M sodium bicarbonate ($NaHCO_3$) buffer, pH 8.5 (2.1 g $NaHCO_3$ in 50 ml uhq-H_2O).
5. Reaction buffer for SulfoLink coupling resin: 0.1 M Tris-HCl (pH 8.5)/10 mM EDTA: 0.22 g Tris-HCl, 0.44 g Tris and 0.186 g Na_2EDTA in 50 ml.
6. Blocking buffer for CNBr Sepharose: 50 mM ethanolamine-HCl in coupling buffer, pH 8.0.
7. Blocking buffer for SulfoLink coupling resin: 10 mM mercaptoethanol.
8. 5 mM EDTA: 0.09 g EDTA in 50 ml.

2.2.4.1.3 *Biotinylation of CT-proET-1 peptides and purified IgG*

N-terminal CT-proET-1 peptide: 1.6 mg of SSEEHLRQTRSC (MWt = 1432; peptide content 75%; ~838 nmol) was dissolved in 750 µl of 5 mM EDTA. 18 µl of peptide (20 nmol) was diluted in 1 ml 0.2% formic acid and injected onto HPLC with detection of peptide peak by absorbance (A_{215}; ACE C18, 4.6 x 250 mm; eluted with a gradient of 8% to 24% CH_3CN containing 0.1% TFA over 40 min at a flow rate of 1 ml/min; elution time 19.1 min). 5.2 mg of EZ-Link Iodoacetyl-PEG-Biotin (MWt = 542) was dissolved in 2.28 ml of Tris-HCl pH 8.5/EDTA (2.28 mg/ml). To characterise the HPLC elution position of the biotinylation reagent and to facilitate identification of reaction products, 5 µl of biotinylation reagent (21 nmol) was diluted in 1 ml of 0.2% formic acid and injected onto HPLC (conditions as above for synthetic peptide; elution time 34.8 min). The biotinylation reagent was reacted with 25% excess over peptide; 250 µl of the biotinylation reagent (1.05 µmol) was added to the remaining peptide, and a further 500 µl of 0.1 M Tris-HCl pH 8.5/10 mM EDTA was added to the reaction mixture before incubation at room temperature in the dark for 1 h. The efficiency of biotinylation reaction was evaluated after 1 h by injecting 20 µl from the reaction mix onto HPLC (conditions as above; elution time of biotinylated peptide product 30.8 min, no unreacted peptide). After verification of the successful reaction the biotinylated peptide was purified by acidifying the reaction mixture with 6 µl 98% formic acid, and loading the entire sample onto HPLC using the same elution conditions as those used for monitoring reaction. The purified biotinylated peptide was retained for subsequent antibody evaluation.

C-terminal CT-proET-1 peptide: 6.2 mg of KYVTHNRAHW peptide (MWt = 1311; peptide content 71.8%; ~3.4 µmol) was dissolved in 680 µl of H_2O (5 µmol/ml), and 0.1 ml (0.5 µmol) was placed on ice. The pH was adjusted to 8.5 by adding 50 µl of 0.5 M $NaHCO_3$, pH 8.5. 1 µl of the C-terminal peptide (5 nmol) was injected onto HPLC with detection of peptide peak by absorbance (A_{215}; ACE C4, 300 Å pore size, 4.6 x 250 mm; eluted with a gradient of 8% to 24% CH_3CN containing 0.1% TFA over 40 min at a flow rate of 1 ml/min; elution time 8.4 min). 2.5 mg of NHS-LC-LC-Biotin reagent (MWt = 568) was dissolved in 176 µl dimethyl formamide (DMF) in a glass tube, and kept on ice (4.4 µmol = 25 µmol/ml). 1 µl of biotinylation reagent (25 nmol) was diluted in 0.2% formic acid and injected onto HPLC with the elution conditions indicated above (elution time 12.8 min). For comparison a sample of biotinylation reagent was hydrolysed in 0.1

M $NaHCO_3$ for 1 h at room temperature and then subjected to HPLC (elution position of hydrolysed reagent 9.8 min). For biotinylation of the C-terminal peptide, 25 µl of biotinylation reagent in DMF (0.625 µmol; 25 % excess) was added to 100 µl of peptide (0.5 µmol) and the reaction mixture was gently mixed and allowed to react on ice for 20 – 30 min and then at room temperature for 2 h. The efficiency of biotinylation reaction was evaluated by HPLC of 1.5 µl samples at A_{215} and A_{280} with the elution conditions described above (elution time for main biotinylated product 18.7 min). The biotinylated peptide was purified by HPLC and retained for subsequent antibody evaluation.

Peptide specific purified IgG: After affinity purification (section 2.2.4.6) of C-terminal (Lys_{203}-CT-proET-$1_{[204 - 212]}$) peptide specific IgG, the fractions containing the highest affinity peptide-specific IgG were determined using the ELISA methodology described in section 2.2.4.5. Highest affinity IgG were determined on the basis of highest binding peptide-specific IgG to the Sepharose gel. Fractions E – F, H – J and I showed highest affinity for the C-terminal peptide. These fractions were concentrated and then subjected to dialysis to remove contaminating reagents that could interfere in the biotinylation reaction; as described in section 2.2.4.6.3 (step 7).

Biotinylation of C-terminal peptide specific IgG was carried out as follows. The pH of IgG samples were adjusted to 8 by adding 0.5 M $NaHCO_3$ (typically 1 in 10 dilution for a post-dialysis IgG solution in 0.9% saline) and then chilled on ice. Biotinylation reagent was added at a 100-fold molar excess based on IgG concentrations (0.15 mg IgG = 1 nmol) determined by Bio-Rad protein assay (section 2.2.5). 5.4 mg of NHS-LC-LC-Biotin reagent (9512 nmol) was dissolved in 288 µl DMF (33 nmol/µl), and 20 µl was added to fractions E – F (1 mg in 150 µl), and 10 µl was added to IgG fractions H – J and I and (both 0.5 mg IgG). The biotin-IgG reaction mixture was kept on ice for 1 h and then reacted for 2 h at room temperature. Biotinylated IgG was dialysed using a 10 kD cut-off membranes against 5 L 0.15 M NaCl/0.05 M sodium phosphate buffer pH 7.2 for 16 – 18 h to remove excess and unbound biotinylation reagent from the biotinylated-IgG. Based on post dialysis sample volumes, biotinylated IgG concentrations were 1.67, 1.0 and 1.25 mg/ml for E – F, H – J and I respectively. Biotinylated IgG were tested at dilutions of ~7.5, 15 and 30 ng/well with 25 µl of the appropriate dilution added per well.

2.2.4.2 Coupling of synthetic N-terminal peptide of CT-proET-1 to an immunogenic carrier protein

1. 40 mg of Imject Mariculture Keyhole limpet Hemocyanin (mcKLH) (± 0.4) (~450 – 13,000 kD) was dissolved in 6 ml 0.1 M phosphate buffer (pH 7.2) and chilled on ice.
2. 10 mg of succinimidyl 4-[p-maleimidophenyl]butyrate (SMPB) (MWt = 356) was dissolved in 250 µl DMF. 120 µl of SMPB solution was added to 6 ml of mcKLH solution (~5 mg of SMPB) and chilled on ice to 4°C (0.35 µmol/mg protein).
3. The tube containing the reaction mix was covered in foil and incubated at room temperature for 2 h to allow the reaction to take place while gently mixing on a flat-bed roller mixer. Then to remove any free SMPB the conjugate mcKLH/SMPB solution was dialysed (MWt cut-off 10 kD) against 10 mM phosphate pH 7.2 in 0.2 M NaCl (5 L) in the dark at 4°C for 2 x 24 h, i.e. changing the dialysis buffer after 24 h. On completion of dialysis mcKLH was centrifuged for 10 min at 3000 rpm to remove any protein that had become insoluble after SMPB reaction.
4. 6.4 mg of SSEEHLRQTRSC (75% peptide by weight, ~5 mg pure peptide) was dissolved in 0.2 M phosphate buffer pH 7.2 containing 10 mM EDTA pre-chilled on ice. The peptide was then added to mcKLH, gently mixed and incubated at room temperature for 2 h.
5. To confirm successful conjugation of peptide to mcKLH carrier protein, a 15 µl aliquot from the reaction mix was diluted in 0.5 ml 0.2% formic acid, subjected to filtration through a 10 kD cut-off filter (Microcon YM-10, Amicon), and the filtrate was injected onto HPLC to demonstrate absence of free unreacted peptide (detection by absorbance A_{215}; column: ACE C18, 5 µm, 4.6 x 250 mm; eluted with a gradient of 8% to 24% CH_3CN containing 0.1% TFA over 40 min at a flow rate of 1 ml/min).
6. CT-proET-1/mcKLH conjugate was dialysed overnight at 4°C using 10 kD MWt cut-off dialysis membranes against 500 ml of 0.9% NaCl.

2.2.4.3 Coupling of synthetic C-terminal peptide of CT-proET-1 to an immunogenic carrier protein

1. KYVTHNRAHW was conjugated to mcKLH with glutaraldehyde. A 20-fold molar excess of glutaraldehyde (95 µl of 0.8 M) was added to 7.1 mg of KYVTHNRAHW (~5 mg pure peptide = 3.8 µmol) dissolved in 1 ml 0.1 M phosphate buffer, and placed in the dark for 30 min at room temperature.
2. mcKLH (20 mg) was dissolved in 4 ml of 0.1 M phosphate buffer and added to the glutaraldehyde activated KYVTHNRAHW peptide. The reaction mixture of mcKLH and glutaraldehyde–KYVTHNRAHW was left in the dark for 1 h at room temperature. Unreacted glutaraldehyde was quenched by the addition of 6 mg glycine dissolved in 5 ml of 0.1 M phosphate buffer.

2.2.4.4 Sheep immunisation protocol

To raise antisera conjugated peptides were sent to Ig-Innovations (Llandysul, Wales). A standardised immunisation procedure was used with pre-immune sera being collected from each sheep before immunisation. For the initial immunisation peptide conjugates were diluted with an equal volume of Complete Freund's adjuvant. Two sheep were immunised with each antigen: N-terminal or C-terminal peptide of CT-proET-1. Booster injections were administered every 4 weeks over a 4 – 5 month period. Test bleeds were collected 2 weeks after each booster injection and evaluated for antigen binding by ELISA. Each new antiserum sample was compared to the previous bleed and pre-immunisation sample.

2.2.4.5 ELISA methodology to evaluate the affinity of antisera

Black, high-binding 96-well plates were coated with 5 µg/ml streptavidin (Thermo Science) and stored at 4°C overnight. On the next day, the plates were blocked with blocking buffer. After washing, 100 µl of the biotinylated peptides for N-terminal CT-proET-1 (ppET-$1_{[169 - 179]}$) or C-terminal CT-proET-1 (ppET-$1_{[204 - 212]}$) (see section 2.2.4.1.3) diluted to 200 pmol/ml were incubated for 4 h at room temperature (N.B. previous studies had established that 10 pmol/well gives maximum signal with this streptavidin-biotin-peptide-IgG complex). Plates were washed 3 times and incubated for 24 h with 100 µl antisera dilutions prepared in assay buffer. Plates were washed 5 times

and end-point detection was carried out by incubating plates for 1 h with rabbit anti-sheep IgG-HRP conjugate, followed by 5 washes before incubation with chemiluminescence substrate.

2.2.4.6 Affinity purification of IgG

2.2.4.6.1 *Coupling of N-terminal peptide of CT-proET-1 to Agarose*

1. 8.2 mg of SSEEHLRQTRSC (4.3 µmol pure peptide) was dissolved in 2 ml of 5 mM EDTA. An aliquot (10 µl, 21.5 nmol) was retained for HPLC characterisation and for comparative estimation of coupling efficiency.
2. SulfoLink coupling resin (10 ml, 50% slurry = 5 ml gel bed volume) was transferred to a column and washed three times with 5 ml reaction buffer (0.1 M Tris-HCl pH 8.5 containing 10 mM EDTA). The gel was vacuum dried after washing, transferred to a 15 ml tube, and then 2 ml peptide and 5 ml reaction buffer was added to react for 1 h at room temperature.
3. The reaction mix (11 ml including gel) was allowed to settle for 10 min. 200 µl of the gel supernatant was transferred to a microcentrifuge tube and centrifuged for 3 min at 14000 rpm to remove all fine gel particles. A sample [110 µl (43 nmol) – equivalent to twice the retained reference sample in step 1] of the resultant supernatant was diluted in 500 µl 0.2% formic acid, the pH adjusted to 3.0 by adding formic acid (98 – 100%), and subjected to HPLC with detection by absorbance (A_{215}; column: ACE C18, 5 µm, 4.6 x 250 mm; eluted with a gradient of 8% to 24% CH_3CN containing 0.1% TFA over 40 min at a flow rate of 1 ml/min). The reaction efficiency was determined by comparison of the peak area with that obtained with initial sample of reconstituted peptide measured at A_{215}. This showed >95% peptide had been coupled to the gel.
4. Unreacted iodo-groups on the SulfoLink gel were blocked by adding 10 mM mercaptoethanol, and reacting at room temperature for 1 h.
5. The column was washed with 3 – 4 column volumes of sterile-filtered PBS. Vacuum dried gel was transferred to a new tube and stored in 10 ml of PBS containing 0.02% azide at 4°C until affinity purification of IgG.

2.2.4.6.2 *Coupling of C-terminal peptide of CT-proET-1 to Sepharose*

1. CNBr Sepharose was prepared according to the protocol described in Corder, 2002. Briefly, 1.3 g CNBr Sepharose was weighed in a sintered glass funnel with a 40 µm porous filter. 1 mM HCl was added to swell the gel, and it was then rinsed four times with 50 ml of 1 mM HCl. Using a clean spatula, the swollen gel was immediately transferred to a 15 ml Falcon tube.
2. 9.2 mg of KYVTHNRAHW was dissolved in 1 ml of H_2O (~5 µmol pure peptide). A sample (1 µl, 5 nmol) was retained for HPLC. The remaining peptide solution was transferred to the swollen gel and 6 ml of 0.2 M $NaHCO_3$ containing 0.5 M NaCl, pH 8.0 was added to initiate the reaction. The gel and the peptide were mixed on a roller-bed mixer at room temperature for 2 h.
3. The reaction efficiency of the 10 ml reaction mix (0.5 nmol/µl) was determined as described above (step 3) by HPLC with monitoring of peptide peaks at A_{280}. No unreacted peptide was detected, indicating 100% coupling efficiency.
4. After coupling of the peptide, the gel was blocked by the addition of ethanolamine-HCl, pH 8.0, to 50 mM, and then incubated at room temperature for 1 h to react.
5. The gel was poured into sintered glass funnel and the tube was washed with 2 mM HCl, and followed by sterile PBS as described in the previous section (step 5). The gel was stored in PBS with 0.02% azide until used for purification of IgG.

2.2.4.6.3 *Sodium Sulphate Precipitation*

Antisera (2 x 40 ml) were measured into 50 ml Falcon tubes. Anhydrous Na_2SO_4 was added to produce an 18% weight per volume (w/v) solution (e.g. 1.8 g per 10 ml antiserum). The tube was inverted immediately several times and then mixed on a roller-bed mixer until all Na_2SO_4 had dissolved. The serum IgG fraction was precipitated by centrifugation at 2000 *g* for 15 min at 20°C. The supernatant was aspirated and the IgG precipitate was reconstituted in PBS to the same volume as the initial antiserum sample volume. Affinity purification of antisera protocol was adapted from the previously described methodologies (Corder, 2002).

1. After precipitation of the antiserum with sodium sulphate as described above, the N-terminal CT-proET-1 Agarose and C-terminal CT-proET-1 Sepharose gels were gently mixed on a roller-bed mixer. Using a glass pipette, the gels were transferred to columns fitted with porous PTFE filters and washed three times with PBS.
2. The reconstituted IgG solutions were passed through the corresponding peptide gel. The gels were washed four times with 5 ml PBS, and then with 5 ml of 0.5 M NaCl to remove non-specifically bound proteins.
3. Specifically bound IgG was eluted into tubes containing 300 µl 0.8 M $NaHCO_3$ per tube for neutralisation with the following elution conditions: **(A)** 3 ml 50 mM $NaCH_3COO$ adjusted to pH 4.5 with acetic acid; **(B)** 2 ml 50 mM $NaCH_3COO$ adjusted to pH 4.0 with formic acid; **(C)** 2 ml 50 mM $NaCH_3COO$ adjusted to pH 3.5 with formic acid; **(D)** 2 ml C + 1 M Urea; **(E)** 2 ml C + 2 M Urea; **(F)** 2 ml C + 4 M Urea; **(G)** 2 ml C + 8 M Urea; **(H)** 2 ml C + 8 M Urea; **(I)** 2 ml C + 2 M G-HCl + 10% CH_3CN; **(J)** 2 ml C + 4 M G-HCl + 10% CH_3CN; **(K)** 2 ml C + 6 M G-HCl + 10% CH_3CN; **(L)** 2 ml C + 6 M G-HCl + 10% CH_3CN; **(M)** 2 ml C + 6 M G-HCl + 10% CH_3CN; **(N)** 2 ml C + 6 M G-HCl + 10% CH_3CN; **(O)** 2 ml C + 6 M G-HCl + 10% CH_3CN; **(P)** 2 ml C + 6 M G-HCl + 10% CH_3CN; **(Q)** 2 ml C + 6 M G-HCl + 10% CH_3CN.
4. 50 µl PBS containing 1% azide was added to each tube as a preservative and mixed gently.
5. Furthermore, 100 µl of each eluate was diluted in tubes containing 1 ml PBS with azide for evaluation of protein/IgG concentration using Bio-Rad protein assay (section 2.2.5) and antigen binding.

6. The gels were washed with 40 ml of PBS with azide and stored at 4°C.
7. Peak fractions from step 5 were pooled and concentrated using centrifugal filter devices (Amicon Ultra, MWt cut-off 100 kD), and then IgG was dialysed against 0.9% NaCl using Float A-Lyser G2 (MWt cut-off 8 – 10 kD) to remove salts that could interfere with biotinylation of IgG or lead to denaturation of IgG on storage.
8. IgG from dialysed fractions were tested as capture antibodies using sandwich ELISA methodology to ensure low non-specific binding and high assay sensitivity. Black, high-binding 96-well plates were coated with 100 µl/well of N-terminal or C-terminal CT-proET-1 specific IgG at 2 µg/ml and stored at 4°C. On the next day, plates were blocked with blocking buffer. CT-proET-1 synthetic standard was prepared in the range 25 – 200 fmol/ml. After washing, 50 µl of standards or SAB (to determine non-specific binding) were added to the N-terminal CT-proET-1 (ppET-$1_{[169 - 179]}$) specific IgG coated wells and mixed at room temperature for 30 min. 25 µl of rabbit anti ppET-$1_{[204 - 212]}$ biotinylated IgG (Table 2.2) was added to all wells and stored at 4°C. C-terminal CT-proET-1 (ppET-$1_{[204 - 212]}$) specific IgG was evaluated with 100 µl/well of the biotinylated-peptide antigen at 10 pmol/ml (section 2.2.4.5). The plate was mixed at room temperature for 30 min and stored at 4°C for end-point detection on the following day.

2.2.5 Bio-Rad protein assay

The protein concentration of the affinity purified fractions was measured from an IgG standard curve as a representative protein solution. IgG was prepared at 1 mg/ml in PBS and the standard curve (concentration range 7.8 – 500 µg/ml) was prepared by 1:2 serial dilutions in PBS. Stock solution of Bio-Rad reagent was prepared at 1:4 dilution of dye reagent concentrate in uhq-H_2O, which was then filtered using a 0.2 µm filter paper and stored at 4°C. In a clear 96-well plate (Sterlin), 50 µl of standards or samples were added in duplicate and 200 µl of the 1:5 diluted (in uhq-H_2O) Bio-Rad reagent was added to all wells. The plate was incubated at room temperature mixing on orbital mixer for 5 min. The absorbance was then measured at 595 nm using a spectrophotometer (Infinite, TECAN).

CHAPTER 3

Release of ET-1 and proET-1 peptide fragments from the conditioned media of EA.hy 926 and A549 cells

3.1 INTRODUCTION

Endothelin-1 is produced from the inactive intermediate big ET-1 by the hydrolysis of $Trp^{21} – Val^{22}$ bond of big ET-1. This process is catalysed by the physiological endothelin converting enzyme (ECE) (Figure 3.1). The first clear evidence of this was provided by inhibition of ET-1 release with high concentrations of a metallopeptidase inhibitor phosphoramidon. This resulted in accumulation of the big ET-1 (Ikegawa *et al.,* 1990). Similarly, in circulation and in isolated vessels, phosphoramidon inhibited the conversion of big ET-1 to ET-1 (McMahon *et al.,* 1991; Corder & Vane, 1995; Battistini *et al.,* 1995). Along with ET-1 a biologically inactive C-terminal fragment (CTF) of big ET-1 is also produced. Phosphoramidon reduced immunoreactive-ET-1 and CTF of big ET-1 (22 – 39) (Ikegawa *et al.,* 1990). This proteolytic step can occur in the extracellular medium and intracellularly in the secretory vesicles prior to its release (Corder *et al.,* 1995b; Harrison *et al.,* 1995). Therefore, big ET-1 can be secreted alone or co-secreted with ET-1 (Plumpton *et al.,* 1994).

Endothelial (EA.hy 926) and epithelial (A549) cells were previously used to study the intracellular biosynthesis of ET-1 as they express ET-1 mRNA and secrete big ET-1 and ET-1 into the culture media in a phosphoramidon-sensitive manner (Saijonmaa *et al.,* 1991; Corder *et al.,* 1995b; Corder *et al.,* 2002). A phosphoramidon-sensitive ECE activity with the characteristics of ECE-1 is localised predominantly in the plasma membrane of EA.hy 926 cells and A549 cells (Waxman *et al.,* 1994; Corder *et al.,* 1995b; Deprez-Roy *et al.,* 2000). However, localisation of ECE-1 to the membranes of Golgi apparatus indicated that ET-1 biosynthesis is primarily intracellular (Gui *et al.,* 1993; Xu *et al.,* 1994) requiring much higher (~10-fold) concentrations of phosphoramidon than those required to inhibit membrane bound ECE-1 (Isaka *et al.,* 2003; Corder *et al.,* 1995b). Thus, phosphoramidon is a more potent inhibitor of exogenous big ET-1 cleavage than the endogenous big ET-1 (Corder *et al.,* 1993a).

EA.hy 926 cells express high NEP-24.11 activity (Waxman *et al.,* 1994), which was shown to degrade ET-1 *in vitro* (Vijayaraghavan *et al.,* 1990) and *in vivo* (Abassi *et al.,* 1992). At lower levels (1 µg/ml), NEP-24.11 resulted in the degradation of secreted ET-1, while at higher levels it resulted in the total cleavage of ET-1 by the $Trp^{21} – Val^{22}$ bond of big ET-1 (Abassi *et al.,* 1993a).

Inhibitory effects of phosphoramidon alone and in combination with thiorphan (NEP-24.11 inhibitor) on the conversion of exogenous big ET-1 to endogenous ET-1 synthesis was studied in human cells using HUVEC, EA.hy 926 and A549 cells (Corder *et al.*, 1995b). While thiorphan (1 µM) had no inhibitory effect on the ECE activity of BAEC, in EA.hy 926 cells thiorphan reduced ECE activity by 30% and when used in the presence of low concentrations of phosphoramidon (up to 0.1 µM), the ECE activity was reduced by 63% (Corder *et al.*, 1995b). In comparison to EA.hy 926 cells, approximately 25% of the ECE activity of HUVEC was attributed to NEP-24.11. Immunoblot analysis identified ECE-1 in the membrane fraction of A549 cells (Deprez-Roy *et al.*, 2000). However, in contrast to EA.hy 926 cells, ECE-1b/c, but not NEP-24.11 is involved in ET-1 production in A549 cells (Aubert *et al.*, 1998).

Although ECE-1 and NEP-24.11 have similar structures (see Table 1.2) (Malfroy *et al.*, 1988) thiorphan, a specific inhibitor of NEP-24.11 has no inhibitory effect on ECE-1 activity. Therefore, it was suggested that NEP-24.11 is unlikely to function as a physiologically relevant ECE-1 activity (Abassi *et al.*, 1993a; Murphy *et al.*, 1994).

Processing of proET-1 at double basic amino acid residues has the potential to produce further peptides that are co-released with ET-1, and which may serve as alternative biomarkers of ET-1 synthesis, or have biological actions that complement those of ET-1. Pilot studies have identified three proET-1 peptides, namely NT-proET-1 (ppET-$1_{[18-50]}$), Endothelin-like Domain Peptide – ELDP (ppET-$1_{[93-166]}$), and CT-proET-1 ppET-$1_{[169-212]}$ (see description of assays in Chapter 2 and Figure 3.1). These proET-1 peptides were shown to be present in conditioned media samples from EA.hy 926 and A549 cell lines using specific immunoassays. However, the effects on regulation of their synthesis with protease inhibitors have not been investigated. Therefore, the goal of this chapter was to examine the effects of phosphoramidon on the synthesis of NT-proET-1, ELDP and CT-proET-1. In addition, the effects of other protease inhibitors were also investigated. Synthetic peptides corresponding to the identified peptides NT-proET-1, ELDP and CT-proET-1 were chemically synthesised and immunoassays were used to measure the release of these peptides in the conditioned media samples of EA.hy 926 and A549 cells.

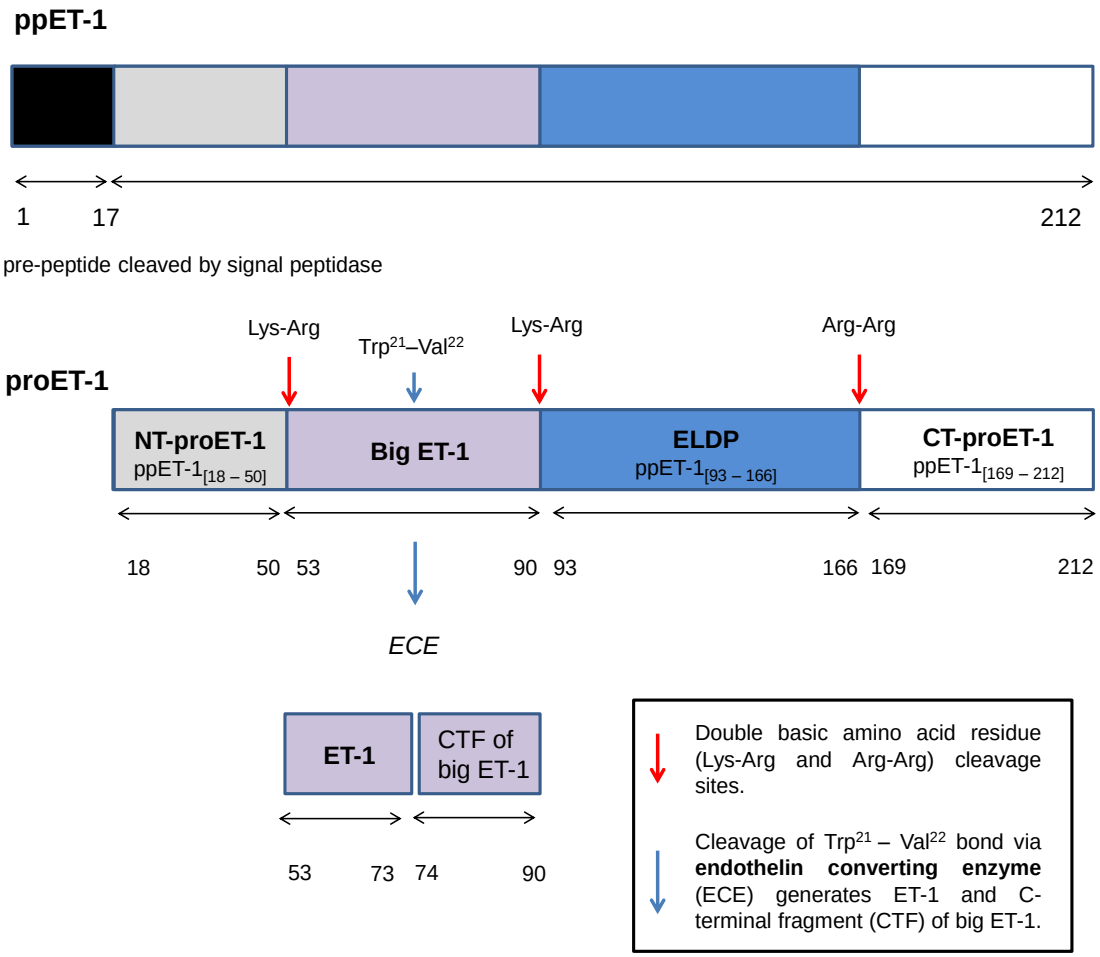

Figure 3.1: ***Scheme for ppET-1 processing and antibody recognition sites for the detection of proET-1 peptides: NT-proET-1, ELDP and CT-proET-1.*** *Specific antisera was raised for NT-proET-1 (ppET-1$_{[18-50]}$); Endothelin-like Domain Peptide–ELDP (ppET-1$_{[93-166]}$); and CT-proET-1 (ppET-1$_{[169-212]}$). Synthetic peptides corresponding to the identified peptides were chemically synthesised.*

3.2 METHODS

3.2.1 Cell culture

EA.hy 926 cells were grown to confluence in T75 cm^2 flasks in Dulbecco's modified Eagle medium (DMEM) supplemented with 4500 mg D-glucose/L with 10% (v/v) foetal calf serum, 2% HAT medium supplement (50x) (100 µM sodium hypoxanthine, 0.4 µM aminopterin, and 16 µM thymidine) and incubated at 37°C in a humidified CO_2 incubator (8% CO_2, 92% air). HAT supplement was also routinely added to DMEM for all incubations with EA.hy 926 cells. A549 cells were cultured under the same conditions, except that HAT supplement was excluded from the DMEM.

Subcultures were prepared by treating confluent flasks using 10% trypsin prepared in warm PBS and seeded into 2 x 24-well plates (2 cm^2 growth area per well/ 2.5 x 10^5 cells per cm^2) in the relevant culture medium containing 10% FCS to give approximately 70 – 80% confluence on the following day. On the next day, protease inhibitors were prepared as described in the next section and incubated on the confluent cells over 6 h and 24 h as described in section 3.2.3. Experiments were performed in DMEM without serum or penicillin/streptomycin.

3.2.2 Protease inhibitor study

The protease inhibitors used to study the stability of ET-1 and proET-1 peptides released from EA.hy 926 and A549 cells included phosphoramidon and an inhibitor cocktail that was composed of 1000 µM bacitracin, 10 µM chymostatin, 10 µM leupeptin, and 1 µM pepstatin A (Table 3.1). Phosphoramidon was prepared as a stock concentration of 100 mM in PBS. Stock solutions of protease inhibitors were prepared by reconstituting leupeptin at 100 mM in uhq-H_2O, chymostatin at 100 mM in DMSO and pepstatin A at 10 mM in DMSO. Furthermore, 1:10 interim dilutions of the stocks were made up in the same solutions and they were stored at -80°C. Bacitracin was prepared fresh on the day of experiment (MWt = 1,422.7) in DMEM. Confluent cells were initially washed with serum-free DMEM and incubated with protease inhibitors (phosphoramidon or inhibitor cocktail) in DMEM without FCS.

Table 3.1: ***The protease inhibitors used in inhibitor cocktail.***

Protease Inhibitor	Protease Family Targeted	Inhibitor Type	Concentration (µM)
Bacitracin	Proline endopeptidases	Reversible	1000
Chymostatin	Chymotrypsin-like serine/(cysteine)	Reversible	10
Leupeptin	Typsin-like serine and some cysteine proteases	Reversible	10
Pepstatin A	Aspartic acid proteases	Reversible	1
Phosphoramidon	Metalloprotease	Reversible	1 – 1000

3.2.3 Cell culture incubations with protease inhibitors

Before the incubation period, confluent cells were rinsed with warmed DMEM (500 µl/well) and then treated with 300 µl/well of the conditions containing protease inhibitor(s). Initial experiments investigated the effect of varying concentrations of phosphoramidon from 1 – 1000 µM on the intracellular processing of ET-1 and proET-1 peptides. The effect of inhibitor cocktail was studied using 10 µM leupeptin, 10 µM chymostatin, 1 µM pepstatin A, and 1000 µM bacitracin. Cells were treated in triplicate with each test condition using 2 x 24-well plates and incubated in a 37°C humidified cell culture incubator with 8% CO_2 for 6 h and 24 h.

3.2.3.1 *Collection of conditioned media and treatment before immunoassay*

After 6 h and 24 h incubation periods, 270 µl of the conditioned media/well were collected into 1.5 ml microcentrifuge tubes. Samples were neutralised by adding 25 µl 0.295 M HCl (prepared from a 100 M stock in fume hood) and heat-treated at 80°C for 10 min with caps open. After cooling, 50 µl N-SAB (Chapter 2, section 2.2.2.1) was added, re-capped and vortexed prior to storing at -20°C for subsequent immunoassay. The remaining medium was aspirated from the 24-well plates and the viability of cells was investigated by an MTT assay as described in section 3.2.4.

3.2.4 Cell viability (MTT) assay

Endothelial cell viability was evaluated using the 3-[4, 5-dimethyliazol-2-yl]-2, 5-diphenyltetrazolium bromide (MTT) colorimetric assay. MTT indicates mitochondrial respiration by quantifying cell-dependent mitochondrial dehydrogenase activity. This assay assesses whether any protease inhibitors have cytotoxic effects on endothelial cells. A stock solution of MTT (M2003, Sigma) was prepared at 2 mg/ml in DMEM containing 10 mM antibiotics (100 Units/ml penicillin and 100 µg/ml streptomycin) and 25 mM HEPES.

On the day of assay, MTT was diluted to 0.4 mg/ml in DMEM, and 300 µl/well (24-well plate) was added immediately after aspiration of conditioned media residues. MTT was incubated with cells for 1 h at 37°C. The medium was then aspirated and the cells were solubilised in 300 µl of dimethyl sulfoxide (DMSO). The absorbance was determined at 550 nm using a 96-well plate reader (Infinite, TECAN).

3.2.5 Immunoassays of ET-1, big ET-1 and proendothelin-1 peptides

Immunoassays of ET-1 and proET-1 peptides are described in detail in Chapter 2 sections 2.2.2.2 and 2.2.2.3, respectively. Primary amino acid sequences in which these specific sandwich immunoassays were developed are shown in Chapter 2, Table 2.2. Briefly, antibody recognition sites used for the detection of ppET-1 derived peptides were illustrated in Figure 3.1.

3.2.6 Data handling and statistical evaluation

The effect of protease inhibitors on ET-1 and proET-1 peptide fragments were expressed as fmol/ml released per 6 h and 24 h. Error bars in the graphs are shown for mean and standard error of mean (s.e.m). Statistical analyses were performed using one-way ANOVA with Fisher`s protected least significant difference (PLSD) as a post-hoc test. In the figures and tables *P* values less than 0.001 are indicated by ***, *P* values from 0.001 to 0.01 are indicated by **, *P* values from 0.01 to 0.05 are indicated by *. *P* values greater than 0.05 are non-significant and indicated by ns.

3.3 RESULTS

Human endothelial EA.hy 926 and epithelial A549 cell lines are well established systems for studying ET-1 biosynthesis. Phosphoramidon is a metalloprotease inhibitor that inhibits ECE and NEP-24.11. This produces a concentration dependent inhibition of the conversion of big ET-1 to ET-1. To investigate the stability of secreted proET-1 peptides, EA.hy 926 and A549 cells were incubated with phosphoramidon alone and in combination with inhibitor cocktail, which is composed of endopeptidase inhibitors at 10 µM leupeptin, 10 µM chymostatin, 1 µM pepstatin A, and 1 mM bacitracin.

3.3.1 EA.hy 926 conditioned medium

3.3.1.1 *Effect of phosphoramidon on the biosynthesis of ET-1 and big ET-1*

EA.hy 926 cells were incubated for 6 h and 24 h with increasing concentrations of phosphoramidon from 1 – 1000 µM. Phosphoramidon inhibited endogenous ET-1 production. This was biphasic with a dramatic increase in ET-1 release at low concentrations (1 – 10 µM) and decreased release at higher concentrations (>10 µM) (Figure 3.2).

In comparison to basal ET-1 release, incubation with 10 µM phosphoramidon over 6 h and 24 h increased the amount of ET-1 present in the medium by 1.4 and 4-fold, respectively. Incubation with phosphoramidon (1 – 10 µM) therefore, prevented degradation of released ET-1 into the culture medium by NEP-24.11. Therefore, the effect of increasing phosphoramidon concentrations on ET-1 synthesis was compared to ET-1 levels at 10 µM phosphoramidon (to reflect basal release without degradation). As a result, at concentrations above 10 µM phosphoramidon, ET-1 synthesis was inhibited to a similar degree over 6 h and 24 h incubation. As such, decrease in ET-1 release at 1000 µM was 78% at 6 h and 80% at 24 h.

Inhibition of ET-1 resulted in the accumulation of big ET-1 at phosphoramidon concentrations >30 µM (Figure 3.2). In the concentration range of 1 – 30 µM, phosphoramidon did not inhibit the processing of big ET-1 to ET-1. Big ET-1 levels accumulated more significantly after 24 h incubation with 1000 µM phosphoramidon, showing a 16-fold increase over 6 h and 24-fold increase over 24 h incubation.

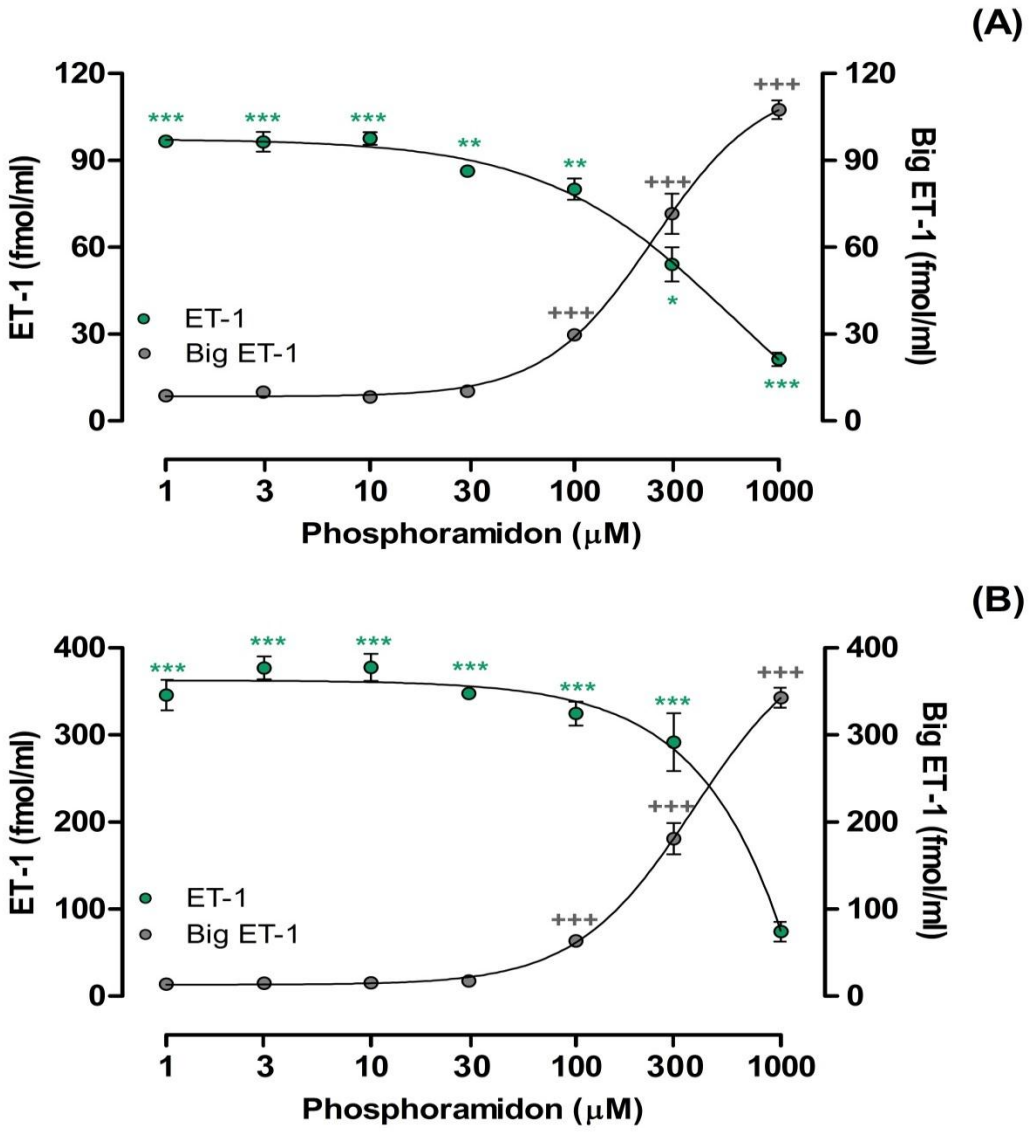

Figure 3.2: ***Effect of phosphoramidon on ET-1 (●) and big ET-1 (○) released from EA.hy 926 cells over (A) 6 h and (B) 24 h.*** *Cells were grown to confluence on 24-well plates and incubated for 6 h and 24 h in the presence of increasing concentrations of phosphoramidon (0 – 1000 μM). Mean results ± s.e.m, from two experiments with incubations in triplicates. * = P <0.05, ** = P <0.01, and *** = P <0.001 comparison of means to control by ANOVA with Fisher`s PLSD. Basal release of ET-1 with no phosphoramidon present was 68.8 ± 2.1 fmol/ml per 6 h and 95.6 ± 15.8 fmol/ml per 24 h. Big ET-1 basal release was 6.8 ± 1.0 fmol/ml per 6 h and 14.4 ± 1.3 fmol/ml per 24 h.*

3.3.1.2 *Effect of inhibitor cocktail on ET-1 and big ET-1 biosynthesis*

EA.hy 926 cells were incubated with 10 µM phosphoramidon, inhibitor cocktail [10 µM leupeptin, 10 µM chymostatin, 1 µM pepstatin A, and 1 mM bacitracin] and a combination of both treatments over 6 h and 24 h. The aim was to investigate the effect of inhibitor cocktail on ET-1 production from endogenous precursors by EA.hy 926 cells.

In comparison to basal ET-1 release, all three conditions significantly elevated ET-1 release from the conditioned medium of EA.hy 926 cells (Figure 3.3A). Incubation with 10 µM phosphoramidon over 24 h showed a 6 – 7-fold increase in ET-1 release. Incubation of EA.hy 926 cells with 10 µM phosphoramidon in combination with inhibitor cocktail increased ET-1 release by approximately 4.6-fold, in which the effect of inhibitor cocktail alone resulted in a 3.7-fold increase.

Basal release of big ET-1 over 6 h incubation (6.8 fmol/ml) was increased by approximately 2.1-fold over 24 h incubation (14.4 fmol/ml) (Figure 3.3B). On the other hand, basal release of ET-1 was only increased by approximately 1.4-fold over 24 h (Figure 3.3A). This suggested that big ET-1 accumulates over time while ET-1 is being degraded.

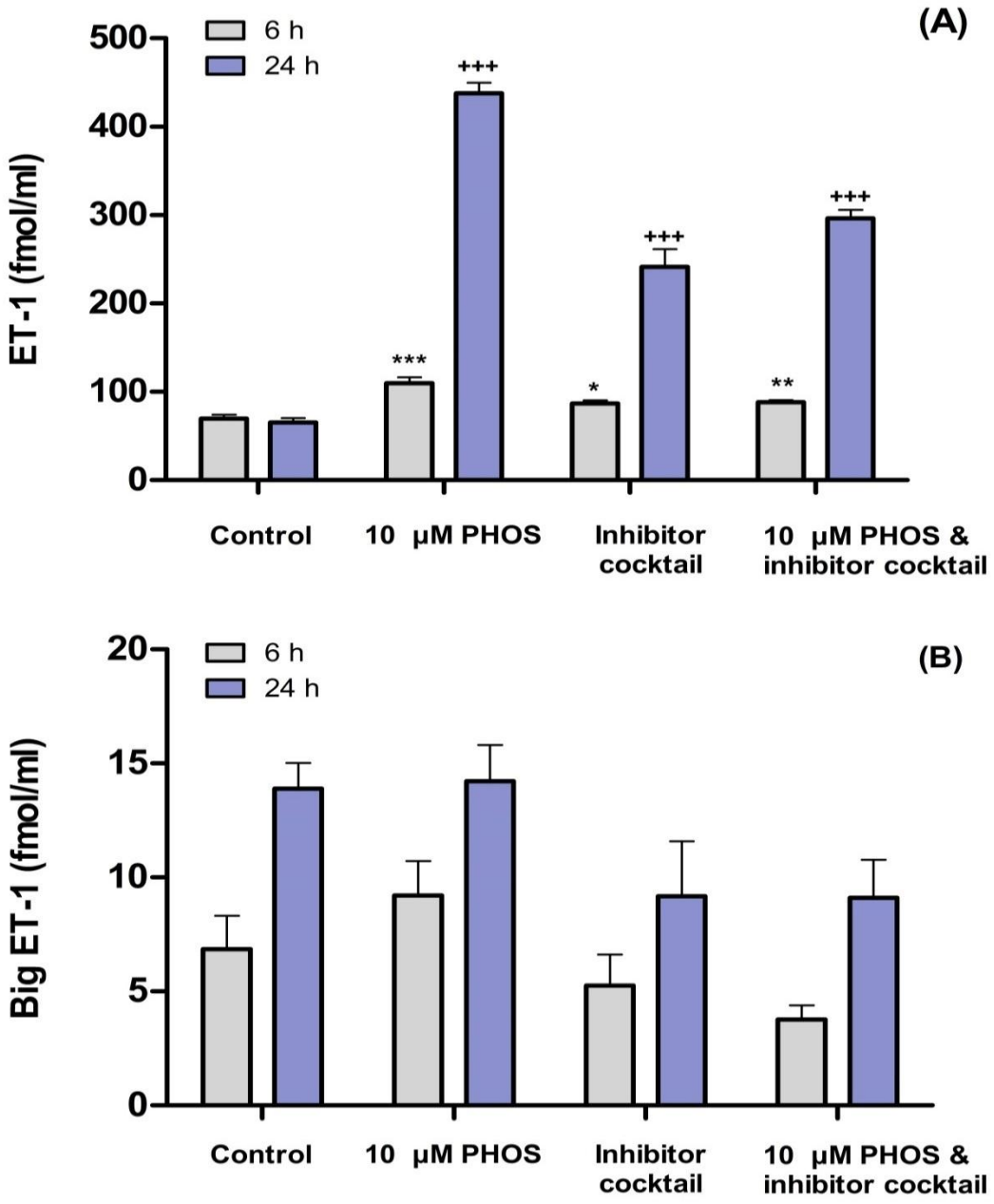

Figure 3.3: ***Effect of inhibitor cocktail on (A) ET-1 and (B) big ET-1 in the conditioned medium of EA.hy 926.*** *Cells were grown to confluence on 24-well plates and incubated for 6 h and 24 h in the presence of 10 µM phosphoramidon, inhibitor cocktail and a combination of 10 µM phosphoramidon with inhibitor cocktail. Mean results ± s.e.m from two experiments with incubations in triplicates were compared to control by ANOVA with Fisher`s PLSD, * = P <0.05, ** = P <0.01, and *** = P <0.001. Basal release of ET-1 (n = 6) immunoreactivity measured in conditioned medium samples from EA.hy 926 was 68.8 fmol/ml per 6 h and 95.6 fmol/ml per 24 h. Basal release of big ET-1 was 6.8 fmol/ml per 6 h and 14.4 fmol/ml per 24 h.*

3.3.2 A549 conditioned medium

3.3.2.1 *Effect of phosphoramidon and inhibitor cocktail on ET-1 and big ET-1 biosynthesis*

Unlike the biphasic pattern of ET-1 release in EA.hy 926 cells, phosphoramidon produced a concentration-dependent inhibition of endogenous synthesis of ET-1 and an enhanced accumulation of big ET-1 in the conditioned medium of A549 cells (Figure 3.4A). Incubation of A549 medium with 1000 µM phosphoramidon inhibited ET-1 synthesis by 84% over 24 h (24 h EC_{50} for ET-1 = 50.9 ± 4.8 µM phosphoramidon). Inhibition of ET-1 synthesis was marked, even for the 6 h incubation, with 1000 µM of phosphoramidon treatment reducing ET-1 accumulation in the medium by 92% (data not shown).

Compared to phosphoramidon alone the combination with inhibitor cocktail produced a more effective inhibition of ET-1 accumulation. The release of ET-1 was reduced by 28% with 10 µM phosphoramidon over 24 h incubation. Phosphoramidon (10 µM) in presence of inhibitor cocktail inhibited the release of ET-1 by 57%, which shows a 2-fold increase in the amount of ET-1 inhibition over 24 h. Although ET-1 released into the conditioned medium of A549 cells was inhibited more effectively with phosphoramidon in combination with inhibitor cocktail, big ET-1 accumulated to a lesser extent with this condition (Figure 3.4B). As such, the levels of big ET-1 accumulated with 10 µM phosphoramidon in presence of inhibitor cocktail (41.1 fmol/ml) were 43% less than that of 10 µM phosphoramidon alone (72.1 fmol/ml). In addition, big ET-1 released into the conditioned medium after 24 h incubation with 1000 µM phosphoramidon was 1.7-fold less than the big ET-1 levels accumulated in EA.hy 926 cells (199 fmol/ml for A549 and 343 fmol/ml for EA.hy 926 cells).

Basal release of ET-1 and big ET-1 from the conditioned medium of A549 cells over 6 h incubation was 102.3 and 8.3 fmol/ml (data not shown), while over 24 h incubation the levels were 557 fmol/ml and 20.1 fmol/ml, respectively. Basal ET-1 release from the conditioned medium of A549 cells was at a greater magnitude (5 – 6-fold) than that of EA.hy 926 cells (95.6 fmol/ml over 24 h incubation).

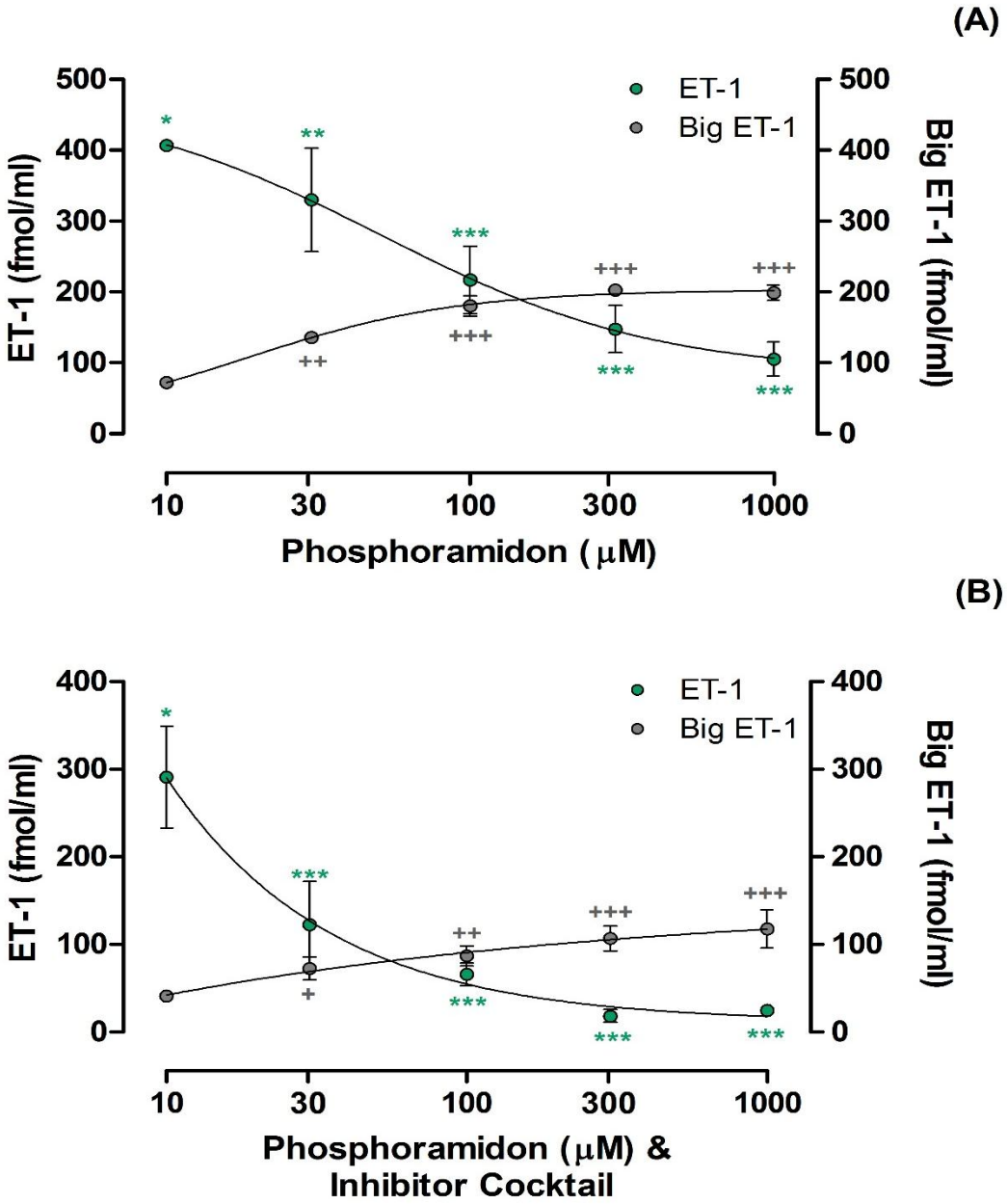

Figure 3.4: ***Stability of ET-1 (●) and big ET-1(○) released from A549 cells incubated with (A) phosphoramidon and (B) phosphoramidon in combination with inhibitor cocktail over 24 h.*** *Cells were grown to confluence on 24-well plates and incubated for 24 h in the presence of increasing concentrations of phosphoramidon (10 – 1000 μM) alone and in presence of inhibitor cocktail. Mean ± s.e.m, from two experiments performed in duplicates were expressed as fmol/ml. * = P <0.05, ** = P <0.01, and *** = P <0.001 comparison of means to basal release of ET-1 by ANOVA. Basal release of ET-1 and big ET-1 was 557 fmol/ml per 24 h and 20.1 fmol/ml per 24 h, respectively.*

3.3.3 Stability of proendothelin-1 peptides (proET-1): NT-proET-1, ELDP and CT-proET-1 released from EA.hy 926 cells

Firstly, EA.hy 926 cells were incubated with increasing concentrations of phosphoramidon (1 – 1000 µM) over 6 h and 24 h. ProET-1 peptides were measured by immunoassays for NT-proET-1 (ppET-$1_{[18-50]}$), ELDP (ppET-$1_{[93-166]}$) and CT-proET-1 (ppET-$1_{[169-212]}$). Release of proET-1 peptides were unaffected by phosphoramidon, indicating that endogenously released proET-1 peptides are fairly stable in the conditioned medium of EA.hy 926 cells (Table 3.2).

Table 3.2: ***Effect of phosphoramidon on NT-proET-1, ELDP and CT-proET-1 in the conditioned medium of EA.hy 926.*** *Cells were grown to confluence on 24-well plates and incubated for 24 h in the presence of increasing concentrations of phosphoramidon (0 – 1000 µM). Mean results ± s.e.m (n = 3) were expressed as a percentage of the control values and each experiment was conditioned in triplicates. Basal release (n = 5) of NT-proET-1, ELDP and CT-proET-1 was 294 fmol/ml, 1389 fmol/ml, and 334 fmol/ml over 24 h incubation.*

Phosphoramidon (µM)	EA.hy 926, 24 h conditioned medium (% of control)		
	NT-proET-1	ELDP	CT-proET-1
0	100 ± 2.9	100 ± 8.7	100 ± 5.1
1	92.0 ± 1.7	107.0 ± 6.6	102.9 ± 3.9
3	95.8 ± 1.6	114.4 ± 6.7	107.1 ± 6.7
10	91.9 ± 2.0	115.8 ± 8.9	104.9 ± 7.0
30	95.2 ± 1.9	105.3 ± 6.7	100.1 ± 8.8
100	103 ± 6.4	107.5 ± 8.3	109.9 ± 10.5
300	96.0 ± 3.5	106.7 ± 8.0	111.5 ± 8.3
1000	87.9 ± 1.7	103.1 ± 10.2	104.9 ± 8.6

Secondly, Table 3.3 summarises the effect of inhibitor cocktail with and without 10 µM phosphoramidon. Incubation with inhibitor cocktail did not show a significant effect over 6 h except slight inhibition of NT-proET-1 released into the conditioned medium of EA.hy 926 cells (data not shown). However, proET-1 peptides were inhibited to a greater extent over 24 h. This inhibition was greatest for NT-proET-1, followed by ELDP and CT-proET-1 at approximately 28% (P <0.001), 23% (P <0.001) and 9%, respectively. Similarly, 10 µM phosphoramidon in combination with inhibitor cocktail inhibited NT-proET-1 and ELDP release at a similar magnitude to that of inhibitor cocktail alone. However, CT-proET-1 levels were unaffected by 10 µM phosphoramidon with inhibitor cocktail and the levels were relatively close to control. Interestingly, proET-1 peptides accumulated slightly with 10 µM phosphoramidon, which increased NT-proET-1, ELDP and CT-proET-1 levels by 8% (P = 0.02), 5% and 11%, respectively.

Table 3.3: ***Effect of phosphoramidon and inhibitor cocktail on NT-proET-1, ELDP and CT-proET-1 in the conditioned medium of EA.hy 926.*** *Cells were grown to confluence on 24-well plates and incubated for 24 h in the presence of treatment conditions (10 µM phosphoramidon, inhibitor cocktail, and a combination of 10 µM phosphoramidon and inhibitor cocktail). Mean results ± s.e.m from two experiments that were conditioned in triplicates was expressed as a percentage of the control values. * = P <0.05 comparison of means to control by ANOVA.*

EA.hy 926, 24 h conditioned medium (% of control)	NT-proET-1	ELDP	CT-proET-1
Control, (DMEM+ only)	100 ± 1.0	100 ± 1.1	100 ± 1.1
10 µM Phosphoramidon	107.5 ± 3.1*	104.5 ± 4.1	110.8 ± 1.6
Inhibitor cocktail	72.3 ± 3.3*	76.7 ± 2.2*	90.9 ± 2.1
10 µM Phosphoramidon and inhibitor cocktail	72.3 ± 1.4*	81 ± 3.2*	99.7 ± 4.1

Although some of these reductions reached significance, the synthesis or degradation of proET-1 peptides was largely unaffected with either of incubations with phosphoramidon, inhibitor cocktail with and without phosphoramidon suggesting that they are fairly stable in the conditioned medium released from EA.hy 926 cells.

3.3.4 Stability of proET-1 peptides: NT-proET-1, ELDP, and CT-proET-1 released from A549 cells

Once again, incubation with phosphoramidon had no effect on proET-1 peptide synthesis (Table 3.4). This in turn suggested that proET-1 peptides released in the conditioned media of both EA.hy 926 and A549 cells were fairly stable. Although increasing phosphoramidon concentrations (10 – 1000 µM) did not show a concentration dependent proET-1 inhibition, CT-proET-1 levels slightly accumulated at 10 µM phosphoramidon by 4% and 15% at 1000 µM over 24 h (Table 3.4).

Table 3.4: ***Effect of phosphoramidon on NT-proET-1, ELDP and CT-proET-1 in the conditioned medium of A549 cells.*** *Cells were grown to confluence on 24-well plates and incubated for 24 h in the presence of increasing concentrations of phosphoramidon. Mean results ± s.e.m from two experiments conditioned in duplicates were expressed as a percentage of the control values. Basal release (n = 4) of NT-proET-1, ELDP and CT-proET-1 was 555 fmol/ml, 1212 fmol/ml, and 279 fmol/ml over 24 h incubation.*

Phosphoramidon (µM)	A549, 24 h conditioned medium (% of control)		
	NT-proET-1	ELDP	CT-proET-1
0	100 ± 1.2	100 ± 1.9	100 ± 3.5
10	95.8 ± 1.6	98.5 ± 2.7	103.9 ± 3.2
30	95.9 ± 0.7	97.9 ± 0.6	101.2 ± 3.0
100	87.9 ± 2.4	93.2 ± 4.5	102.2 ± 2.5
300	95.5 ± 4.2	103 ± 4.4	108.7 ± 4.5
1000	95.8 ± 2.9	100.1 ± 3.6	115.1 ± 1.2

On the other hand, incubation with inhibitor cocktail in the presence of increasing concentrations of phosphoramidon reduced the release of proET-1 peptide fragments. At 6 h incubation, while NT-proET-1 and ELDP were slightly inhibited, CT-proET-1 levels accumulated by 50% with 10 µM phosphoramidon with inhibitor cocktail (data

not shown). When A549 cells were incubated with this treatment over 24 h, accumulated CT-proET-1 was inhibited by 14% (Table 3.5). Increasing phosphoramidon concentrations did not inhibit the release of CT-proET-1. In comparison, NT-proET-1 and ELDP were inhibited more significantly by 62% and 41%, respectively.

Table 3.5: ***Effect of phosphoramidon and inhibitor cocktail on NT-proET-1, ELDP and CT-proET-1 in the conditioned medium of A549 cells.*** *Cells were grown to confluence on 24-well plates and incubated for 24 h in the presence of increasing concentration of phosphoramidon with inhibitor cocktail. Mean results ± s.e.m from two experiments conditioned in duplicates were expressed as a percentage of the control. * = P <0.05 comparison of means by ANOVA.*

Phosphoramidon and inhibitor cocktail (µM)	**A549, 24 h conditioned medium (% of control)**		
	NT-proET-1	**ELDP**	**CT-proET-1**
0	100 ± 1.3	100 ± 4.0	100 ± 1.8
10	37.6 ± 3.8*	58.6 ± 0.4	86.1 ± 1.3
30	41.7 ± 1.4*	62.0 ± 1.5	89.4 ± 4.7
100	42.4 ± 3.4*	56.0 ± 0.1	94.7 ± 2.1
300	43.2 ± 4.0*	59.0 ± 2.5	94.2 ± 2.5
1000	43.9 ± 2.9*	62.8 ± 2.8	93.5 ± 3.5

Although cytotoxic effects of phosphoramidon and inhibitor cocktail were not evaluated in this experiment, in other studies, incubation of A549 cells with inbibitor cocktail (without phosphoramidon) over 24 h resulted in 10% reduction in cell viability when compared to controls. The decreased proET-1 peptide levels observed with phosphoramidon with inhibitor cocktail may be explained by phosphoramidon increasing the cytotoxic effects of inhibitor cocktail. As a result, decrease in proET-1 levels most likely resulted from cytotoxicity rather than inhibition of ECE activity or proET-1 processing.

3.4 DISCUSSION

The aim of this chapter was to characterise the biosynthesis of proET-1 derived peptides from EA.hy 926 and A549 cells. The processing of proET-1 occurs via constitutive secretory vesicles (Harrison *et al.,* 1995) with release of ET-1 together with other fragments of proET-1 (Corder *et al.,* 1995). Previously unpublished pilot studies by our laboratory had shown processing of proET-1 to three peptides: NT-proET-1, ELDP, and CT-proET-1 (Figure 3.1). However, their parallel secretion and stability had not been studied. The proteolytic processing of ET-1 and proET-1 peptide fragments was therefore studied by treating EA.hy 926 and A549 cells with phosphoramidon and inhibitor cocktail and quantifying their release in the conditioned media using specific immunoassays. Synthetic peptides used for NT-proET-1 (ppET-$1_{[18-50]}$), ELDP (ppET-$1_{[93-166]}$) and CT-proET-1 (ppET-$1_{[169-212]}$) peptides do not have any sequence homology with the corresponding sequences of proET-2 and proET-3. Therefore, the assays developed have the advantage of being specific for measuring increased proET-1 synthesis.

Endogenous ET-1 production appeared to be biphasic in EA.hy 926 cells. Lower concentrations of phosphoramidon increased ET-1 levels in the medium samples such that ET-1 release appeared highest at 10 µM showing a 3 – 4-fold increase over 24 h (Figure 3.3). EA.hy 926 cells express NEP-24.11, which at phosphoramidon concentrations <1 µM degrades secreted ET-1 (Abassi *et al.,* 1993a). Phosphoramidon at 10 µM as well inhibiting ECE-1, it also inhibited NEP-24.11. It was shown to prevent degradation of ET-1 by NEP-24.11 at 1 µg/ml (Abassi *et al*., 1993a). The biphasic response of EA.hy 926 cells to phosphoramidon treatment was consistent with previous results (Corder *et al*., 1993b; Xu *et al.,* 1994; Ahn *et al.,* 1995). At higher concentrations of phosphoramidon there was a concentration-dependent inhibition of ET-1 release. Thus, at lower phosphoramidon concentrations ET-1 degradation is prevented then phosphoramidon starts to inhibit ET-1 synthesis at higher concentrations (>10 µM), when the stability of it was at its highest. Inhibition of ET-1 synthesis results in the accumulation of big ET-1 (Figure 3.2). In addition, phosphoramidon (0.01 – 2 mM) was shown to cause a biphasic alteration of ET-1 release in human aortic endothelial cells (Matsumura *et al.,* 1995). Similarly, at lower concentrations increased ET-1

accumulation could be due to inhibition of ET-1 degradation by NEP-24.11. The inhibition of ET-1 synthesis at higher phosphoramidon concentrations was compared to 10 µM phosphoramidon, at which the stability of ET-1 was at its highest. Therefore, when degradation of ET-1 was prevented in presence of 10 µM phosphoramidon, higher phosphoramidon concentrations (>10 µM) had a similar degree of inhibition of ET-1 release over 6 h and 24 h. In addition, others also reported that higher phosphoramidon concentrations were required for intracellular inhibition of ECE (Corder, 2001; Woods *et al.,* 1999). Thus, processing of big ET-1 is, at least in part, intracellular and occurs during vesicle transport from the trans-Golgi network to the cell surface by the constitutive secretory pathway (Harrison *et al.,* 1995; Russel *et al.,* 1998)). This was supported by findings showing localisation of ECE-1 in the membranes of intracellular organelles such as Golgi apparatus (Xu *et al.,* 1994; Barnes *et al.,* 1998; Russel *et al.,* 1998), where it could catalyse the endogenous synthesis of ET-1.

In contrast to the biphasic behaviour of EA.hy 926 cells, phosphoramidon produced a concentration-dependent inhibition of ET-1 synthesis and accumulation of big ET-1 in the conditioned medium of A549 cells (Figure 3.4A). Consistent with phosphoramidon acting as an ECE inhibitor, inhibition of ET-1 synthesis in A549 cells has also been reported by Deprez-Roy *et al.,* 2000. The absence of a biphasic response in this cell line is likely due to the absence of the confounding effects of NEP-24.11 expression (Aubert *et al.,* 1998). Phosphoramidon in combination with inhibitor cocktail was more effective in suppressing ET-1 levels over 24 h (Figure 3.4B). This suggested that inhibitor cocktail might increase the stability of phosphoramidon to have a greater effect in combination. This might be expected to result in a greater increase in big ET-1 levels with phosphoramidon in combination with inhibitor cocktail. However, phosphoramidon alone produced a greater increase in big ET-1 in the conditioned medium of A549 cells (Figure 3.4A). Cell viability assay (MTT), however, showed cytotoxicity of inhibitor cocktail on A549 cells over 24 h incubation. Therefore, reduced release of ET-1 and proET-1 fragments is likely to result from cytotoxicity induced by inhibitor cocktail components rather than inhibition of ECE activity.

Immunoassay results showed that unlike ET-1; NT-proET-1, ELDP and CT-proET-1 released in the conditioned medium of EA.hy 926 cells were unaffected by phosphoramidon treatment (Table 3.2). This implies that at physiological concentrations none of these peptides are degraded by NEP-24.11. In addition, these data suggest that intracellular processing of proET-1 at double basic amino acids is not affected by inhibition of ECE by the metalloprotease inhibitor phosphoramidon. For the three proET-1 peptides investigated, only NT-proET-1 showed a slight reduction whereas ELDP and CT-proET-1 levels were increased slightly (neither were significant changes). Similarly in A549 cells, phosphoramidon had no significant effect on proET-1 peptide levels (Table 3.4). Thus, proET-1 peptides are fairly stable in the conditioned media samples. Hence, phosphoramidon selectively inhibits ECE without affecting proET-1 processing at double basic residues.

The inhibitor cocktail alone or in combination with phosphoramidon over 24 h suppressed proET-1 peptide levels slightly for EA.hy 926 cells when compared to treatment with phosphoramidon alone. However, there was a more marked reduction with A549 cells. In both cell lines a greater reduction with inhibitor cocktail was observed for NT-proET-1 and ELDP than CT-proET-1. These results indicate that for proET-1 peptides released into the conditioned media of EA.hy 926 and A549 cells CT-proET-1 is the most stable, while NT-proET-1 is the least stable peptide. Therefore, these peptide fragments could be alternative and more stable markers of ET-1 synthesis. However, another point to note is that in the conditioned media samples ELDP had the highest concentration of any proET-1 peptide (EA.hy 926 cells 1389 fmol/ml after 24 h, without inhibitors present). ET-1 (for EA.hy 926 cells in the presence of 10 µM phosphoramidon), big ET-1 (EA.hy 926 cells in the presence of 1000 µM phosphoramidon), NT-proET-1 and CT-proET-1 were of the same order of magnitude (~340 fmol/ml after 24 h, without inhibitors present). Whereas, ELDP concentrations were approximately 4-fold higher. Peptide standard concentrations had been carefully matched by using HPLC quantification of synthetic peptides based on A_{280} absorbing residues (Trp and/or Tyr). Therefore other factors affecting stability or clearance (e.g. ET_B-receptor clearance of ET-1) must come into play during these prolonged incubation periods.

Thus it is important to define the optimal fragments of proET-1 for development of the most sensitive and specific diagnostic assay for inferring an elevated level of ET-1

synthesis, which could then be used to guide or optimise treatment. These proET-1 peptide fragments have been identified only by antibody cross-reactivity. Therefore, a detailed characterisation with HPLC and identification using mass spectrometry was considered essential and these studies are described in Chapters 4 and 5, respectively. In addition, the stability of proET-1 peptides, both *in vivo* and *ex vivo,* and their diagnostic utility in patient samples were evaluated in Chapter 6.

CHAPTER 4

Purification and characterisation of proendothelin-1 fragments

4.1 INTRODUCTION

Initial studies showed that three proET-1 fragments: NT-proET-1 ($ppET\text{-}1_{[18\ -\ 50]}$); Endothelin-Like Domain Peptide, ELDP ($ppET\text{-}1_{[93\ -\ 166]}$); and C-terminal fragment, CT-proET-1 ($ppET\text{-}1_{[169-212]}$) were secreted from endothelial (EA.hy 926) and epithelial (A549) cells (Chapter 3). This chapter focuses on purification and characterisation of proET-1 peptides from conditioned media collected from EA.hy 926 and A549 cells.

4.1.1 Types of separation methods

Proteins can be fractionated using different types of chromatography techniques, which include gel filtration (size-exclusion chromatography), ion-exchange chromatography (IEC), hydrophobic interaction chromatography (HIC), and high performance liquid chromatography (HPLC). Separations are based on their physiochemical properties such as molecular size, net charge, and hydrophobicity, respectively (Burgess, 2008; Queiroz *et al.*, 2001). Other protein fractionation methods such as ammonium sulphate [$(NH_4)_2SO_4$] precipitation, isoelectric point focusing, dialysis and ultrafiltration can also be used for separation of proteins. Ammonium sulphate precipitation, IEC and HPLC were among the methods that were used for protein fractionation, purification and characterisation, respectively. These methods are briefly explained here.

4.1.1.1 *Ammonium sulphate precipitation*

The separation of proteins by ammonium sulphate precipitation is based on their solubility; proteins and other macromolecules become progressively less soluble and tend to aggregate and precipitate out of solution with increasing salt concentration. In other words proteins are "salted out". Ammonium sulphate precipitation is often performed as a preliminary step in protein purification either to clean up samples by removal of large molecular weight (MWt) poorly soluble proteins, or to prepare an enriched protein precipitate for chromatography. Removal of ammonium sulphate may be necessary before proceeding to subsequent chromatography methods for purification. Dialysis can be used as a desalting or buffer exchange step, but this increases the sample volume due to an osmotic effect, and is only useful for peptides or proteins that exceed the MWt cut-off for the pore size of the dialysis membrane.

4.1.1.2 *Ion exchange chromatography (IEC)*

Separation of proteins by IEC is based on charge mainly through electrostatic interactions between charged amino acid side chains exposed to the surface of a protein that bind to oppositely charged ligands. Anion exchangers have basic functional groups, which can be either weak or strong. Quaternary ammonium (Q) is an example of a strong anion exchanger with a functional group of $–O\text{-}CH_2N^+\text{-}(CH_3)_3$. Negatively charged side chains (aspartic acid [pKa 3.86] and glutamic acid [pKa 4.25] both with carboxylic acid groups) of proteins bind to anion exchangers, while positively charged side chains (lysine [amino group, pKa 10.79], arginine [guanadino group, pKa 12.48] and histidine [imidazole group, pKa 6.04]) bind to cation exchangers that contain acidic functional groups. These functional groups can be either weak or strong. Carboxymethy (CM) is an example of a weak cation exchanger with a $–O\text{-}CH_2COO^-$ functional group. A protein that has no net charge at a pH equivalent to its isoelectric point (pI) will not interact with a charged medium. However, at a pH *above* its pI, a protein will bind to an anion exchanger (positively charged ligand) and, at a pH *below* its pI, a protein will bind to a cation exchanger (negatively charged ligand). Advantages of using IEC include:

(1) Gradient elution with use of different salt and buffer compositions.

(2) Application to a large volume of sample, which can be used as a concentration step, to recover proteins from a dilute solution.

(3) High recoveries due to carrying out separations in smaller volumes.

(4) High resolving power (Stanton, 2004).

The disadvantages of IEC include: **(1)** application of sample to IEC matrix at a low ionic strength and controlled pH; **(2)** buffers used for elution may not be compatible with further chromatographic separations or assay systems [e.g. high salt concentrations (>1 M)] or guanidine hydrochloride (G-HCl). Thus an additional buffer exchange method may be required (Stanton, 2004).

4.1.1.3 *High performance liquid chromatography (HPLC)*

HPLC is a well-established technique that is used for purification, isolation and analysis of biomolecules. Separations are based on hydrophobicity, size and protein conformation. A high degree of selectivity can be achieved by using various modes of separation including reverse-phase [hydrophobic], normal-phase [hydrophilic], ion exchange, and size exclusion. The surface chemistry of a column is an important

determinant of the sample retention. In particular, characterisation of proET-1 fragments was performed using a reverse-phase HPLC (RP-HPLC) system, where the surface chemistry was based on silanol groups on the silica surface and bonded with alkyl chains (C4 [butyl] or C18 [octadecylsilane]). In RP-HPLC, separation of intact proteins is usually performed with wide pore size and shorter hydrocarbon chains in order to minimise protein denaturation or irreversible binding of the protein to the column. Hydrophobic proteins with longer amino acid sequences are retained strongly by longer alkyl chains and may not elute efficiently, resulting in poor recoveries. Adsorbed peptide or protein is eluted by the addition of an organic solvent (such as acetonitrile (CH_3CN) containing an ionic modifier like trifluoroacetic acid [TFA]) to the mobile phase where the gradient can be either isocratic or gradient elution. Adsorbed peptides are eluted in order of increasing molecular hydrophobicity. HPLC can be used for analysing protein identities such as identification of protein degradation products. For example, peptides that have an oxidised methionine residue can be separated from the native peptide. RP-HPLC is a very powerful technique for the analysis of peptides and proteins because of a number of factors that include:

(1) High resolving power with a wide selection of conditions and choice of columns enabling separation of closely related molecules as well as structurally distinct molecules based on differences in hydrophobicity or molecular conformation.

(2) The experimental ease with which mobile phase can be manipulated for selectivity.

(3) Stability of the sorbent materials under a wide range of mobile phase conditions.

(4) Robust and efficient systems that generally provide high recoveries with good reproducibility of repeated separations carried out over a long time period (Aguilar, 2003; Aguilar & Hearn, 1996; Benedek, 2004).

However, RP-HPLC can cause the irreversible denaturation of protein samples thereby reducing the potential recovery of material in a biologically active form (Aguilar, 2003).

4.1.2 Experimental and theoretical rationale

The aim of this chapter was to purify proET-1 peptides (NT-proET-1, ELDP and CT-proET-1) to obtain sufficient amount of each peptide for confirmation of their identities by mass spectrometry. Table 4.1 shows the amino acid composition, molecular weights and isoelectric points of proET-1 peptides. These parameters were considered in order to select methods and develop a strategy for purification. The workflow for proET-1 characterisation is summarised in Figure 4.1 and the methodology is described here;

(1) Ion exchange chromatography: Q-Sepharose anion exchanger was used to remove acidic peptides and proteins as well as phenol red present in the conditioned media (step 1). This was followed by using a carboxymethyl cation exchanger for the recovery of proET-1 fragments that had passed through the Q-Sepharose anion exchanger without absorption (step 2). Separation in these steps is based on differences in isoelectric points.

(2) After elution from the cation exchanger, CM fractions with the highest ELDP and CT-proET-1 immunoreactivity (section 4.3.1) were subjected to solid-phase extraction (SPE) for buffer exchange and concentration of these peptides prior to characterisation by HPLC (step 3).

(3) However, only low NT-proET-1 immunoreactivity was detected in the CM fractions, requiring additional steps for recovery of NT-proET-1. For EA.hy 926 cells, NT-proET-1 was recovered from the unadsorbed Q-Sepharose sample and 10 mM acetic acid washings by SPE (step 3).

(4) For A549 cells, ammonium sulphate precipitation at 20% saturation was used to remove impurities that blocked the column systems, described above for EA.hy 926 conditioned medium. SPE was used for buffer exchange and concentration for characterisation of proET-1 peptides from A549 cells by HPLC.

(5) Characterisation of fractionated ppET-1 peptide products by HPLC required two steps: semi-preparative (step 4) and analytical HPLC separation (step 5). Presence of proET-1 fragments and identification of fractions with the highest levels of immunoreactivity were achieved with sandwich immunoassays for NT-proET-1 (ppET-$1_{[18-50]}$), ELDP (ppET-$1_{[93-166]}$) and CT-proET-1 (ppET-$1_{[169-212]}$).

Table 4.1: ***Amino acid composition, molecular weights and isoelectric points of proendothelin-1 peptide fragments.*** *Amino acid numbering is based on the 212 amino acid sequence for ppET-1 (Bloch et al., 1989). Molecular weights and theoretical isoelectric points were calculated from the online server http://web.expasy.org/compute_pi/ and net charge at pH 7.0 was calculated from http://vitalonic.narod.ru/biochem/index_en.html.*

Proendothelin-1	Amino acid composition of proET-1 sequences	Molecular weight, MWt (avg):	Isoelectric point, pI	Net charge at pH 7.0	Number of residues
NT-proET-1 ppET-1$_{[18 – 50]}$	APETAVLGAELSAVGENGGEKPTPSPPWRLRRS	3,430.8	6.3	0.0	33
ELDP ppET-1$_{[93 – 166]}$	ALENLLPTKATDRENRCQCASQKDKKCWNFCQAGKEL RAEDIMEKDWNNHKKGKDCSKLGKKCIYQQLVRGRKI	8,642.1	9.4	8.1	74
CT-proET-1 ppET-1$_{[169 – 212]}$	SSEEHLRQTRSETMRNSVKSSFHDPKLKGKPSRERYVT HNRAHW	5,291.9	10.5	5.4	44

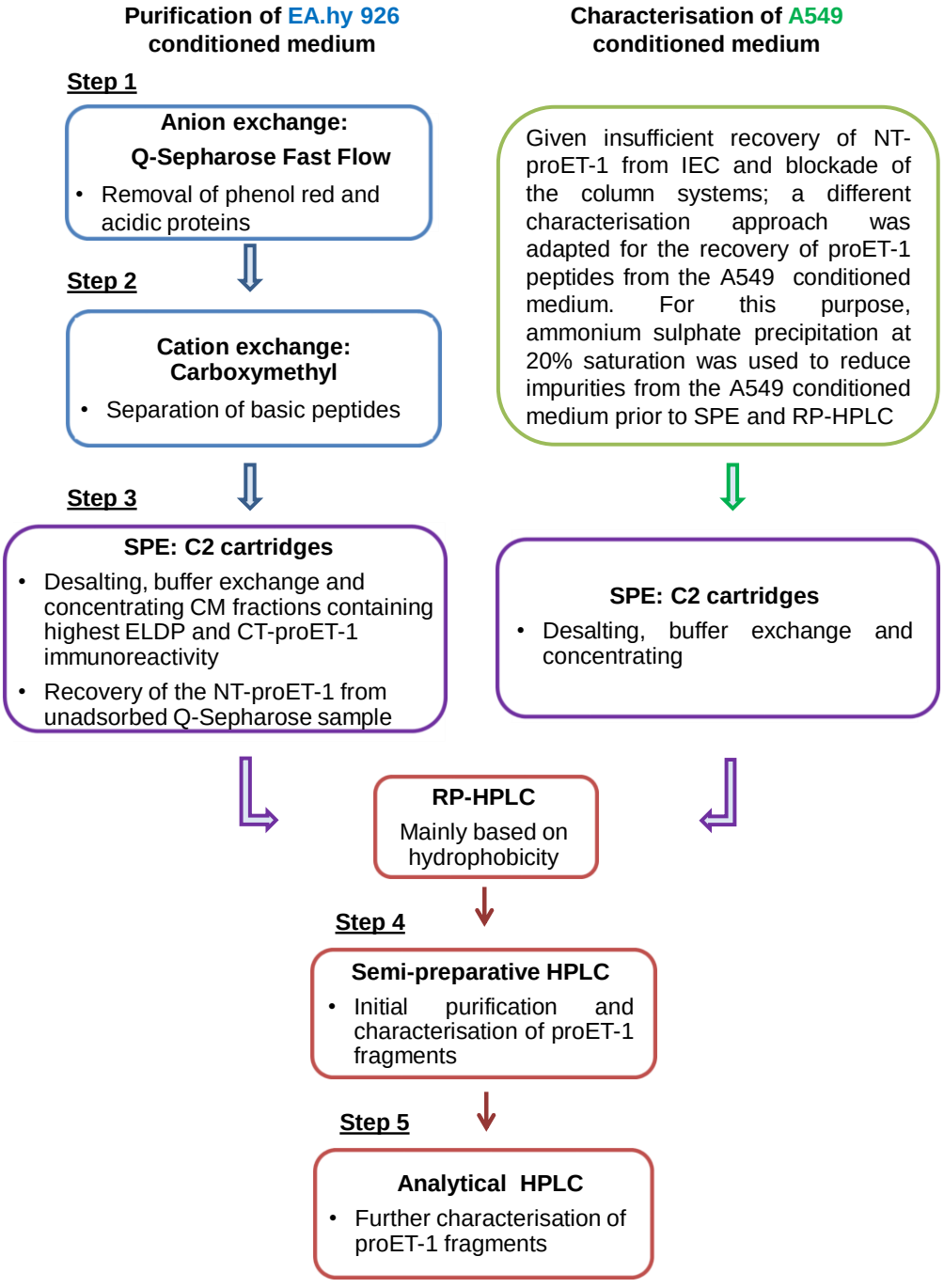

Figure 4.1: ***Approach to purification and characterisation of proET-1 peptides from the conditioned media from EA.hy 926 and A549 cells collected after 48 h incubation.***

4.2 METHODS

4.2.1 Collection of conditioned media for purification and characterisation of proET-1 peptides

Cell culture growth conditions of EA.hy 926 and A549 cells are described in Chapter 3, section 3.2.1. Subcultures of these human cell lines were prepared in four T175 cm^2 flasks at a 1:3 seeding dilution with DMEM supplemented with 4500 mg D-glucose/L, 25% 1 M HEPES and 1% penicillin/streptomycin (DMEM+) and 10% FCS (total volume 30 ml). This resulted in 90 – 100% confluent flasks after 4 – 5 days.

To purify and characterise ppET-1 peptide fragments, conditioned media from EA.hy 926 and A549 cells were collected from confluent cultures of these cell lines grown in four T175 cm^2 flasks, which had been incubated for 48 h at 37°C in a humidified CO_2 incubator (8% CO_2, 92% air). These flasks were washed with 30 ml of DMEM+ and incubated with media (25 ml media/flask), which consisted of DMEM supplemented with 4500 mg D-glucose/L without FCS, peptidase inhibitors or penicillin/streptomycin. After the incubation period, conditioned media was collected and centrifuged at 3000 *g* for 15 min at 4°C. The supernatant was then transferred into fresh tubes and stored at -80°C.

Conditioned medium (900 ml) collected from a total of 36 T175 cm^2 flasks was used for purification of proET-1 peptides from EA.hy 926 cells. The characterisation methodology used for the conditioned medium collected from A549 cells differed from the EA.hy 926 cells (Figure 4.1) and it is described in section 4.2.5.

4.2.2 Characterisation of proET-1 peptides from the EA.hy 926 conditioned medium using ion exchange chromatography

4.2.2.1 *Q-Sepharose Fast Flow columns as a strong anion exchanger*

Q-Sepharose gel was gently swirled and the gel slurry (6 ml) was transferred into 10 ml columns fitted with PTFE filters on a vacuum manifold (Alltech, Fisher Scientific). A small vacuum was applied to allow the gel to settle. The gel was rinsed with (10 ml) 10 mM acetic acid (CH_3COOH) before application of the sample. Conditioned medium (900 ml in DMEM) collected from EA.hy 926 cells after 48 h incubation was acidified with 1.25% CH_3COOH and centrifuged at 3,000 rpm at 4°C for 15 min. Pellets were

reconstituted in SAB and retained for immunoassay to confirm that there was no loss of proET-1 peptides. Supernatants were loaded in equal volumes (30 ml) on to 10 pre-equilibrated Q-Sepharose fast flow columns (6 ml swelled gel per column). The columns were then washed with 15 ml volumes of 10 mM CH_3COOH. Material recovered in the washes was pooled with the unadsorbed sample and then loaded on to a CM column. Q-Sepharose clean-up of EA.hy 926 cell medium followed by recovery of proET-1 peptides by CM ion exchange was performed in 3 batches (300 ml media per batch). Acidic peptides adsorbed on to the Q-Sepharose column were eluted with 15 ml 1 M NaCl containing 0.1 M G-HCl and subjected to immunoassay to confirm absence of proET-1 peptides.

4.2.2.2 *Cation exchange using carboxymethyl column*

Each unadsorbed pooled sample and washings from the Q-Sepharose columns (~45 ml per column) were loaded onto CM Fractogel weak cation exchanger column (2.8 ml) that had been equilibrated with 40 ml of 10 mM CH_3COOH. After loading samples, the columns were then rinsed with 10 ml of 10 mM CH_3COOH. This was combined with the unadsorbed sample from CM column and retained to verify proET-1 peptides had been adsorbed on the CM column. The CM columns were then eluted with increasing concentrations of NaCl and G-HCl (3 ml per elution step):

(1) 0.125 M NaCl,
(2) 0.25 M NaCl,
(3) 0.25 M NaCl + 0.1 M G-HCl,
(4) 0.5 M NaCl + 0.1 M G-HCl,
(5) 1 M NaCl + 0.1 M G-HCl
(6 – 11) 1 M NaCl + 0.5 M G-HCl

All fractions were assayed for NT-proET-1, ELDP and CT-proET-1 according to the immunoassay methodology described in Chapter 2, section 2.2.2.3 Tris-Base (0.55 M) was used to neutralise samples before assay (pH 7.0 – 7.5).

4.2.3 Concentration and desalting of proET-1 peptides

4.2.3.1 *Solid-phase extraction*

Sep-Pak C2 ethyl cartridges (500 mg, Waters) were used according to the manufacturer's instructions with sequential washing of the C2 silica matrix with 10 ml of 100% methanol for full penetration of particles (called priming), which was followed by washing with 10 – 15 ml of 80% acetonitrile, and then 0.1% TFA, prior to the addition of the sample that had been acidified with 0.1% TFA. Table 4.2 shows the C2 extraction procedure applied for proET-1 peptides.

Table 4.2: ***Solid-phase extraction procedure with C2 cartridges.***

Sample preparation	Acidify with 0.1% TFA, optimal pH 2.0
Priming and washing	10 ml, 100% methanol 10 – 15 ml, 80% acetonitrile 10 – 15 ml, 0.1% TFA
Sample addition	
Washing	5 ml, 0.1% TFA
Elution	2 x 2 ml, 80% CH3CN/0.1% TFA

4.2.4 Reverse Phase HPLC

HPLC was performed with a MERCK Hitachi L-6200 Intelligent Pump with 2 ml injection loop. Elution of endothelin-1 and proendothelin-1 fragments and other peptides was monitored at 280 nm using a Shimadzu SPD-6A UV detector. Chromatographic data were collected and processed by PRIME software. Fractions were collected using a Pharmacia LKB Helifrac fraction collector.

Before running the samples, the column was first flushed with 100% CH_3CN containing 0.1% TFA followed by equilibration with 0.1% TFA. Gradient elution was performed with monitoring of eluted peptides by measuring UV absorbance at 280 nm. All samples were filtered using 0.2 µm microcentrifuge filter tubes before injection. Once the column was equilibrated and a stable baseline was confirmed, the samples were injected manually on to the HPLC column.

4.2.4.1 *Semi-preparative RP-HPLC*

This was performed using a Jupiter® column (Phenomenex, Part Number: 00G-4169-N0) packed with butyl-bonded silica C4 with 300 Å pore size and 15 µm particle size (1 x 25 cm). The column was equilibrated with 0.1% TFA and subjected to gradient elution at a flow rate of 2 ml/min: 0 – 15% solvent B (80% CH_3CN with 0.1% TFA) over 2 min, followed by 15 – 60% B over 45 min and further increased to 100% B over 5 min and held at 100% B for 8 min. Following gradient elution the column was re-equilibrated at 0% B before running further samples or standards.

4.2.4.2 *Analytical RP-HPLC*

This was performed using ACE-5 C4-300 (Advanced Chromatography Technologies), 5 µm particle size with 300 Å pore size (4.6 x 250 mm). Samples were eluted at a flow rate of 1 ml/min using gradient of 0 – 10% solvent B (80% CH_3CN with 0.1% TFA) over 2 min, followed by 10 – 30% B over 50 min and further increased to 100% B by 70 min and held at 100% B for another 5 min. After gradient elution the column was re-equilibrated at 0% B before running further samples or standards.

Purified NT-proET-1, ELDP and CT-proET-1 immunoreactivity for both HPLC steps were assessed in aliquots of fractions after they were completely dried under a stream of N_2 at 30°C and reconstituted with 300 µl of SAB.

4.2.5 Characterisation of proET-1 peptides from the A549 conditioned medium

The approach described above for isolating proET-1 peptides from medium collected from EA.hy 926 cells did not work for conditioned medium from A549 cells because of a high level of shed membrane particles that readily blocked the chromatography columns. To overcome this conditioned media was treated to remove these membrane particles. Previous $(NH_4)_2SO_4$ precipitation experiments showed that at 90% saturation proET-1 fragments were precipitated, while at 20% saturation immunoreactivities of NT-proET-1, ELDP and CT-proET-1 could not be detected in the reconstituted precipitates, showing these peptides remained in the supernatant. Thus, $(NH_4)_2SO_4$ precipitation at 20% saturation was used as an intermediate step to remove impurities from the A549 conditioned medium.

4.2.5.1 *Ammonium sulphate precipitation of A549 conditioned medium*

Conditioned medium (20 ml) collected after 48 h incubation with A549 cells was acidified with 0.2 M CH_3COOH to pH 4.0 before the addition of $(NH_4)_2SO_4$ to 20% saturation [2.12 g $(NH_4)_2SO_4$ for 20 ml acidified conditioned medium = 20% saturation]. Acidified conditioned medium was centrifuged at 20,000 rpm for 40 min at 4°C using a Beckman ultracentrifuge (rotor type 70ITI). After the centrifugation step, 0.1% TFA was added to the supernatant (pH 4.0) prior to loading on to a primed SPE C2 cartridge. C2 extraction was carried out as described in Table 4.2 using a vacuum manifold. The peptides were eluted with 2 x 2 ml of 80% CH_3CN containing 0.1% TFA. After applying a stream of N_2 to concentrate the sample, fractions were subjected to NT-proET-1, ELDP and CT-proET-1 immunoassays. Concentrated eluates (1.5 ml) were filtered through 0.2 µm pore size 1.5 ml microcentrifuge tubes and the resultant filtrate was injected onto analytical RP-HPLC (ACE-5 C4-300 column: 5 µm, 4.6 x 250 mm) using the same gradient as described in section 4.2.4.2.

4.2.6 HPLC analysis of synthetic proET-1 peptide standards

Synthetic standards of NT-proET-1 (70 nmol/ml), ELDP (85 nmol/ml) and CT-proET-1 (59 nmol/ml) were diluted (20 µl of each proET-1 peptide) into 1.5 ml of 0.2% formic acid (at a final concentration of 1.4, 1.7 and 1.2 nmol, respectively) and subjected to analytical RP-HPLC (C4 300 Å, 5 µm, 4.6 x 250 mm). The elution position of synthetic standards was only assessed on analytical RP-HPLC monitoring absorbance at 280 nm and by immunoassay. To avoid cross-contamination of purified peptides this was done after samples from conditioned media had been run.

For comparison, NT-proET-1, ELDP and CT-proET-1 standards in quantities similar to those being purified from conditioned media samples were diluted (20 µl) in DMEM (10 ml) at final concentrations of 140, 170 and 120 pmol/ml, respectively. Acidified with 0.1% TFA and extracted on SPE C2 cartridges. After partially drying to remove CH_3CN, filtered eluate was loaded on to analytical RP-HPLC (C4, 5 µm 4.6 x 250 mm) and elution positions of proET-1 fragments were verified by immunoassay.

4.3 RESULTS

4.3.1 Initial purification and characterisation of proET-1 peptide fragments by carboxymethyl ion exchange chromatography

The initial purification step from the EA.hy 926 conditioned medium was carried out using a strong anion exchanger, Q-Sepharose fast flow column (section 4.2.2.1). This was used to remove low MWt contaminants (e.g. phenol red) and acidic proteins from the conditioned medium. Acidic proteins bound to the anion exchanger were eluted with 3 ml of 1 M NaCl containing 0.1 M G-HCl.

Unadsorbed basic proteins including the washes were then loaded on to a weak cation exchanger CM Fractogel column. The CM column was eluted with increasing concentrations of NaCl (ionic strength) and G-HCl (competing cation) concentration. Counter ions (Na^+) in NaCl containing G-HCl displaces the adsorbed peptides from the binding sites in order of their net charge. ProET-1 peptides eluted from the CM IEC were measured by using immunoassays for NT-proET-1, ELDP and CT-proET-1. However, efficient recovery of NT-proET-1 immunoreactivity from EA.hy 926 medium was not achieved using CM IEC.

NT-proET-1 immunoreactivity was mainly present in the unadsorbed pooled sample that had passed through Q-Sepharose column, and then through the CM Fractogel column, indicating inefficient binding of this peptide to the CM column. The mean levels of NT-proET-1 from the three batches of EA.hy 926 conditioned medium processed in this way were 12.6 ± 0.1 fmol/ml. As a result, the unadsorbed pooled sample from Q-Sepharose and CM Fractogel columns was used for the isolation and purification of NT-proET-1 from the EA.hy 926 conditioned medium (section 4.3.2.2).

Both ELDP and CT-proET-1 were mainly eluted in CM fractions 3 – 5 and 6 – 8, which corresponded to an increase in both ionic strength (4 – 5) and competing cation concentration (5 – 6). Therefore, proET-1 peptides mainly eluted according to their isoelectric points (NT-proET-1 [pI 6.3], ELDP [pI 9.4] and CT-proET-1 [pI 10.5]) however, without resolution between ELDP and CT-proET-1 peptides. From EA.hy 926 cells, ELDP levels measured from the pooled fractions 4 – 5 and 6 – 8 were 11.7 and 13.8 pmol/ml, respectively. The recoveries of ELDP and CT-proET-1 from the CM fractions were 57% and 72%, respectively.

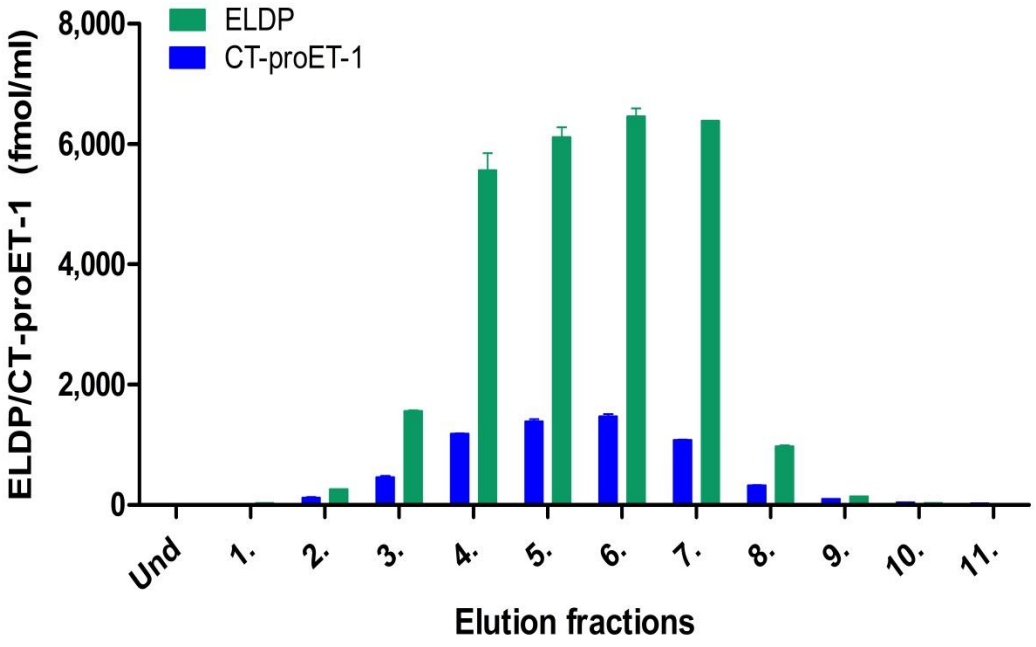

Figure 4.2: ***Carboxymethyl IEC of EA.hy 926 conditioned medium showing elution of ELDP and CT-proET-1 immunoreactivity.*** *Results from a representative batch of 300 ml of conditioned medium loaded onto ten CM fractogel columns after Q-Sepharose pre-treatment. Each CM column was washed with 10 mM acetic acid (10 ml/column) to remove unbound material* ***(Und)****, and then eluted with 3 ml of the following conditions.* ***(1):*** *0.125 M NaCl,* ***(2):*** *0.25 M NaCl,* ***(3):*** *0.25 M NaCl + 0.1 M G-HCl,* ***(4):*** *0.5 M NaCl + 0.1 M G-HCl,* ***(5):*** *1 M NaCl + 0.1 M G-HCl,* ***(6 – 11):*** *1 M NaCl + 0.5 M G-HCl. ELDP and CT-proET-1 were measured by immunoassays; the mean concentrations per fraction for each peptide are indicated.*

4.3.2 Purification and characterisation of NT-proET-1, ELDP and CT-proET-1 using HPLC

4.3.2.1 *EA.hy 926 conditioned medium fractions*

Carboxymethyl IEC fractions containing the highest amounts of ELDP and CT-proET-1 were pooled together (4 – 5 and 6 – 8). These pooled fractions were acidified with 0.1% TFA (pH 2.0) and loaded onto primed C2 cartridges. Adsorbed peptides were eluted with 2 ml of 80% CH_3CN containing 0.1% TFA. Eluates were then concentrated by a gentle stream of N_2 gas to ~400 µl. In order to remove any particulate material before loading on to a semi-preparative RP-HPLC system (Jupiter C4 column, 15 µm, 300 Å and 1 x 25 cm), the concentrated eluate was filtered through 0.2 µm microcentrifuge tubes. Using this semi-preparative HPLC system, the pooled concentrated and filtered eluates were run separately from each other (fractions 4 – 5 and 6 – 8), with two runs per pooled fraction. The column was eluted with a gradient of CH_3CN containing 0.1% TFA at a flow rate of 2 ml/min. Immunoassay of fractions for ELDP and CT-proET-1 showed adequate resolution of the two peptides (Table 4.3), allowing each peptide to be chromatographed separately in subsequent analytical HPLC steps.

Table 4.3: ***Semi-preparative HPLC analysis of EA.hy 926 ELDP and CT-proET-1 from CM IEC.*** *Peak fractions eluted from CM IEC (4 – 5 and 6 – 8) were extracted using C2 columns. Eluted samples were concentrated, pooled as indicated and subjected to semi-preparative RP-HPLC column (Jupiter C4 300 Å, 15 µm, 1 x 25 cm). Collected fractions (2 ml/min) were immunoassayed for ELDP and CT-proET-1.*

Semi-preparative HPLC analysis			
HPLC runs	**CM fractions**	**ELDP**	**CT-proET-1**
1	4 – 5	26 – 27	22 – 23
	6 – 8	25 – 28	22 – 23
2	4 – 5	25 – 27	20 – 21
	6 – 8	25 – 27	21 – 22

Fractions corresponding to peak ELDP and CT-proET-1 immunoreactivity (Table 4.3) were pooled and concentrated under N_2 and filtered using 0.2 µm filters for further purification using the analytical HPLC procedure (C4 column: 5 µm, 4.6 x 250 mm). Collected fractions (1 ml/min) were assayed for ELDP and CT-proET-1.

Analytical HPLC provided better resolution between ELDP and CT-proET-1 peptides. Peak fractions of CT-proET-1 were identified in fractions 27, 28 and 31, whereas ELDP was eluted in fractions 43 and 47 (Figure 4.3A – B).

4.3.2.2 *Recovery of NT-proET-1 from the EA.hy 926 conditioned medium*

NT-proET-1 peptide in conditioned medium from EA.hy 926 cells did not bind to the CM IEC system but was identified in the unadsorbed sample and 10 mM acetic acid wash. To recover NT-proET-1 for further characterisation and to concentrate this dilute sample [1350 ml sample (900 ml EA.hy 926 conditioned medium + 450 ml 10 mM acetic acid wash)], it was subjected to SPE with C2 cartridges. Eluates from the C2 extraction were further concentrated by N_2, filtered using 0.2 µm microcentrifuge tubes before loading on to the semi-preparative RP-HPLC system. The conditions of the semi-preparative HPLC separation were as described for ELDP and CT-proET-1 peptides in section 4.3.2.1. Peak NT-proET-1 immunoreactivity from the semi-preparative HPLC separation was detected in fractions 27 – 29 (data not shown). These fractions were pooled and concentrated with a stream of N_2, filtered and subjected to analytical HPLC. NT-proET-1 immunoreactivity from the analytical HPLC was eluted in fraction 41 (Figure 4.3C).

Synthetic proET-1 standards NT-proET-1, ELDP, and CT-proET-1 were subjected to analytical RP-HPLC (at 1.4, 1.7 and 1.2 nmol, respectively) and their elution positions were verified by monitoring A_{280} and by immunoassay. NT-proET-1, ELDP and CT-proET-1 synthetic standards were eluted at fractions 46, 45 and 28, respectively. Elution positions are indicated by the marked arrows (Figure 4.3).

Comparison of HPLC profiles obtained from synthetic peptides with those of the native proET-1 peptides extracted and purified from EA.hy 926 conditioned medium showed that ELDP and CT-proET-1 synthetic peptides were eluted (fraction 28 for CT-proET-1 and fraction 45 for ELDP) at very close proximities to the native proET-1 peptides (fractions 28, 29 and 31 for CT-proET-1 and fractions 43 and 47 for ELDP). However, the elution profile of ELDP and CT-proET-1 was heterogeneous, which suggest some degree of post-translational modification during purification.

NT-proET-1 synthetic standard (fraction 46) did not co-elute at the same position as the native peptide (fraction 41) that was extracted from the EA.hy 926 conditioned medium. Earlier elution of the native NT-proET-1 peptide in comparison to the synthetic peptide suggested that it may be less hydrophobic.

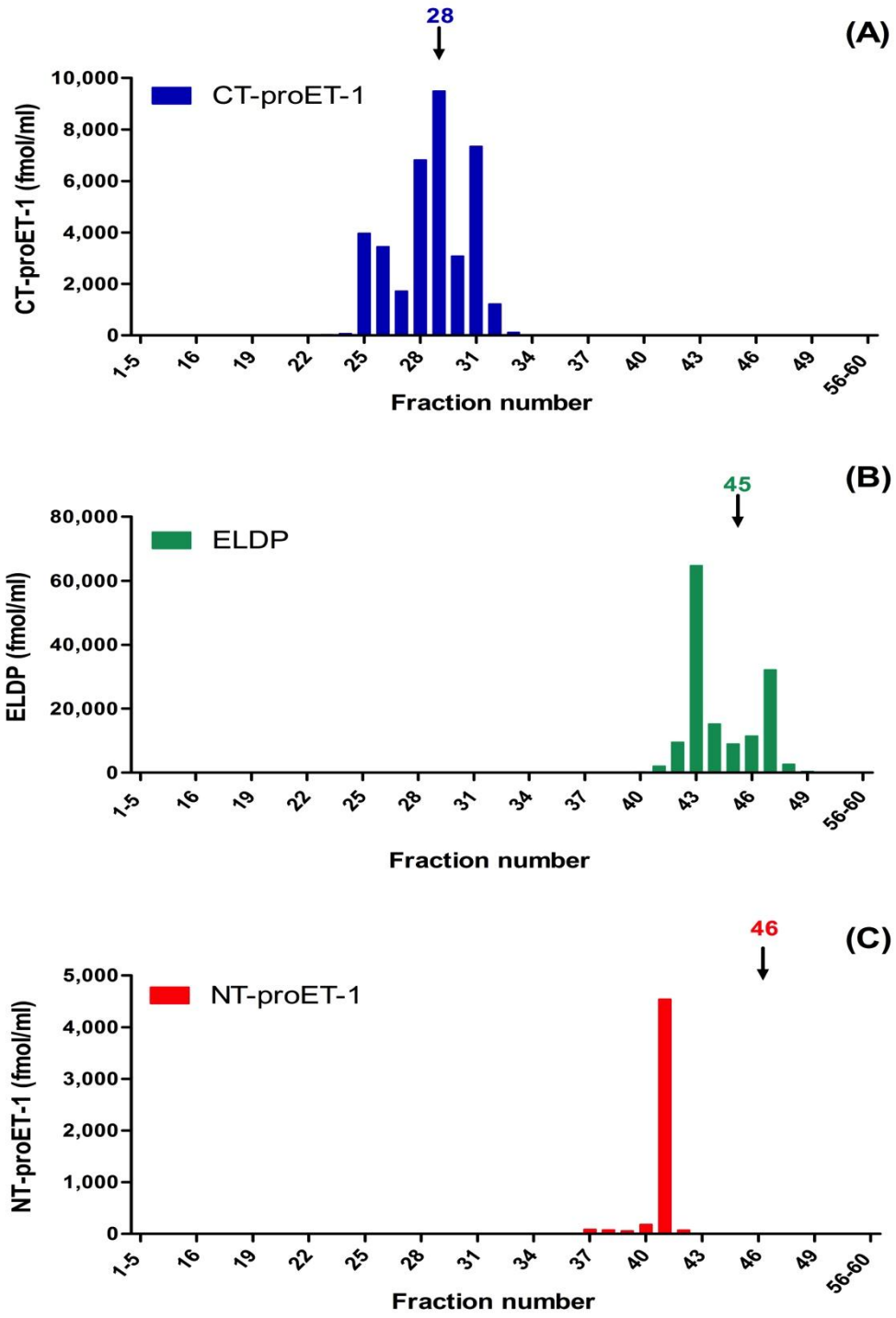

Figure 4.3: ***Analytical HPLC characterisation of proET-1 peptides from EA.hy 926 (A) CT-proET-1, (B) ELDP and (C) NT-proET-1.*** *Peak fractions of CT-proET-1, ELDP and NT-proET-1 from semi-preparative RP-HPLC column (C4 300 Å, 15 µm, 1 x 25 cm) were pooled and subjected to separate analytical RP-HPLC analyses (C4 300 Å, 5 µm, 4.6 x 250 mm). Arrows mark the elution positions of synthetic CT-proET-1, ELDP and NT-proET-1, which eluted in fractions 28, 45 and 46, respectively.*

4.3.2.3 *Characterisation of proET-1 peptides from the A549 conditioned medium*

Characterisation of proET-1 peptides from A549 conditioned medium was problematic. Impurities such as lipoproteins and other lipid material released into the conditioned medium blocked the Q-Sepharose and CM Fractogel IEC columns. This is likely due to cell membrane shedding of microvesicles by tumour cells in culture (Muralidharan-Chari *et al.,* 2010). Thus, to allow further characterisation of proET-1 peptides using HPLC, an alternative approach using $(NH_4)_2SO_4$ precipitation was employed to remove contaminants released from A549 cells into the conditioned medium.

Conditioned medium from A549 cells was subjected to $(NH_4)_2SO_4$ precipitation at 20% saturation to remove particulate material (see section 4.2.5.1). The supernatant was extracted on SPE C2 cartridges, and adsorbed proET-1 peptides were eluted with 80% CH_3CN containing 0.1% TFA. Immunoassays of NT-proET-1, ELDP and CT-proET-1 showed efficient recoveries for all proET-1 fragments. The recovery of NT-proET-1 from SPE was 84%, while ELDP and CT-proET-1 recoveries were ~100%. Eluates were concentrated, pooled together and filtered before subjecting to analytical RP-HPLC (C4 column, 5 µm, 4.6 x 250 mm). Peak fractions of NT-proET-1, ELDP and CT-proET-1 were eluted in 34 – 35, 37 – 40 and 21 – 24, respectively (Figure 4.4), corresponding to 65%, 89%, and 47% recoveries in comparison to C2 extraction. NT-proET-1 and ELDP eluted as single peaks. The elution profile of CT-proET-1 however, showed some heterogeneity with a double peak.

Synthetic peptide standards of NT-proET-1, ELDP and CT-proET-1 were diluted in DMEM and extracted in the same way as previously described for the A549 conditioned medium. Eluates were run on the analytical HPLC and their elution positions were verified by immunoassay. NT-proET-1 and ELDP eluted in the same fractions 43 – 44, while CT-proET-1 eluted in fractions 27 – 28. Hence, proET-1 peptides extracted from the conditioned medium of A549 cells did not closely correspond with the elution positions of the synthetic standards. However, the synthetic standards for ELDP and CT-proET-1 both eluted six fractions later in gradient. NT-proET-1 (43 – 43) on the other hand, was eluted more distant from the native peptide (34 – 35). Elution positions of synthetic peptides were almost identical to the previous calibration of this column after analytical HPLC of peptides isolated from EA.hy 926 conditioned medium. One explanation for the earlier elution of peptides extracted from A549 conditioned medium

is that column had been overloaded with the extracted sample, which underwent limited pre-fractionation before analytical HPLC. The elution characteristics of the column may have been modified by contaminating materials from the conditioned medium so that the column efficiency was compromised. For NT-proET-1, differences between the native and synthetic standards likely contributed to the marked difference in elution times.

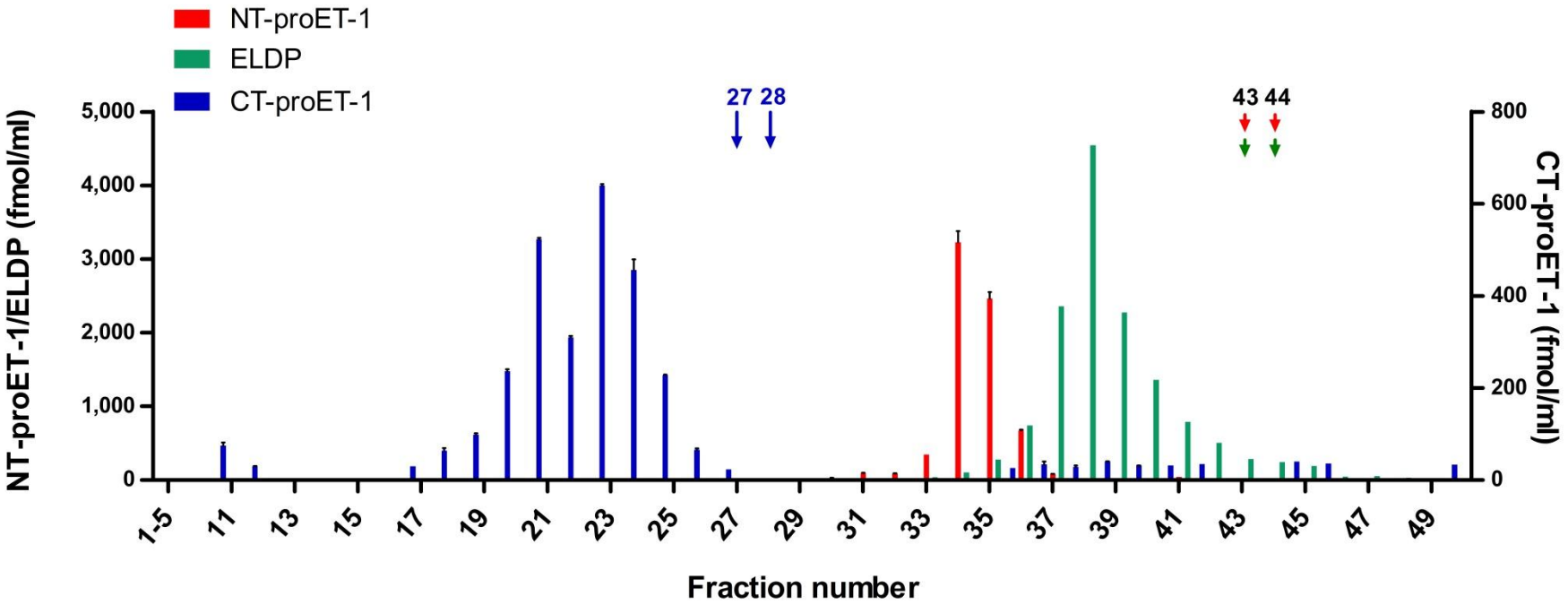

Figure 4.4: ***Analytical HPLC chromatogram showing characterisation of NT-proET-1, ELDP and CT-proET-1 from conditioned medium of A549 cells.*** *A549 conditioned medium was acidified with 0.2 M CH_3COOH to pH 4.0. $(NH_4)_2SO_4$ was added to 20% saturation and centrifuged at 20,000 rpm for 40 min at 4°C. Supernatant was extracted on a C2 cartridge, proET-1 peptides were eluted with 80% CH_3CN containing 0.1% TFA (2 x 2 ml), and concentrated to ~400 µl before analytical RP-HPLC (C4 300 Å, 5 µm, 4.6 x 250 mm). ProET-1 fragments were detected using immunoassays for NT-proET-1, ELDP and CT-proET-1. Arrows marking fractions 27 – 28, indicate the elution positions of CT-proET-1 and 43 – 44 indicate the elution positions of NT-proET-1 and ELDP synthetic peptides.*

4.4 DISCUSSION

A combination of chromatography-based methods was used for purification and characterisation of proET-1 fragments that are co-released with ET-1 from EA.hy 926 and A549 cells. While IEC provided a suitable method of purification for proET-1 peptides from EA.hy 926 conditioned medium, ammonium sulphate precipitation was necessary for characterisation of proET-1 peptides from A549 conditioned medium prior to RP-HPLC characterisation. Both conditioned media samples were then subjected to SPE. This was essential for buffer exchange and to concentrate NT-proET-1, ELDP, and CT-proET-1 peptides for further characterisation using RP-HPLC.

For EA.hy 926 conditioned medium, Q-Sepharose "clean up" to remove acidic proteins or contaminants followed by CM cation exchange chromatography proved to be an efficient process for isolating the basic proET-1 fragments ELDP and CT-proET-1. In pilot experiments to test this two-step procedure with small volumes of medium (20 ml/column), NT-proET-1 was also recovered in the CM fractions. Hence, for the large scale purification the aim was to isolate all three proET-1 fragments for HPLC characterisation. However, NT-proET-1 was present mainly in the unadsorbed pool from CM chromatography, which had been subjected to Q-Sepharose pre-treatment prior to loading on to CM Fractogel. Lack of binding and poor recovery of the NT-proET-1 was likely due to the following reasons:

i. NT-proET-1 has the lowest pI (6.3), so did not bind efficiently to the CM Fractogel.

ii. The binding capacity of the column was exceeded in the large-scale purification, such that NT-proET-1 was readily displaced by other peptides or proteins with higher pIs.

iii. Low levels of NT-proET-1 eluted in multiple CM fractions, but were not detected by the NT-proET-1 immunoassay because G-HCl interferes in this assay resulting in reduced sensitivity. Hence, unless there is adequate dilution of sample to compensate, low amounts of immunoreactivity in fractions are not detected.

Native NT-proET-1 purified from EA.hy 926 (Figure 4.3) and A549 conditioned media samples (Figure 4.4) were eluted after CT-proET-1. This indicated that NT-proET-1 is more strongly retained on the C4 column, and thus has characteristics of a more hydrophobic (non-polar) peptide than the CT-proET-1 requiring a higher concentration of CH_3CN for its desorption. The elution position of native NT-proET-1 peptide purified from EA.hy 926 conditioned medium was earlier (at fraction 41) than the synthetic peptide (at fraction 46). Thus, the native peptide is less hydrophobic than the synthetic peptide. RP-HPLC separation of peptides depends largely on their hydrophobicity. Although this can be influenced by size and conformation/folding and the proportion of hydrophilic amino acids, the overriding determinant is the most hydrophobic sequence providing greatest affinity for the non-polar hydrophobic particle surface of the column. Ion-pairing of basic residues with TFA also increase hydrophobicity and peptide retention on HPLC. It seems likely that the C-terminal sequence of NT-proET-1 (WRLRRS) in the presence of TFA contributes greatly to the overall retention of NT-proET-1, however why there is so much difference between the elution characteristics of the native and synthetic peptides is unclear. The NT-proET-1 immunoassay is very specific for this sequence, and therefore unlikely to detect this peptide if this sequence is not intact.

It is often difficult to synthesise peptides with (poly)proline sequences (Wawra & Fischer, 2006). NT-proET-1 has five proline residues in its amino acid sequence (Table 4.1). The N-terminal sequence of NT-proET-1 has one and the C-terminal sequence has four proline residues in a short six amino acid sequence, including two adjacent residues. Proline is the only natural cyclic amino acid that is unusual in forming cis peptide bonds at a frequency (~5%) much higher than any other naturally occurring amino acid (<0.1%) (Lummis *et al.*, 2005). Therefore, multiple proline residues in the C-terminal sequence of NT-proET-1 may undergo cis/trans isomerisation during chemical synthesis, leading to different structural folding that results in different HPLC elution positions. The synthetic peptide was a single peak, and had been shown to have the correct mass by LC-MS (see Chapter 2, section 2.1.3.1). Because antibody recognition is directed to the N- and C-terminal sequences, internal structural modification may not be detected by immunoassay. Hence, further structural characterisation of the synthetic peptide would be necessary to confirm whether this underlies the differing elution pattern to native peptide. Mass spectrometry provides great resolution and determines

structural features such as amino acid sequence, mass, post-translational modifications and it is also useful for the assignment of disulphide bonds. Therefore, mass spectrometric identification of the purified proET-1 peptide fractions could confirm the peptide identities. This may also define the reasons for heterogeneity, which have resulted from differences in amino acid sequence due to degradation products generated during purification or on storage.

Analytical HPLC of ELDP and CT-proET-1 peptides isolated from the conditioned medium of EA.hy 926 cells did not generate a single peak of immunoreactivity. However, the degree of heterogeneity was low with only two closely eluting peaks for ELDP and three for CT-proET-1 on an acetonitrile gradient with higher resolving potential (gradient increase 0.4% B per min). In both cases the purified native peptides eluted close to the corresponding synthetic peptides. Differences could result from modifications either during the 48 h incubation period where the conditioned medium was in contact with cells, or could have occurred during the various purification steps. Likely modifications could include oxidation of sulphur-containing methionine residues during the course of sample extraction and freeze/thaw process. This is a frequent observation for peptides in acidic solution. The side chain of normal methionine is long, flexible, and non-polar (Richardson & Richardson, 1989; Hoshi & Heinemann, 2001) but when it is oxidised to methionine sulphoxide by the addition of an extra oxygen atom, it becomes stiffer and more polar (hydrophilic) than that of the methionine side chain (Hoshi & Heinemann, 2001). Thus, the oxidised form is eluted before the native peptide. Other possible amino acid modifications during peptide purification under acidic conditions include: hydrolysis of amide side chains of asparagine and glutamine to aspartic acid and glutamic acid; hydroxylation of tyrosine, tryptophan or proline and oxidation of histidine and tryptophan. The reason for two main peaks for ELDP and CT-proET-1 is likely methionine oxidation as both peptides have a single methionine residue. Additional heterogeneity is likely due to a combination of other modifications under the acidic conditions used for the isolation and purification procedure.

Three-dimensional structure of the human ET-1 (PDB: P05305) determined by X-ray crystallography (to 2.18 Å resolution) demonstrated two disulphide bridges at ppET-1

positions 53 – 67 and 55 – 63 (Janes *et al.*, 1994). Similarly, ELDP sequence consists of six cysteine residues, in which the spacing between the first four cysteine residues is the same as in ET-1 sequence. Therefore, it is likely that these residues might form disulphide bridges at amino acid positions 109 – 123, 111 – 119, with a further disulphide bridge at 148 – 155. Disulphide bonds can contribute to protein folding. Correct disulphide bond formation parallels correct folding and formation of secondary structure, which reinforces the stability of a protein (Creighton, 1993; Zhang *et al.*, 2011). Thereby, ELDP can be highly susceptible to protein folding and more compact structure of the folded ELDP can result in prolonged interactions with the hydrocarbon groups of the C4 column.

In general, both HPLC chromatograms showed well resolved peaks of purified proET-1 fragments detected using sensitive immunoassays. Further investigation is required to confirm the sequence identities of the native peptides using mass spectrometry. Mass spectrometric identification of the specific proET-1 fragments identified by the NT-proET-1 (ppET-$1_{[18 - 50]}$), ELDP (ppET-$1_{[93 - 166]}$) and CT-proET-1 (ppET-$1_{[169 - 212]}$) immunoassays was investigated in Chapter 5.

CHAPTER 5

Verification of proendothelin-1 sequence identities using mass spectrometry

5.1 INTRODUCTION

5.1.1 Identification of proteins using mass spectrometry

Peptide mass fingerprinting (PMF) was introduced in 1981 by Henzel and colleagues (1993) and involves digestion of a protein with a specific protease (most often trypsin) to determine the masses of peptides resulting from the proteolytic cleavage (Henzel *et al.,* 2003). Trypsin cleaves at the C-terminal side of lysine and arginine residues with the exception being when the next amino acid is proline (Link & LaBaer, 2011). However, identification of proteins from PMF alone can be inconclusive.

Tandem mass spectrometry (MS/MS) combines peptide separation with fragmentation and provides enhanced specificity for identification of protein mixtures over PMF alone. The "bottom-up" approach involves proteolytic digestion and MS/MS analysis. Molecular weights of proteolytic peptides are submitted to database search engines such as MASCOT or SEQUEST (Eng *et al.,* 1994), which results in a powerful and rapid approach for protein identification. On the other hand, "top-down" approach provides characterisation of intact proteins with no enzymatic digestion. The intact mass and fragmentation data (precursor mass) are matched to search algorithms using absolute mass, sequence tag or a subset of larger sequence (biomarker) (Kellie *et al.,* 2010). This approach provides the potential for full localisation and characterisation of post-translational modifications (PTMs).

5.1.2 Fragmentation of peptides with collision-induced dissociation (CID)

There are several techniques that can generate peptide fragments: Electron Transfer Dissociation (ETD), Electron Capture Dissociation (ECD), and Collision-Induced Dissociation (CID). CID is the main method of fragmenting peptides in ion trap/quadrupole mass spectrometers.

Peptide ions are protonated with electrospray ionisation (ESI). These protonated peptide ions are then fragmented with CID using an inert gas such as helium. This cleavages the weakest amide bond first. Peptide fragmentation mainly occurs on the peptide backbone, often with the transfer of one or two hydrogen(s) to form a stable ion. Under CID peptide fragmentation, a nomenclature proposed by Roepstorff and Fohlman, 1984

was used to define N-terminal and C-terminal fragment ions as *a, b, c* and *x, y, z*, respectively (Figure 5.1) (Roepstorff, 1984). Low energy CID of peptides mainly produces b- and y- type fragment ions (Maleknia & Johnson, 2011).

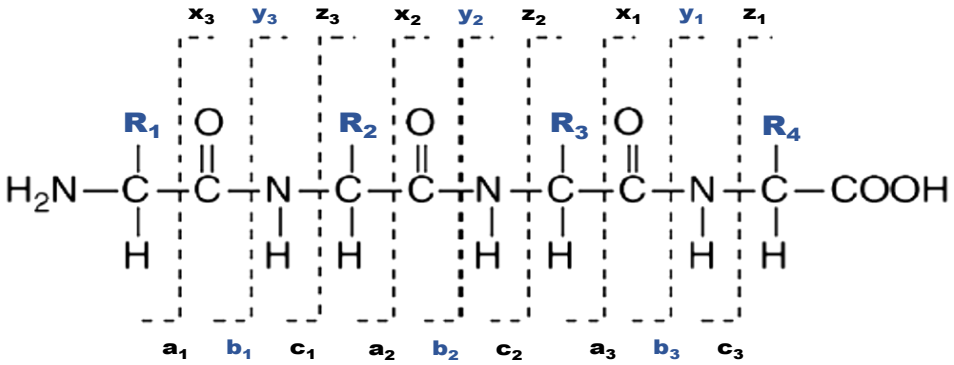

Figure 5.1: ***Roepstorff nomenclature:*** *x, y, and z represent C-terminal fragments and a, b, and c represent N-terminal fragments. Under low-energy CID, b-ion is generated when the charge (proton, H^+) is retained on the N-terminal and y-ion is generated when the charge is retained on the C-terminal end (Modified from Maleknia & Johnson, 2011).*

Fragmentation of precursor/parent ions generates product ions. The mass difference between each product ion corresponds to the mass of the amino acid residue. This defines the amino acid sequence of a peptide. Peptides are often digested to smaller fragments for effective fragmentation. Main fragmentation principles using CID are explained briefly.

(1) Sequencing starts from the C-terminal fragment. In tryptic peptides due to basic C-terminal arginine or lysine residue, more intense *y*-ions are generated (Tabb *et al.*, 2004, 2006).

(2) N-terminal fragment ions (b-ions) are calculated by adding the mass of a proton (H, 1.008 Da) to the residue masses while the C-terminal fragment ions (y-ions) are calculated by adding the mass of water and a proton (19.018 Da) to the residue masses.

(3) The last b-ion loses -17 Da (OH), while the last y-ion loses the mass of the last fragment ion and hydrogen (M+H).

(4) Peptide ions containing aspartic acid, glutamic acid, serine and threonine can neutrally lose water (18 Da) while asparagine, arginine, glutamine and lysine side chains can lose ammonia (17 Da) (Wu *et al.*, 2008; Medzihradszky, 2005). Other amino acids could also lose either water or ammonia.

(5) Proline can produce dominant y-ions, resulting from cleavage on N-terminal side of proline and suppressed b-ions (Breci *et al.*, 2003).

Sequencing tryptic peptides using low energy CID has some limitations. Examples of these include: **(1)** modifications such as disulphide bonds are not typically fragmented by CID (Loo *et al.*, 1990); **(2)** leucine and isoleucine have identical masses and cannot be differentiated (Papayannopoulos, 1995); **(3)** both b_1- and y_1- fragment ions are usually not observed in the spectra due to their low mass range, which is mainly a problem in ion traps but not in QTOF, Orbitrap or quadrupole mass spectrometers. **(4)** In addition, low MWt immonium ions that can confirm the identification/presence of amino acids such as oxidised methionine, histidine and proline at m/z 120, m/z 110 and m/z 70, respectively may not be observed in ion traps. **(5)** The C-terminal side of proline is often not cleaved and not observed (Maleknia & Johnson, 2011). This results from increased gas-phase basicity of the proline nitrogen and the ring structure of the proline side chain that inhibits the attack of the carbonyl on the N-terminal side of the proline (Maleknia & Johnson, 2011).

5.1.3 Identification of post-translational modifications using mass spectrometry

Examples of frequently occurring PTMs in proteins are described here. Some of the modifications are introduced during sample preparation; as such oxidation of methionine residues is the most commonly observed example.

5.1.3.1 *Oxidation*

Methionine, tryptophan, histidine and cysteine residues are susceptible to oxidation. Oxygen and reactive oxygen species (ROS) such as superoxide (O_2^-), hydrogen per oxide (H_2O_2), hydroxyl radical ($^{\bullet}HO$), and hypochlorite (ClO^-) can oxidise methionine. This yields methionine sulphoxide (MetSO). Further oxidation can lead to methionine sulphone (MeS), but to a much lesser extent (Nielsen *et al.,* 1985). Following CID fragmentation, MetSO can be detected with a mass increment of 15.995 Da and MeS with a mass increment of 31.99 Da. Oxidised methionine can also be detected by the presence of additional b- and y-ions that are 64 Da lower in mass than the MetSO ion. This corresponds to a neutral loss of methane-sulphenic acid (CH_3SOH) from the side chain of MetSO (Rebrin *et al.,* 2010). In CID, this characteristic loss of CH_3SOH indicates the presence of MetSO (Guan *et al.,* 2003).

Histidine and tryptophan oxidation is usually mediated by metal-catalysed (Fe(II)/Cu(II)) or ROS (H_2O_2) (Ji *et al.,* 2009). Tryptophan oxidation can result in mass increases of 3.995, 15.995 and 31.99 Da, corresponding to the formation of kynurenine, hydroxytryptophan, and N-formyl-kynurenine/dihydroxytryptophan (doubly oxidised trptophan), respectively (Perdivara *et al.,* 2010; Swiderek *et al.,* 1998). Histidine has an imidazole ring and oxidation can lead to degradation products of asparagine, aspartic acid and 2-oxo-histidine (Uchida & Kawakishi, 1994). Histidine oxidation is usually catalysed with Cu(II) yielding 2-oxo-histidine as the most predominant product (Uchida & Kawakishi, 1994; Li *et al.,* 1995) and it is detected with a mass increment of 31.99.

5.1.3.2 *Deamidation*

Deamidation of asparagine and glutamine residues can generate aspartic acid and glutamic acid. This results in a mass increase of 0.984 Da. Under acidic conditions, deamidation of asparagine via direct hydrolysis generates a mixture of isoaspartate and aspartic acid in a 1:3 ratio (Capasso & Salvadori, 1999). Similarly, direct hydrolysis of the glutamine side chain amide can generate glutamic acid. Under basic or neutral conditions, deamidation arises through the formation of a succinimide ring (cyclic imide) intermediate, which then hydrolyses forming isoaspartate and aspartic acid. At basic or neutral pH, glycine increases the rate of deamidation by providing high local backbone flexibility and lack of steric hindrance imposed by its side chain (Bischoff & Kolbe, 1994). The rate of the reaction can be increased when alanine, serine and aspartic acid are at the C-terminal side of asparagine residue.

5.1.3.3 *Pyro-glutamate formation*

Under acidic conditions, N-terminal glutamine residue can cyclise to form pyroglutamate, which could make it more resistant to proteolytic hydrolysis and degradation (Chelius *et al.*, 2006).

5.1.3.4 *Disulphide bond formation*

Disulphide bonds can be formed by the oxidation of highly reactive sulphydryl groups (–SH) of cysteine residues. They provide stability to the native correctly folded protein.

In this project MS/MS analysis was applied to peak fractions from analytical RP-HPLC purification of proET-1 peptide fragments isolated from EA.hy 926 conditioned medium.

5.1.4 Identification strategy for proET-1 peptide fragments

The identification strategy for purified and characterised proET-1 peptide fragments is summarised in Figure 5.2. Briefly, identification of ELDP and CT-proET-1 was based on fragmentation of tryptic peptides with CID (bottom-up), while NT-proET-1 was analysed in its intact form without digestion (top-down). Samples purified using IEC and HPLC.

HPLC fractions containing the highest immunoreactivity for NT-proET-1 were dried under vacuum with centrifugal force with SpeedVac and reconstituted in 0.1% TFA and analysed using LTQ Orbitrap XL connected online to a nanoflow UPLC with a C4 column. HPLC fractions containing the highest immunoreactivity for ELDP and CT-proET-1 were dried using SpeedVac, reconstituted in H_2O, digested with trypsin, acidified and desalted using Graphitic Carbon C18 spintips. ELDP/CT-proET-1 were dried in the SpeedVac and reconstituted in 0.1% TFA and analysed using LTQ Orbitrap XL connected online to a nanoflow UPLC with a C18 column.

Peptides were initially separated on a reverse-phase column and then directly electrosprayed into LTQ Orbitrap MS. Elution conditions for nanoflow HPLC involved a gradient of CH_3CN with 0.1% formic acid (FA). Pilot experiments with synthetic peptides showed that ELDP and CT-proET-1 do not elute from either C4 or C18 nanoflow columns with CH_3CN/FA, hence the need for tryptic digestion for MS/MS characterisation.

Raw data obtained from MS/MS was subjected to a database search using MASCOT and data analysis provides identification of peptide sequences.

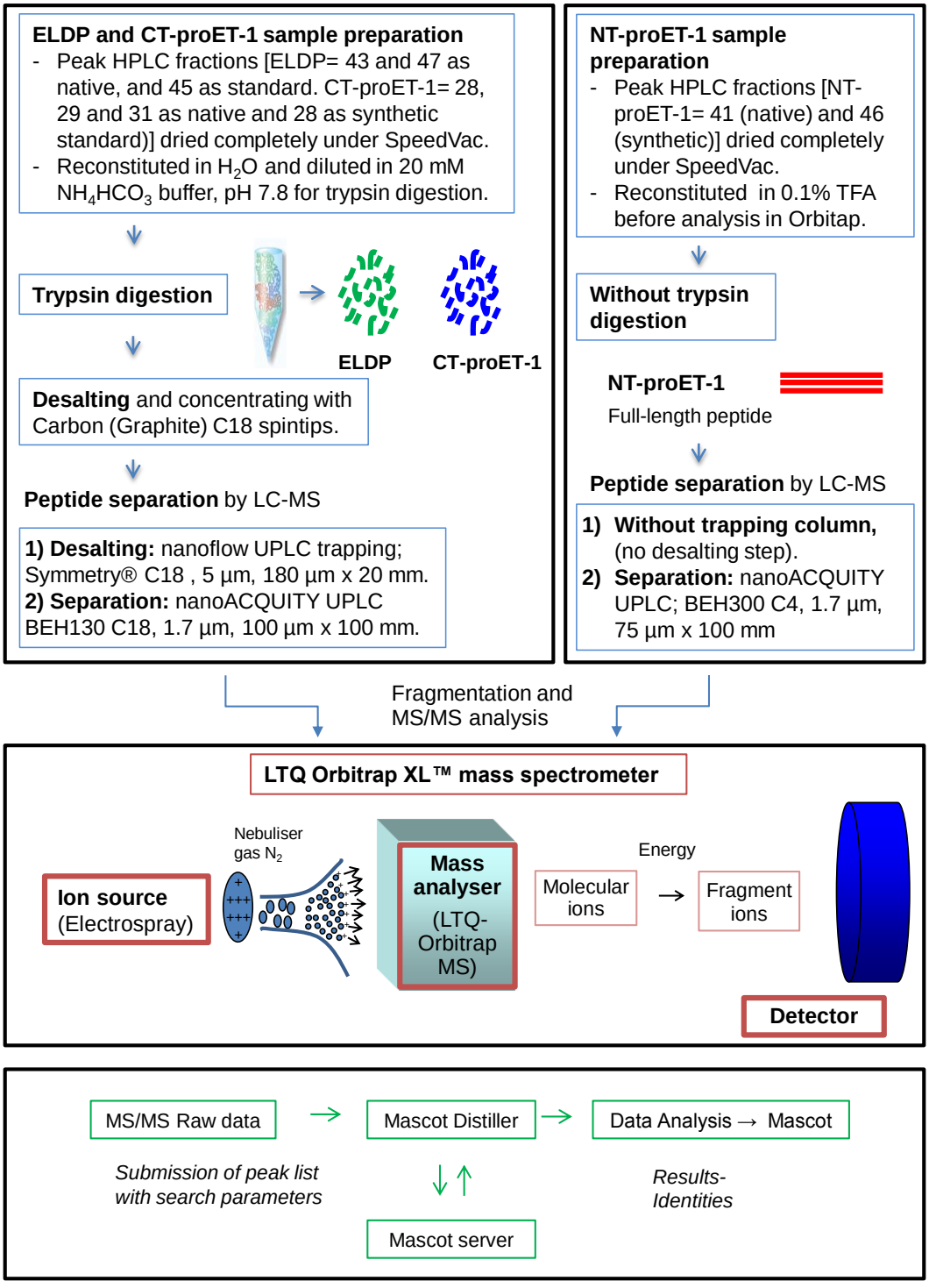

Figure 5.2: ***Workflow of identification strategy for purified and characterised proET-1 peptides from EA.hy 926 conditioned medium using LTQ Orbitrap mass spectrophotometer.***

5.1.5 Hypothesis and aims

Main aims of this chapter were to **(1)** investigate whether the secreted proET-1 peptide sequences corresponded with the inferred amino acid sequences derived from the *EDN1* gene sequence; **(2)** define the reasons for the heterogeneity of elution profiles observed on analytical HPLC (Chapter 4); and **(3)** confirm the presence of disulphide bonds in the endothelin-like domain (Cys^{109} – Cys^{123} and Cys^{111} – Cys^{119}) in which the spacing between cysteine residues is exactly the same as in ET-1 (Cys^{53} – Cys^{67} and Cys^{55} – Cys^{63}) (N.B. Cys numbering based on the full-length ppET-1 sequence).

5.2 METHODS

Synthetic peptides were initially studied to optimise the conditions to ensure efficient fragmentation of proET-1 peptide fragments purified from EA.hy conditioned medium (serum-free). Identification of purified/native proET-1 peptide fragments was performed using LTQ Orbitrap XL MS (Thermo Fisher Scientific, Hemel Hempstead, UK) coupled online to a nanoflow ultrahigh pressure liquid chromatography (UPLC, nanoAcquity, Waters).

5.2.1 Sample preparation for LTQ Orbitrap XL MS

5.2.1.1 *ProET-1 synthetic standards*

NT-proET-1, ELDP and CT-proET-1 were diluted in 0.1% TFA from stock solutions or from HPLC fractions obtained on analytical HPLC of synthetic peptides (NT-proET-1, fraction 41; ELDP, fraction 45; and CT-proET-1, fraction 28). A calibration curve (concentration range 0.98 – 125 fmol/µl) was prepared from stock solutions of synthetic proET-1 peptides. Stock concentrations of synthetic NT-proET-1, ELDP and CT-proET-1 were 70, 85 and 59 nmol/ml, respectively. An equal volume of sample (20 µl) was then transferred into 0.2 ml natural slick-seal tubes (Bioquote) and 4 µl of each sample was injected for each analysis.

5.2.1.2 *HPLC fractions of purified native peptides*

HPLC fractions containing the highest proET-1 immunoreactivity were concentrated using centrifugal force (SpeedVac, CHRIST) and stored at -80°C until the day of analysis. Prior to analysis, NT-proET-1 fractions (native: 41 and synthetic: 46) were reconstituted in 0.1% TFA and diluted at 100 fmol/µl in 0.1% TFA. Of note, the final concentration of purified/native NT-proET-1 (fraction 41) after reconstitution with 50 µl of 0.1% TFA was 89.4 fmol/µl.

HPLC fractions containing the highest ELDP and CT-proET-1 immunoreactivity were digested using trypsin, without reduction or alkylation.

5.2.1.3 *Trypsin digestion*

1. Lyophilized trypsin (20 µg) (Promega) was prepared at 0.5 µg/µl by reconstituting in 40 µl of trypsin resuspension buffer that is composed of 50 mM acetic acid. Reconstituted enzyme was stored at -80°C.
2. HPLC fractions of purified proET-1 peptides were reconstituted in H_2O. Samples were then diluted in 20 mM ammonium bicarbonate buffer, pH 7.8.
3. Modified sequence-grade trypsin (prepared at 0.5 µg/µl) was added at a final trypsin:protein ratio of 1:50 in lo-binding microcentrifuge tubes (Eppendorf, Cat# 022431081). The pH of the resulting mixture should be 7.5 – 8.5.
4. Following a gentle vortex, incubated at 37°C overnight (18 h) on a shaker at 900 rpm.
5. Trypsin was inactivated by acidification with TFA to 0.1% of the final digest volume, followed by chilling the reaction on ice.

5.2.1.4 *Desalting and removal of contaminants from digestion mixtures (Reverse-Phase desalting using Graphitic Carbon C18 spintips)*

Trypsin digested samples were desalted and contaminants were removed by Graphitic Carbon C18 stationary phase spintips (Glygen Corp, USA). Graphitic Carbon can also recover hydrophilic portion of digested fragments. Prior to desalting, samples were acidified with 0.1% TFA and desalting was carried out according to the protocol as shown in Table 5.1. The flow was obtained by centrifugation for 2 min at 1600 *g* at the end of each step, discarding the flow-through until the elution step.

Table 5.1: ***Desalting protocol with Graphitic Carbon C18 spintips.***

Priming	2 x 200 µl of 50% CH_3CN/0.1% TFA Centrifugation 2 x 200 µl 1% CH_3CN/0.1% TFA Centrifugation
Sample addition (200 µl) and washing	200 µl 1% CH_3CN/0.1% TFA Centrifugation 100 µl 1% CH_3CN/0.1% TFA Centrifugation
Elution	4 x 50 µl 50% CH_3CN/0.1% TFA

At the end of elution step, samples were centrifuged for 2 min at 13,000 rpm and transferred to a fresh lo-bind 2 ml microcentrifuge tube, dried under vacuum at room temperature using a rotational vacuum concentrator and stored at -80°C. Dried samples were reconstituted in 0.1% TFA prior to analysis with LTQ Orbitrap.

5.2.2 LTQ Orbitrap MS/MS Analysis

Flow from the nanoacquity UPLC system was directed to a LTQ Orbitrap XL MS equipped with a nano-ESI source (positive mode). NT-proET-1 separation was performed directly in nanoACQUITY UPLC BEH300 (Ethylene Bridged Hybrid) C4 reverse-phase column with 1.7 µm particle size, 75 µm x 100 mm in dimensions and 300 Å pore size (Waters, 186004639) without on-line trapping/desalting. Injection volume was set to 4 µl, which was followed by a gradient elution at 300 nl/min over 50 min. Gradient elution was from 99% A (A = 0.1% FA in LC-MS grade H_2O), 5% B (B = 0.1% FA in LC-MS grade CH_3CN) to 50% CH_3CN followed by a 25 min wash with H_2O.

Trypsin digested ELDP and CT-proET-1 fragments were loaded onto a trapping nanoAcquity UPLC™ column, Symmetry® C18, 5 µm, 180 µm x 20 mm (Waters). The nanoflow UPLC loading flow rate was set at 2 µl/min for 8 min, which operated with a back pressure of about 3,000 psi and sample elution at a flow rate of 300 nl/min. Peptide separation was performed on a nanoAcquity UPLC BEH130 column packed with C18 resin, 1.7 µm, 100 µm inner diameter x 100 mm (Waters, Part No 186003546) using a linear gradient of 1 – 35% in 10 min, followed by an increase to 85% B in 10 min and held at 85% B for another 10 min. The gradient was followed by a gradual decrease to 1% B in 10 min, which was followed by a 25 min H_2O wash.

Full scan survey spectra (m/z 375 – 1800) were acquired by the Orbitrap with a resolution of 30,000 at m/z 400. A data dependent analysis was employed in which the five most abundant multiply charged ions present in the survey spectrum were automatically mass-selected, fragmented by CID (normalised collision energy 35%) and analysed in the LTQ (m/z 50 – 2000).

5.2.3 Peptide Identification via MASCOT Database Search

ProET-1 peptide fragments were identified by an automated database MASCOT Daemon (Matrix Science Ltd, London, UK). MASCOT Daemon 2.2 server was used to process mass spectrometry raw data. MASCOT Daemon automates the use of MASCOT Distiller (v2.3.2.), to smooth and centroid the MS/MS data, and MASCOT search engine (v2.2.02), to search for the target protein sequence against all known proteins present in mammalian genomes using UniProt database (http://www.uniprot.org).

The search was performed by using the following parameters: no enzymatic digestion for NT-proET-1, and trypsin as the digestion enzyme for ELDP and CT-proET-1. Up to two missed cleavages were allowed in all searches. Variable modifications included in the search criteria were oxidation of methionine (15.995 Da), Gln->pyro-Glu (N-term Q) and deamidation of asparagine and glutamine residues to aspartic acid and glutamic acid (0.984 Da). Data sets were searched with a mass accuracy of ± 10 ppm (parts-per-million), peptide charge +2 +3, –MS/MS tolerance of ± 600 mmu (milli-mass units). Ions with single and unrecognized charge states were excluded.

MASCOT data output includes the identification of peptides (amino acid sequence), parent ion m/z, retention time and confidence scores based on the probability (Perkins *et al.*, 1999). MASCOT calculates ions score using -10*Log(P), where P is the probability that the observed match is a random event.

Precursor ion tolerance in LTQ Orbitrap was 5 – 20 ppm. Instrument type was ESI FT ICR CID (Fourier Transform Ion Cyclotron Resonance). Product ion tolerance in LTQ Orbitrap was set at 0.5 – 0.8 Da for ion trap mode and 0.01 – 0.02 Da for Orbitrap mode.

Monoisotopic masses of the proET-1 peptides were calculated using ProteinProspector (http://prospector.ucsf.edu/). The following parameters were selected: MS product → maximum charge 8 → instrument ESI FT ICR CID. *EDN1* gene (endothelin-1, P05305) was identified for the proET-1 peptides. Raw chromatograms were subsequently processed and analysed using Xcalibur.

Ion fragments of each trypsin digested ELDP and CT-proET-1 peptides were obtained from ProteinProspector. Fragment ions were identified in the MS/MS spectra from Qual Browser and labelled manually for the b- and y-ions, confirming MS/MS fragmentation from MASCOT.

In order to ensure correct identification, all samples were run twice on two separate days and only peptides that were present in all analyses are shown here.

5.3 RESULTS

The workflow for proET-1 identification strategy is illustrated in Figure 5.2 for the proET-1 peptides purified and characterised from EA.hy 926 conditioned medium. In addition to the native purified peptides, synthetic standard peptides were added to medium samples and subjected to the same extraction and HPLC procedures (Chapter 4). A calibration curve (concentration range 0.98 – 125 fmol/µl) prepared with each proET-1 synthetic standard was used to optimise a methodology to enable identification of each purified proET-1 peptide using LTQ Orbitrap MS.

Following MASCOT database search of the MS/MS data, NT-proET-1 amino acid sequence was not identified from the native/purified sample (fraction 41) but was detected from the NT-proET-1 synthetic standard (fraction 46). Therefore, the identity of the native NT-proET-1 could not be confirmed with MS/MS.

Precursor ion masses of trypsin digested ELDP and CT-proET-1 fragments were obtained from MASCOT. Initially these m/z values were identified in the extracted ion chromatogram (XIC) acquired on a LTQ Orbitrap with their corresponding charges (data not shown) and these were manually verified in MS/MS spectra.

5.3.1 Peptide sequences of ELDP and CT-proET-1 identified using MASCOT

Peptide identities of ELDP and CT-proET-1 were determined from partial sequences obtained from trypsin digestion. Detailed list of ELDP and CT-proET-1 peptide sequences are shown in Table 5.2 and Table 5.3, respectively.

5.3.1.1 *MASCOT identification of purified native ELDP*

Tryptic peptides identified from HPLC fractions 43 and 47 purified (native peptide), and 45 (synthetic standard) are shown in Table 5.2A – C. These data include residue numbers of the tryptic proET-1 fragments, parent ion m/z (monoisotopic), ion score, peptide charge and identification.

The first peptide fragment identified in both fractions was ELRAEDIMEK, where M represents an oxidised methionine residue. Methionine oxidation results in a mass increment of 15.995 Da. Fraction 47 also contained non-oxidised form of this fragment. The N-terminal fragment of the ELDP (ppET-$1_{[93-101]}$) corresponding to ALENLLPTK (m/z at 499.799^{2+}) was not detected in either 43 or 47 fractions but was an abundant fragment from the synthetic peptide (ion score 63).

The second peptide fragment identified with two missed-cleavages was ELRAEDIMEKDWNNHK. Fraction 43 contained a precursor ion at m/z 681.999^{3+} and 511.744^{4+}, corresponding to oxidised methionine and both oxidation of methionine and deamidation of asparagine, respectively. Deamidation of asparagine results in a monoisotopic mass increment of 0.984 Da. Fraction 47 contained precursor ions at m/z 676.657^{3+} (no modification), m/z 681.990^{3+} (methionine oxidation), and m/z 687.321^{3+} (both methionine and tryptophan oxidation).

The third peptide fragment identified was AEDIMEK, which had an oxidised methionine in fraction 43 and both oxidised and unoxidised forms in fraction 47.

The fourth peptide fragment identified with a missed-cleavage was AEDIMEKDWNNHK. Two precursor ions were detected at m/z 823.367^{2+} and m/z 549.247^{3+}. In addition, fractions 47 also contained the native peptide with no PTMs as well as a fragment with both oxidation of methionine and histidine. This fragment was also detected with an additional missed-cleavage of lysine at the C-terminal.

The fifth peptide fragment was a precursor ion at m/z 540.287^{2+} corresponding to CIYQQLVR. This fragment is the closest fragment to the C-terminal of the ELDP sequence and was identified in both fractions.

Table 5.2: ***MASCOT identification of tryptic peptides from purified native ELDP fractions (A) 43, (B) 47 and synthetic ELDP standard (C) 45.*** *Data show start-end residue masses corresponding to the ppET-1 peptide sequence (ELDP; ppET-1 residues 93 – 166), monoisotopic and experimental average masses, charge, score and peptide identification. Underlined* ***M*** *and* **W** *indicate oxidation of the corresponding methionine and tryptophan, respectively. Underlined* ***N*** *indicates deamidation of asparagine. Bold m/z values correspond to peptide ions that were selected for MS/MS to provide data for primary structure determination.*

(A) Purified native ELDP, fraction 43:

ppET-1 Residues Start-End	Observed mass, m/z (Da)	Experimental Mass (MWt expt)	Charge	Score	Peptide
128 – 137	**625.308**	1,248.602	2	44	ELRAEDI**M**EK
128 – 143	681.990	2,042.948	3	26	ELRAEDI**M**EKDWNNHK
	511.744	2,042.948	4	12	ELRAEDI**M**EKDW**N**NHK
131 – 137	426.195	850.375	2	26	AEDI**M**EK
131 – 143	823.368	1,644.721	2	61	AEDI**M**EKDWNNHK
	549.247	1,644.721	3	36	
131 – 144	**887.414**	1,772.814	2	43	AEDI**M**EKDWNNHKK
	591.942	1,772.805	3	26	AEDI**M**EKDW**N**NHKK
	597.277	1,788.810	3	35	AEDI**M**EKD**W**NNHKK
155 – 162	**540.287**	1,078.560	2	49	CIYQQLVR

(B) Purified native ELDP, fraction 47:

ppET-1 Residues Start-End	Observed mass, m/z (Da)	Experimental Mass (MWt expt)	Charge	Score	Peptide
128 – 137	617.310	1,232.605	2	34	ELRAEDIMEK
	625.308	1,248.602	2	50	ELRAEDI**M**EK
128 – 143	676.657	2,026.950	3	47	ELRAEDIMEKDWNNHK
	681.990	2,042.948	3	21	ELRAEDI**M**EKDWNNHK
	687.321	2,058.942	3	21	ELRAEDI**M**EKD**W**NNHK
131 – 137	418.197	834.380	2	47	AEDIMEK
	426.194	850.374	2	26	AEDI**M**EK
131 – 143	815.369	1,628.723	2	34	AEDIMEKDWNNHK
	543.915	1,628.724	3	28	
	549.247	1,644.719	3	39	AEDI**M**EKDWNNHK
	823.367	1,644.719	2	35	
	554.579	1,660.716	2	23	AEDI**M**EKDWNN**H**K
131 – 144	879.417	1,756.820	2	56	AEDIMEKDWNNHKK
	586.61	1,756.808	3	50	
	887.415	1,756.815	2	46	AEDI**M**EKDWNNHKK
	591.943	1,772.808	3	28	
	591.945	1,772.814	3	33	AEDIMEKDWNN**H**KK
	597.606	1,789.795	3	23	AEDI**M**EKD**W**N**N**HKK
155 – 162	540.287	1,078.559	2	49	CIYQQLVR

(C) Synthetic ELDP, fraction 45:

ppET-1 Residues Start-End	Observed mass, m/z (Da)	Experimental Mass (MWt expt)	Charge	Score	Peptide
93 – 101	499.798	997.582	2	57	ALENLLPTK
	499.798	997.581	2	18	AL**EN**LLPTK
93 – 105	721.404	1,440.793	2	64	ALENLLPTKATDR
93 – 108	920.997	1,839.979	2	24	AL**EN**LLPTKATDRENR
	614.334	1,839.981	3		
128 – 137	617.311	1,232.607	2	37	ELRAEDIMEK
	625.308	1,248.601	2	35	ELRAEDI**M**EK
128 – 143	1,014.483	2,026.951	2	46	ELRAEDIMEKDWNNHK
	676.658	2,026.952	3	38	
	1,022.482	2,042.949	2	60	ELRAEDI**M**EKDWNNHK
	511.744	2,042.947	4	25	ELRAEDIMEKD**W**NNHK
	681.990	2,042.947	3	22	ELRAEDIMEKDWNN**H**K
	687.321	2,058.942	3	24	ELRAEDI**M**EKD**W**NNHK
	1,030.478	2,058.941	2	38	ELRAEDI**ME**KD**WN**NHK
131 – 137	426.195	850.375	2	26	AEDI**M**EK
131 – 143	815.370	1,628.724	2	42	AEDIMEKDWNNHK
	543.915	1,628.724	3	38	
	823.367	1,644.720	2	62	AEDI**M**EKDWNNHK
	549.247	1,644.720	3	37	

Table 5.2 continued; (C) Synthetic ELDP, fraction 45:

ppET-1 Residues Start-End	Observed mass, m/z (Da)	Experimental Mass (MWt expt)	Charge	Score	Peptide
131 – 143	554.580	1,660.717	2	33	AEDI**M**EKDWNN**H**K
	549.575	1,645.703	2	27	AEDI**M**EKDW**N**NHK
	831.364	1,660.714	2	74	AEDI**M**EKD**W**NNHK
131 – 144	879.417	1,756.820	2	68	AEDIMEKDWNNHKK
	586.614	1,756.820	3	80	
	887.415	1,756.815	2	46	AEDI**M**EKDWNNHKK
	591.943	1,772.806	2	25	
	887.415	1,772.815	2	41	AEDIMEKD**W**NNHKK
	591.945	1,772.814	3	33	AEDIMEKDWNN**H**KK
	591.945	1,772.813	3	25	AEDI**M**EKDWNNHKK
	895.412	1,788.810	2	50	AEDI**M**EKD**W**NNHKK
	597.278	1,788.811	3	40	
	879.910	1,757.805	2	35	AEDIMEKDWN**N**HKK
	597.606	1,789.795	3	23	AEDI**M**EKD**W**N**N**HKK
151 – 162	483.618	1,447.833	3	27	LGKKCIYQQLVR
154 – 162	575.820	1,149.625	2	25	KCIYQQLVR
	576.314	1,150.614	2	17	KCIY**Q**QLVR
155 – 162	540.286	1,078.557	2	44	CIYQQLVR

5.3.1.2 *MASCOT identification of purified native CT-proET-1*

MASCOT identification of CT-proET-1 was only confirmed from HPLC fraction 28. Identified tryptic peptides are shown in Table 5.3. No peptide fragments corresponding to *EDN1* were detected in fraction 29. A precursor ion at m/z 395.203^{2+}, corresponding to YVTHNR (ppET-$1_{[204 - 209]}$) was detected in fraction 31 (P = 0.006). However, following an error tolerant search (Creasy & Cottrell, 2002), SSFHDPKLKGKPSRER (m/z 625.674^{3+}) containing 4 missed-cleavages was also identified in both fractions 29 and 31 on re-analysis.

The first tryptic fragment identified in fraction 28 was SSEEHLRQTRSETMR (m/z 461.735^{4+}). The ion score assigned by MASCOT was low and therefore the identification was not statistically significant. This peptide was also identified in the fraction 28 for the synthetic peptide with a low ion score that was insufficient for peptide identification (Table 5.3B). However, detection of a smaller fragment, SSEEHLRQTR (m/z 414.878^{3+}) with a higher ion score supported the identification of this sequence in the synthetic peptide. This sequence corresponds to the proposed N-terminal sequence of CT-proET-1.

Table 5.3: ***MASCOT identification of CT-proET-1 tryptic peptides from (A) purified native peptide (fraction 28) and (B) synthetic peptide (fraction 28_std).*** *Data shows start-end residue masses corresponding to the ppET-1 peptide sequence (CT-proET-1; ppET-1 residues 169 – 212), monoisotopic and experimental average mass, charge, score and peptide identification. Underlined* ***M*** *indicates oxidation of the corresponding methionine. Bold m/z values correspond to peptide ions that were selected for MS/MS to provide data for primary structure determination.*

(A) Purified native CT-proET-1, fraction 28

ppET-1 Residues Start-End	Observed mass, m/z (Da)	Experimental Mass (MWt expt)	Charge	Score	Peptide
169 – 183	**461.735**	1,842.911	4	2	SSEEHLRQTRSETMR
179 – 187	**534.261**	1,066.508	2	23	SET**M**RNSVK
184 – 196	496.273	1,485.796	3	20	NSVKSSFHDPKLK
188 – 196	529.786	1,057.557	2	30	SSFHDPKLK
188 – 201	**528.627**	1,582.86	3	60	SSFHDPKLKGKPSR
	396.722	788.393	2	20	SSFHDPKLKGKPSR
204 – 209	**395.204**	788.393	2	12	YVTHNR

(B) Synthetic CT-proET-1, fraction 28_std

ppET-1 Residues Start-End	Observed mass, m/z (Da)	Experimental Mass (MWt expt)	Charge	Score	Peptide
169 – 178	414.878	1,241.611	3	14	SSEEHLRQTR
	414.878	1,241.611	3	16	SSE<u>E</u>HLR**<u>Q</u>**TR
169 – 183	616.627	1,846.860	3	7	SSEEHLR**<u>Q</u>**TRSETMR
176 – 183	496.235	990.455	2	42	QTRSETMR
179 – 187	526.755	1,051.495	2	16	SETMR**<u>N</u>**SVK
184 – 196	743.904	1,485.794	2	25	NSVKSSFHDPKLK
188 – 194	409.196	816.378	2	23	SSFHDPK
204 – 209	395.204	788.393	2	12	YVTHNR

5.3.2 Verification of ELDP and CT-proET-1 peptide identities from the MS/MS spectra

Both C-terminal (y-ions) and N-terminal (b-ions) fragment ions were obtained from MASCOT and y-ions were manually labelled in the MS/MS spectra along with their corresponding amino acid residues. This provided amino acid composition, confirming the identification of the corresponding peptide sequences with their assigned PTM(s).

5.3.2.1 *Evaluation of the MS/MS spectra for purified native ELDP (fraction 43):*

Figure 5.3 illustrates three low-energy CID MS/MS spectra for precursor ions at m/z (A) 625.308^{2+}, (B) 887.414^{2+}, and (C) 540.287^{2+}, corresponding to ELRAEDIMEK, AEDIMEKDWNNHKK and CIYQQLVR, respectively.

The first tryptic peptide corresponded to ELRAEDIMEK (ppET-1 residues 128 – 137) consisted of an oxidised methionine. This was illustrated with a y_3 ion at m/z 359.193 (KEM) (Figure 5.3A). It was 63.998 Da lower than the unmodified methionine residue. This was corresponding to a neutral loss of methane-sulphenic acid (CH_3SOH) from the side chain of methionine sulphoxide. In the spectrum, y_2-H_2O (m/z 258.144), b_6-H_2O (m/z 696.331), and b_7-H_2O (m/z 809.415) ions had a neutral loss of H_2O (-18 Da) while y_9-NH_3 (m/z 1,039.542) had a neutral loss of NH_3 (-17 Da). To note, there were also a few unassigned peaks at m/z 529.024, 584.365, 593.522, and these are likely to belong to contaminating peptides.

The MS/MS spectrum of AEDIMEKDWNNHKK (Figure 5.3B) had a dominance of y-ions with almost full identification of the amino acid residues in the peptide sequence. This spectrum also contained unknown abundant peaks whose identity could not be confirmed by manual inspection of the MS/MS spectrum.

Figure 5.3C shows the MS/MS spectrum of CIYQQLVR, which represents sequence closest to the C-terminal of ELDP peptide that could be identified after tryptic digestion.

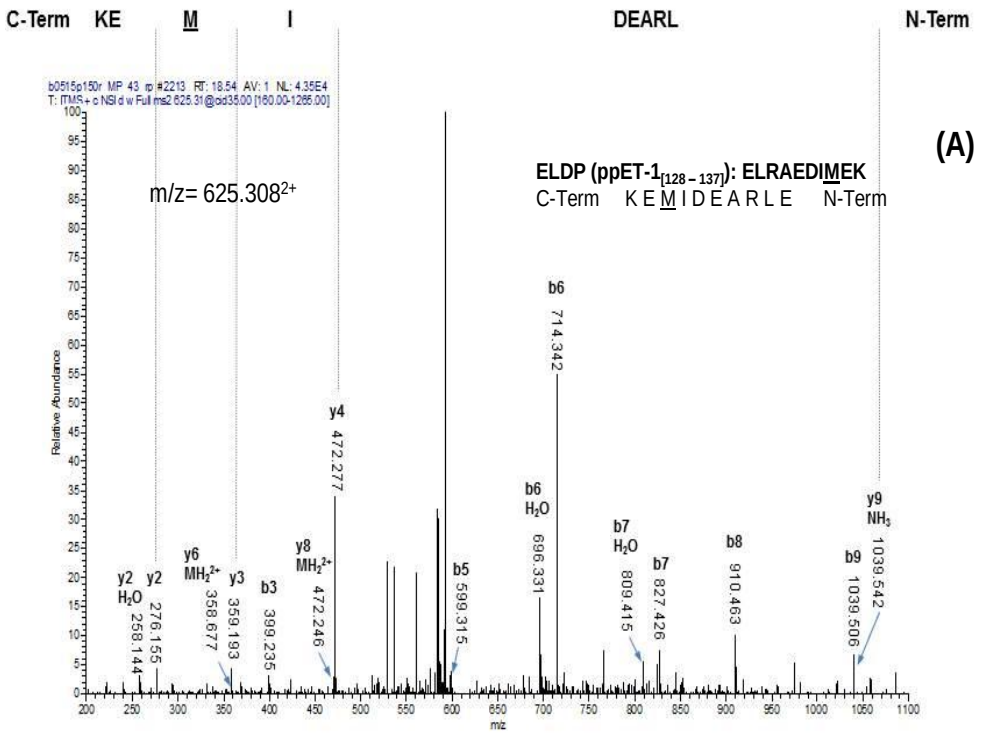
C-Term KE M I DEARL N-Term
b0515p150r MP 43 sp #2213 RT: 18.54 AV: 1 NL: 4.35E4
T: ITMS + c NSI d w Full ms2 625.31@cid35.00 [160.00-1265.00]
m/z= 625.308 2+
ELDP (ppET-1 [128 – 137]): ELRAEDIMEK
C-Term K E M I D E A R L E N-Term
(A)
Relative Abundance
m/z
b6 714.342
y4 472.277
b6 H2O 686.331
b7 H2O 809.415
b7 827.426
b8 910.463
y9 NH3 1039.542
b9 1039.506
b5 599.315
y8 MH2 2+ 472.246
y6 MH2 2+ 358.677
y3 359.193
b3 399.235
y2 H2O 258.144
y2 276.155

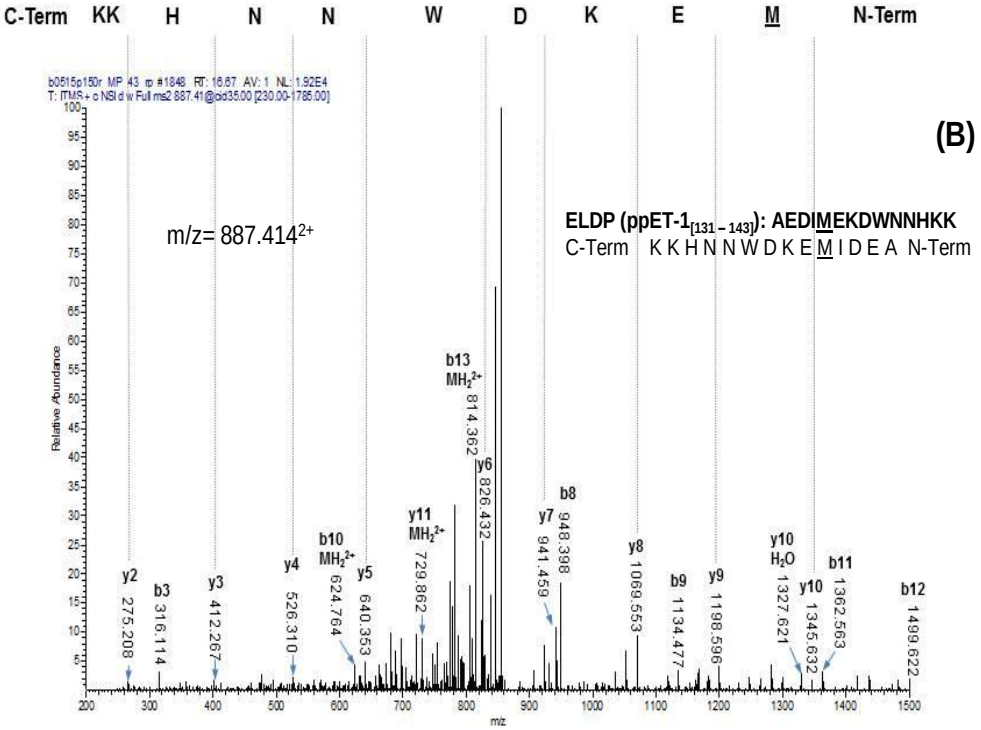
C-Term KK H N N W D K E M N-Term
b0515p150r MP 43 sp #1848 RT: 16.67 AV: 1 NL: 1.92E4
T: ITMS + c NSI d w Full ms2 887.41@cid35.00 [230.00-1785.00]
m/z= 887.414 2+
ELDP (ppET-1 [131 – 143]): AEDIMEKDWNNHKK
C-Term K K H N N W D K E M I D E A N-Term
(B)
Relative Abundance
m/z
b13 MH2 2+ 814.362
y6 826.432
b8
y7 948.398
y11 MH2 2+ 729.862
b10 MH2 2+ 624.764
y4 526.310
y5 640.353
y2 275.208
b3 316.114
y3 412.267
y8 1069.553
b9 1134.477
y9 1198.596
y10 H2O 1327.621
y10 1345.632
b11 1362.563
b12 1499.622

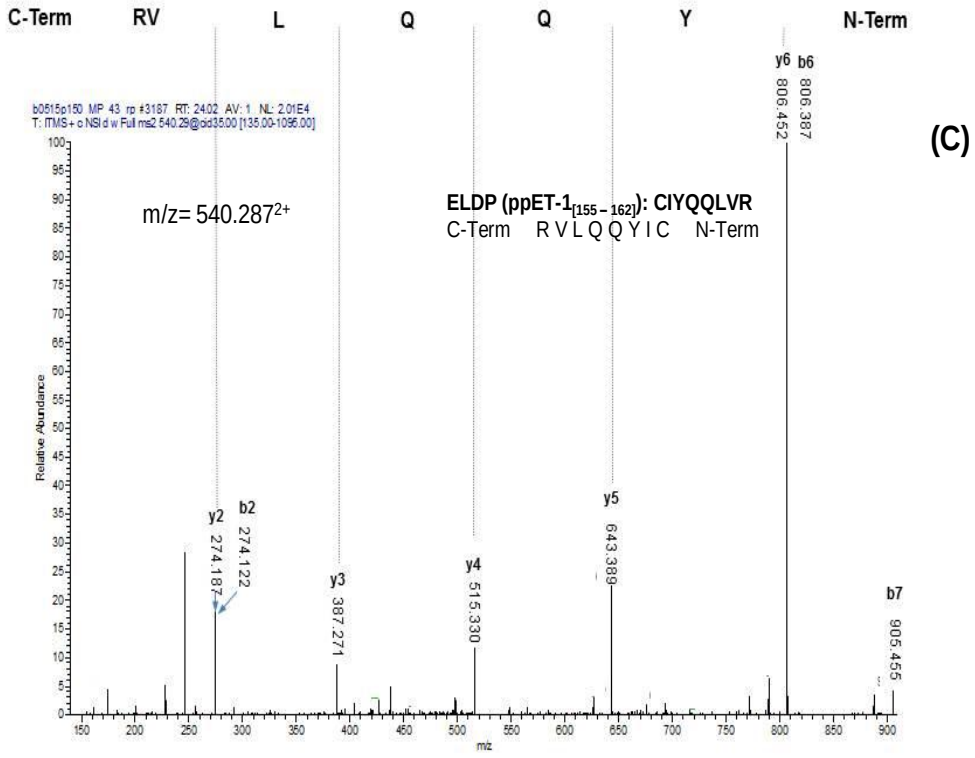

Figure 5.3: ***MS/MS spectra of purified/native ELDP (fraction 43) precursor ions at m/z (A) 625.308^{2+}, (B) 887.414^{2+} and (C) 540.287^{2+}.*** *MS/MS spectra were manually annotated for C-terminal fragment ions (y-) and N-terminal fragment ions (b-) confirming the sequence identities of the precursor ions obtained from MASCOT. The mass differences between the y-ion series indicate amino acid residues of the corresponding fragment ions, which are shown above the spectrum. Annotations of –NH_3 or H_2O at b- and y-ions represent a loss of ammonia or water at the corresponding fragment ions with a loss of 17 and 18 Da, respectively.*

5.3.2.2 *Evaluation of the MS/MS spectra for purified native CT-proET-1 (fraction 28):*

Figure 5.4 illustrates four MS/MS spectra (A – D) showing precursor ions at m/z (A) 461.735^{4+}, (B) 534.261^{2+}, (C) 528.627^{3+} and (D) 395.204^{2+}. The MS/MS spectrum shown in Figure 5.4A corresponds to the N-terminal sequence of CT-proET-1, SSEEHLRQTRSETMR with 2 missed-cleavages. The spectrum contained highly abundant background ions, resulting in a low signal-to-noise ratio. Of note, the quality of the spectrum was poor and the ion score obtained from MASCOT was not significant. However, despite the poor quality spectrum, isomeric leucine was identified (m/z 113.084) correctly. The identification of the peptide accounted mostly doubly charged y-ions. These were y_{12}-MH_2^{2+} (EHLRQTRSETMR), y_{10}-MH_2^{2+}, y_9-MH_2^{2+}, and y_8-MH_2^{2+}. From the N-terminal fragment ions, only b_2 ion corresponding to serine (m/z 175.071) was detected. However, this ion could also be y_1 ion corresponding to arginine (m/z 175.119).

This fragment was also found in CT-proET-1 synthetic standard with a precursor ion at m/z 616.627^{2+} containing a deamidated glutamine residue (see Table 5.3B). The signal intensity was low resulting in a low ion score. Moreover, there were two shorter peptides SSEEHLRQTR (m/z 414.878^{3+}) with deamidation of glutamine and QTRSETMR (m/z 496.235^{2+}) with the N-terminal glutamine converted to pyro-glutamic acid. These fragments had better ion scores than the longer peptide. However, neither of these were detected in the sample of purified native peptide.

Figure 5.4B shows the MS/MS spectrum of a precursor ion at m/z 534.261^{2+}, corresponding to SETMRNSVK with an oxidised methionine residue. There was a neutral loss of 64 Da ($HSOCH_3$) from MetS. Although the peak at m/z 502.406 was unassigned, it may represent the neutral loss of 64 Da (32 m/z difference x 2 charges).

Figure 5.4C shows the MS/MS spectrum of a precursor ion at m/z 528.627^{3+}, which corresponded to SSFHDPKLKGKPSR.

Figure 5.4D shows the MS/MS spectrum of a precursor ion at m/z 395.204^{2+}. Although none of the b-ions were detected in this spectrum dominated C-terminal ions generated a high quality spectrum with full identification of the peptide sequence corresponding to YVTHNR. The most abundant peak generated for y_4 ion at m/z 527.269 corresponded to RNHT.

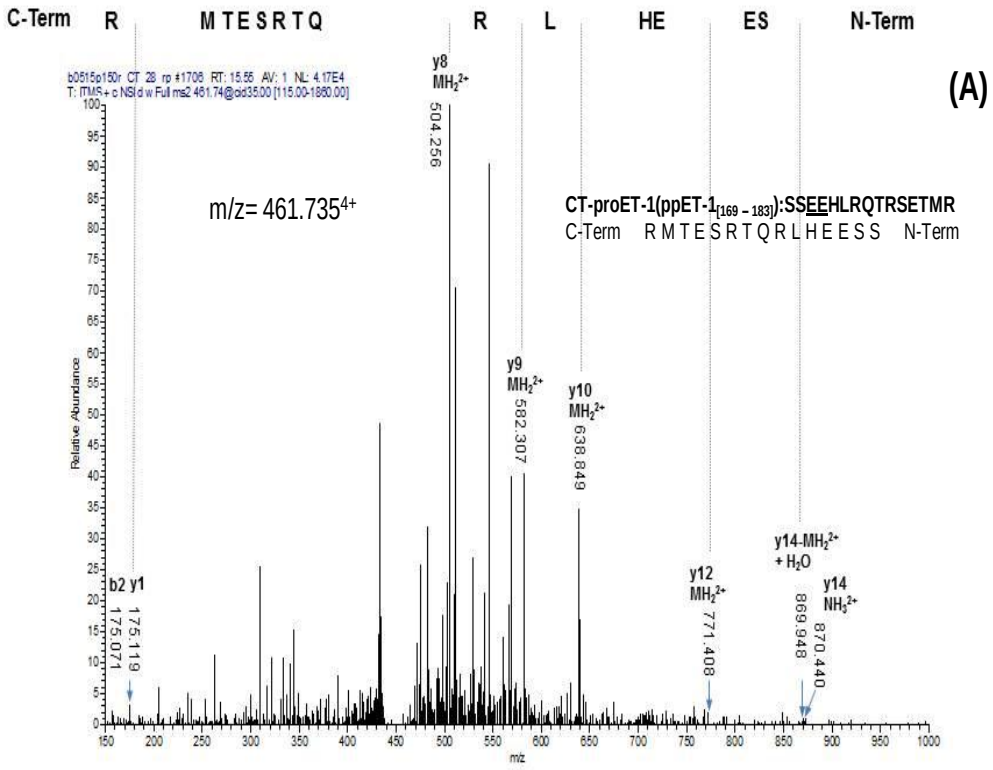
C-Term R M T E S R T Q R L HE ES N-Term
(A)
m/z= 461.735 4+
CT-proET-1(ppET-1 (169 – 183)):SSEEHLRQTRSETMR
C-Term R M T E S R T Q R L H E E S S N-Term
y8 MH2 2+ 504.256
y9 MH2 2+ 582.307
y10 MH2 2+ 638.849
y12 MH2 2+ 771.408
y14-MH2 2+ + H2O 869.948
y14 NH3 2+ 870.440
b2 y1 175.119 175.071
Relative Abundance
m/z

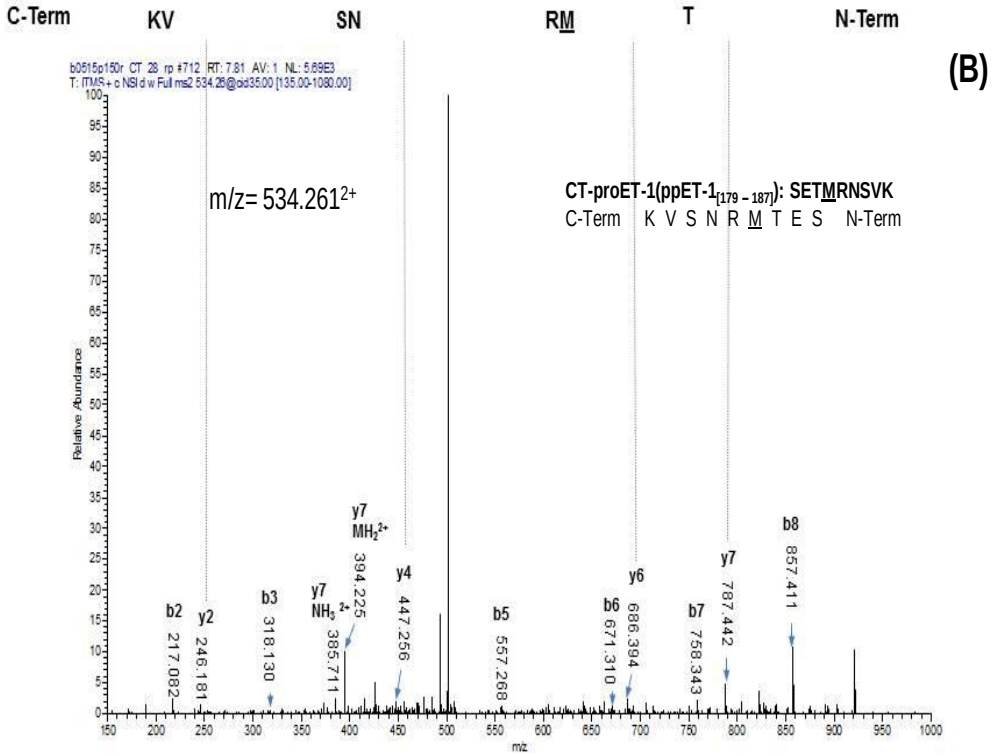
C-Term KV SN RM T N-Term
(B)
m/z= 534.261 2+
CT-proET-1(ppET-1 (179 – 187)): SETMRNSVK
C-Term K V S N R M T E S N-Term
y7 MH2 2+ 394.225
y4 447.256
y7 NH3 2+ 385.711
b3 318.130
b2 217.082
y2 246.181
b5 557.268
b6 671.310
y6 686.394
b7 758.343
y7 787.442
b8 857.411
Relative Abundance
m/z

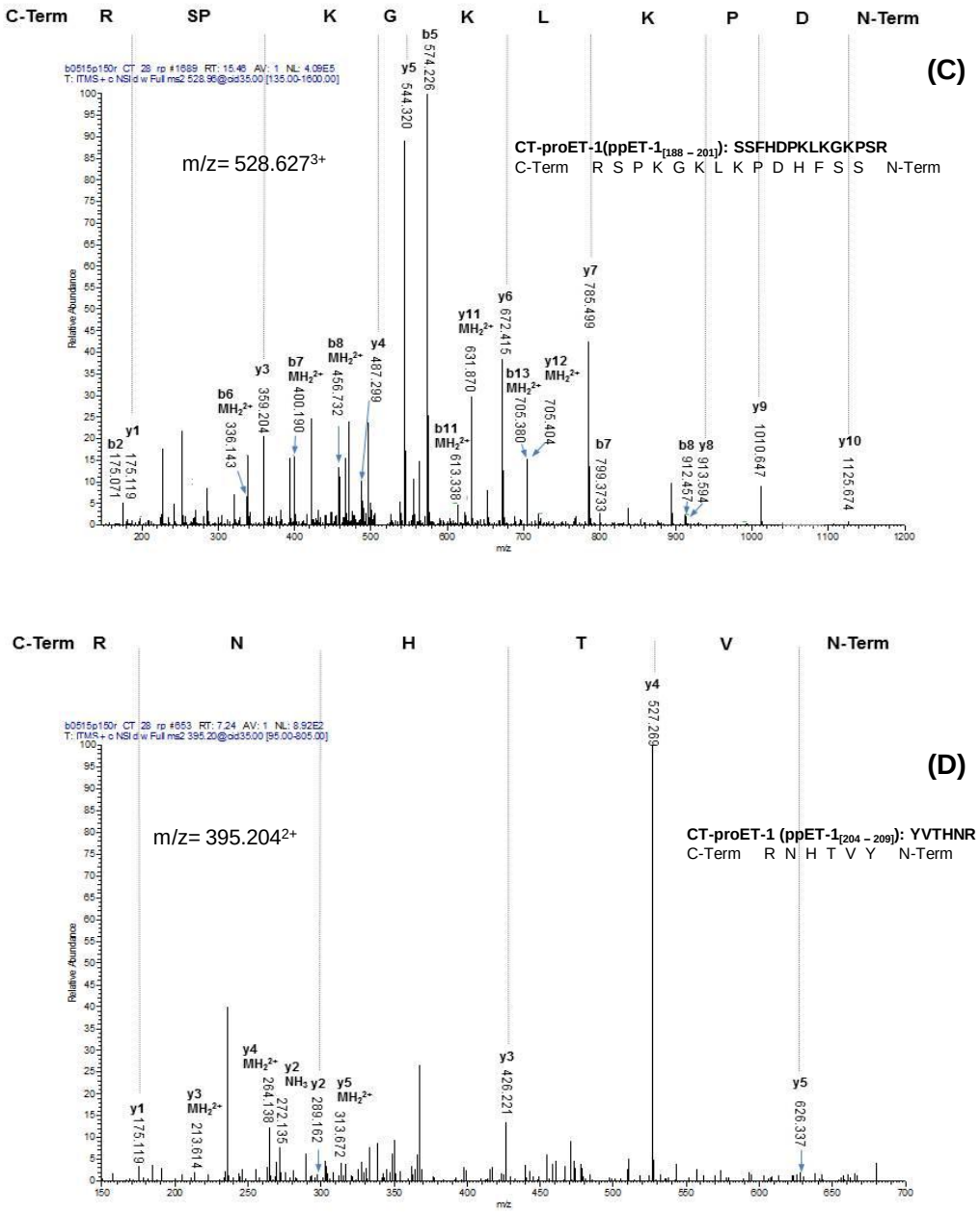

Figure 5.4: ***MS/MS spectra of purified/native CT-proET-1 (fraction 28) precursor ions at m/z (A) 461.735^{4+}, (B) 534.261^{2+}, (C) 528.627^{3+} and (D) 395.204^{2+}.*** *MS/MS spectra were manually annotated for C-terminal fragment ions (y-) and N-terminal fragment ions (b-) confirming the sequence identities of the precursor ions obtained from MASCOT. The mass differences between the y-ion series indicate amino acid residues of the corresponding fragment ions, which are shown above the spectrum. Annotations of –NH_3 or H_2O at b- and y-ions represent a loss of ammonia or water at the corresponding fragment ions with a loss of 17 and 18 Da, respectively.*

5.4 DISCUSSION

The aim of this chapter was to verify the identities of the purified native proET-1 peptides that were initially characterised using a combination of IEC, HPLC and immunoassay (Chapter 4). Here, a mass spectrometric approach was pursued with an initial series of experiments using synthetic peptide standards for optimisation of the methodology. Native proET-1 peptides purified from EA.hy 926 conditioned medium were analysed according to the methodology as shown in Figure 5.2.

The identity of the undigested native purified NT-proET-1 peptide (fraction 41) was not confirmed using mass spectrometry. Nevertheless, the same methodology identified this *EDN1* derived peptide from fraction 46, which represented the synthetic standard in medium and in the calibration curve prepared with NT-proET-1 synthetic standard. All samples were run with the same analysis parameters, suggesting that the problem was related to the purified sample itself rather than being associated with the methodology. The main limitation for identification of NT-proET-1 was insufficient peptide, so that the levels were below the detection limit of the method. This is likely the result of: **(1)** low levels of NT-proET-1 in the EA.hy 926 conditioned medium; **(2)** poor recovery following IEC; **(3)** degradation during sample concentration. Both HPLC fractions were dried overnight under vacuum with centrifugal force with SpeedVac (at room temperature), and stored at -80°C until the day of proteomic analysis. Degradation further reduces peptide levels and this is likely to contribute to poor recovery and identification of NT-proET-1 peptide. The fact that fraction 46 was dried in the same way, similar rate of peptide loss was expected from the native/purified sample. However, the final concentration of the native NT-proET-1 following reconstitution in 0.1% TFA was 132-fold less than the synthetic standard; 89 and 11,774 fmol/µl, respectively. This may result in differences in the rate of recovery. Thus, the resulting peptide concentration may not be sufficient or may be lower than the detection limit (<62.5 fmol/µl). In contrast, fraction 46 could be degraded to a lesser extent, in which the final levels were still sufficient for its identification.

Analysis of full-length ELDP and CT-proET-1 with an analytical UPLC BEH130 C18 column (1.7 µm, 100 µm x 100 mm) produced poor ionisation and fragmentation. Due to longer amino acid sequences and hydrophobicity, elution from the analytical column was not sufficient for analysis. In principle, this directly affects the number of peptides being subjected to ESI, which then directs ions into the LTQ before being sent to the Orbitrap for mass analysis (Schwartz *et al.*, 2002).

The first step for ELDP and CT-proET-1 identification involved trypsin digestion. This was followed by desalting prior to MS analysis. Buffers containing salts compromise ESI-MS performance leading to ion suppression. Following solvent exchange and concentration, samples were analysed using LTQ Orbitrap coupled online to a nanoflow UPLC equipped with a C18 column. Peptide sequences of ELDP and CT-proET-1 were manually verified from the MS/MS spectra (Figures 5.3 and 5.4). The relative abundance of fragment ions was normalised according to the most abundant fragment ion in the same MS/MS spectrum. Co-elution of contaminating or unknown fragment ions can result in ion suppression, and this reduces the intensity of fragment ions. This presents difficulties for detection of low abundance peptides particularly those closer to the signal-to-noise ratio. The presence of an intense contaminating fragment ion was an associated limitation for identification of less abundant proET-1 fragment ions (Figures 5.3A and 5.4B).

The N-terminal fragment of synthetic ELDP corresponded to ALENLLPTK (ppET-$1_{[93 - 101]}$). This fragment was only identified in the synthetic standard (fraction 45) (Table 5.2C) but not in the native peptide samples (fractions 43 and 47). Comparison of the XICs between the synthetic and the native peptide samples failed to identify a precursor ion at m/z 499.798^{2+}, which corresponded to ALENLLPTK (data not shown). Moreover, the intensity of the purified/native samples was very low for this precursor ion suggesting that the peptide is either not sufficiently abundant for detection or not present. However, because the purification procedure for ELDP (and CT-proET-1) focussed on recovery of peptides with high pI, it is likely that contaminating peptides would be rich in lysine and arginine. Hence, such contaminants would have competed as substrates for trypsin or potentially acted as trypsin inhibitors. This could affect digestion efficiency, resulting in longer peptides and these may not have been recovered from the trapping column.

ELDP contains an evolutionary conserved endothelin-like domain (ppET-$1_{[109 - 123]}$). Importantly, the positioning of the first four cysteine residues was exactly the same as in ET-1 (see Tables 1.1 and 1.6). Based on this similarity, disulphide bonds have been proposed to be formed between ppET-1 residues 109 – 123 and 111 – 119 [**C**^{109}Q**C**^{111}ASQKDKK**C**^{119}WNF**C**^{123}QAGK] without supporting experimental evidence (Uniport). Correct disulphide linkages are likely important for correct folding and structural stability (Zhang *et al.*, 2011). Therefore, a biological function associated with this peptide is likely to be preserved with correct folding. Thus, it was particularly important to show whether purified/native ELDP samples were forming these two intra-linked disulphide bonds as expected. In addition, ELDP consists of two more cysteine residues in its C-terminal end that were also likely to form disulphide bridges between Cys^{148} – Cys^{155}. In order to confirm the presence of disulphide bonds, ELDP analysis was carried out under non-denaturing conditions keeping cysteine residues intact. However, MASCOT database was unable to identify a tryptic peptide belonging to this region, either from the purified/native or the synthetic ELDP sample. In order to ensure that a peptide belonging to this region was absent from the MS/MS spectra, precursor ion masses (calculated from ProteinProspector) of both the full-length fragment containing non-cleaved DKK residues (CQCASQKDKKCWNFCQAGK) and the fragment with cleaved DKK residues (CQCASQK−−−CWNFCQAGK) were searched from the XICs. Searching further precursor ion masses with missed-cleavages (e.g. ENRCQCASQKDKKCWNFCQAGK, ENRCQCASQK−−−CWNFCQAGK, and ENRCQCASQK−−KCWNFCQAGK) and considering possible amino acid modifications such as deamidation of an asparagine (N) and glutamine (Q) residues, both individually and in combination failed to detect potential peptides. However, none of the calculated masses were detected for the purified native sample of ELDP or the synthetic peptide standard. In part, this might be explained by **(i)** inaccessibility of trypsin into the core of ELDP for cleavage; **(ii)** insufficient recovery of the resulting peptide from the separation column; or **(iii)** the presence of unexpected modifications. Moreover, it is well known that cysteine residues yield limited fragmentation and disulphide bonds are generally resistant to cleavage by low collision energies using CID fragmentation (Loo *et al.*, 1990). Furthermore, MASCOT and Sequest rely on fragmentation efficiency of peptides and this limits identification of peptides with disulphide bridges under non-denaturing conditions. Possibly, these factors are likely to contribute to the inability to identify this region of the ELDP peptide sequence. On the

other hand, synthetic ELDP was shown to naturally form three disulphide bonds on refolding at pH 8 (MWt 8,636.32 compared to 8,642.37 for unfolded peptide in which the mass difference of 6.05 Da represents loss of six hydrogens).

In support of the identification of ELDP sequence, the processing is likely to occur at the Lys-Arg and Arg-Arg at ppET-1 positions 91/92 and 167/168, respectively. Although ELDP sequence has four other processing sites, these were unlikely to yield a cleaved peptide. Cleavage at these other dibasic processing sites (Lys-Lys and Arg-Lys) occurs less frequently. In addition, the specificity of the PCs to cleave at these dibasic processing sites can be influenced by the conformation and the characteristics of the amino acid residue adjacent to the dibasic processing site (e.g. cleavage is less likely to occur if the next residue is proline). Secondary and tertiary structures influence accessibility of the PCs for cleavave. For example, cleavage is less likely to occur if the dibasic processing site is within a disulphide bond, making the site inaccessible by the proteolytic enzyme. This is likely to be the case for ppET-1 residues 127/128 (Lys-Lys) and 153/154 (Lys-Lys).

All peptide fragments with a methionine residue were oxidised to methionine sulphoxide (MetSO), resulting in a mass increment of 16 Da. Methionine oxidation can display a neutral loss of 64 Da, corresponding to methane-sulphenic acid (CH_3SOH). The MS/MS spectrum of a precursor ion at m/z 625.308^{2+} (ELRAEDIMEK) (Figure 5.3A) and other ions at m/z 625.308^{2+}, 681.990^{3+}, 823.368^{2+}, 549.247^{3+} and 887.414^{2+} (data not shown) all displayed this characteristic loss. Although oxidation of methionine is among the most common PTM, it could also be a potential by-product resulting from the purification/digestion and/or storage conditions. Oxidation to MetSO, 2-oxo-histidine, and hydroxytryptophan usually occur as a result of sample handling following protein separation (Perdivara *et al.,* 2010). MASCOT results have shown more PTMs to be associated with fraction 43, in comparison to fraction 47. This was in agreement with previous HPLC elution profiles in which fraction 43 was eluted earlier that fraction 47 (Chapter 4, Figure 4.3). Oxidation can alter folding and structural stability of a protein (Torchinsky, 1981). In addition, deamidation of asparagine or glutamine may change the conformation by transforming a neutral amide side chain to a negatively charged carboxylic acid ($-NH_2 \rightarrow -CO$). Oxidised peptide becomes more polar (hydrophilic) than the unoxidised peptide and as a result elutes earlier. Similarly, deamidated peptide elutes earlier than the unmodified peptide.

CT-proET-1 peptide sequence was confirmed by detection of both the N-terminal and C-terminal fragment ions corresponding to SSEEHLRQTRSETMR (ppET-$1_{[169 - 183]}$) and YVTHNR (ppET-$1_{[204 - 209]}$), respectively (see Figure 5.4). The identification of native CT-proET-1 was only confirmed from fraction 28 without identification of an *EDN1* peptide from fractions 29 and 31. On the day of analysis, final concentration of CT-proET-1 fractions 28, 29 and 31 (51.9, 60.3, and 43.3 fmol/µl, respectively) were ~2-fold less than the optimal sample concentration (100 fmol/µl), and this as a result can limit the identification of less abundant fragments ions.

The MS/MS spectrum for SSEEHLRQTRSETMR had poor resolution for both the synthetic and native CT-proET-1 samples (Figure 5.4A). This could result from: **(1)** inefficient ionisation of the adjacent serine and acidic glutamine residues. In particular, non-volatile materials (e.g. endogenous metabolites) and molecules with a higher mass (Annesley, 2003) contribute to ion suppression. More polar samples are also more sensitive to ion suppression (Bonfiglio *et al.,* 1999). **(2)** Poor recovery following desalting. **(3)** Inefficient elution from the separation column. The theoretical pI of this peptide was calculated as 6.5. The analytical column is packed with silica particles, which are stable under acidic conditions. Yet, the acidic peptide may not be eluted effectively under acidic conditions. **(4)** Low ion scores from MASCOT could simply suggest low abundance. Moreover, considering low ion scores and poor quality spectra, the difference between the experimental (1,842.911) and the calculated mass (1,842.923) was -0.118 Da, and the determined sequence was within a -6.43 ppm precision.

In summary, accessibility of peptides to trypsin for proteolytic cleavage, solubility and ionisation efficiency (nebulisation) of the tryptic digest combine to influence peptide fragmentation and detection using mass spectrometry. Differences in these factors may produce different signal intensities and affect the quality of an MS/MS spectrum. The results showed close agreement with experimental and calculated MWts showing correct identification of proET-1 peptide fragments.

In conclusion, these data confirm that the peptides ELDP and CT-proET-1 identified by sandwich immunoassay and purified from conditioned medium of EA.hy 926 cells are authentic proET-1 fragments. For CT-proET-1 (ppET-$1_{[169 - 212]}$) the MS data fully confirm for the first time the identity of this peptide. For the novel proET-1 derived

peptide ELDP (ppET-$1_{[169-212]}$), the MS data in combination with immunoassay results, and elution profile on HPLC relative to synthetic peptide standard all provide evidence of the correct identification of this peptide. But key structural features such as the disulphide bonds of the endothelin-like domain sequence could not be confirmed. For NT-proET-1 isolation of further peptide is required to confirm the sequence of this peptide and to determine the reasons underlying the differences in HPLC elution characteristics of the purified native peptide and the synthetic standard.

CHAPTER 6

Evaluation of ELDP and CT-proET-1 as biomarkers of cardiovascular and renal disease

6.1 INTRODUCTION

6.1.1 Metabolism and clearance of ET-1

ET-1 has a short circulating half-life (30 – 60 s) (Gasic *et al.,* 1992; Corder & Vane, 1994). Rapid clearance and low circulating levels of ET-1 results from a combination of factors: **(i)** most ET-1 is released abluminally (Wagner *et al.,* 1992) and then acts in a paracrine or autocrine manner on endothelial and smooth muscle cells; **(ii)** binding to ET_B receptors that are primarily located in the pulmonary vascular endothelium accounts for the majority (53%) of clearance (Wagner *et al.,* 1992; Dupuis *et al.,* 1996b), but also contributing to clearance from the kidney; and **(iii)** degradation by NEP-24.11 (Abassi *et al.,* 1992; Vijayaraghavan *et al.,* 1990; D'Orléans-Juste *et al*., 2003). Therefore, measuring plasma concentrations may not correctly reflect ET-1 biosynthesis as this mainly reflects the spillover of total synthesis (Dupuis *et al.,* 1996). There is a well-coordinated regulation between biosynthesis and clearance.

6.1.2 Physiological role of ET-1 in cardiovascular and renal function

Physiological actions of ET-1 are mediated by activation of ET receptors, ET_A and ET_B. ET_A receptors predominate on the underlying VSMC throughout the cardiovascular system and mediate vasoconstriction. ET_B receptors are less abundant (15%) also mediate vasoconstriction (Davenport & Maguire, 1994; Haynes *et al.,* 1995). In contrast, in the renal system, ET_B receptors predominate and mediate vasodilatation, natriuresis and diuresis (Davenport & Maguire, 2006).

Endothelial cell-specific deletion of ET_B results in impaired clearance of exogenous ET-1 however, without increasing blood pressure (BP) (Bagnall *et al.,* 2006). In contrast, inner medullary collecting duct (IMCD) specific deletion of ET_B results in salt-sensitive hypertension without altering the clearance of ET-1 (Bagnall *et al.,* 2006; Ge *et al.,* 2006). Therefore, these results suggested that while endothelial ET_B receptors mainly contribute to clearance, IMCD ET_B receptors mediate natriuretic action of ET-1. Some studies that defined the role of ET-1 for the maintenance of vascular tone and BP are briefly explained in the next section.

6.1.2.1 *Effects of ET-1 in the regulation of basal vascular tone*

In healthy man, brachial artery infusion of ET-1 produces concentration-dependent vasoconstrictor and pressor responses. After infusion, an initial transient vasodilatation [indicated by increased forearm blood flow (FBF)] was followed by a slowly developing but sustained vasoconstriction that lasted for 2 h (Clarke *et al.,* 1989; Kiowski *et al.,* 1991). In general, while selective ET_A (BQ-123) or $ET_{A/B}$ receptor (TAK-044) antagonism resulted in vasodilatation (minimal) and reduced BP (Haynes, 1995; Haynes *et al.,* 1996; Schmetter *et al.,* 1998; Hand *et al.,* 1999; Verhaar *et al.,* 1998), selective ET_B receptor antagonism caused vasoconstriction (Spratt *et al.,* 2001). This suggested that endogenous ET-1 contributes to basal vascular tone by mediating vasoconstriction through ET_A receptor activation and that selective ET_A receptor antagonists could have superior therapeutic benefits.

6.1.2.2 *Effects of ET-1 in renal physiology and haemodynamics*

ET-1 is synthesised by most renal cell types. In pig, the synthesis of ET-1 was shown to be higher in the IMCD than any other organ (Kitamura *et al.,* 1989). Renal vasculature is also more sensitive to ET-1 than other vascular beds (Pernow *et al.,* 1989).

Exogenous ET-1 at low concentrations reduced renal plasma flow (RPF) and Na^+ excretion without having an effect on BP. At higher concentrations, ET-1 reduced glomerular filtration rate (GFR) and increased renal vascular resistance (Weitzberg *et al.,* 1991) (Table 6.1). Physiological actions of ET-1 (at low and high doses) differed depending on the experimental model, receptor localisation, and relative subtype abundance. Selective ET_A antagonism (BQ-123) in chronic kidney disease (CKD) patients increased renal blood flow (RBF), reduced BP and effective filtration fraction (FF) suggesting ET_A mediated preferential efferent arteriolar constriction without changing GFR (Goddard *et al.,* 2004). Selective ET_B receptor antagonism (BQ-788) caused renal vasoconstriction both in chronic renal failure and in healthy controls (Goddard *et al.,* 2004). The physiological role of ET-1 and its receptors in renal system were defined by specific knockout (KO) studies and some of these results are summarised in Table 6.2.

Table 6.1: ***Haemodynamic effects of exogenous ET-1 in healthy man.*** *BP = blood pressure, GFR = glomerular filtration rate, FBF = forearm blood flow, FF = filtration fraction, RBF = renal blood flow, RPF = renal plasma flow, HR = heart rate, CO = cardiac output, MAP = mean arterial blood pressure.*

Doses of exogenous ET-1 administered in the forearm of healthy man	**Effects of ET-1**	**Reference(s)**
<1 pmol/kg/min	● Decreased Na^+ excretion by 36%, without having an effect on systemic or renal haemodynamics.	Rabelink *et al.,* 1994
2.5 pmol/kg/min	● Balanced GFR, thus relatively constant FF. ● Increased RBF and induced natriuresis and diuresis by inhibiting apical Na^+ and water reabsorption.	Kaasjager *et al.,* 1995
1.5 and 3 pmol/kg/min	● Decreased HR and CO, increased systemic vascular resistance and impaired left and right ventricular diastolic filling.	Kiely *et al.,* 1997
≤4 pmol/kg/min	● Reduced FBF and increased MAP.	Haynes & Webb, 1998
4 pmol/kg/min	● Reduced RPF and GFR and increase renal vascular resistance. ● Increased glomerular capillary pressure and MAP. ● Reduced FF. ● Reduced urinary Na^+ and water excretion (urine volume).	Weitzberg *et al.,* 1991 Vuurmans *et al.,* 2004 Sørensen *et al.,* 1994 Rabelink *et al.,* 1994

Table 6.2: ***Physiological role of ET-1 in the regulation of blood pressure and renal function: A perspective from collecting duct (CD) specific knockouts (KO) of ET-1, ET_A and ET_B receptors.***

Model of study	Effects of ET-1 and ET_A/ET_B receptors	Reference(s)
CD ET-1 KO mice	● Salt-sensitive hypertension in which high salt diet further increased BP. ● Amiloride, which is a direct inhibitor of epithelial Na^+ channel (ENaC), partly restored BP. This indicated that Na^+ epithelial channel is involved in regulation of Na^+ excretion. ● Impaired ability to excrete Na^+ and acute water load. Increased arginine vasopressin (AVP)-induced cAMP accumulation.	Ahn *et al.*, 2004 Kurihara *et al.*, 1994 Kisanuki *et al.*, 2010 Ge *et al.*, 2005a
CD ET_A KO mice	● Normal BP and urinary Na^+ excretion even after a high salt diet. ● Reduced water reabsorption associated with lower AVP-stimulated IMCD cAMP accumulation. Increased diuresis after water load.	Ge *et al.*, 2005b Tomita *et al.*, 1993
CD ET_B KO rats	● Salt-sensitive hypertension that is partly restored with amiloride. ET_B was suggested to regulate Na^+ excretion at the epithelial Na^+ channel in CD cells. ● Increase in BP was smaller (50%) in comparison to CD ET-1 KO and combined $ET_{A/B}$ KO.	Gariepy *et al.*, 2000 Webb *et al.*, 1998 Ge *et al.*, 2006; 2008 Schneider *et al.*, 2008

6.1.3 ELDP and CT-proET-1 as biomarkers of vascular and renal disease

6.1.3.1 *Chronic heart failure*

Plasma levels of ET-1 are elevated in patients with heart failure (HF) (Stewart *et al.,* 1992; Rodeheffer *et al.,* 1992; McMurray *et al.,* 1992) and in experimental models (e.g. dogs) (Motte *et al.,* 2003) through increased ET-1 synthesis by cardiomyocytes, vascular endothelial cells and cardiac fibroblasts (Porter & Turner, 2009). Plasma levels of ET-1 directly correlate with pulmonary artery pressure (Moraes *et al.,* 2000). ET-1 expression is increased in lung tissue and in the circulation of patients with pulmonary artery hypertension (PAH) (Giaid *et al*., 1993; Bauer *et al.,* 2002). In contrast, hypertensive patients had lower ET-1 levels with the exception of black Africans (Ergul *et al.,* 1996).

6.1.3.2 *Chronic kidney disease*

Renal ET-1 production is upregulated in CKD (Orisio *et al*., 1993). Increased plasma (Goddard *et al*., 2007) and urinary (Dhaun *et al.,* 2009) ET-1 levels correlate with declining renal function measured as estimated GFR (eGFR). Moreover, urinary ET-1 excretion is independent of plasma ET-1 concentrations (Serneri *et al*., 1995). It is mainly derived from renal tubular secretion and reflects renal ET-1 production (Benigni *et al.,* 1991). Thus, urinary ET-1 excretion was suggested as a potential biomarker for renal disease (Ohta *et al.,* 1991).

CKD is strongly associated with increased cardiovascular disease risk (Go *et al.,* 2004). According to the National Kidney Foundation (USA), classification of CKD is based on albumin-creatinine ratio in spot urine and eGFR from serum creatinine measurements (National Kidney Foundation, 2002).

Proteinuria is a risk factor associated with progression of renal disease (Lea *et al.,* 2005) and reported as a marker of renal failure in CKD (Dhaun *et al.,* 2011). Increased ET-1 production in CKD contributes to excessive protein filtration (increased protein excretion) through its haemodynamic effects leading to increased glomerular capillary pressure via ET_A mediated renoconstriction of efferent arterioles (Barton, 2008) and glomerular permeability (Saleh *et al.,* 2010).

6.1.4 Hypothesis and aims

Despite strong evidence that ET-1 is involved in cardiovascular and renal disease pathology, plasma measurements of ET-1 have a number of limitations (described in section 6.1.1) and have yielded inconsistent findings (Schiffrin *et al.,* 1997; Goddard & Webb, 2000). Early identification of these diseases still remains a challenge. Hence, stable fragments of proET-1 synthesis may have greater utility over current markers for earlier diagnosis, assessing disease progression and treatment outcomes, and may provide a non-invasive measure of cardiovascular function that directly reflects BP or cardiac changes. Therefore, the aim of this chapter was to **(i)** identify stable proET-1 peptide fragment(s) as alternative markers of ET-1 synthesis and **(ii)** test their potential as markers of cardiovascular and renal diseases. Accordingly, to test this hypothesis, initially clearance rates in rats, and the stability of proET-1 peptides were evaluated. Their usefulness as biomarkers of cardiovascular and renal disease was then assessed using samples collected in four studies:

Study 1: The effects of TNF-α infusion on proET-1 levels in healthy man.

Study 2: ProET-1 levels in mild/pre-hypertension and in chronic HF.

Study 3: ProET-1 levels in CKD.

Study 4: The effects of sitaxentan on plasma concentrations of proET-1 peptides. Assess correlation of proET-1 peptide levels with functional parameters that were previously reported in Dhaun *et al.,* 2011, 2013.

6.2 METHODS

6.2.1 Stability and metabolism of proET-1 peptides

Clearance and metabolism of proET-1 peptides were evaluated using synthetic NT-proET-1 (ppET-$1_{[18-50]}$), ELDP (ppET-$1_{[93-166]}$) and CT-proET-1 (ppET-$1_{[169-212]}$).

6.2.1.1 *Clearance rates of proET-1 peptides in vivo in rat circulation*

Four male Wistar rats (Charles River UK Limited) with a mean ± s.e.m weight of 345 ± 6 g were anaesthetised with sodium thiopentone intraperitoneally (i.p.) (120 mg/kg). Polyethylene catheters (PE-50) were inserted into the left carotid artery for blood collection. A 25G needle was attached to the PE-50 catheter containing saline.

A mixed peptide solution containing 1 nmol/ml of each proET-1 peptide (NT-proET-1, ELDP and CT-proET-1) was prepared in 0.9% NaCl/0.1% BSA and filtered (0.2 µm) before use. An initial blood sample (1 ml) was collected at -5 min at rest, before injecting the proET-1 peptide solution. A bolus dose containing 1 nmol/kg of each proET-1 peptide was administered intravenously (*i.v.*) into the femoral vein.

After injection, arterial blood samples (500 µl) were collected through the carotid artery at 0.5, 1, 2, 5, 10, 20 and 40 min into chilled 1.5 ml microcentrifuge tubes containing 50 Units/ml of heparin as an anticoagulant. Samples were kept on ice until the end of 40 min. Plasma was then collected after centrifugation of samples at 12,000 rpm for 2 min at 4°C and transferred into fresh 1.5 ml microcentrifuge tubes avoiding red blood cell contamination. Small aliquots of samples were stored at -80ºC for subsequent analyses. NT-proET-1, ELDP and CT-proET-1 were assayed using magnetic bead-based multiplex assays using Luminex methodology (see Chapter 2, section 2.2.3).

6.2.1.2 *Stability of proET-1 peptides in human whole blood and plasma*

Blood was withdrawn from a forearm vein of a healthy volunteer and collected into a syringe containing heparin (50 Units/ml). In order to carry out plasma incubations of synthetic peptides, one third of whole blood was immediately separated into chilled 2.0 ml microcentrifuge tubes and centrifuged at 12,000 rpm for 2 min at 4°C to collect plasma. Heparin anticoagulated plasma was separated into fresh 2.0 ml microcentrifuge tubes and kept on ice.

Peptide mix (1 nmol/ml) stock solution was diluted in freshly prepared saline (0.9% NaCl/0.1% BSA, 0.2 µm filtered before use). This interim dilution was added into the remaining whole blood and to the plasma giving a final concentration of 500 fmol/ml of each proET-1 peptide. The tubes were mixed gently by inverting several times. Aliquots of whole blood (750 µl) and plasma (250 µl) were separated into 1.5 ml microcentrifuge tubes and incubated at room temperature (22 – 24°C) and on ice (4°C) for 5, 10, 20, 40, and 60 min. At the end of each time point, whole blood was centrifuged and the separated plasma samples were stored on ice until the end of incubation. Samples had no visible evidence of haemolysis. Samples from the plasma incubations were frozen immediately after each incubation time. All samples were stored at -80°C. Concentrations of proET-1 peptides were determined using double-site sandwich based immunoassay (Chapter 2, section 2.2.2.4).

6.2.2 Biomarker investigation study details

6.2.2.1 *The effects of TNF-α infusion on ELDP and CT-proET-1 levels*

Collection of samples used for this investigation was described in Patel *et al.,* 2002. ET-1 release in response to TNF-α infusion was studied in 6 healthy subjects (mean age 56 years; male:female 5:1). Briefly, FBF and plasma flow responses to acetylcholine (ACh) and sodium nitroprusside (SNP) were monitored before and during TNF-α infusion over 6 h. TNF-α was administered to the brachial artery aiming to achieve a local concentration of 200 pg/ml (in venous blood, observed concentration was 40 pg/ml). Arterial and venous blood samples were collected at baseline and during TNF-α infusion for up to 300 min.

6.2.2.2 *Heart failure*

Blood samples from patients with chronic stable HF study were collected at the London Chest Hospital, Barts Health NHS Trust with the approval of the local research ethics committees and the written informed consent of each subject (East London and the City Research Ethics Committee – reference number 07/Q0604/24). The levels of proET-1 peptides in patients with chronic HF (HF, n = 24) were compared with untreated subjects with pre-hypertension/mild hypertension (pre-H, n = 24) collected in the Centre for Clinical Pharmacology, William Harvey Research Institute, Charterhouse Square (East London and the City Research Ethics Committee – reference number 07/Q0605/44). Subject demographic data are shown in Table 6.3. After patients had been at rest for at least 15 min, blood samples were collected into pre-chilled EDTA tubes, placed on ice and centrifuged within 10 min using a cooled centrifuge (4000 rpm for 10 min at 4ºC). Supernatant plasma was stored at -80ºC until immunoassay.

Table 6.3: ***Demographic and clinical characteristics of patients in heart failure study.*** *Values are given as mean ± s.e.m. NA indicates measurements for which data was not available.*

	Heart Failure	**Pre-hypertension**
n	24	24
Age (years)	70 ± 2.0	55.4 ± 1.5
Male gender	20 (80%)	24 (100%)
Weight (kg)	85.7 ± 4.3	80.4 ± 3.0
Body Mass Index (kg/m^2)	29.6 ± 1.2	26.7 ± 0.5
Systolic Blood Pressure (mmHg)	126.3 ± 3.6	144.8 ± 2.1
Diastolic Blood Pressure (mmHg)	71.0 ± 2.0	87.1 ± 1.3
Heart rate (bpm)	64.0 ± 1.4	69.3 ± 2.0
NYHA chronic HF Class II/III	20 (80%)/ 4 (20%)	NA
LVEF (%)	31.2 ± 2.0	NA
NT-proBNP (pg/ml)	1970 ± 288	NA

6.2.2.3 *Chronic Kidney Disease*

Plasma and urine samples were obtained through collaboration with Prof. David J. Webb at the University of Edinburgh. CKD patients classified as stage 1 to 5 based on the Kidney Disease Outcome Quality Initiative (K/DOQI) classification criteria (National Kidney Foundation, 2002) had renal disease without co-existing morbidities. Venous plasma and urine samples were collected after a 12 h fast and stored frozen at -80ºC until ELDP and CT-proET-1 analysis. Details of these patients and sample collection have been described previously (Lilitkarntakul *et al.*, 2011).

6.2.2.4 *Proteinuric CKD receiving renoprotective treatment*

Plasma and urine samples were from a clinical trial conducted by Dhaun *et al.*, 2011, 2013. This was a randomized, double-blind, three-way crossover study in 27 patients with proteinuric CKD, which investigated the effects of sitaxentan (Thelin, Encysive Pharmaceuticals), nifedipine and placebo on proteinuria, BP, arterial stiffness and urine ET-1/creatinine (renal ET-1 production). Cardiovascular indices were monitored at baseline, week 3, and week 6 of each treatment period and samples were collected for biochemical analyses. Oral administration of sitaxentan (100 mg/day) (Dhaun *et al.*, 2007a) and nifedipine (30 mg/day) were as once daily doses. Both were recommended therapeutic doses for human.

6.2.3 Evaluation of CT-proET-1 antibodies for biomarker investigations

Sheep were immunised with N-terminal (ppET-$1_{[169-179]}$) and C-terminal (ppET-$1_{[204-212]}$) CT-proET-1 peptides to produce highly specific and sensitive antibodies for capture and detection with low cross-reactivity. The aim of this approach was to reduce non-specific binding, as this is crucial for accurate detection of lower peptide concentrations and for increasing assay sensitivity. The assay performance of the new antibodies was compared with the existing CT-proET-1 antibodies to determine the best antibody combination to use for the analysis of plasma samples in Chapter 6.

Affinity purification of antisera (see section 2.2.4.6.3) obtained from sheep immunised with C-terminal CT-proET-1 (Lys_{203}-CT-proET-$1_{[204-212]}$) peptide produced the highest binding IgG in fractions I, H – J and E – F (from the 3rd bleed sample, obtained 2 weeks after the 4th immunisation with peptide antigen). These IgG fractions were biotinylated (section 2.2.4.1.3) and compared to the existing rabbit anti ppET-$1_{[204-212]}$ biotinylated IgG. For this comparison, black clear bottom Costar 96 well plates were coated with the CT-proET-1 capture antibody [sheep anti ppET-$1_{[169-186]}$ IgG] at 1 µg/ml, and incubated with SAB (0 fmol/ml) to determine background signal/non-specific binding or CT-proET-1 standard at 5 and 50 fmol/ml. Detection of bound peptide was achieved with biotinylated rabbit anti ppET-$1_{[204-212]}$ IgG diluted at 1:100 or with biotinylated sheep anti ppET-$1_{[204-212]}$ IgG fractions I, H – J and E – F, each tested at three dilutions corresponding to ~30, 15 or 7.5 ng/well (Table 6.4). The assay methodology was carried out as described in section 2.2.2.3.

Table 6.4: ***Comparison of existing biotinylated antibody (rabbit anti ppET-1$_{[204 – 212]}$) with affinity purified biotinylated sheep anti CT-proET-1 IgG fractions I, H – J and E – F.*** *Sheep anti CT-proET-1(ppET-1$_{[169 – 186]}$) IgG capture antibody (1 µg/ml) was incubated with assay buffer or CT-proET-1 standard at 5 and 50 fmol/ml followed by the biotinylated detection antibodies I, H – J and E – F (~30, 15 and 7.5 ng/well).*

	0	**5**		**50**	
	Mean	**Mean**	**S:N**	**Mean**	**S:N**
Rabbit anti IgG at 1:100	3,185.7	8,941.5	2.8	60,107.9	18.9
I at 1:1,000	2,722.9	19,649.5	7.2	135,146.6	49.6
I at 1:2,000	429.7	16,779.7	39.1	128,154.9	298.2
I at 1:4,000	120.7	14,624.2	121.2	119,148.0	987.1
H – J at 1:800	1,983.3	18,843.8	9.5	129,847.8	65.5
H – J at 1:1,600	400.7	15,701.9	39.2	122,594.6	306.0
H – J at 1:3,200	99.2	13,497.9	136.1	112,750.0	1,136.6
E – F at 1:1,400	436.8	8,709.8	20.0	75,940.0	173.9
E – F at 1:2,800	73.4	4,136.6	56.4	44,352.3	604.3
E – F at 1:5,600	30.6	1,264.4	41.3	22,333.3	729.8

Detection with affinity purified biotinylated IgG [sheep anti ppET-1$_{[204 – 212]}$] fractions I (at 1:4,000) and H – J (at 1:3,200) (i.e. both IgG diluted to ~7.5 ng/well) produced very similar results with lower non-specific binding and greater signal-to-noise ratio (S:N) when compared to biotinylated rabbit anti ppET-1$_{[204 – 212]}$ IgG (Table 6.4).

Affinity purification of IgG from antisera collected from sheep immunised with N-terminal CT-proET-1 (CT-proET-$1_{[169 - 179]}$) resulted in elution of highest binding antibodies in fractions H – I and E – F. These fractions were used as capture antibodies at 2 µg/ml, with the same standard concentrations and biotinylated antibody dilutions being used as described above. The signal from the new coating antibodies was compared to the existing capture antibody (Table 6.5).

Table 6.5: ***Comparison of biotinylated rabbit anti ppET-$1_{[204 - 212]}$ IgG with affinity purified sheep anti ppET-$1_{[204 - 212]}$ IgG fractions I, H – J and E – F with the capture antibody sheep anti ppET-$1_{[169 - 179]}$ IgG fractions E – F.***

	0	**5**		**50**	
	Mean	**Mean**	**S:N**	**Mean**	**S:N**
Rabbit anti IgG at 1:100	102,256.0	105,825.6	1.0	145,945.6	1.4
I at 1:1,000	132,328.4	150,649.0	1.1	208,684.3	1.6
I at 1:2,000	88,191.8	104,299.6	1.2	181,241.3	2.1
I at 1:4,000	57,866.1	73,651.6	1.3	157,748.3	2.7
H – J at 1:800	149,430.8	160,939.2	1.1	213,543.7	1.4
H – J at 1:1,600	89,202.9	105,512.3	1.2	178,999.4	2.0
H – J at 1:3,200	53,283.4	71,084.1	1.3	153,866.5	2.9
E – F at 1:1,400	92,123.2	99,935.3	1.1	154,673.4	1.7
E – F at 1:2,800	64,129.0	73,251.4	1.1	128,163.6	2.0
E – F at 1:5,600	46,022.2	52,662.8	1.1	91,335.0	2.0

Sheep anti ppET-$1_{[169 - 179]}$ (H – I) IgG used as the capture antibody did not produce any binding (data not shown), while sheep anti ppET-$1_{[169 - 179]}$ (E – F) IgG produced higher background signal than the existing capture antibody [sheep anti ppET-$1_{[169 - 186]}$ IgG]

(Table 6.5). As a result, the main improvement for the CT-proET-1 immunoassay was achieved with the new C-terminal CT-proET-1 anti-sheep biotinylated IgG I at 1:4,000 dilution or H – J at 1:3,200 with the existing N-terminal CT-proET-1 sheep anti ppET-$1_{[169-186]}$ IgG. Biotinylated anti ppET-$1_{[204-212]}$ sheep IgG fraction I was chosen as the detection antibody for further characterisation and application in biomarker studies because the total antibody purified in this fraction was ~5 times more than in the pooled side fractions H – J.

6.2.3.1 *Analysis of matrix effects of plasma and serum on ELDP and CT-proET-1 standard curves*

To determine matrix effect of human plasma in ELDP and CT-proET-1 assays the standard curves (concentration range 3.125 – 200 fmol/ml) were prepared in assay buffer, horse serum and heparin anticoagulated plasma using the assay methodology described in section 2.2.2.4. These studies were performed in high-binding white plates (Costar), which increase by more than 100-fold the chemiluminescence signal generated during assay end-point measurement. Here, after blocking as usual, standard curves were prepared by adding 25 µl nSAB to all wells, followed by 25 µl of each matrix (nSAB, horse serum, or plasma) and 50 µl of standards.

Figure 6.1 shows close similarity between all three matrixes at the higher concentration range. However, both ELDP and CT-proET-1 standards prepared in heparin anticoagulated plasma had higher counts at the lower range of the standard curve (0 – 12.5 fmol/ml) (Figure 6.1). This finding was also consistent for standard curves prepared in EDTA anticoagulated human plasma (data not shown). The signal observed with the low concentrations of proET-1 standards is likely primarily due to endogenous peptide present in the test plasma. This was a consistent observation across all plasma samples evaluated. Therefore, standard curves prepared in human plasma (either heparin or EDTA anticoagulated) were unsuitable for determining ELDP and CT-proET-1 concentrations in patient samples. In comparison, the background signal from horse serum was very similar to that obtained when standards were diluted in assay buffer. This is expected as horse proET-1 has only low homology over the sequences used to generate specific antibodies for ELDP and CT-proET-1 (http://www.ensembl.org *Equus_caballus EDN1* gene ENSECAG00000011618), so even if present would not cross react in these assays. Standard curves prepared in horse serum were more similar to standards diluted in nSAB showing it as a more suitable matrix for preparation of standard curves than human plasma. However, horse serum did not appear to provide any advantages over standard curves prepared in nSAB. Therefore, for biomarker assays ELDP and CT-proET-1 peptide concentrations were determined from standard curves diluted in nSAB.

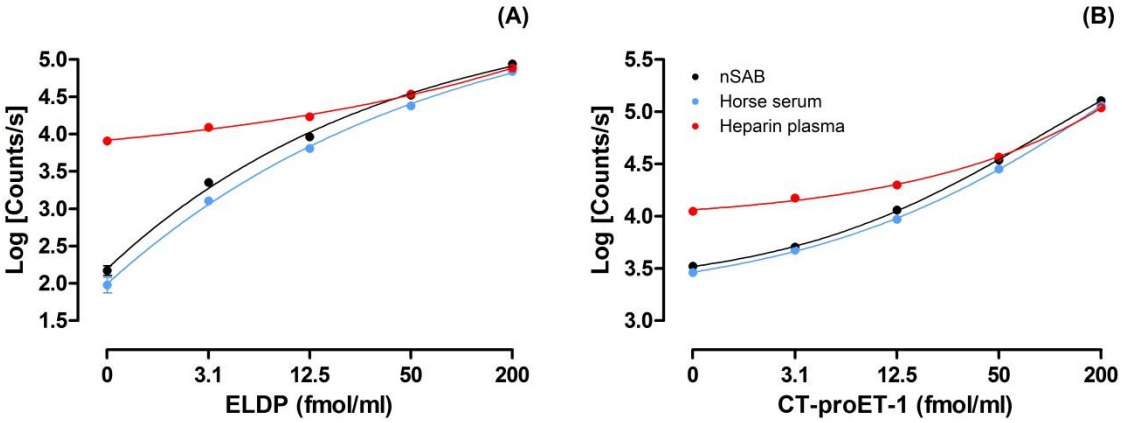

Figure 6.1: ***Standard curves of (A) ELDP and (B) CT-proET-1 prepared in nSAB, horse serum and heparin anticoagulated plasma.***

Figure 6.2 demonstrates the reproducibility of ELDP and CT-proET-1 immunoassays with standard curves (concentration range 0.09 – 200 fmol/ml for ELDP and 0.27 – 200 fmol/ml for CT-proET-1) prepared in nSAB for the analysis of plasma samples obtained from patients analysed in Chapter 6.

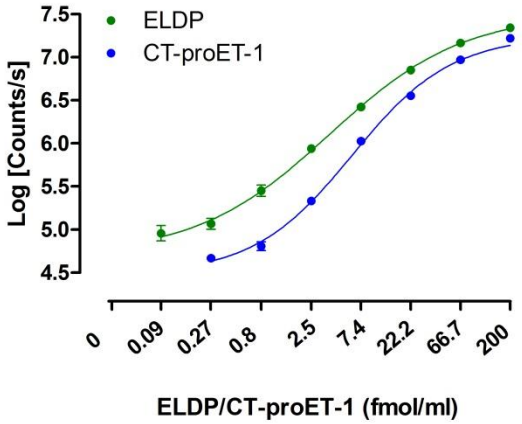

Figure 6.2: ***Reproducibility of ELDP and CT-proET-1 standard curves produced during biomarker investigations.*** *ELDP (n = 6) and CT-proET-1 (n = 7) standard curves generated during analysis of plasma samples.*

6.2.4 Immunoassays for plasma and urinary ELDP and CT-proET-1 measurements

Specific double-recognition site sandwich ELISAs were optimised for plasma measurements of ELDP and CT-proET-1. All samples in the biomarker investigation were analysed using the immunoassay assay methodologies described in Chapter 2, section 2.2.2.4. The lower limit of detection for ELDP (n = 12) in plasma was 0.3 fmol/ml and 0.09 fmol/ml in urine. The detection limit for CT-proET-1 (n = 18) in plasma was 0.6 fmol/ml and 0.34 fmol/ml in urine. These were calculated using the formula "mean of background + (3 x standard deviation of background)" and the values used were from the standard curves used for the analysis of samples described in this chapter. All assays were performed blinded to the sample code.

6.2.5 Statistical analysis

Plasma levels were expressed as mean ± s.e.m (fmol/ml). Changes in ELDP and CT-proET-1 levels between baseline and different time points or groups were compared using one-way ANOVA with Bonferroni post-hoc test. Plasma levels of ELDP and CT-proET-1 after TNF-α infusion and in pre-hypertension and chronic HF were compared using Student's *t*-test (unpaired, two-tailed) and by two-way ANOVA with Bonferroni post-hoc test. Effects of treatments (sitaxentan, nifedipine, and placebo) on plasma levels of ELDP and CT-proET-1 were shown as percentage change (%) from baseline. The difference in plasma levels at week 3 and week 6 of each treatment was compared to baseline levels and significance was determined by ANOVA with repeated measures. Relationships between proET-1 peptides and other cardiovascular and renal parameters (e.g. eGFR or 24 h Na^+ excretion) were investigated using linear regression analysis (GraphPad Prism 5). In the scatter plots *P* values and r^2 (linearity of the data) are reported.

6.3 RESULTS

6.3.1 Clearance and metabolism of proET-1 peptides

6.3.1.1 *Clearance rates of proET-1 peptides in rat circulation*

A mixed proET-1 peptide solution was administered as a bolus dose of 1 nmol/kg. Arterial plasma levels determined before injection (-5 min) and at 0.5, 1, 2, 5, 10, 20 and 40 min following injection showed markedly different elimination rates for the proET-1 peptides (P <0.001; one-way ANOVA) (Figure 6.3). At 30 sec after the injection, the levels of NT-proET-1, ELDP and CT-proET-1 were 287 ± 23, 3648 ± 234, and 11736 ± 639 fmol/ml, respectively. Assuming 100 g body weight (BW) of a rat has a circulating blood volume of 7.2 ± 0.3 ml (Argent *et al.,* 1994), then according to mean weight of Wistar rats (345 ± 6 g), the total circulating blood volume was 24.8 ± 1.8 ml. The maximum observed concentration of proET-1 peptides was likely to be 23 – 35 pmol/ml assuming a haematocrit of 40 – 60%. According to these assumptions with a haematocrit of 50%, the percentage of NT-proET-1, ELDP and CT-proET-1 remaining 0.5 min after the injection was ~1%, ~13%, and ~42% of the administered peptide, respectively.

The time coarse of measurements showed NT-proET-1 had the most rapid clearance (<5 min) in which only 1.8 ± 0.8% of initial values (at 0.5 min) remained 5 min after injection in the plasma (estimated half-life <1 min). ELDP and CT-proET-1 had slower clearance rates, in which 2.5 ± 0.2% and 13.3 ± 1.0% of initial values remained 20 min after injection, respectively. Clearance rates for ELDP and CT-proET-1 both showed two phases with estimated half-lifes of 0.52 and 0.74 min for phase 1, and 5.73 and 7.25 min for phase 2 (Figure 6.3).

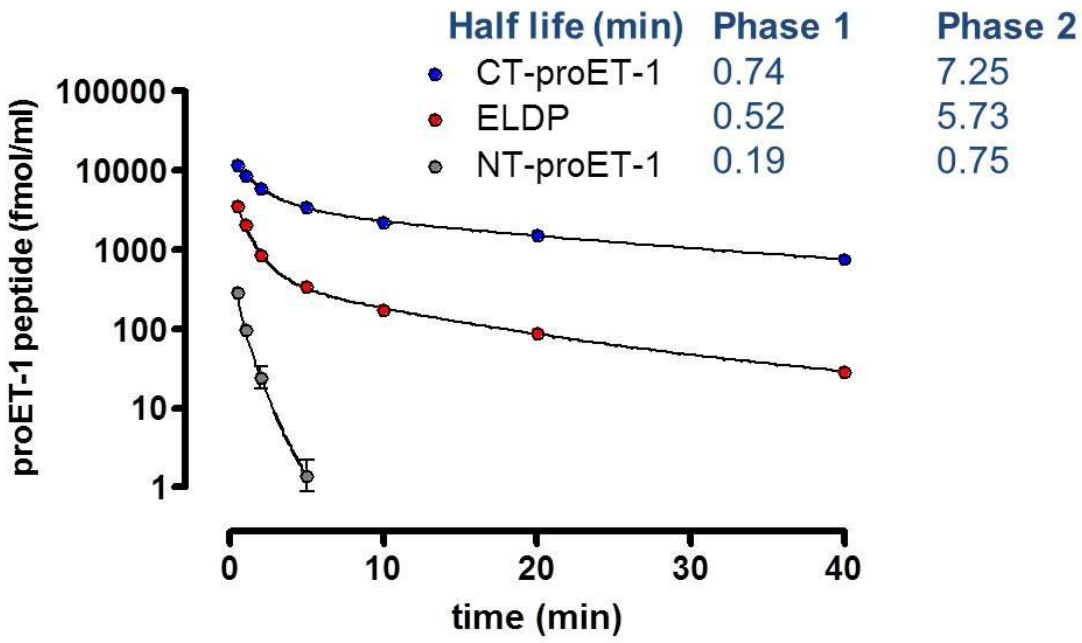

Figure 6.3: ***Clearance rates of NT-proET-1 ( ), ELDP ( ) and CT-proET-1 ( ) in vivo.*** *A bolus dose of 1 nmol/kg of each proET-1 peptide was injected through the femoral vein of male Wistar rats (n = 4). Arterial plasma concentrations of NT-proET-1, ELDP and CT-proET-1 were determined using Luminex based assay methodology. Data were expressed as fmol/ml and values represent mean ± s.e.m from a single experiment.*

6.3.1.2 *Stability of proET-1 peptides in whole blood and plasma*

To evaluate the effect of blood samples not being centrifuged immediately after collection, or plasma not being frozen rapidly, the stability of proET-1 peptides were investigated with room temperature incubation (22°C) of blood samples. Addition of NT-proET-1, ELDP and CT-proET-1 peptides at 500 fmol/ml (from 1 nmol/ml of peptide stock) showed relative stability of ELDP and CT-proET-1 over 60 min incubation at 22°C. In whole blood, 92.7 ± 3.1% and 94.6 ± 3.6% of initial ELDP and CT-proET-1 concentrations remained after 60 min incubation, respectively (Figure 6.4A). In plasma, 99.4 ± 0.7% and 104.3 ± 1.4% of initial ELDP and CT-proET-1 concentrations remained after 60 min incubation with plasma, respectively (Figure 6.4B).

In contrast, degradation of NT-proET-1 occurred rapidly at 22°C. In whole blood, 24.2 ± 4.1% of initial NT-proET-1 concentration remained after 60 min incubation in whole blood and 25.4 ± 1.4% of initial NT-proET-1 concentration remained after 60 min incubation in plasma (Figure 6.4A and 6.4B). NT-proET-1 levels were significantly lower than ELDP and CT-proET-1 over 60 min incubation (P <0.001 at all time-points; two-way ANOVA).

There were no significant differences between whole blood and plasma whether NT-proET-1 was incubated on ice or at 22°C. In whole blood 56.1% of initial NT-proET-1 concentration remained after 60 min incubation while in plasma 81.3% of initial NT-proET-1 concentration remained after 60 min incubation on ice (data not shown).

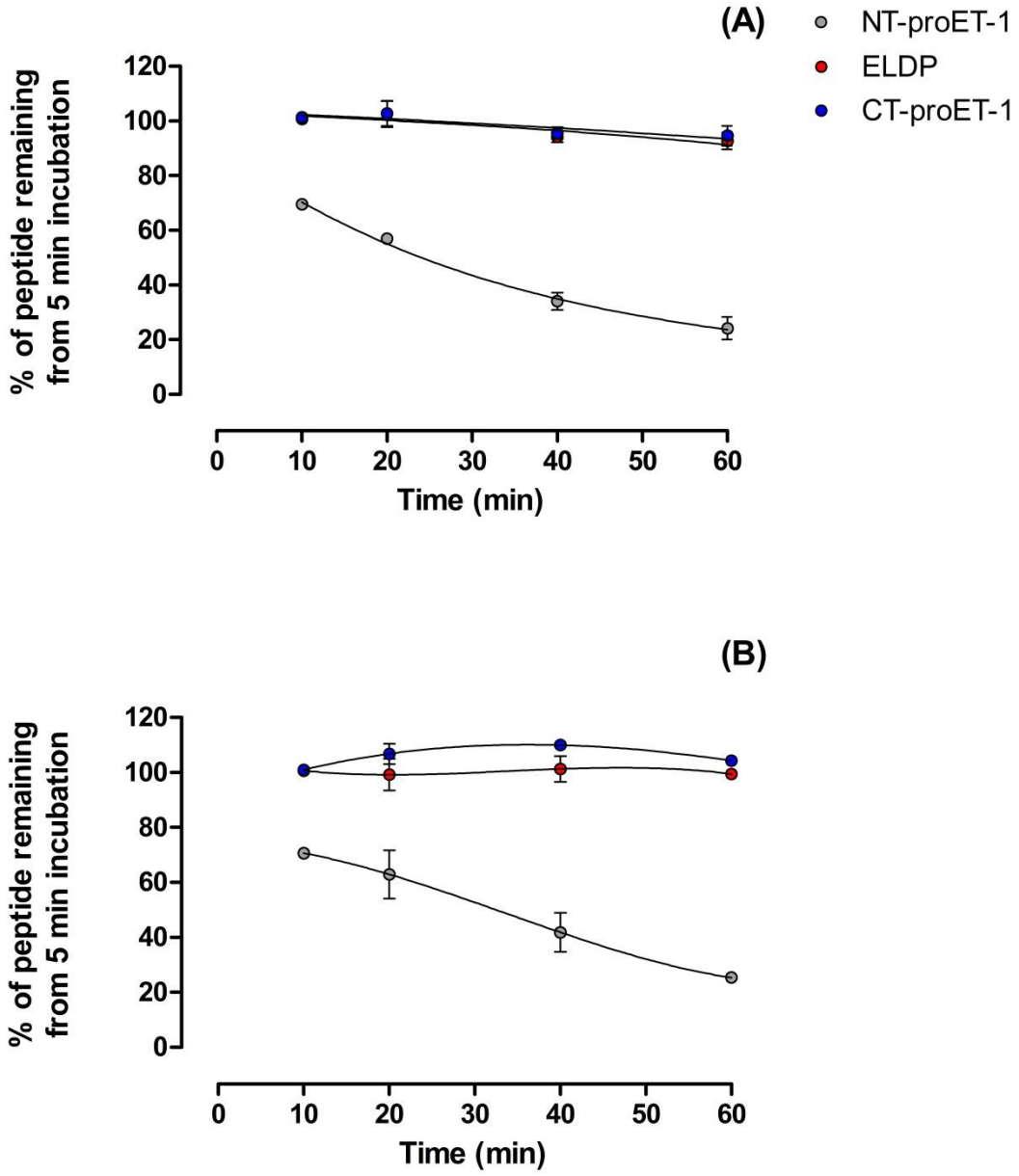

Figure 6.4: ***Ex vivo stability of NT-proET-1 (○), ELDP (●) and CT-proET- 1 (●) synthetic peptides (at 500 fmol/ml) following room temperature incubation in: (A) Whole blood and (B) Plasma.*** *At the end of each time point, whole blood was centrifuged and plasma was kept on ice. NT-proET-1, ELDP, and CT-proET-1 were measured using double-recognition site sandwich immunoassay. Values are expressed as a percentage remaining relative to initial sample measured after 5 min incubation of proET-1 peptides (mean ± s.e.m) (n = 2).*

6.3.1.3 *Stability of ELDP and CT-proET-1 synthetic standards in urine*

ELDP and CT-proET-1 synthetic standards were diluted at 200 fmol/ml and 1 in 3 serial dilutions were prepared (concentration range 0.27 – 200 fmol/ml) in urine that was centrifuged at 8,000 rpm for 5 min at 4°C. Aliquots of each sample containing equal volumes were separated into 1.5 ml microcentrifuge tubes and incubated on ice and at 25°C for 1 h. For comparison, synthetic standards of ELDP and CT-proET-1 were diluted in nSAB and serial dilutions were prepared in the same concentration range and these were incubated at room temperature for 1 h. At the end of 1 h incubation, all samples were stored at -80°C. Concentrations of ELDP and CT-proET-1 were determined using the optimised urine immunoassay (section 2.2.2.4). There were no temperature dependent changes in the stability of either ELDP or CT-proET-1 (Figure 6.5).

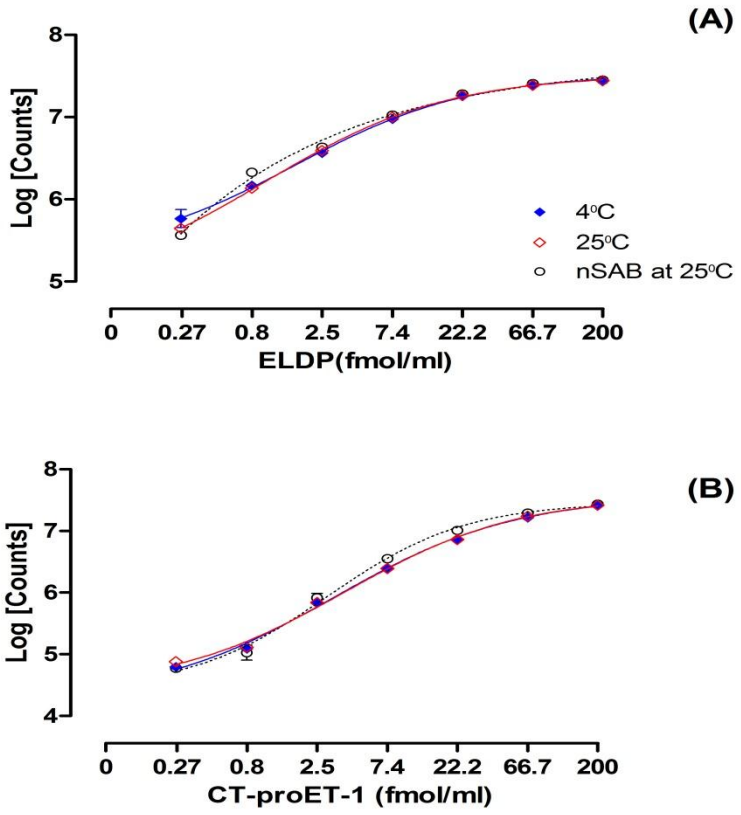

Figure 6.5: ***The stability of (A) ELDP and (B) CT-proET-1 synthetic standards in urine.*** *Dilution curves prepared with each synthetic standard were incubated at 4°C and at 25°C for 1 h and the peptide levels were measured using double-recognition site sandwich immunoassay.*

6.3.2 Plasma levels of ELDP and CT-proET-1 in response to TNF-α administration

Arterial and venous plasma levels of ELDP and CT-proET-1 were measured at baseline and after *i.v.* TNF-α infusion over 250 min in healthy control subjects. Arterial levels of ELDP at baseline and post-TNF-α were 5.7 ± 0.4 fmol/ml and 7.5 ± 0.6 fmol/ml, respectively (unpaired, two-tailed *t*-test, $P = 0.02$). Venous levels of ELDP at baseline and post-TNF-α were 6.6 ± 0.4 fmol/ml and 8.0 ± 0.9 fmol/ml, respectively. The change between venous ELDP levels at baseline and post TNF-α was not significant (Figure 6.6A). However, overall ELDP levels after TNF-α infusion for arterial and venous samples together were significantly greater than combined baseline arterial and venous values (2-way ANOVA, $P = 0.009$). There was no significant difference between arterial and venous levels at baseline or after TNF-α infusion.

Arterial levels of CT-proET-1 at baseline and post-TNF-α were 6.5 ± 1.5 fmol/ml and 9.6 ± 2.0 fmol/ml, respectively. Venous levels of CT-proET-1 at baseline and post-TNF-α were 6.2 ± 1.6 fmol/ml and 7.4 ± 2.1 fmol/ml, respectively. In comparison to venous levels of CT-proET-1, arterial levels showed a greater increase after TNF-α infusion (Figure 6.6B). However, neither arterial nor venous levels were significantly changed after TNF-α infusion.

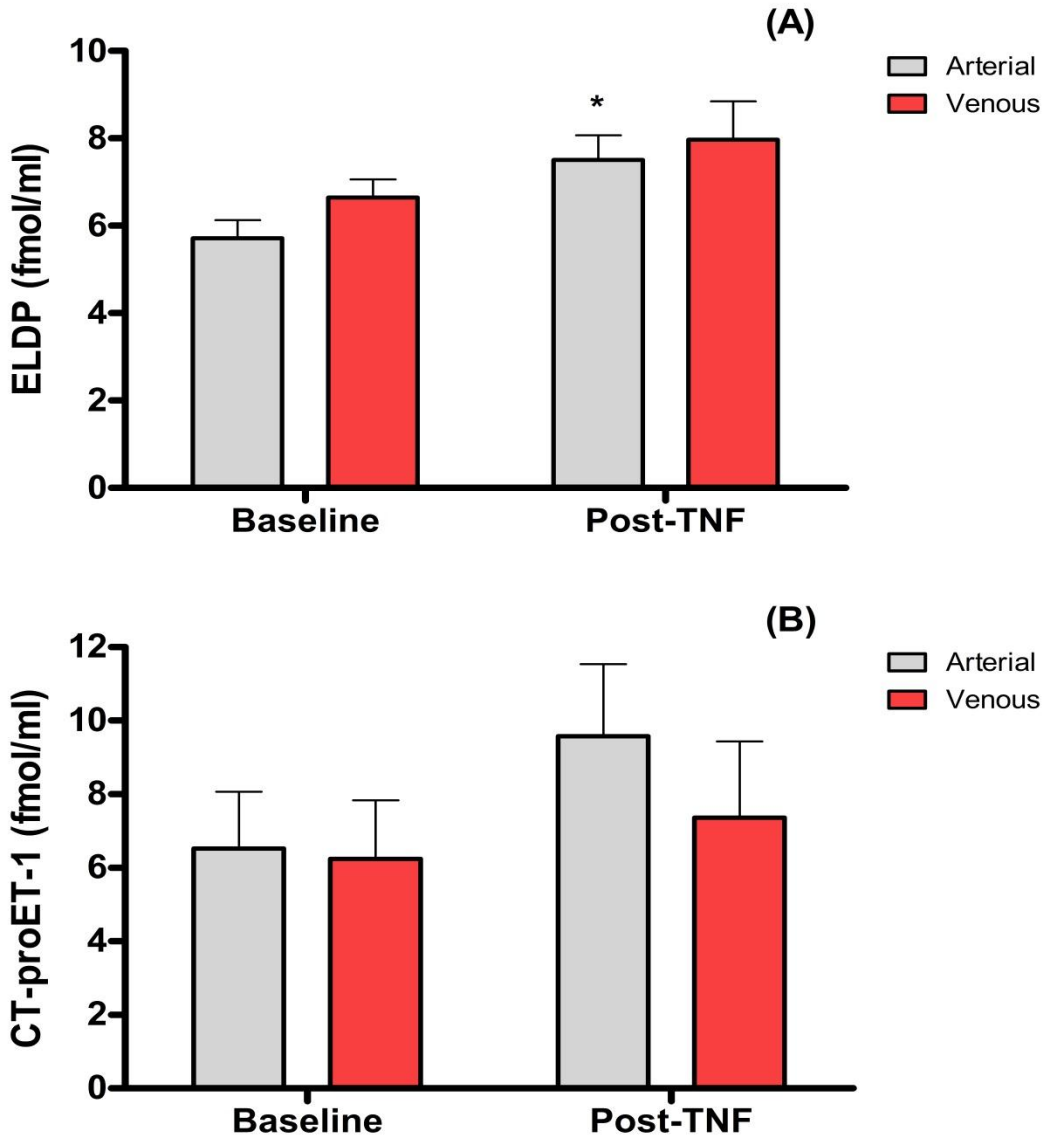

Figure 6.6: ***Arterial and venous plasma concentrations of (A) ELDP and (B) CT-proET-1 after TNF-α infusion.*** *Results shown are plasma levels of ELDP and CT-proET-1 (fmol/ml) at baseline and post-TNF-α. The data were expressed as mean ± s.e.m. A comparison between arterial and venous levels at baseline and post-TNF-α was performed using a Student's t-test (unpaired, two-tailed). * represents a significant increase in ELDP levels from arterial plasma following TNF-α infusion (P = 0.02).*

6.3.3 Evaluation of ELDP and CT-proET-1 as biomarkers of cardiovascular disease

6.3.3.1 *Comparison of ELDP and CT-proET-1 levels in pre-hypertension/mild hypertension and chronic heart failure*

Baseline levels of ELDP and CT-proET-1 were measured in untreated subjects with pre-H (n = 24) and in patients with chronic HF (n = 24). Plasma levels of ELDP were significantly different between pre-H and chronic HF (P <0.001; unpaired t-test) (Figure 6.7A). Plasma levels (mean ± s.e.m) of ELDP were 6.5 ± 0.2 and 7.8 ± 0.3 fmol/ml for pre-H and chronic HF, respectively (95% CI of 6.1 – 6.8 and 7.3 – 8.3, respectively).

Similarly, CT-proET-1 showed a significant difference between the two patient groups (P <0.001; unpaired t-test), with CT-proET-1 being significantly greater than ELDP in each group (P <0.05; one-way ANOVA) (Figure 6.7A). Plasma levels of CT-proET-1 in pre-H and in chronic HF were 9.9 ± 0.5 and 16.3 ± 0.8 fmol/ml, respectively (95% CI of 8.9 – 11.0 and 14.7 – 18.0, respectively).

There was a positive correlation between plasma levels of ELDP and CT-proET-1 (P <0.001, $r^2 = 0.44$) in which patients with chronic HF had higher proET-1 peptide levels and patients with pre-H had lower proET-1 peptide levels (Figure 6.7B).

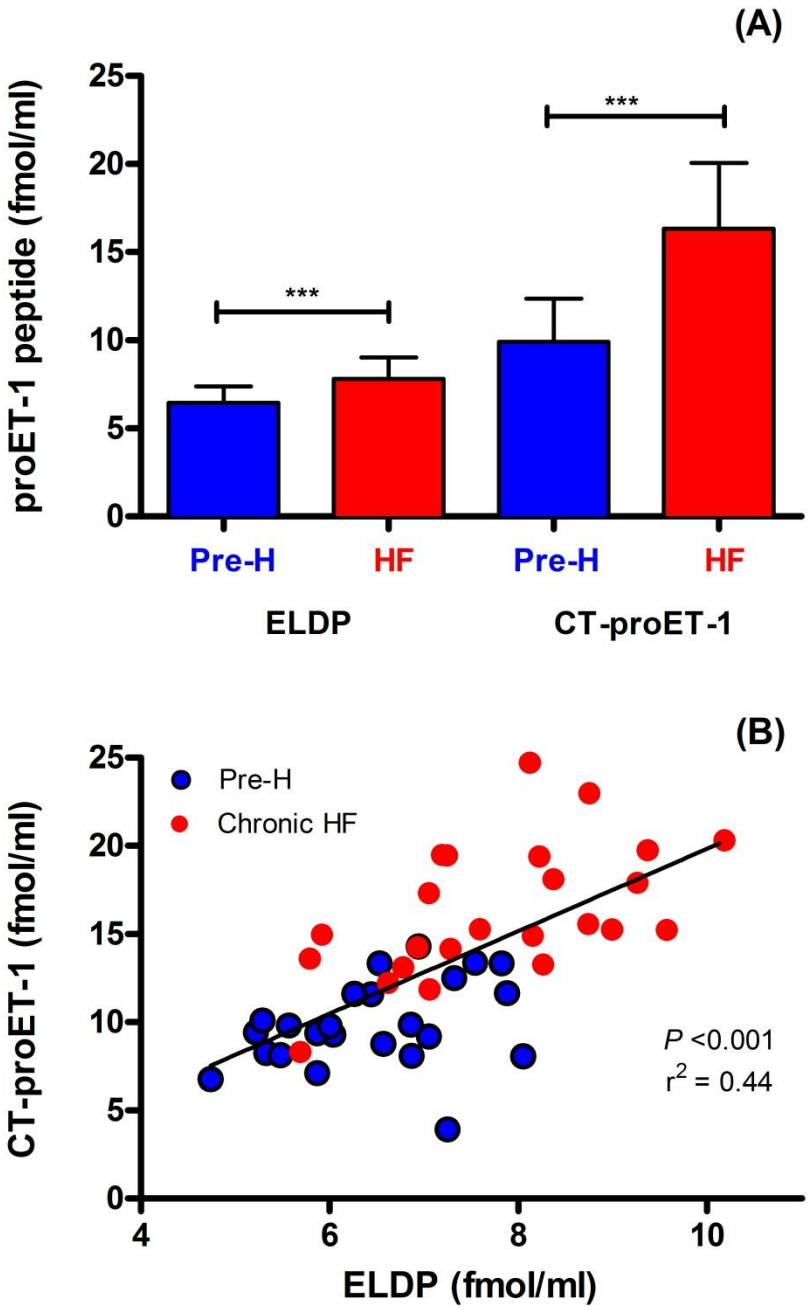

Figure 6.7: (A) ***Plasma ELDP and CT-proET-1 (fmol/ml) levels in pre-hypertension and chronic heart failure. (B) Scatter plot comparing plasma levels of ELDP with plasma levels of CT-proET-1.*** *(A) Results are expressed as mean ± s.e.m. Concentrations of ELDP and CT-proET-1 in each group were compared by Student`s t-test, *** = P <0.001. (B) Linear regression analysis comparing plasma ELDP with CT-proET-1 showed a positive correlation.*

6.3.4 Evaluation of ELDP and CT-proET-1 as biomarkers of chronic kidney disease

6.3.4.1 *Plasma measurements in CKD*

Plasma levels of ELDP (mean ± s.e.m) were 6.3 ± 0.4 for control subjects (n = 16) and 6.2 ± 0.3 (n = 31), 7.0 ± 0.4 (n = 30), 7.7 ± 0.3 (n = 29), 9.8 ± 0.8 (n = 10) and 12.4 ± 2.0 (n = 5) fmol/ml for CKD stages 1 to 5, respectively (P <0.05 for the overall trend; comparison of means by ANOVA). In comparison to healthy controls, similar levels of ELDP were observed in CKD stages 0 – 3, but there was a significant increase in CKD stages 4 – 5 (P <0.001 ANOVA) (Figure 6.8A).

Plasma levels of CT-proET-1 were 8.9 ± 1.3 for control subjects (n = 14) and 9.4 ± 1.0 (n = 29), 11.4 ± 1.2 (n = 30), 16.4 ± 1.3 (n = 28), 19.7 ± 2.1 (n = 11), and 29.6 ± 3.5 (n = 5) fmol/ml for CKD stages 1 to 5, respectively (P <0.001 for the linear trend; comparison of means by ANOVA). In comparison to healthy controls, CT-proET-1 levels were significantly higher from CKD stages 3 – 5 (Figure 6.8B).

Scatter plots of eGFR (ml/min/1.73m^2) against plasma concentrations of ELDP and CT-proET-1 (Figure 6.8C and 6.8D) had a negative linear correlation (P <0.001 and r^2 = 0.26 for ELDP and P <0.001 and r^2 = 0.29 for CT-proET-1). Thus, with increasing eGFR, proET-1 peptide concentrations tended to be lower. There was a positive correlation between plasma levels of ELDP and CT-proET-1 (P <0.001, and r^2 = 0.40) (data not shown).

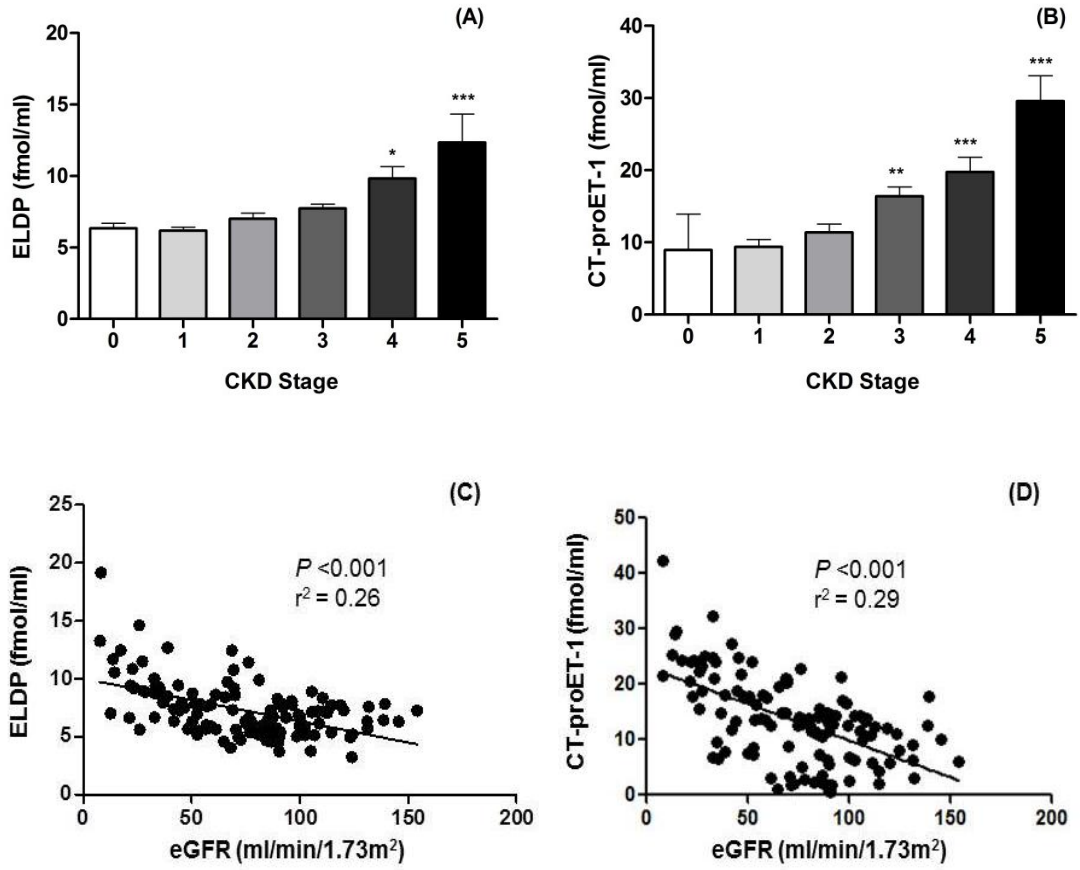

Figure 6.8: ***Plasma levels of ELDP and CT-proET-1 in chronic kidney disease (A – B) and their correlation with eGFR (C – D).*** *Bar graphs in the upper panel show mean ± s.e.m for plasma concentrations (fmol/ml) of (A) ELDP and (B) CT-proET-1. ** = P <0.01, and *** = P <0.001 comparison of means to control (CKD stage 0) by ANOVA. Scatter plots in the lower panel show plasma levels of (C) ELDP (P <0.001, r^2 = 0.26) and (D) CT-proET-1 (P <0.001, r^2 = 0.29) against eGFR (ml/min/1.73m^2). The relationship between proET-1 peptide levels and eGFR was assessed by linear regression analysis.*

6.3.4.2 *Urinary ELDP and CT-proET-1 in CKD*

Urinary ELDP levels did not increase with increasing CKD stages (Table 6.6). Mean ELDP levels were 1.1 ± 1.2 pmol/L, but there was a marked difference (>70-fold) between the minimum and maximum values of 0.09 and 6.7 pmol/L. There was no relationship between urinary ELDP and eGFR (data not shown). Urinary ELDP levels also did not correlate with plasma ELDP levels (data not shown).

Table 6.6: ***ELDP concentrations in urine from patients with chronic kidney disease.*** *Mean ELDP levels are expressed as pmol/L. SD = standard deviation and n = the number of samples analysed.*

CKD stage	Mean ELDP (pmol/L)	SD	n
0	0.7	0.8	23
1	1.3	1.6	29
2	1.0	1.3	22
3	1.0	1.3	22
4	1.7	1.1	16
5	1.2	0.8	7

CT-proET-1 had very low levels in CKD urine samples, which were mostly lower than the detection limit of the assay (0.34 fmol/ml).

6.3.4.3 Effects of sitaxentan on ELDP and CT-proET-1 in patients with CKD

The effects of an ET_A receptor antagonist sitaxentan (100 mg/day), a long-acting formulation of calcium-channel blocker nifedipine (30 mg/day), and placebo were compared at baseline and after 3 and 6 weeks of treatment.

Baseline levels of ELDP and CT-proET-1 were similar in all treatment groups with mean plasma levels being 11.7 ± 0.6 and 20.0 ± 1.1 fmol/ml, respectively (data not shown). Placebo treatment did not cause any significant changes in plasma levels of ELDP or CT-proET-1 between baseline, week 3 and week 6 (mean decrease in ELDP: -4% and CT-proET-1: -0.2%). Sitaxentan treatment resulted in significant increases in ELDP at both 3 and 6 weeks when compared to baseline (Figure 6.9A). Mean increase of plasma ELDP following sitaxentan treatment was 16.2 ± 3.3% (95% CI, 6.6% – 21.0%) (P <0.001). Similarly, CT-proET-1 levels significantly increased after 3 and 6 weeks of sitaxentan treatment (Figure 6.9B). Mean increase of plasma CT-proET-1 was 13.6 ± 2.3% (95% CI, 8.9% – 18.7%) (P <0.001 by repeated measures ANOVA; comparison to baseline for both peptides).

After treatment with nifedipine, there were no significant differences in ELDP or CT-proET-1 levels compared to baseline at week 3 and week 6 (mean increase ELDP: 5.4% and CT-proET-1: 3.4%) (Figure 6.9A and 6.9B).

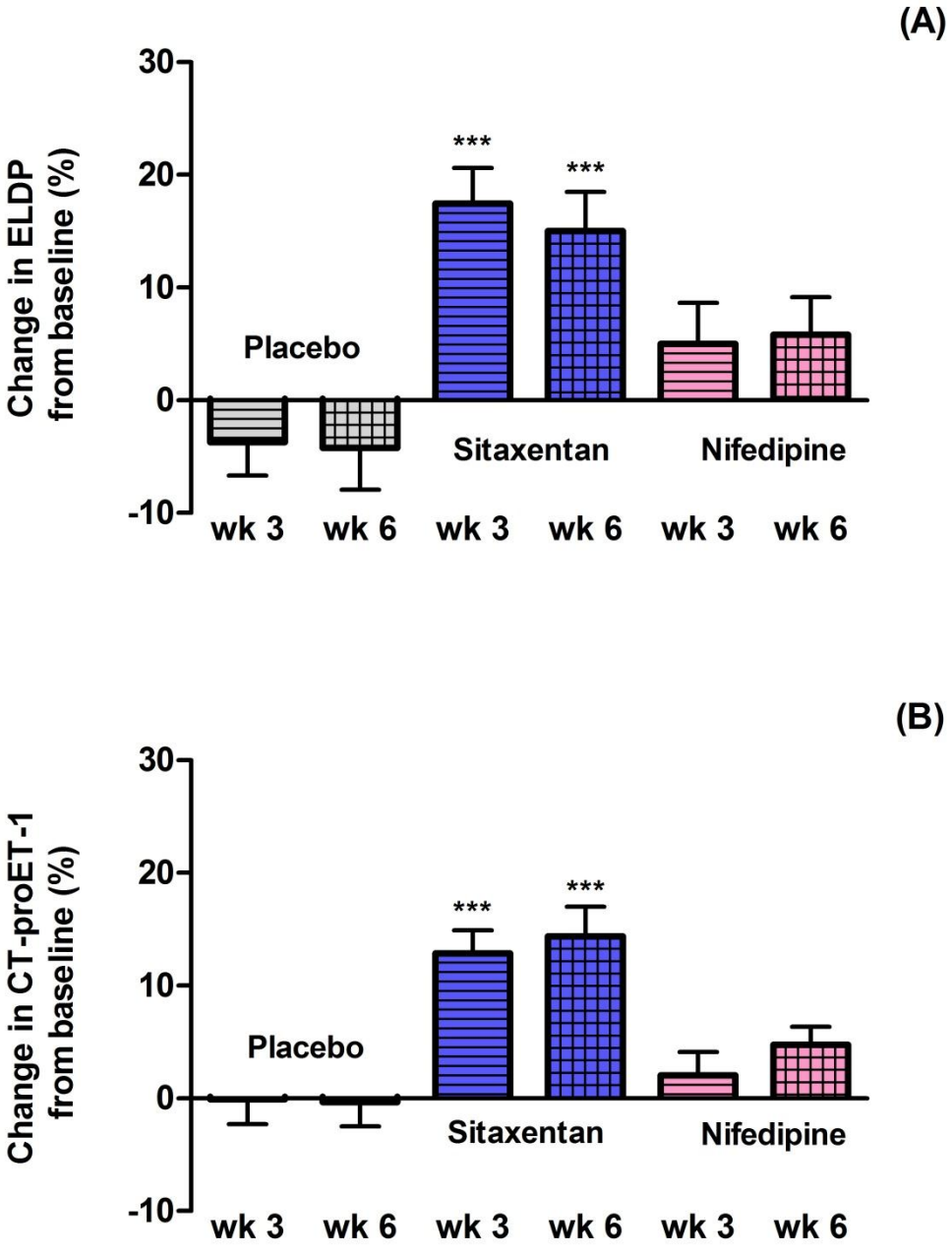

Figure 6.9: ***Effects of placebo, sitaxentan, and nifedipine on plasma levels of (A) ELDP and (B) CT-proET-1.*** *Values (mean ± s.e.m) represent percent change of plasma ELDP and CT-proET-1 from baseline. Mean baseline levels of ELDP and CT-proET-1 were 11.7 ± 0.6 and 20.0 ± 1.1 fmol/ml, respectively. *** represents P <0.001 by ANOVA with repeated measures for the comparisons made between baseline and after 3 and 6 weeks of each treatment.*

There was no difference between urinary ELDP levels at baseline and after 6 weeks of receiving placebo, sitaxentan and nifedipine (Table 6.7). Again, CT-proET-1 levels were mostly undetectable in urine (data not shown).

Table 6.7: ***Effects of placebo, sitaxentan, and nifedipine on urinary ELDP concentrations.*** *ELDP levels were expressed as mean ± SD (pmol/L) and measured at baseline and after 6 weeks of each treatment.*

Treatment	Baseline (pmol/L)	Week 6
Placebo	0.8 ± 0.7	0.9 ± 0.8
Sitaxentan	0.9 ± 0.7	0.8 ± 0.6
Nifedipine	0.8 ± 0.6	0.8 ± 1.1

6.3.5 Correlation of ELDP and CT-proET-1 levels with changes in clinical parameters

ELDP and CT-proET-1 levels from CKD and proteinuric CKD after sitaxentan treatment were compared with cardiovascular and renal parameters, which were previously measured in Dhaun *et al.*, 2011, 2013. These parameters were: BP [systolic blood pressure (SBP), diastolic blood pressure (DBP), MAP and pulse pressure (PP)]; FMD to assess endothelial function; pulse wave velocity (PWV) and central augmentation index-C as a measure of arterial stiffness; urine Na^+, albumin:creatinine ratio (ACR), blood creatinine, urine creatinine, urine ET-1, and fractional excretion of ET-1. Parameters that showed significant correlations with plasma levels of ELDP and CT-proET-1 are discussed here.

6.3.5.1 *Patients with proteinuric CKD receiving renoprotective treatment*

There was no correlation between plasma ELDP or CT-proET-1 levels with 24 h Na^+ excretion at baseline or after 3 weeks of sitaxentan treatment. However, after 6 weeks, plasma levels of ELDP and CT-proET-1 correlated negatively with 24 h Na^+ excretion (ELDP: $P = 0.01$, $r^2 = 0.21$ and CT-proET-1: $P = 0.01$, $r^2 = 0.22$) (Figure 6.10).

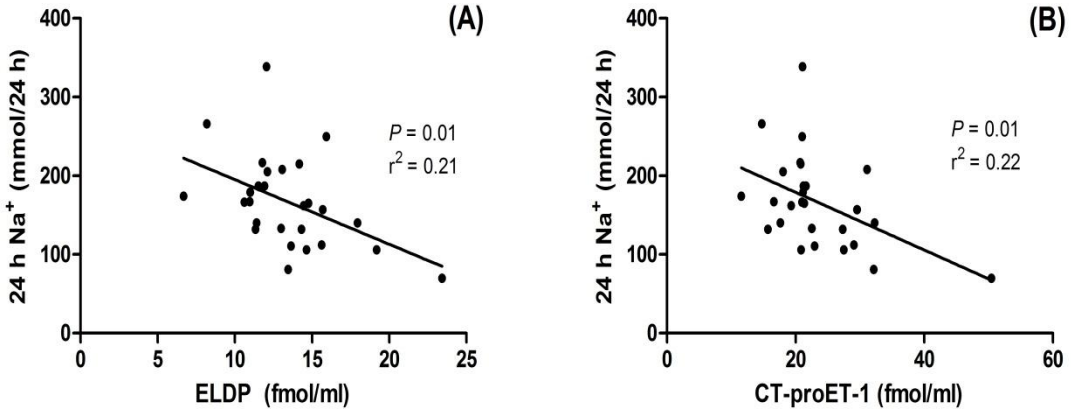

Figure 6.10: ***Relationship between plasma levels of (A) ELDP and (B) CT-proET-1 with 24 h Na^+ excretion (mmol/24 h) after 6 weeks of sitaxentan treatment.*** *ELDP and CT-proET-1 had negative linear correlation with 24 h Na^+ excretion (as assessed by linear regression analysis). 24 h Na^+ excretion was expressed as mmol/24 h.*

In the sitaxentan treatment group, changes in plasma ELDP and CT-proET-1 did not correlate with changes in urinary protein excretion (UPE), protein:creatinine ratio (PCR), 24 h Na^+ excretion, MAP, SBP, DBP and PWV.

In the nifedipine treatment group, there was no correlation between plasma ELDP or CT-proET-1 levels and 24 h Na^+ excretion. However, changes in plasma levels of ELDP and CT-proET-1 after 6 weeks of treatment correlated with changes in 24 h Na^+ excretion (ELDP: $P = 0.04$, $r^2 = 0.17$; CT-proET-1: $P = 0.005$, $r^2 = 0.28$) (Figure 6.11).

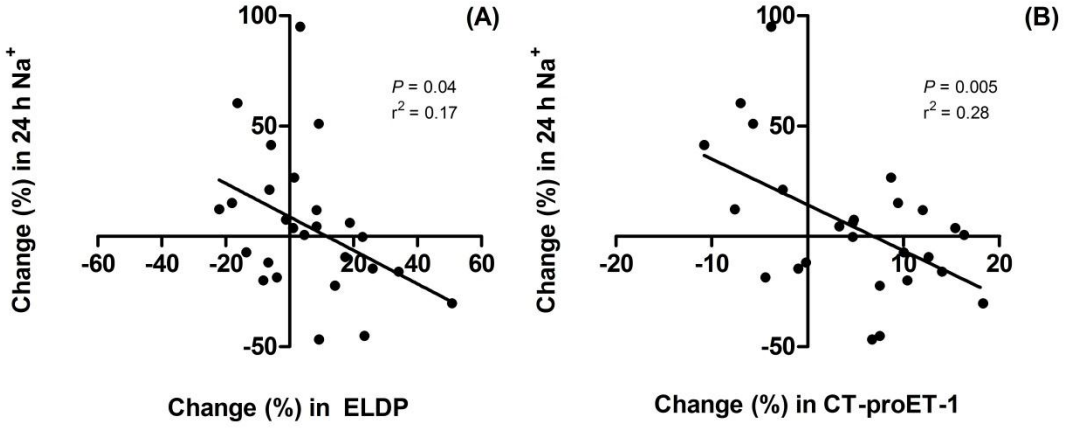

Figure 6.11: ***Scatter plots showing changes (%) in plasma levels of (A) ELDP and (B) CT-proET-1 with changes (%) in 24 h Na^+ excretion (mmol/24 h) following nifedipine treatment over 6 weeks.***

6.4 DISCUSSION

In this chapter the potential of proET-1 peptides as biomarkers was investigated in rat and human studies. Firstly, their clearance rates were investigated in anaesthetised rats. Then in human studies ELDP and CT-proET-1 were measured after TNF-α infusion in healthy volunteers, in patients with chronic HF, and in patients with CKD.

Slower clearance from the circulation and greater stability in whole blood/plasma favoured ELDP and CT-proET-1 as potential biomarkers of ET-1 synthesis. In comparison, NT-proET-1 had rapid clearance and degradation, and therefore has limited potential as a biomarker. Clearance of peptides from the circulation can be mediated by receptor-binding, proteolytic degradation, diffusion into interstitial fluid, and renal clearance. The exact mechanism that underlies relative short half-life of NT-proET-1 is unclear. The peptides were administered *i.v.* and arterial blood samples were collected. The very rapid disappearance of NT-proET-1 (Figure 6.3) was indicative of pulmonary clearance. This is similar to that observed with ET-1 (Sirviö *et al.*, 1990; de Nucci *et al.*, 1988; Dupuis *et al.*, 1996b), which is mainly due to receptor binding (Fukuroda *et al.*, 1994a; Dupuis *et al.*, 1996a; Burkhardt *et al.*, 2000). In comparison, angiotensin I is largely metabolised to angiotensin II by angiotensin converting enzyme (ACE) (Soubrier *et al.*, 1993) as it passes through the pulmonary vasculature. The concentration of NT-proET-1, ELDP and CT-proET-1 measured after 30 s of injection were 287 ± 23, 3648 ± 234, and 11736 ± 639 fmol/ml, respectively. If interstitial fluid is also included in the volume of distribution of peptides [volume of distribution = volume of extracellular fluid (15 – 20% of total BW)], then peptide concentrations would be expected in the 5 – 6.6 pmol/ml. Hence, the levels of proET-1 peptides reflect both dilution in plasma and diffusion into interstitial fluid, as well as metabolism. Whether clearance of NT-proET-1 is due to receptor binding or proteolytic degradation needs further investigation. Nevertheless, temperature dependent decreases in NT-proET-1 (section 6.3.1.2 , Figure 6.4) were indicative of increased sensitivity to degradation by proteolytic enzymes.

In the first human study, the effects of TNF-α on proET-1 release were investigated by measuring the plasma levels of more stable fragments, ELDP and CT-proET-1. TNF-α is a pro-inflammatory cytokine and stimulates both mRNA expression and ET-1 peptide synthesis in endothelial and vascular smooth muscle cells (Corder *et al.,* 1995; Woods *et al.,* 1999). TNF-α can induce vascular inflammation and the levels are increased in patients with endothelial dysfunction and ischaemic heart disease (Ridker *et al.,* 2000). Administering TNF-α to healthy individuals' increased ET-1 release, measured in both arterial and venous blood (Patel *et al.,* 2002). In response to TNF-α, the increase in ET-1 release was greater in venous plasma in comparison to arterial levels. As a follow up to these investigations, plasma levels of ELDP and CT-proET-1 were measured in the same set of plasma samples. When compared to baseline, there was a slight increase in ELDP and CT-proET-1 levels after TNF-α. This elevation however was only significant in arterial ELDP (Figure 6.6A). To note, venous levels of ELDP at baseline were slightly higher than arterial levels (6.6 ± 0.4 *vs.* 5.7 ± 0.4 fmol/ml). A regional difference in vascular sensitivity to ET-1 was previously reported (Lüscher *et al.,* 1990; Kelly & Whitworth, 1999) and higher ET-1 levels in venous plasma (at baseline) was also reported by Patel *et al.,* 2002. However, after TNF-α infusion, the increase in ELDP in venous blood was minor. Post-TNF-α CT-proET-1 levels showed a greater increase in arterial plasma (1.5-fold) when compared to venous plasma. The reason for the differences observed between arterial and venous plasma levels of ET-1 and proET-1 peptides is unclear. However, as the samples had been stored at -80º C for more than 12 years prior to assay for ELDP and CT-proET-1, the long-term stability of these peptides may be an important factor affecting the observed plasma levels.

The limitations of this study included small sample size. Due to invasiveness of the brachial artery catheterisation, the study was limited to 6 volunteers. Bigger sample size and limited freeze/thaw process of stored plasma samples could have increased the confidence of results. Nevertheless, increases in proET-1 peptide levels support the relationship with inflammatory and vasoconstrictor processes induced by TNF-α (Klemm *et al.,* 1995).

In a second study of human samples, diagnostic utility of ELDP and CT-proET-1 was evaluated in patients with pre-H and chronic HF. Plasma levels of CT-proET-1 were comparatively higher than ELDP levels and in patients with chronic HF there was a more pronounced elevation with CT-proET-1 (1.6-fold increase) in comparison to ELDP (1.2-fold increase). Nevertheless, lower and upper 95% CI of means showed differentiation between pre-H and chronic HF with both proET-1 peptides (ELDP: 6.1 – 6.8 and 7.3 – 8.3; CT-proET-1: 8.9 – 11.0 and 14.7 – 18.0, respectively). The results of this study suggested that CT-proET-1 may be a better biomarker to distinguish patients with HF. The higher CT-proET-1 levels relative to ELDP are consistent with the relative difference in clearance rates of these peptides. Importantly, pre-H patients were not receiving any treatment and represented a rare population in which plasma measurements would reflect changes in proET-1 without drug interactions.

Currently, diagnosis of HF is difficult during emergency conditions where a rapid, non-invasive, easily accessible biomarker is critical for identification. NT-proBNP is the most powerful predictor of HF (Cowie *et al.,* 1997; Maisel *et al.,* 2002) and the diagnosis of acute coronary syndromes are accompanied by cardiac troponins and creatinine kinase MB. The first CT-proET-1 immunoassay (B.R.A.H.M.S GmbH, Hennigsdorf/Berlin, Germany) was described by Papassotiriou *et al.,* 2006 is a chemiluminescence sandwich assay and uses polyclonal antibodies for the detection of ppET-1 residues 168 – 212. A comparison between CT-proET-1 (ppET-$1_{[168 – 212]}$) and NT-proBNP demonstrated that CT-proET-1 increases the prognostic value for assessing patients with chronic HF (Dieplinger *et al.,* 2009; Jankowska *et al.,* 2011). In addition, a variety of HF studies investigated the prognostic potential of CT-proET-1 along with other biomarkers such as plasma mid-regional pro-adrenomedullin (MR-proADM) (Adlbrecht *et al.,* 2009), and the GISSI-HF trial measuring mid-regional pro-atrial natriuretic peptide (MR-proANP), MR-proADM, C-terminal pro-vasopressin (CT-proAVP or copeptin) (Masson *et al.,* 2010) and showed promising results with CT-proET-1. Clinical trials investigating the prognostic potential of CT-proET-1 along with other cardiovascular biomarkers were summarised in Chapter 1, Table 1.8. Of note, the CT-proET-1 (ppET-$1_{[168 – 212]}$) assay described in these studies differed from the CT-proET-1 (ppET-$1_{[169 – 212]}$) assay used in this thesis, as the antigen included an arginine at ppET-1 residue 168 (ppET-1 ^{167}-R**R** SSEEHLRQTRS) that is likely to be removed

during the processing. However, an assay for ppET-$1_{[168 - 212]}$ may be able to detect unprocessed fragments of ppET-1 as well as the fully processed peptide ppET-$1_{[169 - 212]}$.

In a previous study of CKD patients with minimal comorbidity, plasma ET-1 levels were increased linearly with declining renal function (declining GFR), while fractional excretion of ET-1 was increased exponentially (Goddard *et al.,* 2007; Dhaun *et al.,* 2009). Therefore, plasma levels of ELDP and CT-proET-1 were investigated in CKD. In comparison to healthy controls, ELDP levels were significantly increased from CKD stage 4, while CT-proET-1 levels were increased from CKD stage 3 (Figure 6.8A and 6.8B). Both proET-1 peptides lacked the sensitivity to differentiate between earlier CKD stages, which are crucial for prognosis and for preventing disease progression. The inverse relationship between plasma levels of ET-1 and eGFR (Goddard *et al.,* 2007) was confirmed for plasma levels of ELDP and CT-proET-1 (reduced eGFR with increasing proET-1 peptides) (Figure 6.8C and 6.8D). In CKD, this was consistent with decreased renal filtration and thus removal of peptides from the circulation resulting in higher plasma levels. Furthermore, in comparison to plasma levels of ET-1 (Dhaun *et al.,* 2009) linear regression curves of ELDP and CT-proET-1 had higher r^2 values (ET-1: $r^2 = 0.22$ *vs.* ELDP: $r^2 = 0.26$ and CT-proET-1: $r^2 = 0.29$) indicating slightly better curve fittings and a closer relationship to renal filtration rates. Alternatively, increasing r^2 values may reflect the ability to detect increased synthesis of ppET-1 with increasing severity of CKD. This finding is also consistent with CT-proET-1 having the longest circulating half-life.

Earlier studies have indicated that urinary and plasma ET-1 concentrations are independent of each other (Serneri *et al.,* 1995; Goddard *et al.,* 2007) and the concentration of urinary ET-1 was well correlated with ET-1 production (Benigni *et al.,* 1991). Urinary ET-1 levels are elevated in CKD (Dhaun *et al.,* 2006). These suggested that urinary ET-1 (instead of plasma ET-1) could be a better biomarker of renal disease. Here, this hypothesis was evaluated for proET-1 peptides. However, urinary ELDP levels were low (mean 1.1 ± 1.2 pmol/L) and did not change with the severity of disease either in CKD or in proteinuric CKD patients receiving renoprotective treatments and placebo. In addition, urinary CT-proET-1 levels were mostly undetectable. This suggested that the peptides (particularly CT-proET-1) might be differently metabolised in the kidney and that antibodies may not be recognising excreted fragments of ELDP and CT-proET-1 in urine. To support this hypothesis and to rule out the possibility of

stability issues in urine, synthetic standards of ELDP and CT-proET-1 prepared at 0.27 – 200 fmol/ml were incubated for 1 h at room temperature and on ice. There was no temperature dependent change in the stability of peptides between the two incubation temperatures (25°C and 4°C) and they were relatively comparable to the standard curve prepared in nSAB (Figure 6.5). This suggested that the most likely reason is renal tubule proteolytic degradation. Abassi *et al.,* 1993b showed that NEP-24.11, located at the brush border of renal proximal tubule degraded filtered ET-1. Therefore, it is likely that CT-proET-1 is excreted as proteolytic fragments rather than the full length peptide. Excretion of smaller fragments is also documented for plasma proteins such as albumin and transferrin (Burne *et al.,* 1999). It may also be possible that, due to their larger MWt, only small amounts of ELDP and CT-proET-1 were excreted in urine. Identification of stable CT-proET-1 fragments excreted in urine is needed in order to fully evaluate and interpret the utility of measuring urinary ppET-1 fragments in patients with CKD.

In a second study of patients with CKD, the effects of nifedipine, sitaxentan and placebo on the plasma and urinary levels of ELDP and CT-proET-1 were evaluated. The main aim of these investigations was to establish whether plasma levels of proET-1 peptides were modified with sitaxentan or nifedipine treatments, and if any changes in proET-1 peptide levels were related to cardiovascular parameters (e.g. proteinuria, BP, and arterial stiffness, which modify systemic and renal haemodynamics). The clinical trial initially described in Dhaun *et al.,* 2013 compared these changes with plasma and urine ET-1 concentrations. In this study, sitaxentan did not affect plasma levels of ET-1 whereas urine ET-1/creatinine, which reflects renal ET-1 production, was reduced. Interestingly, in contrast to these findings, plasma levels of ELDP and CT-proET-1 were significantly elevated at 3 and 6 weeks after receiving sitaxentan (Figure 6.9). In general, ET-1 levels are not affected with selective ET_A antagonist treatments (such as SB 247083) (Douglas *et al.,* 1998). Whereas, blocking ET_B receptors either through an ET_B selective antagonist (Fukuroda *et al.,* 1994a) or endothelial cell-specific ET_B KO (Bagnall *et al.,* 2006; Kelland *et al.,* 2010) was associated with increased circulating ET-1 levels probably as a result of reduced clearance. In contrast, Opgenorth *et al.,* 2000 observed increased plasma ET-1 levels with selective ET_A and ET_B receptor antagonism in healthy humans in which the increase with ET_B receptor antagonism was greater than that of ET_A. More importantly, combined ET_A and ET_B receptor blockade increased ET-

1 levels more than ET_B alone. Based on this finding, Opgenorth *et al.,* 2000 suggested this was due to blocking a negative feedback effect mediated via ET_A receptors. Therefore, the mechanism underlying increased plasma levels of ELDP and CT-proET-1 could be due to ET_A blockade of a negative feedback mechanism leading to increased synthesis. Decreased fractional filtration after sitaxentan could also alter renal clearance, which would lead to a change in half-life of proET-1 peptides.

Correlations between plasma levels of ELDP and CT-proET-1 with 24 h Na^+ excretion and proteinuria markers confirmed previous findings of Dhaun *et al.,* 2011, 2013 that acute selective ET_A receptor blockade modifies cardiovascular parameters (reduces proteinuria, BP and arterial stiffness) in proteinuric CKD and may confer protection against disease progression. There was no change between sitaxentan and nifedipine in reducing BP parameters. Yet, a reduction seen in proteinuria with sitaxentan was greater than that of nifedipine (Dhaun *et al.,* 2013). Plasma levels of ELDP and CT-proET-1 had a negative correlation with 24 h Na^+ excretion after 6 weeks of sitaxentan treatment. Thus, increasing concentrations of ELDP and CT-proET-1 were associated with reductions in 24 h Na^+ excretion. The role of ET_A receptors in regulation of Na^+ homeostasis is not well defined. Therefore, anti-natriuretic effect of sitaxentan is unclear. Most evidence from gene targeting studies suggested that ET-1 mediated natriuresis (increased Na^+ excretion) is mainly regulated by the activation of ET_B receptors (Ahn *et al.,* 2004). Active reabsorption of Na^+ and Cl^- are mainly inhibited in the proximal tubule and thick ascending limb where ET_B receptors have the highest density without ET_A localisation (Kohan *et al.,* 2011). Thus, the contribution of ET_A receptors to Na^+ homeostasis is expected to be minor. Results from CD specific KO experiments indicated that (Table 6.2):

(1) Specific CD ET_A KO mice did not affect Na^+ excretion or systemic BP (Ge *et al.,* 2005).

(2) Urine volume and Na^+ excretion were similar between inducible nephron-specific ET_A KO mice (iET_A) and control mice, on a normal or high Na^+ intake (Stuart *et al.,* 2012).

(3) ET_A blockers had no effect on ET-1 inhibition of ENaC activity in isolated rat cortical CD (Bugaj *et al.,* 2012).

(4) In contrast, CD $ET_{A/B}$ KO mice were shown to be more hypertensive and retain more Na^+ than mice with CD ET_B KO alone (Ge *et al.,* 2008).

Taking all these evidences together, there is a possibility that ET_A receptors might contribute to regulation of Na^+ homeostasis. This is possibly as a secondary effect through alterations on the renal haemodynamics. Sitaxentan was shown to reduce RBF, GFR, effective FF in CKD patients (Dhaun *et al.,* 2011) and in a previous study these alterations in haemodynamics were shown to reduce urinary Na^+ and water excretion (Claria *et al.,* 1991). In support of the role of ET_A receptors on Na^+ homeostasis, Stuart *et al.,* 2013 has shown that ET_A antagonist-induced fluid retention was mediated by CD ET_A receptors. In this study, ambrisentan and atrasentan (both at 100 mg/kg/day over 2 weeks) were used as ET_A receptor antagonists and their effect on fluid retention was investigated in control mice and in cell-specific ET_A KO mouse lines [cardiomyocyte-specific ET_A KO, VSMC ET_A KO (ET_A KO of all SMCs), CD ET_A KO, and nephron ET_A KO].

In the nifedipine treatment group plasma levels of ELDP and CT-proET-1 did not correlate with any of the parameters tested. However, there was a relationship between changes in ELDP and CT-proET-1 levels and changes in 24 h Na^+ excretion (Figure 6.11).

In summary, clearance and metabolism of proET-1 peptides demonstrated the superiority of CT-proET-1 as a biomarker of ET-1 synthesis. This was based on the longer half-life and greater differences observed in chronic HF and CKD stages, which is likely to be reflected by its longer stability in comparison to ELDP. However, the prognostic value of both peptides was limited for identification of CKD stages 1 – 2. Nevertheless, correlations with 24 h Na^+ excretion and proteinuria markers indicated a relation with disease progression, suggesting measurements of ELDP and CT-proET-1 may be useful for the assessment of kidney pathology and responses to treatment. In addition, increased plasma levels of ELDP and CT-proET-1 after sitaxentan treatment (plasma ET-1 levels were unchanged) suggested that ET_A antagonists might block a negative feedback effect of ET-1 on *EDN1* gene expression (Stow *et al.,* 2011). This requires further investigation, but observations of limited efficacy of ERAs in clinical

trials of HF suggest that ET_A receptor blockade creates a vicious circle where the more effective the blockade the greater the upregulation of *EDN1* gene expression. Measuring proET-1 peptides not only provide advantages over limitations associated with plasma measurements of ET-1, but also may be useful to assess responses associated with ET_A receptor antagonism. Fluid retention (oedema) was an important side effect of ET receptor antagonism and increased morbidity in the clinical trials (Dhaun *et al.*, 2007b; Ritz & Wenzel, 2010) (see Table 1.4, page 29). Although it requires further investigation, proET-1 peptides may serve useful in monitoring side effects associated with ET_A receptor antagonism.

CHAPTER 7

Discussion and general conclusions

7 DISCUSSION AND GENERAL CONCLUSIONS

7.1 Remaining questions from functional studies investigating the role of ET-1 and its receptors

Over the past 25 years strong evidence has accumulated showing that ET-1, the most potent vasoconstrictor peptide known, plays a key role in the regulation of vascular tone and renal function. Genetic models of endothelial-specific deletion of *EDN1* have demonstrated a physiological role of the ET system in regulation of BP (Kisanuki *et al.*, 2010). Similarly, cell specific deletions of *EDN1*, or ET_A and ET_B receptors have revealed important roles for ET-1 in the regulation of renal function and blood pressure (Kedzierski *et al.*, 2003; Bagnall *et al.*, 2006; Kelland *et al.*, 2010). However, research to date has focused exclusively on the pathophysiological roles of the 21 amino acid peptide ET-1, rather than other peptide products of the 212 amino acid precursor – ppET-1. Yet, the contribution *EDN1* might play in human hypertension or regulation of BP is still not well understood.

Cardiac overexpression of the human *EDN1* gene in mice resulted in cardiac inflammation and hypertrophy (Yang *et al.*, 2004). However, although it was anticipated that these changes were due to increased ET-1 synthesis, ERAs were unable to block the resulting lethal HF (Yang *et al.*, 2004). Moreover, ERAs had either little or no benefit in human clinical trials of hypertension and left ventricular HF (Weber *et al.*, 2009; Battistini *et al.*, 2006; Mann *et al.*, 2010; Galiè *et al.*, 2011). Instead, treatment with ERAs was associated frequently with side effects including fluid retention. Following these investigations the unresolved question has been whether additional proET-1 peptides, co-released with ET-1, contribute to the biological actions of *EDN1* and lead to effects that are resistant to inhibition with ERAs.

Plasma levels of ET-1 are an unreliable measure of vascular synthesis. Earlier diagnosis of patients at a higher risk of developing hypertension or HF is still clinically challenging. Indeed, there is an unmet need for a biomarker to enable earlier diagnosis of patients that are at a greater risk to develop cardiovascular or renal disease. Although $ppET\text{-}1_{[168\ -\ 212]}$ (referred to as CT-proET-1) was proposed as an alternative biomarker of ET-1 synthesis on the basis of the assay described by Papassotiriou *et al.*, 2006, detailed characterisation of ppET-1 processing was not carried out. The possibility of

processing to alternative peptides, which may be better biomarkers of ET-1 synthesis, therefore cannot be excluded.

7.2 Characterisation and identification of proET-1 peptide sequences

The initial work of our laboratory identified ppET-1 derived peptides from the EA.hy 926 and A549 conditioned media samples based on antibody recognition using specific immunoassays and HPLC. These human cell lines are fast-growing and well characterised in terms of the ET-1 system (Waxman *et al.,* 1994; Corder *et al.,* 1993a; Corder *et al.,* 1995; Deprez-Roy *et al.,* 2000). Therefore, conditioned media collected after 48 h incubation allowed large-scale purification of proET-1 derived peptides. As a result of further purification and characterisation using IEC and HPLC, the identified secreted proET-1 peptides has shown processing results in three main fragments: NT-proET-1 (ppET-$1_{[18-50]}$), ELDP (ppET-$1_{[93-166]}$), and CT-proET-1 (ppET-$1_{[169-212]}$). Detection of these proET-1 peptides was achieved with double-recognition sandwich immunoassays.

7.2.1 *NT-proET-1*

Identification of the native NT-proET-1 sequence using mass spectrometry was not completed. This was primarily due to isolation of insufficient peptide. Definitive identification of NT-proET-1 was important for two main reasons. Firstly, NT-proET-1 synthetic peptide (fraction 46) eluted later than the purified native peptide (fraction 41) (Figure 4.3C). So mass spectrometry could have confirmed whether the sequence of synthetic peptide (ppET-$1_{[18-50]}$) corresponded to that of the native peptide. Secondly, the amino acid sequence of this peptide is based on a prediction (Bloch *et al.,* 1989); with the first amino acid in its sequence following that of the proposed signal peptide sequence (ppET-1 residues 1 – 17). Thus, identification of the N-terminal sequence of NT-proET-1 could confirm both the amino acid sequence of signal peptide and the processing site for NT-proET-1.

Rapid clearance of synthetic NT-proET-1 from the circulation of rats (Figure 6.3), and the susceptibility of the synthetic peptide to proteolytic degradation (Figure 6.4) showed limited potential of this peptide as a biomarker. Attempts to measure native peptide in plasma samples were also unsuccessful, suggesting that native peptide was also rapidly degraded or cleared from the circulation. Although the amino acid sequence of NT-proET-1 (ppET-$1_{[18-50]}$) is highly conserved (e.g. 67% homology between human and sheep), there is not yet any evidence for a biological activity.

7.2.2 *ELDP and CT-proET-1*

Amino acid sequences of purified ELDP and CT-proET-1 peptides were determined from partial sequences on the basis of trypsin digestion. The N-terminal sequence of ELDP (ppET-$1_{[93-101]}$) was not identified from the purified native samples (fractions 43 and 47) (Table 5.2A and 5.2B). In contrast, under the same methodological conditions, the N-terminal sequence was identified from the purified synthetic sample (fraction 45) (Table 5.2C). Confirmation of disulphide bonds in the endothelin-like domain sequence (ppET-$1_{[109-123]}$) from either native or synthetic ELDP samples was not achieved. Identification of these sequences could be limited by a number of factors including: **(i)** loss of lower abundance peptides during the extraction or C18 clean-up; **(ii)** poor chromatographic separation of the trypsin digested peptides; **(iii)** low amounts of purified native peptide sample; or **(iv)** non-specific proteolytic cleavage of proteins. Digestion with additional proteases with different cleavage capabilities could increase the amino acid sequence coverage and the confidence of results. Trypsin is the most commonly used digestion enzyme. However, in the case for ELDP, the use of this enzyme had two disadvantages. Firstly, abundance of lysine and arginine residues in a sequence produces high numbers of short peptides that are difficult to identify using mass spectrometry. The sequence of endothelin-like domain is rich in lysine and had 4 potential cleavage sites. Peptide identification using database search engines is designed for linear peptides only. Therefore identification of additional peptides requires manual inspection of the raw data. Although all potential peptides were searched manually in the MS/MS spectra, greater number of potential peptides is likely to complicate identification. Secondly, the basic pH required for optimal trypsin digestion can cause disulphide bond rearrangement (Sanger, 1953; Ryle & Sanger, 1955). For both cases,

endopeptidase Glu-C could be advantageous for two reasons: **(1)** it cleaves peptide bonds C-terminal to glutamic acid residue (or at aspartic acid residue depending on the buffer) producing endothelin-like domain as a single fragment; and **(2)** has the option of carrying digestion under more acidic conditions (pH 4 or 8) (Lippincott & Apostol, 1999).

The sequence of endothelin-like domain is highly conserved (Table 1.6) and the spacing between first four cysteine residues is exactly the same as in ET-1 (see Table 1.1, page 3). Although this was suggestive of a biological activity, previous attempts have failed to show this for ppET-$1_{[110–130]}$ (Cade *et al.*, 1990). However, the C-terminal sequence of ELDP has two more cysteine residues (Cys^{148} and Cys^{155}), which are also highly conserved. Therefore, the C-terminal sequence of ELDP could be necessary for receptor binding, and hence for biological activity.

The proteolytic processing of peptides commonly occurs at double basic amino acid residues (most frequently at Lys-Arg and Arg-Arg). Identification of the C-terminal sequence of ELDP: CIYQQLVRGR (ppET-$1_{[155 – 162]}$); and the N-terminal sequence of CT-proET-1: SSEEHLRQTRSETMR (ppET-$1_{[169 – 183]}$), confirmed Arg-Arg at ppET-1 residues 167 – 168 as the cleavage site for CT-proET-1 ($_{155}$-CIYQQLVRGRKI**RR**SSEEHLRQTRSETMR-$_{183}$). The results shown in Figure 5.4 also confirmed the sequence identity of CT-proET-1 (ppET-$1_{[169 – 212]}$). The amino acid sequence of this peptide is highly divergent across species. As such, the human N-terminal sequence of CT-proET-1 (SSEEHLRQTR) corresponding to ppET-1 residues 169 – 178 is completely absent from other species. In addition to these observations, slow clearance of CT-proET-1 suggested that it is biologically inert.

Although mass spectrometry of the purified proET-1 peptides yielded only limited data, the peptide sequences that were identified based on antibody recognition using double-recognition site sandwich immunoassays, as well as HPLC elution characteristics of synthetic and native peptides strongly support the identities of ELDP and CT-proET-1 as ppET-$1_{[93 – 166]}$ and ppET-$1_{[169 – 212]}$, respectively. However, the arrangement of disulphide bridges in ELDP were not confirmed by these studies.

7.3 ELDP and CT-proET-1 peptides as potential biomarkers of cardiovascular and renal disease

The usefulness of ELDP and CT-proET-1 as biomarkers of cardiovascular and renal disease was assessed in plasma samples obtained from patients with pre-H, chronic HF and CKD. Consistent with previous studies showing upregulation of ET-1 in disease states, the levels of ELDP and CT-proET-1 were increased in chronic HF and CKD. Although plasma levels of CT-proET-1 were previously assessed in patients with HF (see Table 1.8), the results shown in Chapter 6 were the first to evaluate plasma levels of ELDP and CT-proET-1 in CKD. Comparison of plasma ELDP and CT-proET-1 levels in patients with pre-H and chronic HF showed higher CT-proET-1 levels (65% *vs.* 21% increase from pre-H) (Figure 6.7). Similarly in CKD, the levels of CT-proET-1 were higher than plasma levels of ELDP (Figure 6.8). This is likely a consequence of slower clearance of CT-proET-1 from the circulation. In addition, earlier increase in CT-proET-1 levels (CKD stages 3 – 5) highlighted its superiority over ELDP (CKD stages 4 – 5). However, the diagnostic ability of both peptides was limited for early CKD stages.

On the other hand, creatinine-based measurements form the basis of renal function assessment and are commonly used in the clinic. Creatinine has a non-linear relationship with GFR and the levels start to increase as GFR $\leq$60/ml/min/1.73 m^2 (National Kidney Foundation, 2002). Plasma levels of ELDP and CT-proET-1 had an inverse linear relationship with GFR (Figure 6.8C and 6.8D), which was consistent with the inverse linear relationship previously observed for plasma ET-1 (Goddard *et al.,* 2007; Dhaun *et al.,* 2009 and Lilitkarntakul *et al.,* 2011) but more importantly, their levels increased earlier in the CKD classification. This is advantageous over the inaccuracy of creatinine measurements in the lower range and highlights the potential of proET-1 peptides as useful biomarkers of CKD. Furthermore, proET-1 assays have advantages over the limitations associated with ET-1 measurements. These are **(1)** immunoassays performed directly without the need of an extraction/purification step; **(2)** due to greater stability or lower degree of degradation their measurements are more accurate and reliable; and **(3)** avoid the cross-reactivity that is associated between ET isoforms.

The negative linear relationship between plasma levels of proET-1 peptides and GFR (decrease in GFR while ELDP and CT-proET-1 increase) suggested reduced renal

filtration and therefore reduced renal clearance. In patients with chronic HF or CKD, there is already an existing upregulation of ET-1 synthesis due to the underlying pathology. Thus, increases in ELDP and CT-proET-1 could be due to increased *EDN1* expression and proET-1 synthesis. Increases in ELDP and CT-proET-1 levels as GFR declines provided further evidence that ET axis contributes to the progression of CKD.

Pathological actions of ET-1 are mainly mediated by activation of ET_A receptors. However, whether blocking ET_A receptors is the best choice of treatment with ERAs still remains controversial. In patients with CKD, blocking ET_A receptors has additional effects on renal haemodynamics and has been proposed to be superior to either dual or ET_B receptor blockade (Goddard *et al.,* 2004). Blocking ET_A receptors in the treatment of CKD improved cardiovascular parameters (Dhaun *et al.,* 2011) as such sitaxentan increased GFR, and reduced proteinuria and BP (Dhaun *et al.,* 2013). However, plasma levels of ET-1 were unchanged after 6 weeks of treatment. As ET-1 measurements may not accurately reflect *EDN1* peptide synthesis, plasma levels of ELDP and CT-proET-1 were investigated in these plasma samples. The observed increases in ELDP and CT-proET-1 levels provided a new insight into the effects of ET_A receptor antagonism, which might be a consequence of increased synthesis. Plasma levels of ET-1 are mainly regulated by the ET_B-mediated clearance. Blockade of ET_B receptors increases plasma ET-1 levels mainly as a result of blocking pulmonary clearance (Fukuroda *et al.,* 1994a; Dupuis *et al.,* 1996a; Burkhardt *et al.,* 2000), but this also in part reduces renal clearance of ET-1 (Gasic *et al.,* 1992). As a result, ET_B receptor blockade contributes to increased ET-1 levels (Goddard *et al.,* 2007). In sitaxentan and nifedipine treatment groups, there was no correlation between changes in proET-1 levels and the reduction in GFR. Thus, from this data, increases in proET-1 peptides are less likely due to reduced renal clearance and the most likely explanation could therefore be increased *EDN1* expression leading to proET-1 synthesis. Increases in ELDP and CT-proET-1 after ET_A receptor blockade shows the first clinical evidence that increases previously observed in plasma ET-1 (Opgenorth *et al.,* 2000; Verhaar *et al.,* 2000) could be due to upregulation of its synthesis.

After 6 weeks of sitaxentan treatment, increases in plasma levels of ELDP and CT-proET-1 were correlated with reductions in 24 h urine Na^+ excretion (Figure 6.10).

Although an increase in ET_B-mediated natriuresis (increased Na^+ excretion) was expected after ET_A antagonist treatment, the reverse occurred. This finding suggests a potential link with adverse side effects (such as increased Na^+ and possibly water retention) associated with ET_A receptor antagonists in previous clinical trials (see Table 1.4, page 29) and might explain the inefficiency of ERAs in clinical trials of HF. These side effects resulted in premature termination of clinical trials due to increased morbidity and mortality, and hence there is a requirement for a sensitive biomarker that would enable identification of patients that are more likely to develop oedema, which again lacks a good biomarker. Thus, measuring stable peptide fragments of proET-1 synthesis could be useful in this setting to provide more reliable measurements of active or upregulated ET-1 synthesis. In conjunction, a biomarker that reflects associated side effects of ERAs would enable better control on development/progression of side effects by adjusting the dose of antagonists to achieve maximal efficacy with minimal side effects.

If increases in ELDP and CT-proET-1 levels were due to upregulation of ET-1 synthesis, then sitaxentan treatment blockade of the physiological negative feedback mechanism regulating *EDN1* expression is likely to contribute to disease progression through alternative pathways. Renin-angiotensin-aldosterone system (RAAS) plays an important role in regulation of vascular homeostasis, fluid electrolyte balance and vascular growth (Fyhrquist & Saijonmaa, 2008). ET-1 reduced renin secretion from cultured mouse renal juxtaglomerular cells (Ackermann *et al.*, 1995; Ritthaler *et al.*, 1995), as well as directly increasing aldosterone secretion through the adrenal cortex (Nussdorfer *et al.*, 1997). As interactions between ET-1 and aldosterone (Rossi *et al.*, 2001) and Ang II (Emori *et al.*, 1991; Park & Schiffrin, 2001) are evident, increased Na^+ and fluid retention could be induced by increased aldosterone secretion. The mechanism of aldosterone stimulation is mainly regulated by Ang II and there is no clinical evidence to show a link between ET-1 and aldosterone release. However, increased proET-1 peptide levels and Na^+ and fluid retention following sitaxentan treatment may suggest that the underlying mechanism for Na^+ and fluid retention, in part, could be regulated **(i)** directly by ELDP; or **(ii)** ELDP-mediated release of aldosterone secretion. The reason of suggesting ELDP as a potential contributor to this mechanism lies beneath its biological action to

potentiate vasoconstrictor activity of ET-1 (Yuzugulen *et al.*, 2012). Therefore, it may also potentiate the action of another mediator that results in aldosterone secretion. **(iii)** ET-1 through ET_B receptors. Although ET_B-mediated natriuresis is largely evident, in rats, ET-1-induced aldosterone secretion was mediated by ET_B receptors while ET_A receptors had no direct effect (Belloni *et al.*, 1996).

7.4 Limitations and future experiments for biomarker investigations

The sample size of TNF-α and chronic HF studies were limited to a small sample size in which samples were stored over a long time. Therefore, further validation of proET-1 peptide levels in studies consisting of a larger sample size could provide further insights into their value as biomarkers. However, although CT-proET-1 had high stability in short-term incubations, the factors affecting its stability in long-term storage are not known. Sample collection may be improved by collecting blood samples into chilled microcentrifuge tubes containing protease inhibitors with analysis of peptide levels from freshly collected samples without the interference of peptide degradation or freeze/thaw process. Tests should be done to evaluate the impact of freeze/thaw cycles on CT-proET-1 stability, in case activation of clotting factors contributes to instability as this is a recognised consideration for repeated analysis of samples particularly after long-term storage.

Biomarker investigations with ELDP and CT-proET-1 opened a new window in the ET field. The results of this study raised further questions, which require additional experiments:

(1) Do selective ET_A receptor antagonists block the physiological negative feedback of ET-1, resulting in increased *EDN1* synthesis? One approach to test this hypothesis is measuring ppET-1 mRNA levels after sitaxentan treatment. Analysing ppET-1 mRNA levels from the plasma samples used in this study would be inaccurate due to degradation. However, investigating the mRNA levels in cultured cells and proET-1 peptides in freshly collected culture medium (e.g. ECs or VSMC) after treatment with sitaxentan at a clinically relevant concentration could provide useful insights into this mechanism.

(2) Further work is needed to confirm that increases in plasma levels of ELDP and CT-proET-1 in other studies of ET_A receptor antagonism and to understand whether this is a class specific effect. As such, chronic administration of atrasentan (ABT-627, ET_A selective antagonist) to healthy subjects increased ET-1 levels at a dose-dependent manner (Verhaar *et al.,* 2000). Thus, analysing plasma levels of proET-1 peptides in similar studies could be advantageous.

(3) Do ET_A receptor antagonists (e.g. sitaxentan) reverse underlying cardiovascular risk factors in CKD, but at the same time contribute to the associated side effects (Na^+ and water retention) observed in clinical trials? Therefore, the potential mechanism by which ELDP regulates aldosterone secretion needs to be investigated. One approach could be evaluation of arterial plasma levels of aldosterone in rats before and after *i.v.* infusion of synthetic ELDP (through femoral vein). Moreover, what would be more interesting is to measure ELDP, CT-proET-1 and aldosterone levels in patients with an existing oedema following treatment with ERAs. This could provide further clues on the underlying mechanism linking ET_A receptor antagonist treatment and Na^+ retention.

(4) Although weight gain or free water clearance was not measured in CKD study, it would be very important to confirm this link between water retention and increases in proET-1 peptide levels in patients treated with ET_A receptor antagonists.

(5) CKD patients involved in the study had minimal co-morbidities and a further investigation which includes other cohorts of patients would be useful. In particular, patients that are less responsive to treatment or at a higher risk of developing adverse effects that are linked to ET_A receptor antagonism can be determined.

(6) Although the ET system is an important contributor to the underlying pathology of PAH, ERAs are less likely to be used as the only line of treatment. In persistent PAH, advanced therapy includes ERAs in combination with phosphodiesterase type 5 (PDE5) inhibitors and prostaglandin analogues. There is a need for less expensive and more effective therapies. It would be interesting to investigate whether proET-1 peptide levels are increased in patients with PAH, and whether proET-1 peptide levels increase in patients treated with bosentan ($ET_{A/B}$ selective) or ambrisentan (ET_A selective). This could provide an opportunity to evaluate whether increases in proET-1 levels correlate with Na^+ or water retention, and determine whether this can distinguish patients that are more likely to develop oedema as a result of ET_A receptor blockade.

(7) Crosstalk between ET receptors: where blockade of a single receptor subtype may influence or account for the deleterious effects of the other receptor subtype has been reported in a number of studies (Mickley *et al.*, 1997; Ozaki *et al.*, 1997; Adner *et al.*, 2001; Davenport & Kuc, 2004). Thus, comparing the effects of selective ET_A and ET_B and dual $ET_{A/B}$ receptor antagonism on increases in plasma levels of ELDP and CT-proET-1 would be useful. Macitentan ($ET_{A/B}$ receptor antagonist with high tissue affinity) increased plasma ET-1 levels at ten times lower doses that were required to increase ET-1 levels to a similar extent with bosentan (moderate volume of distribution) (Weber *et al.*, 1996). This shows an important consideration for the tissue distribution/selectivity of ERAs being investigated. Macitentan (Opsumit®) received its first approval for the treatment of PAH in USA (Patel & McKeage, 2014; Dingemanse *et al.*, 2014) and further investigations of the effects of this antagonist on proET-1 peptide levels might be of value.

7.5 Summary of conclusions and future work

In summary, results presented in this thesis identified a novel ppET-1 derived peptide, which was referred to as ELDP and confirmed the processing of CT-proET-1. These proET-1 peptides are stable in the circulation and therefore their measurement is superior to ET-1. Increases in proET-1 peptide levels in plasma samples obtained from patients with chronic HF and CKD highlighted their potential as useful biomarkers. However, at this stage, they cannot be considered as diagnostic tools for routine use. Increases in proET-1 peptide levels after ET_A receptor blockade provided the first clinical evidence for which increases previously observed in plasma ET-1 could be as a consequence of increased *EDN1* synthesis. The correlation between increased proET-1 peptide levels and Na^+ (and hence fluid) retention after ET_A receptor blockade suggests a link with the adverse side effects associated with ERAs.

Low levels of ELDP and CT-proET-1 detected in urine samples from CKD patients suggested that their metabolism in urine could lead to shorter peptide fragments, which the antibodies being used did not recognise. Hence, identification of excreted peptide fragments in urine would be particularly useful. These immunoassays can be more

favourable than plasma immunoassays as interference of plasma proteins can be excluded.

Further investigations are required to understand the role of ELDP. In addition, identification of its receptor would enable investigations to determine whether a clinical benefit can be achieved by blocking its biological activity. For instance, GPCR-37 or ET_B receptor-like protein-1 (Uniprot: O15354) (Marazziti *et al.*, 1997) could be a potential receptor to investigate. It would be very interesting to obtain X-ray crystallography data for ELDP to determine potential surface residues that are important in receptor binding. This requires a highly purified and a larger amount of ELDP. However, such investigations might enable identification of structural similarities between ELDP and ET-1 and provide insights for the development of antagonists.

References

Abassi ZA, Golomb E, Bridenbaugh R, Keiser HR. (1993a) **Metabolism of endothelin-1 and big endothelin-1 by recombinant neutral endopeptidase EC.3.4.24.11.** *Br J Pharmacol.* 109(4):1024-8.

Abassi ZA, Klein H, Golomb E, Keiser HR. (1993b) **Urinary endothelin: a possible biological marker of renal damage.** *Am J Hypertens*. 6(12):1046-54.

Abassi ZA, Tate JE, Golomb E, Keiser HR. (1992) **Role of neutral endopeptidase in the metabolism of endothelin.** *Hypertension.* 20(1):89-95.

Ackermann M, Ritthaler T, Riegger G, Kurtz A, Krämer BK. (1995) **Endothelin inhibits cAMP-induced renin release from isolated renal juxtaglomerular cells.** *J. Cardiovasc Pharmacol.* 26 Suppl 3:S135-7.

Adlbrecht C, Hülsmann M, Strunk G, Berger R, Mörtl D, Struck J, Morgenthaler NG, Bergmann A, Jakowitsch J,Maurer G, Lang IM, Pacher R. (2009) **Prognostic value of plasma midregional pro-adrenomedullin and C-terminal-pro-endothelin-1 in chronic heart failure outpatients.** *Eur J Heart Fail.* 11(4):361-6.

Adner M, Shankley N, Edvinsson L. (2001) **Evidence that ET-1, but not ET-3 and S6b, ET_A receptor mediated contractions in isolated rat mesenteric arteries are modulated by co-activation of ET_B receptors.** *Br J Pharmacol.* 133: 927–935.

Advenier C, Sarria B, Naline E, Puybasset L, Lagente V. (1990) **Contractile activity of three endothelins (ET-1, ET-2 and ET-3) on the human isolated bronchus.** *Br J Pharmacol.* 100(1):168-72.

Aguilar MI. (2003) **HPLC of Peptides and Proteins: Methods and Protocols.** *Methods in Molecular Biology.* 251: 45-53.

Aguilar MI. and Hearn MT. (1996) **High resolution reversed phase high performance liquid chromatography of peptides and proteins.** *Meth. Enzymol.*270: 3–26.

Ahn D, Ge Y, Stricklett PK, Gill P, Taylor D, Hughes AK, Yanagisawa M, Miller L, Nelson RD, Kohan DE. (2004) **Collecting duct-specific knockout of endothelin-1 causes hypertension and sodium retention**. *J Clin Invest.* 114(4):504-11.

Amiri F, Virdis A, Neves MF, Iglarz M, Seidah NG, Touyz RM, Reudelhuber TL, Schiffrin EL. (2004) **Endothelium-restricted overexpression of human endothelin-1 causes vascular remodeling and endothelial dysfunction.** *Circulation.* 110(15):2233-40.

Anand I, McMurray J, Cohn JN, Konstam MA, Notter T, Quitzau K, Ruschitzka F, Lüscher TF; EARTH investigators. (2004) **Long-term effects of darusentan on left-ventricular remodelling and clinical outcomes in the EndothelinA Receptor Antagonist Trial in Heart Failure (EARTH): randomised, double-blind, placebo-controlled trial.** *Lancet.* 364(9431):347-54.

Annesley TM. (2003) **Ion suppression in mass spectrometry.** *Clin Chem.* 49(7):1041-4.

Argent NB, Liles J, Rodham D, Clayton CB, Wilkinson R, Baylis PH. (1994) **A new method for measuring the blood volume of the rat using 113mIndium as a tracer.** *Lab Anim.* 28(2):172-5.

Arinami T, Ishikawa M, Inoue A, Yanagisawa M, Masaki T, Yoshida MC, Hamaguchi H. (1991) **Chromosomal assignments of the human endothelin family genes: the endothelin-1 gene (EDN1) to 6p23-p24, the endothelin-2 gene (EDN2) to 1p34, and the endothelin-3 gene (EDN3) to 20q13.2-q13.3.** *Am J Hum Genet.* 48(5):990-6.

Atkins GB. and Jain MK. (2007**) Role of krüppel-like transcription factors in endothelial biology**. *Circ Res*. 100:1686-1695.

Aubert JD, Carnal B, Ricou J, Fioroni P, Juillerat-Jeanneret L, Pinet F. (1998) **Characterization of the enzyme involved in the processing of big endothelin-1 in human lung epithelial cells.** *Pulm Pharmacol Ther.*11(2-3):209-13.

Bacon CR, Cary NR, Davenport AP. (1996) **Endothelin peptide and receptors in human atherosclerotic coronary artery and aorta.** *Circ Res.* 79(4):794-801.

Bagnall AJ, Kelland NF, Gulliver-Sloan F, Davenport AP, Gray GA, Yanagisawa M, Webb DJ, and Kotelevtsev YV. (2006). **Deletion of endothelial cell endothelin B receptors does not affect blood pressure or sensitivity to salt.** *Hypertension.* 48, 286-293.

Bakris GL, Lindholm LH, Black HR, Krum H, Linas S, Linseman JV, Arterburn S, Sager P, Weber M. (2010) **Divergent results using clinic and ambulatory blood pressures: report of a darusentan-resistant hypertension trial.** *Hypertension.* 56(5):824-30.

Barker S, Khan NQ, Wood EG, Corder R. (2001) **Effect of an antisense oligodeoxynucleotide to endothelin-converting enzyme-1c (ECE-1c) on ECE-1c mRNA, ECE-1 protein and endothelin-1 synthesis in bovine pulmonary artery smooth muscle cells**. *Mol Pharmacol.* 59(2):163-9.

Barnes K, Brown C, Turner AJ. (1998) **Endothelin-converting enzyme: ultrastructural localization and its recycling from the cell surface**. *Hypertension.* 31(1):3-9.

Barton M, Cosentino F, Brandes RP, Moreau P, Shaw S, Lüscher TF. (1997a) **Anatomic heterogeneity of vascular aging: role of nitric oxide and endothelin.** *Hypertension*. 30(4):817-24.

Barton M, Shaw S, d'Uscio LV, Moreau P, Lüscher TF. (1997b) **Angiotensin II increases vascular and renal endothelin-1 and functional endothelin converting enzyme activity in vivo: role of ETA receptors for endothelin regulation.** *Biochem Biophys Res Commun.* 238(3):861-5.

Barton M. (2008) **Reversal of proteinuric renal disease and the emerging role of endothelin.** *Nat Clin Pract Nephrol.* 4(9):490-501.

Battistini B, Chailler P, D'Orléans-Juste P, Brière N, Sirois P. (1993) **Growth regulatory properties of endothelins.** *Peptides.* 14(2):385-99.

Battistini B, Woods M, O'Donnell LJ, Warner TD, Corder R, Fournier A, Farthing MJ, Vane JR. (1995) **Contractile activity of endothelin precursors in the isolated gallbladder of the guinea-pig: presence of an endothelin-converting enzyme.** *Br J Pharmacol.* 114(7):1383-90.

Battistini B, Berthiaume N, Kelland NF, Webb DJ, Kohan DE. (2006) **Profile of past and current clinical trials involving endothelin receptor antagonists: the novel "-sentan" class of drug.** *Exp Biol Med (Maywood).* 231(6):653-95.

Bauer M, Wilkens H, Langer F, Schneider SO, Lausberg H, Schäfers HJ. (2002) **Selective upregulation of endothelin B receptor gene expression in severe pulmonary hypertension.** *Circulation.* 105: 1034–1036.

Belloni AS, Rossi GP, Andreis PG, Neri G, Albertin G, Pessina AC, Nussdorfer GG. (1996) **Endothelin adrenocortical secretagogue effect is mediated by the B receptor in rats.** *Hypertension.* 27(5):1153-9.

Benedek K. (2004) **High-Performance Hydrophobic Interaction Chromatography.** *Methods Mol Biol.* 251:45-54.

Benigni A, Perico N, Gaspari F, Zoja C, Bellizzi L, Gabanelli M, Remuzzi G. (1991) **Increased renal endothelin production in rats with reduced renal mass.** *Am J Physiol*. 260(3 Pt 2):F331-9.

Bergeron F, Leduc R, Day R. (2000) **Subtilase-like pro-protein convertases: from molecular specificity to therapeutic applications**. *J Mol Endocrinol.* 24(1):1-22.

Bischoff R. and Kolbe HV. (1994) **Deamidation of asparagine and glutamine residues in proteins and peptides: structural determinants and analytical methodology.** *J Chromatogr B Biomed Appl.* 662(2):261-78.

Blais V, Fugère M, Denault JB, Klarskov K, Day R, Leduc R. (2002) **Processing of proendothelin-1 by members of the subtilisin-like pro-protein convertase family.** *FEBS Lett.* 524(1-3):43-8.

Blankenberg S, McQueen MJ, Smieja M, Pogue J, Balion C, Lonn E, Rupprecht HJ, Bickel C, Tiret L, Cambien F, Gerstein H, Münzel T, Yusuf S; HOPE Study Investigators. (2006) **Comparative impact of multiple biomarkers and N-Terminal pro-brain natriuretic peptide in the context of conventional risk factors for the prediction of recurrent cardiovascular events in the Heart Outcomes Prevention Evaluation (HOPE) Study.** *Circulation.* 114(3):201-8.

Bloch KD, Friedrich SP, Lee ME, Eddy RL, Shows TB, Quertermous T. (1989) **Structural organization and chromosomal assignment of the gene encoding endothelin.** *J Biol Chem.* 264(18):10851-7.

Böhm F, Johansson BL, Hedin U, Alving K, Pernow J. (2002) **Enhanced vasoconstrictor effect of big endothelin-1 in patients with atherosclerosis: relation to conversion to endothelin-1.** *Atherosclerosis.* 160(1):215-22.

Bonfiglio R, King RC, Olah TV, Merkle K. (1999) **The effects of sample preparation methods on the variability of the electrospray ionization response for model drug compounds.** *Rapid Commun Mass Spectrom*.13:1175–85.

Bosselmann H, Egstrup M, Rossing K, Gustafsson I, Gustafsson F, Tonder N, Kistorp CN, Goetze JP, Schou M. (2013) **Prognostic significance of cardiovascular biomarkers and renal dysfunction in outpatients with systolic heart failure: A long term follow-up study.** *Int J Cardiol.* pii: S0167-5273(13)01908-6.

Boulanger C. and Lüscher TF. (1990) **Release of endothelin from the porcine aorta. Inhibition by endothelium-derived nitric oxide**. *J Clin Invest.* 85:587–590.

Boulanger CM, Tanner FC, Bea ML, Hahn AWA, Wener A, Lüscher TF. (1992) **Oxidized low density lipoproteins induce mRNA expression and release of endothelin from human and porcine endothelium.** *Circ Res.* 70:1191–1197.

Boyer B, Hart KW, Sperling MI, Lindsell CJ, Collins SP. (2012) **Biomarker changes during acute heart failure treatment.** *Congest Heart Fail.* 18(2):91-7.

Braasch I, Volff JN, Schartl M. (2009) **The endothelin system: evolution of vertebrate-specific ligand-receptor interactions by three rounds of genome duplication.** *Mol Biol Evol.* 26(4):783-99.

Breci LA, Tabb DL, Yates JR III, Wysocki VH. (2003) **Cleavage N-terminal to proline: analysis of a database of peptide tandem mass spectra**. *Anal. Chem.* 75:1963–1971.

Bugaj V, Mironova E, Kohan DE, Stockand JD. (2012) **Collecting duct-specific endothelin B receptor knockout increases ENaC activity.** *Am J Physiol Cell Physiol.* 302(1):C188-94.

Burgess RR. (2008) **Protein Purification**. In: Nothwang HG. and Pfeiffer SE eds., Proteomics of the Nervous System. Weinheim, Germany, WILEY-VCH, pp. 1-17.

Burkhardt M, Barton M, Shaw SG. (2000) **Receptor- and non-receptor-mediated clearance of big-endothelin and endothelin-1: differential effects of acute and chronic ETA receptor blockade.** *J Hypertens.*18(3):273-9.

Burne MJ, Osicka TM, Comper WD. (1999) **Fractional clearance of high molecular weight proteins in conscious rats using a continuous infusion method.** *Kidney Int.* 55(1):261-70.

Cade C, Lumma WC Jr, Mohan R, Rubanyi GM, Parker-Botelho LH. (1990) **Lack of biological activity of preproendothelin [110-130] in several endothelin assays.** *Life Sci.* 47(23):2097-103.

Calderón E, Gómez-Sánchez CE, Cozza EN, Zhou M, Coffey RG, Lockey RF, Prockop LD, Szentivanyi A. (1994) **Modulation of endothelin-1 production by a pulmonary epithelial cell line. I. Regulation by glucocorticoids.** *Biochem Pharmacol.* 48(11):2065-71.

Capasso S. and Salvadori S. (1999) **Effect of the three-dimensional structure on the deamidation reaction of ribonuclease A.** *J Pept Res.* 54(5):377-82.

Cardillo C, Campia U, Kilcoyne CM, Bryant MB, Panza JA. (2002) **Improved endothelium-dependent vasodilation after blockade of endothelin receptors in patients with essential hypertension**. *Circulation.* 105(4):452-6.

Cattaruzza M, Dimigen C, Ehrenreich H, Hecker M. (2000) **Stretch-induced endothelin B receptor-mediated apoptosis in vascular smooth muscle cells.** *FASEB J.* 14(7):991-8.

Celermajer DS, Sorensen KE, Spiegelhalter DJ, Georgakopoulos D, Robinson J, Deanfield JE. (1994) **Aging is associated with endothelial dysfunction in healthy men years before the age-related decline in women.** *J Am Coll Cardiol*. 24:471–476.

Chelius D, Jing K, Lueras A, Rehder DS, Dillon TM, Vizel A, Rajan RS, Li T, Treuheit MJ, Bondarenko PV. (2006) **Formation of pyroglutamic acid from Nterminal glutamic acid in immunoglobulin gamma antibodies.** *Anal. Chem.* 78:2370–2376.

Chen SJ, Chen YF, Meng QC, Durand J, Dicarlo VS, Oparil S. (1995) **Endothelin-receptor antagonist bosentan prevents and reverses hypoxic pulmonary hypertension in rats.** *J Appl Physiol.* 79:2122–2131.

Claria J, Jimenez W, La Villa G, Asbert M, Castro A, Llibre JL, Arroyo V, Rivera F. (1991) **Effects of endothelin on renal haemodynamics and segmental sodium handling in conscious rats.** *Acta Physiol Scand.* 141(3):305-8.

Clarke JG, Benjamin N, Larkin SW, Webb DJ, Davies GJ, Maseri A. (1989) **Endothelin is a potent long-lasting vasoconstrictor in men.** *Am J Physiol.* 257(6 Pt 2):H2033-5.

Clozel M, Gray GA, Breu V, Loffler BM, Osterwalder R.(1992) **The endothelin ET (B) receptor mediates both vasodilation and vasoconstriction in vivo.** *Biochem. Biophys. Res. Commun.* 186:867–873.

Cohn JN, Quyyumi AA, Hollenberg NK, Jamerson KA. (2004) **Surrogate markers for cardiovascular disease: functional markers.** *Circulation.* 109(25 Suppl 1):IV31-46.

Coletta A, Thackray S, Nikitin N, Cleland JG. (2002) **Clinical trials update: highlights of the scientific sessions of The American College of Cardiology 2002: LIFE, DANAMI 2, MADIT-2, MIRACLE-ICD, OVERTURE, OCTAVE, ENABLE 1 & 2, CHRISTMAS, AFFIRM, RACE, WIZARD, AZACS, REMATCH, BNP trial and HARDBALL.** *Eur J Heart Fail.* 4(3):381-8.

Coletta AP. and Cleland JG. (2001) **Clinical trials update: highlights of the scientific sessions of the XXIII Congress of the European Society of Cardiology--WARIS II, ESCAMI, PAFAC, RITZ-1 and TIME.** *Eur J Heart Fail.* 3(6):747-50.

Corder R, Carrier M, Khan N, Klemm P, Vane JR. (1995a) **Cytokine regulation of endothelin-1 release from bovine aortic endothelial cells.** *J Cardiovasc Pharmacol.* 26 Suppl 3:S56-8.

Corder R, Harrison VJ, Khan N, Anggård EE, Vane JR. (1993a) **Effects of phosphoramidon in endothelial cell cultures on the endogenous synthesis of endothelin-1 and on conversion of exogenous big endothelin-1 to endothelin-1.** *J Cardiovasc Pharmacol.* 22 Suppl 8:S73-6.

Corder R, Khan N, Anggård EE, Vane JR. (1993b) **Calcium ionophores inhibit the release of endothelin-1 from endothelial cells**. *J Cardiovasc Pharmacol.* 22 Suppl 8:S42-5.

Corder R. and Vane JR. (1995) **Radioimmunoassay evidence that the pressor effect of big endothelin-1 is due to local conversion to endothelin-1.** *Biochem Pharmacol.* 49(3):375-80.

Corder R, Khan N, Harrison VJ. (1995b) **A simple method for isolating human endothelin converting enzyme free from contamination by neutral endopeptidase 24.11.** *Biochem Biophys Res Commun.* 207(1):355-62.

Corder R. (1996) **The conformation of human big endothelin-1 favours endopeptidase hydrolysis of the TRP21-VAL22 bond.** *Biochem Pharmacol*. 51(3):259-66.

Corder R. (2001) **Identity of endothelin-converting enzyme and other targets for the therapeutic regulation of endothelin biosynthesis**. In: Warner TD. ed., Handbook of Experimental Pharmacology: Endothelin and Its Inhibitors. Germany, Springer-Verlag, 152: 35–67.

Corder R. (2002) **Evaluation of Endothelin-Converting Enzyme Inhibitors Using Cultured Cells**. In: Maguire JJ. and Davenport AP. eds., Peptide Research Protocols Methods in Molecular Biology. Totowa, NJ, Humana Press Inc., pp. 147-162.

Corder R. and Barker S. (1999) **The expression of endothelin-1 and endothelin converting enzyme-1 (ECE-1) are independently regulated in bovine aortic endothelial cells.** *J. Cardiovasc. Pharmacol.* 33, 671–677.

Cowie MR, Struthers AD, Wood DA, Coats AJ, Thompson SG, Poole-Wilson PA, Sutton GC. (1997) **Value of natriuretic peptides in assessment of patients with possible new heart failure in primary care.** *Lancet.* 350(9088):1349-53.

Creasy DM, and Cottrell JS. (2002) **Error tolerant searching of uninterpreted tandem mass spectrometry data.** *Proteomics.* 2:1426–1434.

Creighton T. (1993) **Proteins: Structures and Molecular Properties**. 2nd ed. New York, Freeman.

Dashwood MR, Barker SG, Muddle JR, Yacoub MH, Martin JF. (1993) **[125I]-endothelin-1 binding to vasa vasorum and regions of neovascularization in human and porcine blood vessels: a possible role for endothelin in intimal hyperplasia and atherosclerosis.** *J Cardiovasc Pharmacol*. 22:S343–S347.

Dashwood MR, Mehta D, Izzat MB, Timm M, Bryan AJ, Angelini GD, and Jeremy JY. (1998) **Distribution of endothelin-1 (ET) receptors (ETA and ETB) and immunoreactive ET-1 in porcine saphenous vein carotid artery interposition grafts.** *Atherosclerosis*. 137: 233-242.

Dashwood MR, Noertersheuser P, Kirchengast M, and Munter K. (1999) **Altered endothelin-1 binding following balloon angioplasty of pig coronary arteries: effect of the ETA receptor antagonist, LU 135252.** *Cardiovascular research.* 43: 445-456.

Davenport AP. and Kuc RE. (2004) **Down-regulation of ETA receptors in ETB receptor-deficient mice.** *J Cardiovasc Pharmacol*. 44 Suppl 1:S276-8.

Davenport AP. and Kuc RE. (2002) **Analysis of Endothelins by Enzyme-Linked Immunosorbent Assay and Radioimmunoassay**. In: Maguire JJ & Davenport AP eds., Methods in Molecular Biology, Peptide Research Protocols: Endothelin. Totowa, NJ. Humana Press Inc., pp. 21-36.

Davenport AP, O'Reilly G, Kuc RE. (1995) **Endothelin ETA and ETB mRNA and receptors expressed by smooth muscle in the human vasculature: majority of the ETA sub-type.** *Br J Pharmacol.* 114(6):1110-6.

Davenport AP. (2002) International Union of Pharmacology. XXIX. **Update on endothelin receptor nomenclature**. *Pharmacol Rev.* 54: 219-226.

Davenport AP. and Maguire JJ. (1994) **Is endothelin-induced vasoconstriction mediated only by ETA receptors in humans?** *Trends Pharmacol Sci*. 15(1):9-11.

Davenport AP. and Maguire JJ. (2006) **Endothelin.** In: Moncada S. and Higgs A. eds., The Vascular Endothelium I, Handb Exp Pharmacol. Germany, Springer (176 Pt 1):295-329.

Davie N, Haleen SJ, Upton PD, Polak JM, Yacoub MH, Morrell NW, Wharton J. (2002) **ET(A) and ET(B) receptors modulate the proliferation of human pulmonary artery smooth muscle cells**. *Am J Respir Crit Care Med.* 165(3):398-405.

de Nucci G, Thomas R, D'Orleans-Juste P, Antunes E, Walder C, Warner TD, Vane JR. (1988) **Pressor effects of circulating endothelin are limited by its removal in the pulmonary circulation and by the release of prostacyclin and endothelium-derived relaxing factor**. *Proc Natl Acad Sci U S A.* 85(24):9797-800.

Deanfield JE, Halcox JP, Rabelink TJ. (2007) **Endothelial function and dysfunction: testing and clinical relevance.** *Circulation.* 115(10):1285-95.

deFilippi CR, de Lemos JA, Christenson RH, Gottdiener JS, Kop WJ, Zhan M, Seliger SL. (2010) **Association of serial measures of cardiac troponin T using a sensitive assay with incident heart failure and cardiovascular mortality in older adults.** *JAMA.* 304(22):2494-502.

Denault JB, Claing A, D'Orléans-Juste P, Sawamura T, Kido T, Masaki T, Leduc R. (1995) **Processing of proendothelin-1 by human furin convertase.** *FEBS Lett*. 362(3):276-80.

Deng LY, Day R, Schiffrin EL. (1996) **Localization of sites of enhanced expression of endothelin-1 in the kidney of DOCA-salt hypertensive rats**. *J Am Soc Nephrol.* 7:1158–1164.

Deprez-Roy I, Coge F, Bertry L, Galizzi JP, Feletou M, Vanhoutte PM, Canet E. (2000) **Endothelin-1 pathway in human alveolar epithelial cell line A549 and human umbilical vein endothelial cells.** *Acta Pharmacol Sin.* 21(6):499-506.

Dhaun N, Goddard J, Webb DJ. (2006) **The endothelin system and its antagonism in chronic kidney disease**. *J Am Soc Nephrol* 17:943-55.

Dhaun N, Lilitkarntakul P, Macintyre IM, Muilwijk E, Johnston NR, Kluth DC, Webb DJ, Goddard J. (2009) **Urinary endothelin-1 in chronic kidney disease and as a marker of disease activity in lupus nephritis**. *Am J Physiol Renal Physiol.* 296(6):F1477-83.

Dhaun N, Melville V, Kramer W, Stavros F, Coyne T, Swan S, Goddard J, Webb DJ. (2007a) **The pharmacokinetic profile of sitaxsentan, a selective endothelin receptor antagonist, in varying degrees of renal impairment.** *Br J Clin Pharmacol.* 64(6):733-7.

Dhaun N, Pollock DM, Goddard J, Webb DJ. (2007b) **Selective and mixed endothelin receptor antagonism in cardiovascular disease.** *Trends Pharmacol Sci.* 28:573-579.

Dhaun N, Melville V, Blackwell S, Talwar DK, Johnston NR, Goddard J, Webb DJ. (2013) **Endothelin-A receptor antagonism modifies cardiovascular risk factors in CKD.** *J Am Soc Nephrol*. 24(1):31-6.

Dhaun N, MacIntyre IM, Kerr D, Melville V, Johnston NR, Haughie S, Goddard J, Webb DJ. (2011) **Selective endothelin-A receptor antagonism reduces proteinuria, blood pressure, and arterial stiffness in chronic proteinuric kidney disease.** *Hypertension*. 57(4):772-9.

Dieplinger B, Gegenhuber A, Struck J, Poelz W, Langsteger W, Haltmayer M, Mueller T. (2009) **Chromogranin A and C-terminal endothelin-1 precursor fragment add independent prognostic information to amino-terminal proBNP in patients with acute destabilized heart failure**. *Clin Chim Acta.* 400(1-2):91-6.

Dingemanse J, Sidharta PN, Maddrey WC, Rubin LJ, Mickail H. (2014) **Efficacy, safety and clinical pharmacology of macitentan in comparison to other endothelin receptor antagonists in the treatment of pulmonary arterial hypertension.** *Expert Opin Drug Saf.* 13(3):391-405.

D'Orléans-Juste P, Plante M, Honoré JC, Carrier E, Labonté J. (2003) **Synthesis and degradation of endothelin-1.** *Can J Physiol Pharmacol*. 81(6):503-10.

Douglas SA, Nambi P, Gellai M, Luengo JI, Xiang JN, Brooks DP, Ruffolo RR Jr, Elliott JD, Ohlstein EH. (1998) **Pharmacologic characterization of the novel, orally available endothelin-A--selective antagonist SB 247083**. *J Cardiovasc Pharmacol.* 31 Suppl 1:S273-6.

Douthwaite JA, Lees DM, Corder R. (2003) **A role for increased mRNA stability in the induction of endothelin-1 synthesis by lipopolysaccharide**. *Biochem Pharmacol.* 66(4):589-94.

Drion I, Kleefstra N, Landman GW, Alkhalaf A, Struck J, Groenier KH, Bakker SJ, Bilo HJ. (2012) **Plasma COOH-terminal proendothelin-1: a marker of fatal cardiovascular events, all-cause mortality, and new-onset albuminuria in type 2 diabetes? (ZODIAC-29).** *Diabetes Care.* 35(11):2354-8.

Dupuis J, Goresky CA, Fournier A. (1996a) **Pulmonary clearance of circulating endothelin-1 in dogs in vivo: exclusive role of ET_B receptors**. *J. Appl. Physiol*. 81(4): 1510-1515.

Dupuis J, Stewart DJ, Cernacek P, Gosselin G. (1996b) **Human pulmonary circulation is an important site for both clearance and production of endothelin-1.** *Circulation.* 94(7):1578-84.

Edgell CJ, McDonald CC, Graham JB. (1983) **Permanent cell line expressing human factor VIII-related antigen established by hybridization.** *Proc Natl Acad Sci U S A.* 80(12):3734-7.

Eguchi S, Hirata Y, Ihara M, Yano M, Marumo F. (1992) **A novel ETA antagonist (BQ-123) inhibits endothelin-1-induced phosphoinositide breakdown and DNA synthesis in rat vascular smooth muscle cells.** *FEBS Lett.* 302(3):243-6.

Ehrenreich H, Anderson RW, Fox CH, Rieckmann P, Hoffman GS, Travis WD, Coligan JE, Kehrl JH, Fauci AS. (1990) **Endothelins, peptides with potent vasoactive properties, are produced by human macrophages**. *J Exp Med.* 172(6):1741-8.

Elkayam U, Khan S, Mehboob A, Ahsan N. (2002) **Impaired endothelium-mediated vasodilation in heart failure: clinical evidence and the potential for therapy.** *J Card Fail.* 8(1):15-20.

Emori T, Hirata Y, Ohta K, Kanno K, Eguchi S, Imai T, Shichiri M, Marumo F. (1991) **Cellular mechanism of endothelin-1 release by angiotensin and vasopressin.** *Hypertension.* 18(2):165-70.

Emori T, Hirata Y, Ohta K, Shichiri M, Shimokado K. and Marumo F. (1989) **Concomitant secretion of big endothelin and its C-terminal fragment from human and bovine endothelial cells**. *Biochem. Biophys. Res. Commun.* 162(1):217-23.

Emoto N, Yanagisawa M. (1995) **Endothelin-converting enzyme-2 is a membrane-bound, phosphoramidon-sensitive metalloprotease with acidic pH optimum.** *J Biol Chem.* 270(25):15262-8.

Eng JK, McCormack AL and Yates JR, (1994) **An approach to correlate tandem mass spectral data of peptides with amino acid sequences in a protein database**. *J. Am. Soc. Mass Spectrom.* 5:(11) 976-89.

Ergul S, Parish DC, Puett D, Ergul A. (1996) **Racial differences in plasma endothelin-1 concentrations in individuals with essential hypertension.** *Hypertension.* 28(4):652-5.

Fang ZY, Marwick TH. (2002) **Vascular dysfunction and heart failure: epiphenomenon or etiologic agent?** *Am Heart J.* 143(3):383-90.

Feinberg MW, Lin Z, Fisch S, Jain MK. (2004) **An emerging role for Krüppel-like factors in vascular biology**. *Trends Cardiovasc Med.* 14(6):241-6.

Fernandez-Patron C, Radomski MW, Davidge ST. (1999) **Vascular matrix metalloproteinase-2 cleaves big endothelin-1 yielding a novel vasoconstrictor**. *Circ Res.* 85(10):906-11.

Foley RN, Murray AM, Li S, Herzog CA, McBean AM, Eggers PW, Collins AJ. (2005) **Chronic kidney disease and the risk for cardiovascular disease, renal replacement,**

and death in the United States Medicare population, 1998 to 1999. *J Am Soc Nephrol.* 16(2):489-95.

Fukuroda T, Fujikawa T, Ozaki S, Ishikawa K, Yano M, Nishikibe M. (1994a) **Clearance of circulating endothelin-1 by ETB receptors in rats.** *BiochemBiophys Res Commun.* 199(3):1461-5.

Fukuroda T, Kobayashi M, Ozaki S, Yano M, Miyauchi T, Onizuka M, Sugishita Y, Goto K, Nishikibe M. (1994b) **Endothelin receptor subtypes in human versus rabbit pulmonary arteries.** *J Appl Physiol.* 76:1976–1982.

Fukuroda T, Noguchi K, Tsuchida S, Nishikibe M, Ikemoto F, Okada K, Yano M. (1990) **Inhibition of biological actions of big endothelin-1 by phosphoramidon.** *Biochem Biophys Res Commun.* 172(2):390-5.

Fuller RS BA. and Thorner J. (1989) **Intracellular targeting and structural conservation of a prohormone-processing endoprotease.** *Science.* 246(4929):482-6.

Fyhrquist F. and Saijonmaa O. (2008) **Renin-angiotensin system revisited**. *J Intern Med*. 264:224–236.

Galiè N, Hoeper MM, Simon J, Gibbs R, Simonneau G; Task Force for the Diagnosis and Treatment of Pulmonary Hypertension of the European Society of Cardiology (ESC) and the European Respiratory Society (ERS) (2011) **Liver toxicity of sitaxentan in pulmonary arterial hypertension.** *Eur Heart J.* 32(4):386-7.

Gariepy CE, Ohuchi T, Williams SC, Richardson JA, Yanagisawa M. (2000) **Salt-sensitive hypertension in endothelin-B receptor-deficient rats.** *J Clin Invest.* 105(7):925-33.

Gasic S, Wagner OF, Vierhapper H, Nowotny P, Waldhäusl W. (1992) **Regional hemodynamic effects and clearance of endothelin-1 in humans: renal and peripheral tissues may contribute to the overall disposal of the peptide.** J *Cardiovasc Pharmacol.* 19(2):176-80.

Ge Y, Ahn D, Stricklett PK, Hughes AK, Yanagisawa M, Verbalis JG, Kohan DE. (2005a) **Collecting duct-specific knockout of endothelin-1 alters vasopressin regulation of urine osmolality**. *Am J Physiol Renal Physiol.* 288(5):F912-20.

Ge Y, Bagnall A, Stricklett PK, Webb D, Kotelevtsev Y, Kohan DE. (2008) **Combined knockout of collecting duct endothelin A and B receptors causes hypertension and sodium retention**. *Am J Physiol Renal Physiol.* 295(6):F1635-40.

Ge Y, Stricklett PK, Hughes AK, Yanagisawa M, Kohan DE. (2005b) **Collecting duct-specific knockout of the endothelin A receptor alters renal vasopressin responsiveness, but not sodium excretion or blood pressure.** *Am J Physiol Renal Physiol*. 289(4):F692-8.

Ge Y, Bagnall A, Stricklett PK, Strait K, Webb DJ, Kotelevtsev Y, Kohan DE (2006) **Collecting duct-specific knockout of the endothelin B receptor causes hypertension and sodium retention.** *Am J Physiol Renal Physiol.* 291(6):F1274-80.

Ghafourifar P, Asbury ML, Joshi SS, Kincaid ED. (2005) **Determination of mitochondrial nitric oxide synthase activity.** *Methods Enzymol.* 396:424–444.

Giaid A. and Saleh D. (1995) **Reduced expression of endothelial nitric oxide synthase in the lungs of patients with pulmonary hypertension.** *N Engl J Med.* 333(4):214-21.

Giaid A, Yanagisawa M, Langleben D, Michel RP, Levy R, Shennib H, Kimura S, Masaki T, Duguid WP, Stewart DJ. (1993) **Expression of endothelin-1 in the lungs of patients with pulmonary hypertension.** *N Engl J Med.* 328: 1732–1739.

Go AS, Chertow GM, Fan D, McCulloch CE, Hsu CY. (2004) **Chronic kidney disease and the risks of death, cardiovascular events, and hospitalization.** *N Engl J Med*. 351(13):1296-305.

Goddard J, Johnston NR, Cumming AD, Webb DJ. (2007) **Fractional urinary excretion of endothelin-1 is reduced by acute ETB receptor blockade.** *Am J Physiol*. 293:1433-8.

Goddard J, Johnston NR, Hand MF, Cumming AD, Rabelink TJ, Rankin AJ, Webb DJ: (2004) **Endothelin-A receptor antagonism reduces blood pressure and increases renal blood flow in hypertensive patients with chronic renal failure: A comparison of selective and combined endothelin receptor blockade**. *Circulation.* 109:1186–1193.

Goddard J. and Webb DJ. (2000) **Plasma endothelin concentrations in hypertension.** *J Cardiovasc Pharmacol*. 35(4 Suppl 2):S25-31.

Goettsch W, Lattmann T, Amann K, Szibor M, Morawietz H, Münter K, Müller SP, Shaw S, Barton M. (2001) **Increased expression of endothelin-1 and inducible nitric oxide synthase isoform II in aging arteries in vivo: implications for atherosclerosis.** *Biochem Biophys Res Commun*. 280(3):908-13.

Goto K, Hama H, Kasuya Y. (1996) **Molecular pharmacology and pathophysiological significance of endothelin.** *Jpn J Pharmacol*. 72(4):261-90.

Granchi S, Brocchi S, Bonaccorsi L, Baldi E, Vinci MC, Forti G, Serio M, Maggi M. (2001) **Endothelin-1 production by prostate cancer cell lines is up-regulated by factors involved in cancer progression and down-regulated by androgens.** *Prostate.* 49(4):267-77.

Gui G, Xu D, Emoto N, Yanagisawa M. (1993) **Intracellular localization of membrane-bound endothelin-converting enzyme from rat lung.** *J Cardiovasc Pharmacol.* 22 Suppl 8:S53-6.

Habib A, Al-Omari MA, Khaleghi M, Morgenthaler NG, Struck J, Bergmann A, Mosley TH, Turner ST, Kullo IJ. (2010) **Plasma C-terminal pro-endothelin-1 is associated with target-organ damage in African Americans with hypertension.** *Am J Hypertens.* 23(11):1204-8.

Hahn AW, Resink TJ, Scott-Burden T, Powell J, Dohi Y, Bühler FR. (1990) **Stimulation of endothelin mRNA and secretion in rat vascular smooth muscle cells: a novel autocrine function.** *Cell Regul.* 1(9):649-59.

Halcox JP, Nour KR, Zalos G, Quyyumi AA. (2001) **Coronary vasodilation and improvement in endothelial dysfunction with endothelin ET(A) receptor blockade.** *Circ Res.* 89:969–976.

Hand MF, Haynes WG, Webb DJ. (1999) **Reduced endogenous endothelin-1-mediated vascular tone in chronic renal failure**. *Kidney Int.* 55(2):613-20.

Harrison VJ, Barnes K, Turner AJ, Wood E, Corder R, Vane JR. (1995) **Identification of endothelin-1 and big endothelin-1 in secretory vesicles isolated from bovine aortic endothelial cells.** *Proc Natl Acad Sci USA.* 92:6344.

Hasdai D, Holmes DR Jr, Garratt KN, Edwards WD, Lerman A. (1997) **Mechanical pressure and stretch release endothelin-1 from human atherosclerotic coronary arteries in vivo.** *Circulation.* 95(2):357-62.

Hasegawa H, Hiki K, Sawamura T, Aoyama T, Okamoto Y, Miwa S, Shimohama S, Kimura J, Masaki T. (1998) **Purification of a novel endothelin-converting enzyme specific for big endothelin-3**. *FEBS Lett.* 428(3):304-8.

Haynes WG, Ferro CJ, O'Kane KP, Somerville D, Lomax CC, Webb DJ. (1996) **Systemic endothelin receptor blockade decreases peripheral vascular resistance and blood pressure in humans.** *Circulation.* 93(10):1860-70.

Haynes WG. and Webb DJ. (1994) **Contribution of endogenous generation of endothelin-1 to basal vascular tone.** *Lancet.* 344(8926):852-4.

Haynes WG. and Webb DJ. (1998) **Endothelin as a regulator of cardiovascular function in health and disease**. *J Hypertens.* 16(8):1081-98.

Haynes WG. (1995) **Endothelins as regulators of vascular tone in man**. *Clin Sci (Lond).* 88(5):509-17.

Haynes WG, Strachan FE, Gray GA, Webb DJ. (1995) **Forearm vasoconstriction to endothelin-1 is mediated by ETA and ETB receptors in vivo in humans.** *J Cardiovasc Pharmacol*. 26 Suppl 3:S40-3.

Hemsén A, Ahlborg G, Ottosson-Seeberger A, Lundberg JM. (1995) **Metabolism of Big endothelin-1 (1-38) and (22-38) in the human circulation in relation to production ofendothelin-1 (1-21).** *Regul Pept.* 55(3):287-97.

Henrich S, Cameron A, Bourenkov GP, Kiefersauer R, Huber R, Lindberg I, Bode W, Than ME (2003) **The crystal structure of the proprotein processing proteinase furin explains its stringent specificity**. *Nat Struct Biol.* 10(7):520-6.

Henzel WJ, Billeci TM, Stults JT, Wong SC, Grimley C, Watanabe C. (1993) **Identifying proteins from two-dimensional gels by molecular mass searching of peptide fragments in protein sequence databases.** *Proc. Natl. Acad. Sci. U. S. A. 90*, 5011– 5015.

Henzel WJ, Watanabe C, Stults JT. (2003) **Protein identification: the origins of peptide mass fingerprinting.** *J Am Soc Mass Spectrom.* 14(9):931-42.

Hewitt SM, Dear J, Star RA. (2004) **Discovery of protein biomarkers for renal diseases.** *J Am Soc Nephrol.* 15:1677-1689.

Hirata Y, Yoshimi H, Takata S, Watanabe TX, Kumagai S, Nakajima K, Sakakibara S. (1988) **Cellular mechanism of action by a novel vasoconstrictor endothelin in cultured rat vascular smooth muscle cells.** *Biochem Biophys Res Commun.* 154(3):868-75.

Hishikawa K, Nakaki T, Marumo T, Suzuki H, Kato R, Saruta T. (1995) **Pressure enhances endothelin-1 release from cultured human endothelial cells.** *Hypertension.* 25(3):449-52.

Hoang MV, Turner AJ. (1997) **Novel activity of endothelin-converting enzyme: hydrolysis of bradykinin.** *Biochem J.* 327(Pt 1):23-6.

Hoshi T. and Heinemann S. (2001) **Regulation of cell function by methionine oxidation and reduction**. *J Physiol.* 531(Pt 1):1-11.

Howard PG, Plumpton C, Davenport AP. (1992) **Anatomical localization and pharmacological activity of mature endothelins and their precursors in human vascular tissue**. *J Hypertens.* 10(11):1379-86.

Hyndman KA, Evans DH. (2007) **Endothelin and endothelin converting enzyme-1 in the fish gill: evolutionary and physiological perspectives.** *J Exp Biol.* 210(Pt 24):4286-97.

Hyndman KA, Miyamoto MM, Evans DH. (2009) **Phylogeny, taxonomy, and evolution of the endothelin receptor gene family**. *Mol Phylogenet Evol.* 52(3):677-87.

Ihling C, Göbel HR, Lippoldt A, Wessels S, Paul M, Schaefer HE, Zeiher AM. (1996) **Endothelin-1-like immunoreactivity in human atherosclerotic coronary tissue: a detailed analysis of the cellular distribution of endothelin-1.** *J Pathol.* 179(3):303-8.

Ihling C, Szombathy T, Bohrmann B, Brockhaus M, Schaefer HE, Loeffler BM. (2001) **Coexpression of endothelin-converting enzyme-1 and endothelin-1 in different stages of human atherosclerosis.** *Circulation.* 104(8):864-9.

Ikegawa R, Matsumura Y, Tsukahara Y, Takaoka M, Morimoto S. (1990) **Phosphoramidon, a metalloproteinase inhibitor, suppresses the secretion of endothelin-1 from cultured endothelial cells by inhibiting a big endothelin-1 converting enzyme**. *Biochem Biophys Res Commun*. 171(2):669-75.

Ikegawa R, Matsumura Y, Tsukahara Y, Takaoka M, Morimoto S. (1991) **Phosphoramidon inhibits the generation of endothelin-1 from exogenously applied big endothelin-1 in cultured vascular endothelial cells and smooth muscle cells.** *FEBS Lett.* 293(1-2):45-8.

Imai T, Hirata Y, Emori T, Yanagisawa M, Masaki T, Marumo F. (1992) **Induction of endothelin-1 gene by angiotensin and vasopressin in endothelial cells.** *Hypertension.* 19(6 Pt 2):753-7.

Inoue A, Yanagisawa M, Takuwa Y, Mitsui Y, Kobayashi M, Masaki T. (1989) **The human preproendothelin-1 gene. Complete nucleotide sequence and regulation of expression.** *J Biol Chem.* 264(25):14954-9.

Iqbal N, Wentworth B, Choudhary R, Landa Ade L, Kipper B, Fard A, Maisel AS. (2012) **Cardiac biomarkers: new tools for heart failure management.** *Cardiovasc Diagn Ther*. 2(2):147-64.

Isaka D, Emoto N, Raharjo SB, Yokoyama M, Matsuo M. (2003) **The effects of phosphoramidon on the expression of human endothelin-converting enzyme-1 (ECE-1) isoforms.** *J Cardiovasc Pharmacol*. 42(1):136-41.

Ito H, Hirata Y, Adachi S, Tanaka M, Tsujino M, Koike A, Nogami A, Murumo F, Hiroe M. (1993) **Endothelin-1 is an autocrine/paracrine factor in the mechanism of angiotensin II-induced hypertrophy in cultured rat cardiomyocytes.** *J Clin Invest.* 92(1):398-403.

Ito H, Hirata Y, Hiroe M, Tsujino M, Adachi S, Takamoto T, Nitta M, Taniguchi K, Marumo F. (1991) **Endothelin-1 induces hypertrophy with enhanced expression of muscle-specific genes in cultured neonatal rat cardiomyocytes**. *Circ Res.* 69(1):209-15.

James ND, Caty A, Payne H, Borre M, Zonnenberg BA, Beuzeboc P, McIntosh S, Morris T, Phung D, Dawson NA. (2010) **Final safety and efficacy analysis of the specific endothelin A receptor antagonist zibotentan (ZD4054) in patients with metastatic castration-resistant prostate cancer and bone metastases who were pain-free or mildly symptomatic for pain: a double-blind, placebo-controlled, randomized Phase II trial.** *BJU Int.* 106(7):966-73.

Janes RW, Peapus DH, Wallace BA. (1994) **The crystal structure of human endothelin.** *Nat Struct Biol*. 1(5):311-9.

Jankowska EA, Filippatos GS, von Haehling S, Papassotiriou J, Morgenthaler NG, Cicoira M, Schefold JC, Rozentryt P, Ponikowska B, Doehner W, Banasiak W, Hartmann O, Struck J, Bergmann A, Anker SD, Ponikowski P. (2011) **Identification of chronic heart failure patients with a high 12-month mortality risk using biomarkers including plasma C-terminal pro-endothelin-1.** *PLoS One.* 6(1):e14506.

Jersmann HP, Hii CS, Ferrante JV, Ferrante A. (2001) **Bacterial lipopolysaccharide and tumor necrosis factor alpha synergistically increase expression of human endothelial adhesion molecules through activation of NK-kappaB and p38 mitogen activated protein kinase signalling pathway**. *Infect. Immun.* 69(3):1273-9.

Ji JA, Zhang B, Cheng W, Wang YJ. (2009) **Methionine, tryptophan, and histidine oxidation in a model protein, PTH: mechanisms and stabilization**. *J Pharm Sci*. 98(12):4485-500

Johnson GD, Stevenson T, Ahn K. (1999) **Hydrolysis of peptide hormones by endothelin-converting enzyme-1. A comparison with neprilysin.** *J Biol Chem.* 274(7):4053-8.

Jones GT, van Rij AM, Solomon C, Thomson IA, Packer SG. (1996) **Endothelin-1 is increased overlying atherosclerotic plaques in human arteries.** *Atherosclerosis.* 124(1):25-35.

Jones RC, Francis GS, Lauer MS. (2004) **Predictors of mortality in patients with heart failure and preserved systolic function in the Digitalis Investigation Group trial.** *J Am Coll Cardiol.* 44(5):1025-9.

Kaasjager KA, van Rijn HJ, Koomans HA, Rabelink TJ. (1995) **Interactions of nifedipine with the renovascular effects of endothelin in humans**. *J Pharmacol Exp Ther.* 275(1):306-11.

Kahler J, Ewert A, Weckmüller J, Stobbe S, Mittmann C, Köster R, Paul M, Meinertz T, Münzel T. (2001) **Oxidative stress increases endothelin-1 synthesis in human coronary artery smooth muscle cells.** *J Cardiovasc Pharmacol.* 38:49–57.

Kang BY, Kleinhenz JM, Murphy TC, Hart CM. (2011) **The PPARγ ligand rosiglitazone attenuates hypoxia-induced endothelin signaling in vitro and in vivo.** *Am J Physiol Lung Cell Mol Physiol.* 301(6):L881-91.

Kelland NF, Kuc RE, McLean DL, Azfer A, Bagnall AJ, Gray GA, Gulliver-Sloan FH, Maguire JJ, Davenport AP, Kotelevtsev YV, Webb DJ. (2010) **Endothelial cell-specific ETB receptor knockout: autoradiographic and histological characterisation and crucial role in the clearance of endothelin-1.** *Can J Physiol Pharmacol.* 88(6):644-51.

Kellie JF, Tran JC, Lee JE, Ahlf DR, Thomas HM, Ntai I, Catherman AD, Durbin KR, Zamdborg L, Vellaichamy A, Thomas PM, Kelleher NL. (2010) **The emerging process of Top Down mass spectrometry for protein analysis: biomarkers, protein-therapeutics, and achieving high throughput.** *Mol Biosyst.* 6(9):1532-9.

Kelly JJ. and Whitworth JA. (1999) **Endothelin-1 as a mediator in cardiovascular disease.** *Clin Exp Pharmacol Physiol*. 26(2):158-61.

Khan MA, Dashwood MR, Mumtaz FH, Thompson CS, Mikhailidis DP, Morgan RJ (1999) **Upregulation of Endothelin A Receptor Sites in the Rabbit Diabetic Kidney: Potential Relevance to the Early Pathogenesis of Diabetic Nephropathy**. *Nephron*. 83:261–267.

Kido T, Sawamura T, Hoshikawa H, D'Orléans-Juste P, Denault JB, Leduc R, Kimura J, Masaki T. (1997) **Processing of proendothelin-1 at the C-terminus of big endothelin-1 is essential for proteolysis by endothelin-converting enzyme-1 in vivo.** *Eur J Biochem*. 244(2):520-6.

Kiely DG, Cargill RI, Struthers AD, Lipworth BJ. (1997) **Cardiopulmonary effects of endothelin-1 in man.** *Cardiovasc Res*. 33(2):378-86.

Kinlay S, Behrendt D, Wainstein M, Beltrame J, Fang JC, Creager MA, Selwyn AP, Ganz P. (2001) **Role of endothelin-1 in the active constriction of human atherosclerotic coronary arteries**. *Circulation.* 104(10):1114-8.

Kiowski W, Lüscher TF, Linder L, Bühler FR. (1991) **Endothelin-1-induced vasoconstriction in humans. Reversal by calcium channel blockade but not by nitrovasodilators or endothelium-derived relaxing factor.** *Circulation.* 83(2):469-75.

Kisanuki YY, Emoto N, Ohuchi T, Widyantoro B, Yagi K, Nakayama K, Kedzierski RM, Hammer RE, Yanagisawa H, Williams SC, Richardson JA, Suzuki T, Yanagisawa

M. (2010) **Low blood pressure in endothelial cell-specific endothelin 1 knockout mice.** *Hypertension.* 56(1):121-8.

Kitamura K, Tanaka T, Kato J, Eto T, Tanaka K. (1989) **Regional distribution of immunoreactive endothelin in porcine tissue: abundance in innermedulla of kidney.** *Biochem Biophys Res Commun.* 161(1):348-52.

Kitazumi K, Tasaka K. (1993) **The role of c-Jun protein in thrombin-stimulated expression of preproendothelin-1 mRNA in porcine aortic endothelial cells**. *Biochem Pharmacol*. 46(3):455-64.

Klemm P, Warner TD, Hohlfeld T, Corder R, Vane JR. (1995) **Endothelin 1 mediates ex vivo coronary vasoconstriction caused by exogenous and endogenous cytokines.** *Proc Natl Acad Sci U S A.* 92(7):2691-5.

Kloog Y, Ambar I, Sokolovsky M, Kochva E, Wollberg Z, Bdolah A. (1988) **Sarafotoxin, a novel vasoconstrictor peptide: phosphoinositide hydrolysis in rat heart and brain**. *Science.* 242(4876):268-70.

Kohan DE, Rossi NF, Inscho EW, Pollock DM. (2011) **Regulation of blood pressure and salt homeostasis by endothelin.** *Physiol Rev*. 91(1):1-77.

Kohno M, Yokokawa K, Horie T, Yasunari K, Murahawa K, Ikeda M, Takeda T. (1992) **Release mechanism of endothelin-1 and big endothelin-1 after stimulation with thrombin in cultured porcine endothelial cells.** *J Vasc Res*. 29*:*56-*63.*

Komuro I, Kurihara H, Sugiyama T, Yoshizumi M, Takaku F, Yazaki Y. (1988) **Endothelin stimulates c-fos and c-myc expression and proliferation of vascular smooth muscle cells.** *FEBS Lett.* 238(2):249-52.

Kourembanas S, Marsden PA, McQuillan LP, Faller DV. (1991) **Hypoxia induces endothelin gene expression and secretion in cultured human endothelium.** *J Clin Invest.* 88(3):1054-7.

Kuc RE, Karet FE, Davenport AP. (1995) **Characterization of peptide and nonpeptide antagonists in human kidney.** *J Cardiovasc Pharmacol.* 26 Suppl 3:S373-5.

Küng CF. and Lüscher TF. (1995) **Different mechanisms of endothelial dysfunction with aging and hypertension in rat aorta.** *Hypertension.* 25:194-200.

Kurihara Y, Kurihara H, Suzuki H, Kodama T, Maemura K, Nagai R, Oda H, Kuwaki T, Cao WH, Kamada N, et al. (1994) **Elevated blood pressure and craniofacial abnormalities in mice deficient in endothelin-1.** *Nature.* 368(6473):703-10.

Lambers C, Roth M, Zhong J, Campregher C, Binder P, Burian B, Petkov V, Block L.H (2013) **The Interaction of Endothelin-1 and TGF-β1 Mediates Vascular Cell Remodeling.** *PLoS One.* 8(8): e73399.

Landan G, Bdolah A, Wollberg Z, Kochva E, Graur D. (1991) **Evolution of the sarafotoxin/endothelin superfamily of proteins.** *Toxicon.* 29(2):237-44.

Larivière R, Day R, Schiffrin EL. (1993) **Increased expression of endothelin-1 gene in blood vessels of deoxycorticosterone acetate-salt hypertensive rats**. *Hypertension.* 21:916–920.

Latini R, Masson S, Pirelli S, Barlera S, Pulitano G, Carbonieri E, Gulizia M, Vago T, Favero C, Zdunek D, Struck J, Staszewsky L, Maggioni AP, Franzosi MG, Disertori M; GISSI-AF Investigators. (2011) **Circulating cardiovascular biomarkers in recurrent atrial fibrillation: data from the GISSI-atrial fibrillation trial.** *J Intern Med.* 269(2):160-71.

Lea J, Greene T, Hebert L, Lipkowitz M, Massry S, Middleton J, Rostand SG, Miller E, Smith W, Bakris GL. (2005) **The relationship between magnitude of proteinuria reduction and risk of end-stage renal disease:results of the African American study of kidney disease and hypertension.** *Arch Intern Med.* 25;165(8):947-53.

Lee S, Zambas ED, Marsh WL, Redman CM. (1991) **Molecular cloning and primary structure of Kell blood group protein**. *Proc. Natl. Acad. Sci. USA.* 88: 6353-6357.

Lepailleur-Enouf D, Valdenaire O, Philippe M, Jandrot-Perrus M, Michel JB. (2000) **Thrombin induces endothelin expression in arterial smooth muscle cells.** *Am J Physiol Heart Circ Physiol.* 278(5):H1606-12.

Lerman A, Edwards BS, Hallett JW, Heublein DM, Sandberg SM, Burnett JC Jr. (1991) **Circulating and tissue endothelin immunoreactivity in advanced atherosclerosis**. *N Engl J Med.* 325:997-1001.

Lerman A. and Zeiher AM. (2005) **Endothelial function: cardiac events.** *Circulation.* 111: 363–368.

Li JS, Larivière R, Schiffrin EL. (1994) **Effect of a nonselective endothelin antagonist on vascular remodeling in deoxycorticosterone acetate-salt hypertensive rats. Evidence for a role of endothelin in vascular hypertrophy.** *Hypertension.* 24(2):183-8.

Li S, Schöneich C, Borchardt RT. (1995) **Chemical instability of protein pharmaceuticals: Mechanisms of oxidation and strategies for stabilization**. *Biotechnol Bioeng.* 48(5):490-500.

Li Z, Froehlich J, Galis ZS, Lakatta EG. (1999) **Increased expression of matrix metalloproteinase-2 in the thickened intima of aged rats**. *Hypertension.* 33:116–123.

Lilitkarntakul P, Dhaun N, Melville V, Blackwell S, Talwar DK, Liebman B, Asai T, Pollock J, Goddard J, Webb DJ. (2011) **Blood pressure and not uraemia is the major determinant of arterial stiffness and endothelial dysfunction in patients with chronic kidney disease and minimal co-morbidity.** *Atherosclerosis.* 216(1):217-25.

Link AJ. and LaBaer J. (2011) **Solution protein digest.** Cold Spring Harb Protoc. 2011(2):pdb.prot5569.

Lippincott J. and Apostol I. (1999) **Carbamylation of cysteine: a potential artifact in peptide mapping of hemoglobins in the presence of urea.** *Anal Biochem.* 267(1):57-64.

Loo JA, Edmonds CG, Udseth HR, Smith RD. (1990) **Effect of reducing disulfide-containing proteins on electrospray ionization mass spectra**. *Anal Chem*. 62(7):693-8.

Louis A, Cleland JG, Crabbe S, Ford S, Thackray S, Houghton T, Clark A. (2001) **Clinical Trials Update: CAPRICORN, COPERNICUS, MIRACLE, STAF, RITZ-2, RECOVER and RENAISSANCE and cachexia and cholesterol in heart failure. Highlights of the Scientific Sessions of the American College of Cardiology, 2001.** *Eur J Heart Fail.* 3(3):381-7.

Love MP, Ferro CJ, Haynes WG, Plumpton C, Davenport AP, Webb DJ, McMurray JJ. (2000) **Endothelin receptor antagonism in patients with chronic heart failure.** *Cardiovasc Res.* 47(1):166-72.

Lowenstein CJ, Morrell CN, Yamakuchi M. (2005) **Regulation of Weibel-Palade body exocytosis.** *Trends Cardiovasc Med.* 15(8):302-8.

Lummis SC, Beene DL, Lee LW, Lester HA, Broadhurst RW, Dougherty DA. (2005) **Cis-trans isomerization at a proline opens the pore of a neurotransmitter-gated ion channel.** *Nature.* 438(7065):248-52.

Lüscher TF, Enseleit F, Pacher R, Mitrovic V, Schulze MR, Willenbrock R, Dietz R, Rousson V, Hürlimann D, Philipp S, Notter T, Noll G, Ruschitzka F; Heart Failure ET(A) Receptor Blockade Trial. (2002) **Hemodynamic and neurohumoral effects of selective endothelin A (ET(A)) receptor blockade in chronic heart failure: the Heart Failure ET(A) Receptor Blockade Trial (HEAT).** *Circulation.* 106(21):2666-72.

Lüscher TF, Yang Z, Tschudi M, von Segesser L, Stulz P, Boulanger C, Siebenmann R, Turina M, Bühler FR. (1990) **Interaction between endothelin-1 and endothelium-derived relaxing factor in human arteries and veins**. *Circ Res.* 66(4):1088-94.

Macarthur H, Warner TD, Wood EG, Corder R, Vane JR. (1994) **Endothelin-1 release from endothelial cells in culture is elevated both acutely and chronically by short periods of mechanical stretch**. *Biochem Biophys Res Commun.* 200(1):395-400.

Maguire JJ. and Davenport AP. (1995) **ETA receptor-mediated constrictor responses to endothelin peptides in human blood vessels in vitro.** *Br J Pharmacol.* 15(1):191-7.

Maguire JJ. And Davenport AP. (1998) **Increased response to big endothelin-1 in atherosclerotic human coronary artery: functional evidence for up-regulation of endothelin-converting enzyme activity in disease.** *Br J Pharmacol.* 125:238–240.

Maguire JJ. and Davenport AP. (2004) **Alternative pathway to endothelin-converting enzyme for the synthesis of endothelin in human blood vessels.** *J Cardiovasc Pharmacol.* 44 Suppl 1:S27-9.

Maier C, Clodi M, Neuhold S, Resl M, Elhenicky M, Prager R, Moertl D, Strunk G, Luger A, Struck J, Pacher R, Hülsmann M. (2009) **Endothelial markers may link kidney function to cardiovascular events in type 2 diabetes.** *Diabetes Care.* 32(10):1890-5.

Maisel AS, Krishnaswamy P, Nowak RM, McCord J, Hollander JE, Duc P, Omland T, Storrow AB, Abraham WT, Wu AH, Clopton P, Steg PG, Westheim A, Knudsen CW, Perez A, Kazanegra R, Herrmann HC, McCullough PA; Breathing Not Properly Multinational Study Investigators. (2002) **Rapid measurement of B-type natriuretic peptide in the emergency diagnosis of heart failure.** *N Engl J Med.* 347(3):161-7.

Malek AM, Greene AL, Izumo S. (1993) **Regulation of endothelin 1 gene by fluid shear stress is transcriptionally mediated and independent of protein kinase C and cAMP**. *Proc Natl Acad Sci U S A.* 90(13):5999-6003.

Malek AM, Zhang J, Jiang J, Alper SL, Izumo S. (1999) **Endothelin-1 gene suppression by shear stress: pharmacological evaluation of the role of tyrosine kinase, intracellular calcium, cytoskeleton, and mechanosensitive channels.** *J Mol Cell Cardiol.* 31(2):387-99.

Maleknia SD. and Johnson R. (2011) **Mass Spectrometry of Amino Acids and Proteins.** In: Hughes AB. ed., Amino Acids, Peptides and Proteins in Organic Chemistry: Analysis and Function of Amino Acids and Peptides. Weinheim, Germany, Wiley-VCH Verlag GmbH & Co, pp. 1-50.

Malfroy B, Kuang WJ, Seedburg PH, Mason AJ, and Schofield PR. (1988) **Molecular cloning and amino acid sequence of human enkephalinase (neutral endopeptidase).** *FEBS Lett.* 229: 206-210.

Mann JF, Green D, Jamerson K, Ruilope LM, Kuranoff SJ, Littke T, Viberti G; ASCEND Study Group. (2010) **Avosentan for overt diabetic nephropathy.** *J Am Soc Nephrol*. 21(3):527-35.

Marazziti D, Golini E, Gallo A, Lombardi MS, Matteoni R, Tocchini-Valentini GP. (1997) **Cloning of GPR37, a gene located on chromosome 7 encoding a putative G-protein-coupled peptide receptor, from a human frontal brain EST library.** *Genomics.* 45(1):68-77.

Markewitz BA, Farrukh IS, Chen Y, Li Y, Michael JR. (2001) **Regulation of endothelin-1 synthesis in human pulmonary arterial smooth muscle cells. Effects of transforming growth factor-beta and hypoxia.** *Cardiovasc Res.* 49(1):200-6.

Marsen TA, Simonson MS, Dunn MJ. (1995) **Thrombin induces the preproendothelin-1 gene in endothelial cells by a protein tyrosine kinase-linked mechanism.** *Circ Res.* 76(6):987-95.

Martin-Nizard F, Houssaini HS, Lestavel-Delattre S, Duriez P, Fruchart JC. (1991) **Modified low density lipoproteins activate human macrophages to secrete immunoreactive endothelin.** *FEBS Lett.* 293(1-2):127-30.

Masson S, Latini R, Anand IS, Vago T, Angelici L, Barlera S, Missov ED, Clerico A, Tognoni G, Cohn JN; Val-HeFT Investigators. (2006) **Direct comparison of B-type natriuretic peptide (BNP) and amino-terminal proBNP in a large population of patients with chronic and symptomatic heart failure: the Valsartan Heart Failure (Val-HeFT) data.** *Clin Chem.* 52(8):1528-38.

Masson S, Latini R, Carbonieri E, Moretti L, Rossi MG, Ciricugno S, Milani V, Marchioli R, Struck J, Bergmann A, Maggioni AP, Tognoni G, Tavazzi L; GISSI-HF

Investigators. (2010) **The predictive value of stable precursor fragments of vasoactive peptides in patients with chronic heart failure: data from the GISSI-heart failure (GISSI-HF) trial.** *Eur J Heart Fail.* 12(4):338-47.

Matsumoto T, Yoshiyama S, Kobayashi T, Kamata K. (2004) **Mechanisms underlying enhanced contractile response to endothelin-1 in diabetic rat basilar artery.** *Peptides.* 25(11):1985-94.

McCulloch KM, Docherty C, MacLean MR. (1998) **Endothelin receptors mediating contraction of rat and human pulmonary resistance arteries: effect of chronic hypoxia in the rat.** *Br J Pharmacol*. 123(8):1621-30.

McMahon EG, Palomo MA, Moore WM, McDonald JF, Stern MK. (1991) **Phosphoramidon blocks the pressor activity of porcine big endothelin-1-(1-39) in vivo and conversion of big endothelin-1-(1-39) to endothelin-1-(1-21) in vitro.** *Proc Natl Acad Sci U S A.* 88(3):703-7.

McMurray JJ, Adamopoulos S, Anker SD, Auricchio A, Böhm M et al; ESC Committee for Practice Guidelines. (2012) **ESC guidelines for the diagnosis and treatment of acute and chronic heart failure 2012: The Task Force for the Diagnosis and Treatment of Acute and Chronic Heart Failure 2012 of the European Society of Cardiology. Developed in collaboration with the Heart Failure Association (HFA) of the ESC**. *Eur J Heart Fail.* 14(8):803-69.

McMurray JJ, Ray SG, Abdullah I, Dargie HJ, Morton JJ. (1992) **Plasma endothelin in chronic heart failure**. *Circulation.* 85(4):1374-9.

Medzihradszky KF. (2005) **Peptide sequence analysis**. *Methods Enzymol.* 402:209-44.

Mickley EJ, Gray GA, Webb DJ. (1997) **Activation of endothelin ETA receptors masks the constrictor role of endothelin ETB receptors in rat isolated small mesenteric arteries.** *Br J Pharmacol.* 120(7):1376-82.

Minamino T, Kurihara H, Takahashi M, Shimada K, Maemura K, Oda H, Ishikawa T, Uchiyama T, Tanzawa K, Yazaki Y. (1997) **Endothelin-converting enzyme expression in the rat vascular injury model and human coronary atherosclerosis.** *Circulation.* 95(1):221-30.

Mockridge JW, Kuc RE, Huskisson NS, Barker PJ, Davenport AP. (1998) **Characterization of site-directed antisera against endothelin-converting enzymes.** *J Cardiovasc Pharmacol.* Suppl 1:S35-7.

Moncada S, Vane JR. (1979) **Pharmacology and endogenous roles of prostaglandin endoperoxides, thromboxane A2 and prostacyclin.** *Pharmacol Rev.* 30*:* 293–331.

Moraes DL, Colucci WS, Givertz MM. (2000) **Secondary pulmonary hypertension in chronic heart failure: the role of the endothelium in pathophysiology and management.** *Circulation.* 102:1718-1723.

Morawietz H, Talanow R, Szibor M, Rueckschloss U, Schubert A, Bartling B, Darmer D, Holtz J. (2000) **Regulation of the endothelin system by shear stress in human endothelial cells.** *J Physiol.* 525 Pt 3:761-70.

Morey AK, Razandi M, Pedram A, Hu RM, Prins BA, Levin ER. (1998) **Oestrogen and progesterone inhibit the stimulated production of endothelin-1.** *Biochem J.* 330 (Pt 3):1097-105.

Morin C, Asselin C, Boudreau F, Provencher PH. (1998) **Transcriptional regulation of pre-pro-endothelin-1 gene by glucocorticoids in vascular smooth muscle cells.** *Biochem Biophys Res Commun*. 244(2):583-7.

Motte S, van Beneden R, Mottet J, Rondelet B, Mathieu M, Havaux X, Lause P, Clercx C, Ketelslegers JM, Naeije R, McEntee K. (2003) **Early activation of cardiac and renal endothelin systems in experimental heart failure**. *Am J Physiol Heart Circ Physiol.* 285(6):H2482-91.

Murakoshi N, Miyauchi T, Kakinuma Y, Ohuchi T, Goto K, Yanagisawa M, Yamaguchi I. (2002) **Vascular endothelin-B receptor system in vivo plays a favorable inhibitory role in vascular remodeling after injury revealed by endothelin-B receptor-knockout mice.** *Circulation.* 106(15):1991-8.

Muralidharan-Chari V, Clancy JW, Sedgwick A, D'Souza-Schorey C. (2010) **Microvesicles: mediators of extracellular communication during cancer progression.** *J Cell Sci.* 123(Pt 10):1603-11.

Murphy LJ, Corder R, Mallet AI, Turner AJ. (1994) **Generation by the phosphoramidon-sensitive peptidases, endopeptidase-24.11 and thermolysin, of endothelin-1 and c-terminal fragment from big endothelin-1.** *Br J Pharmacol*. 113(1):137-42.

Nakano J, Takizawa H, Ohtoshi T, Shoji S, Yamaguchi M, Ishii A, Yanagisawa M, Ito K. (1994) **Endotoxin and pro-inflammatory cytokines stimulate endothelin-1 expression and release by airway epithelial cells.** *Clin Exp Allergy.* 24(4):330-6.

Nakano A, Kishi F, Minami K, Wakabayashi H, Nakaya Y, Kido H. (1997) **Selective conversion of big endothelins to tracheal smooth muscle-constricting 31-amino acid-length endothelins by chymase from human mast cells.** *J Immunol.* 159(4):1987-92.

National Kidney Foundation. (2002) **K/DOQI clinical practice guidelines for chronic kidney disease: evaluation, classification, and stratification**. *Am J Kidney Dis*. 39(Suppl): S1–266.

Nelson JB, Chan-Tack K, Hedican SP, Magnuson SR, Opgenoth TJ, Bova GS, Simons J. W. (1996) **Endothelin–1 and decreased endothelin B receptor expression in advanced prostate cancer.** *Cancer Res.* 56:663–668.

Neuhofer W. and Pittrow D. (2009) **Endothelin receptor selectivity in chronic kidney disease: rationale and review of recent evidence.** *Eur J Clin Invest*. 39 Suppl 2:50–67.

Nielsen HK, Löliger J, Hurrell RF. (1985) **Reactions of proteins with oxidizing lipids. 1. Analytical measurements of lipid oxidation and of amino acid losses in a whey protein-methyl linolenate model system**. *Br. J. Nutr.* 53, 61-73.

Nunez DJ, Brown MJ, Davenport AP, Neylon CB, Schofield JP, Wyse RK. (1990) **Endothelin-1 mRNA is widely expressed in porcine and human tissues.** *J Clin Invest.* 85(5):1537-41.

Nussdorfer GG, Rossi GP, Belloni AS. (1997) **The role of endothelins in the paracrine control of the secretion and growth of the adrenal cortex.** *Int Rev Cytol.* 171:267-308.

Ohta K, Hirata Y, Shichiri M, Kanno K, Emori T, Tomita K, Marumo F. (1991) **Urinary excretion of endothelin-1 in normal subjects and patients with renal disease.** *Kidney Int.* 39(2):307-11.

Oliver FJ, de la Rubia G, Feener EP, Lee ME, Loeken MR, Shiba T, Quertermous T, King GL. (1991) **Stimulation of endothelin-1 gene expression by insulin in endothelial cells**. *J Biol Chem.* 266(34):23251-6.

Opgenorth TJ, Wessale JL, Dixon DB, Adler AL, Calzadilla SV, Padley RJ, Wu-Wong JR. (2000) **Effects of endothelin receptor antagonists on the plasma immunoreactive endothelin-1 level.** *J Cardiovasc Pharmacol.* 36(5 Suppl 1):S292-6.

Orisio S, Benigni A, Bruzzi I, Corna D, Perico N, Zoja C, Benatti L, Remuzzi G. (1993) **Renal endothelin gene expression is increased in remnant kidney and correlates with disease progression.** *Kidney Int*. 43(2):354-8.

Ozaki S, Ohwaki K, Ihara M, Ishikawa K, Yano M. (1997) **Coexpression studies with endothelin receptor subtypes indicate the existence of intracellular cross-talk between ET(A) and ET(B) receptors.** *J Biochem.* 121(3):440-7.

Pacher R, Stanek B, Hülsmann M, Koller-Strametz J, Berger R, Schuller M, Hartter E, Ogris E, Frey B, Heinz G, Maurer G. (1996) **Prognostic impact of big endothelin-1 plasma concentrations compared with invasive hemodynamic evaluation in severe heart failure.** *J Am Coll Cardiol.* 27: 633–641.

Packer M, McMurray J, Massie BM, Caspi A, Charlon V, Cohen-Solal A, Kiowski W, Kostuk W, Krum H, Levine B, Rizzon P, Soler J, Swedberg K, Anderson S,Demets DL. (2005) **Clinical effects of endothelin receptor antagonism with bosentan in patients with severe chronic heart failure: results of a pilot study.** *J Card Fail.* 11(1):12-20.

Palmer MJ. (2009) **Endothelin receptor antagonists: status and learning 20 years on.** *Prog Med Chem*. 47:203-37.

Panettieri RA Jr, Goldie RG, Rigby PJ, Eszterhas AJ, Hay DW (1996) **Endothelin-1-induced potentiation of human airway smooth muscle proliferation: an ETA receptor-mediated phenomenon.** *Br J Pharmacol.* 118: 191-197.

Papassotiriou J, Morgenthaler NG, Struck J, Alonso C, Bergmann A (2006) **Immunoluminometric assay for measurement of the C-terminal endothelin-1 precursor fragment in human plasma**. *Clin Chem* 52: 1144–1151.

Park JB. and Schiffrin EL. (2001) **ET(A) receptor antagonist prevents blood pressure elevation and vascular remodeling in aldosterone-infused rats.** *Hypertension.* 37(6):1444-9.

Patel T, McKeage K. (2014) **Macitentan: First Global Approval.** *Drugs.* 74(1):127-33.

Patel JN, Jager A, Schalkwijk C, Corder R, Douthwaite JA, Yudkin JS, Coppack SW, Stehouwer CD. (2002) **Effects of tumour necrosis factor-alpha in the human forearm: blood flow and endothelin-1 release**. *Clin Sci (Lond).* 103(4):409-15.

Perdivara I, Deterding LJ, Przybylski M, Tomer KB. (2010) **Mass spectrometric identification of oxidative modifications of tryptophan residues in proteins: chemical artifact or post-translational modification?** *J Am Soc Mass Spectrom.* 21(7):1114-7.

Perkins DN, Pappin DJ, Creasy DM, Cottrell JS. (1999) **Probability-based protein identification by searching sequence databases using mass spectrometry data**. *Electrophoresis.* 20(18):3551-67.

Pernow J, Franco-Cereceda A, Matran R, Lundberg JM: (1989) **Effect of endothelin-1 on regional vascular resistance in the pig.** *J Cardiovasc Pharmacol.* 13[Suppl 16]: S205–S206.

Plumpton C, Kalinka S, Martin RC, Horton JK, Davenport AP. (1994) **Effects of phosphoramidon and pepstatin A on the secretion of endothelin-1 and big endothelin-1 by human umbilical vein endothelial cells: measurement by two-site enzyme-linked immunosorbent assays.** *Clin Sci (Lond).* 87(2):245-51.

Plumpton C, Haynes WG, Webb DJ, Davenport AP. (1995) **Measurement of C-terminal fragment of big endothelin-1: a novel method for assessing the generation of endothelin-1 in humans.** *J Cardiovasc Pharmacol.* 26 Suppl 3:S34-6.

Pönicke K, Vogelsang M, Heinroth M, Becker K, Zolk O, Böhm M, Zerkowski HR, Brodde OE. (1998) **Endothelin receptors in the failing and nonfailing human heart.** *Circulation.* 97(8):744-51.

Porter KE. and Turner NA. (2009) **Cardiac fibroblasts: at the heart of myocardial remodeling.** *Pharmacol Ther.* 123(2):255-78.

Potenza MA, Marasciulo FL, Chieppa DM, Brigiani GS, Formoso G, Quon MJ, Montagnani M. (2005) **Insulin resistance in spontaneously hypertensive rats is associated with endothelial dysfunction characterized by imbalance between NO and ET-1 production**. *Am J Physiol Heart Circ Physiol.* 289(2):H813-22.

Pousset F, Isnard R, Lechat P, Kalotka H, Carayon A, Maistre G, Escolano S, Thomas D, Komajda M. (1997) **Prognostic value of plasma endothelin-1 in patients with chronic heart failure.** *Eur Heart J.* 18(2):254-8.

Prasad SK, Dargie HJ, Smith GC, Barlow MM, Grothues F, Groenning BA, Cleland JG, Pennell DJ. (2006) **Comparison of the dual receptor endothelin antagonist enrasentan with enalapril in asymptomatic left ventricular systolic dysfunction: a cardiovascular magnetic resonance study.** *Heart.* 92(6):798-803.

Prins BA, Hu RM, Nazario B, Pedram A, Frank HJ, Weber MA, Levin ER. (1994) **Prostaglandin E2 and prostacyclin inhibit the production and secretion of endothelin from cultured endothelial cells.** *J Biol Chem.* 269(16):11938-44.

Queiroz JA, Tomaz CT, Cabral JM. (2001) **Hydrophobic interaction chromatography of proteins.** *J Biotechnol.* 87(2):143 – 59.

Rabelink TJ, Kaasjager KA, Boer P, Stroes EG, Braam B, Koomans HA. (1994) **Effects of endothelin-1 on renal function in humans: implications for physiology and pathophysiology**. *Kidney Int.* 46(2):376-81.

Reriani M, Raichlin E, Prasad A, Mathew V, Pumper GM, Nelson RE, Lennon R, Rihal C, Lerman LO, Lerman A. (2010a) **Long-term administration of endothelin receptor antagonist improves coronary endothelial function in patients with early atherosclerosis.** *Circulation.* 122(10):958-66.

Reriani MK, Lerman LO, Lerman A. (2010b) **Endothelial function as a functional expression of cardiovascular risk factors**. *Biomark Med.* 4(3):351-60.

Resink TJ, Hahn AW, Scott-Burden T, Powell J, Weber E, Bühler FR. (1990) **Inducible endothelin mRNA expression and peptide secretion in cultured human vascular smooth muscle cells.** *Biochem Biophys Res Commun.* 168(3):1303-10.

Richardson JS. and Richardson DC. (1989) **Principles and patterns of protein conformation**. In: Fasman GD ed., Prediction of Protein Structure and the Principles of Protein Conformation. New York, Plenum Press, pp. 1–98.

Ridker PM, Brown NJ, Vaughan DE, Harrison DG, Mehta JL. (2004) **Established and emerging plasma biomarkers in the prediction of first atherothrombotic events.** *Circulation.* 109(25 Suppl 1):IV6-19.

Ridker PM, Rifai N, Pfeffer M, Sacks F, Lepage S, Braunwald E. (2000) **Elevation of tumor necrosis factor-alpha and increased risk of recurrent coronary events after myocardial infarction.** *Circulation.*101(18):2149-53.

Ritthaler T, Scholz H, Ackermann M, Riegger G, Kurtz A, Kramer BK. (1995) **Effects of endothelins on renin secretion from isolated mouse renal juxtaglomerular cells**. *Am J Physiol Renal Fluid Electrolyte Physiol*. 268: F39–F45.

Ritz E. and Wenzel R. (2010) **Endothelin receptor antagonists in proteinuric renal disease: Every rose has its thorn.** *J Am Soc Nephrol.* 21:392-394.

Rockwell NC, Thorner JW (2004) **The kindest cuts of all: crystal structures of Kex2 and furin reveal secrets of precursor processing.** *Trends Biochem Sci.* 29(2):80-7.

Rodeheffer RJ, Lerman A, Heublein DM, Burnett JC Jr. (1992) **Increased plasma concentrations of endothelin in congestive heart failure in humans.** *Mayo Clin Proc.* 67(8):719-24.

Rossi GP, Albertin G, Franchin E, Sacchetto A, Cesari M, Palù G, Pessina AC. (1995) **Expression of the endothelin-converting enzyme gene in human tissues.** *Biochem Biophys Res Commun.* 211(1):249-53.

Rossi GP, Cavallin M, Nussdorfer GG, Pessina AC. (2001) **The endothelin-aldosterone axis and cardiovascular diseases.** *J Cardiovasc Pharmacol.* 38 Suppl 2:S49-52.

Rubanyi GM. and Polokoff MA. (1994) **Endothelins: molecular biology, biochemistry, pharmacology, physiology, and pathophysiology**. *Pharmacol Rev*. 46:325-415.

Rubin LJ, Badesch DB, Barst RJ, Galie N, Black CM, Keogh A, Pulido T, Frost A, Roux S, Leconte I, Landzberg M, Simonneau G. (2002) **Bosentan therapy for pulmonary arterial hypertension.** *N Engl J Med.* 346(12):896-903.

Rubinstein I, Gurbanov K, Hoffman A, Better OS, Winaver J. (1995) **Differential effect of endothelin-1 on renal regional blood flow: role of nitric oxide.** *J Cardiovasc Pharmacol.* 26 Suppl 3:S208-10.

Ruef J, Moser M, Kubler W, Bode C. (2001) **Induction of endothelin-1 expression by oxidative stress in vascular smooth muscle cells.** *Cardiovasc Pathol.* 10:311–315.

Ruetten H. and Thiemermann C. (1997) **Endothelin-1 stimulates the biosynthesis of tumour necrosis factor in macrophages: ET-receptors, signal transduction and inhibition by dexamethasone.** *J Physiol Pharmacol*. 48(4):675-88.

Ruschitzka F, Shaw S, Gygi D, Noll G, Barton M, Lüscher TF. (1999) **Endothelial dysfunction in acute renal failure: role of circulating and tissue endothelin-1.** *J Am Soc Nephrol*. 10(5):953-62.

Russell FD. and Davenport AP. (1996) **Characterization of the binding of endothelin ETB selective ligands in human and rat heart.** *Br J Pharmacol.* 119(4): 631–636.

Russell FD. and Davenport AP. (1999) **Secretory pathways in endothelin synthesis.** *Br J Pharmacol.* 126(2):391-8.

Russell FD, Skepper JN, Davenport AP. (1998) **Human endothelial cell storage granules: a novel intracellular site for isoforms of the endothelin-converting enzyme.** *Circ Res.* 83(3):314-21.

Ryle AP. and Sanger F. (1955) **Disulphide interchange reactions.** *Biochem. J.* 60(4):535-540.

Sabatine MS, Morrow DA, de Lemos JA, Omland T, Sloan S, Jarolim P, Solomon SD, Pfeffer MA, Braunwald E. (2012) **Evaluation of multiple biomarkers of cardiovascular stress for risk prediction and guiding medical therapy in patients with stable coronary disease.** *Circulation.* 125(2):233-40.

Saijonmaa O, Nyman T, Hohenthal U, Fyhrquist F. (1991) **Endothelin-1 is expressed and released by a human endothelial hybrid cell line (EA.hy 926).** *Biochem Biophys Res Commun*. 181(2):529-36.

Sakai S, Miyauchi T, Kobayashi M, Yamaguchi I, Goto K, Sugishita Y. (1996) **Inhibition of myocardial endothelin pathway improves long-term survival in heart failure.** *Nature.* 384(6607):353-5.

Sakurai T, Yanagisawa M, Takuwa Y, Miyazaki H, Kimura S, Goto K, Masaki T. (1990) **Cloning of a cDNA encoding a non-isopeptide-selective subtype of the endothelin receptor.** *Nature.* 348(6303):732-5.

Saleh MA, Boesen EI, Pollock JS, Savin VJ, Pollock DM. (2010) **Endothelin-1 increases glomerular permeability and inflammation independent of blood pressure in the rat.** *Hypertension.* 56(5):942-9.

Sanger F. (1953) **A disulphide interchange reaction.** *Nature.* 171(4362):1025-6.

Sansom CE, Hoang VM, Turner AJ. (1995) **Molecular modeling of the active site of endothelin-converting enzyme.** *J Cardiovasc Pharmacol.* 26 Suppl 3:S75-7.

Sansom CE, Hoang MV, Turner AJ. (1998) **Molecular modelling and site-directed mutagenesis of the active site of endothelin-converting enzyme.** *Protein Eng.* 11(12):1235-41.

Sawamura T, Kasuya Y, Matsushita Y, Suzuki N, Shinmi O, Kishi N, Sugita Y, Yanagisawa M, Goto K, Masaki T, et al. (1991) **Phosphoramidon inhibits the intracellular conversion of big endothelin-1 to endothelin-1 in cultured endothelial cells.** *Biochem Biophys Res Commun.* 174(2):779-84.

Schiffrin EL, Deng LY, Sventek P, Day R. (1997) **Enhanced expression of endothelin-1 gene in resistance arteris in severe human essential hypertension.** *J Hypertens*. 15:57-63.

Schmetter L, Dallinger S, Bobr B, Selenko N, Eichler H-G, Woltz M. (1998) **Systemic and renal effects of an ETA receptor subtype-specific antagonist in healthy subjects.** *Br J Pharmacol* 124: 930–934.
Schneider MP, Ge Y, Pollock DM, Pollock JS, Kohan DE. (2008) **Collecting duct-derived endothelin regulates arterial pressure and Na excretion via nitric oxide.** *Hypertension.* 51(6):1605-10.

Schweizer A, Valdenaire O, Nelbock P, Deuschle U, Edwards JBDM, Stumpf JG, Loffler BM. (1997) **Human endothelin-converting enzyme (ECE-1): three isoforms with distinct subcellular localisations.** *Biochem. J.* 328:871–877.

Seissler J, Feghelm N, Then C, Meisinger C, Herder C, Koenig W, Peters A, Roden M, Lechner A, Kowall B, Rathmann W. (2012) **Vasoregulatory peptides pro-endothelin-1 and pro-adrenomedullin are associated with metabolic syndrome in the population-based KORA F4 study.** *Eur J Endocrinol.* 167(6):847-53

Selvais PL, Robert A, Ahn S, van Linden F, Ketelslegers JM, Pouleur H, Rousseau MF. (2000) **Direct comparison between endothelin-1, N-terminal proatrial natriuretic factor, and brain natriuretic peptide as prognostic markers of survival in congestive heart failure.** *J Card Fail.* 6(3):201-7.

Serneri GG, Modesti PA, Cecioni I, Biagini D, Migliorini A, Costoli A, Colella A, Naldoni A, Paoletti P. (1995) **Plasma endothelin and renal endothelin are two distinct systems involved in volume homeostasis.** *Am J Physiol*. 268(5 Pt 2):H1829-37.

Sharefkin JB, Diamond SL, Eskin SG, McIntire LV, Dieffenbach CW. (1991) **Fluid flow decreases preproendothelin mRNA levels and suppresses endothelin-1 peptide release in cultured human endothelial cells.** *J Vasc Surg.* 14(1):1-9.

Shichiri M, Hirata Y, Nakajima T, Ando K, Imai T, Yanagisawa M, Masaki T, Marumo F. (1991) **Endothelin-1 is an autocrine/paracrine growth factor for human cancer cell lines.** *J Clin Invest.* 87(5):1867-71.

Sirviö ML, Metsärinne K, Saijonmaa O, Fyhrquist F. (1990) **Tissue distribution and half-life of 125I-endothelin in the rat: importance of pulmonary clearance.** *BiochemBiophys. Res Commun.* 167(3):1191-5.

Sokolovsky M. (1994) **Endothelins and sarafotoxins: receptor heterogeneity.** *Int J Biochem.* 26(3):335-40.

Sørensen SS, Madsen JK, Pedersen EB. (1994) **Systemic and renal effect of intravenous infusion of endothelin-1 in healthy human volunteers.** *Am J Physiol.* 266(3 Pt 2):F411-8.

Soubrier F, Hubert C, Testut P, Nadaud S, Alhenc-Gelas F, Corvol P. (1993) **Molecular biology of the angiotensin I converting enzyme: I. Biochemistry and structure of the gene**. *J. Hypertens.* 11(5):471-6.

Spratt JCS, Goddard J, Patel N, Strachan FE, Rankin AJ, Webb DJ. (2001) **Systemic ETA receptor antagonism with BQ-123 blocks ET-1 induced forearm vasoconstriction and decreases peripheral vascular resistance in healthy men.** *Br J Pharmacol* 134: 648–654.

Stanton P. (2004) **Ion-exchange chromatography.** *Methods Mol Biol.* 251:23-44.

Stewart DJ, Cernacek P, Costello KB, Rouleau JL. (1992) **Elevated endothelin-1 in heart failure and loss of normal response to postural change.** *Circulation.* 85(2):510-7.

Stow LR, Jacobs ME, Wingo CS, Cain BD. (2011) **Endothelin-1 gene regulation.** *FASEB J.* 25:16-28.

Struck J, Morgenthaler NG, Bergmann A. (2005) **Proteolytic processing pattern of the endothelin-1 precursor in vivo.** *Peptides.* 26: 2482–2486.

Stuart D, Chapman M, Rees S, Woodward S, Kohan DE. (2013) **Myocardial, smooth muscle, nephron, and collecting duct gene targeting reveals the organ sites of endothelin A receptor antagonist fluid retention.** *J Pharmacol Exp Ther.* 346(2):182-9.

Stuart D, Rees S, Woodward SK, Koesters R, Strait KA, Kohan DE. (2012) **Disruption of the endothelin A receptor in the nephron causes mild fluid volume expansion.** *BMC Nephrol.* 13:166.

Sütsch G, Kiowski W, Yan XW, Hunziker P, Christen S, Strobel W, Kim JH, Rickenbacher P, Bertel O. (1998) **Short-term oral endothelin-receptor antagonist therapy in conventionally treated patients with symptomatic severe chronic heart failure.** *Circulation.* 98(21):2262-8.

Suwaidi JA, Hamasaki S, Higano ST, Nishimura RA, Holmes DR Jr, Lerman A. (2000) **Long-term follow-up of patients with mild coronary artery disease and endothelial dysfunction.** *Circulation.* 101(9):948-54.

Swiderek KM, Davis MT, Lee TD**.** (1998) **The identification of peptide modifications derived from gel-separated proteins using electrospray triple quadrupole and ion trap analyses.** *Electrophoresis.* 19(6):989-97.

Tabb DL, Friedman DB, Ham AJ. (2006) **Verification of automated peptide identifications from proteomic tandem mass spectra.** *Nat Protoc.* 1(5):2213-22.

Tabb DL, Huang Y, Wysocki VH, Yates JR III. (2004) **Influence of basic residue content on fragment ion peak intensities in low-energy collision-induced dissociation spectra of peptides.** *Anal. Chem*. 76:1243-1248.

Takahashi M, Fukuda K, Shimada K, Barnes K, Turner AJ, Ikeda M, Koike H, Yamamoto Y, Tanzawa K. (1995) **Localization of rat endothelin-converting enzyme to vascular endothelial cells and some secretory cells**. *Biochem J*. 311 (Pt 2):657-65.

Takasaki C, Itoh Y, Onda H, Fujino M. (1992) **Cloning and sequence analysis of a snake, Atractaspis engaddensis gene encoding sarafotoxin S6c.** *Biochem Biophys Res Commun.* 189(3):1527-33.

Tasaka K, Kitazumi K. (1994) **The control of endothelin-1 secretion.** *Gen Pharmacol.* 25(6):1059-69.

Tchekneva E, Lawrence ML, Meyrick B. (2000) **Cell-specific differences in ET-1 system in adjacent layers of main pulmonary artery. A new source of ET-1.** *Am J Physiol Lung Cell Mol Physiol.* 278(4):L813-21.

Teerlink JR, McMurray JJ, Bourge RC, Cleland JG, Cotter G, Jondeau G, Krum H, Metra M, O'Connor CM, Parker JD, Torre-Amione G, Van Veldhuisen DJ, Frey A, Rainisio M, Kobrin I; VERITAS Investigators. (2005) **Tezosentan in patients with acute heart failure: design of the Value of Endothelin Receptor Inhibition with Tezosentan in Acute heart failure Study (VERITAS).** *Am Heart J.* 150(1):46-53.

Tirapelli CR, Casolari DA, Yogi A, Montezano AC, Tostes RC, Legros E, D'Orléans-Juste P, de Oliveira AM. (2005) **Functional characterization and expression of endothelin receptors in rat carotid artery: involvement of nitric oxide, a vasodilator prostanoid and the opening of K+ channels in ETB-induced relaxation.** *Br J Pharmacol.* 146(6):903-12.

Tomita K, Nonoguchi H, Terada Y, Marumo F. (1993) **Effects of ET-1 on water and chloride transport in cortical collecting ducts of the rat**. *Am J Physiol*. 264(4 Pt 2):F690-6.

Torchinsky YM. (1981) **Properties of SH groups, in Sulfur in Proteins.** In: Metzler DE. ed., Peroxiredoxin Systems: Structures and Functions. Oxford, England, Pergamon, pp. 52-53.

Touyz RM. and Schiffrin EL. (2004) **Reactive oxygen species in vascular biology: implications in hypertension**. *Histochem Cell Biol.* 122:339–352.

Turner A. and Tanzawa K. (1997) **Mammalian membrane metallopetidases: NEP, ECE, Kell and PEX.** *FASEB J.* 11:355–364.

Turner AJ. and Murphy LJ. (1996) **Molecular pharmacology of endothelin converting enzymes.** *Biochem Pharmacol.* 51(2):91-102.

Uchida K. and Kawakishi S. (1994) **Identification of oxidized histidine generated at the active site of Cu, Zn-superoxide dismutase exposed to H2O2. Selective generation of 2-oxo-histidine at the histidine 118.** *J Biol Chem*. 269(4):2405-10.

Valdenaire O, Rohrbacher E, Mattei MG. (1995) **Organization of the gene encoding the human endothelin-converting enzyme (ECE-1).** *J Biol Chem.* 270:29794–8.

Valdenaire O, Lepailleur-Enouf D, Egidy G, Thouard A, Barret A, Vranckx R, Tougard C, Michel JB. (1999) **A fourth isoform of endothelin-converting enzyme (ECE-1) is generated from an additional promoter molecular cloning and characterization.** *Eur J Biochem.* 264(2):341-9.

Vallance P, Leone A, Calver A, Collier J, Moncada S. (1992) **Accumulation of an endogenous inhibitor of nitric oxide synthesis in chronic renal failure.** *Lancet.* 339:572–575.

Vanhoutte PM, Shimokawa H, Tang EHC, Feletou M (2009) **Endothelial dysfunction and vascular disease**. *Acta Physiologica.* 196(2):193–222.

Vanhoutte PM. (2004) **Endothelium-dependent hyperpolarizations: the history.** *Pharmacol Res.* 49(6):503-8.

Vasan RS. (2006) **Biomarkers of cardiovascular disease: molecular basis and practical considerations.** *Circulation.* 113(19):2335-62.

Vásquez-Vivar J, Whitsett J, Martásek P, Hogg N, Kalyanaraman B. (2001) **Reaction of tetrahydrobiopterin with superoxide: EPR-kinetic analysis and characterization of the pteridine radical.** *Free Radic Biol Med*. 31:975–985.

Vásquez-Vivar J, Kalyanaraman B, Martásek P. (2003) **The role of tetrahydrobiopterin in superoxide generation from eNOS: enzymology and physiological implications.** *Free Radic Res.* 37(2):121-7.

Vatter H. and Seifert V. (2006) **Ambrisentan, a non-peptide endothelin receptor antagonist.** *Cardiovasc Drug Rev.* 24(1):63-76.

Verhaar MC, Grahn AY, van Weerdt AWN, Honing MLH, Morrison PJ, Yang YP, Padley RJ, Rabelink TJ. (2000) **Pharmacokinetics and pharmacodynamic effects of abt-627, an oral eta selective endothelin antagonist, in humans**. *Br J Clin Pharmacol*. 49:562-573.

Verhaar MC, Strachan FE, Newby DE, Cruden NL, Koomans HA, Rabelink TJ, Webb DJ. (1998) **Endothelin-A receptor antagonist-mediated vasodilatation is attenuated by inhibition of nitric oxide synthesis and by endothelin-B receptor blockade.** *Circulation.* 97: 752–756.

Verma S, Lovren F, Dumont AS, Mather KJ, Maitland A, Kieser TM, Kidd W, McNeill JH, Stewart DJ, Triggle CR, Anderson TJ. (2001) **Endothelin receptor blockade improves endothelial function in human internal mammary arteries.** *Cardiovasc Res*. 49(1):146-51.

Vessières E, Guihot AL, Toutain B, Maquigneau M, Fassot C, Loufrani L, Henrion D. (2013) **COX-2-derived prostanoids and oxidative stress additionally reduce endothelium-mediated relaxation in old type 2 diabetic rats.** *PLoS One.* 8(7):e68217.

Vijayaraghavan J, Scicli AG, Carretero OA, Slaughter C, Moomaw C, Hersh LB. (1990) **The hydrolysis of endothelins by neutral endopeptidase 24.11 (enkephalinase).** *J Biol Chem.* 265(24):14150-5.

Virmani R, Avolio AP, Mergner WJ, et al. (1991) **Effect of aging on aortic morphology in populations with high and low prevalence of hypertension and atherosclerosis: comparison between occidental and Chinese communities.** *Am J Pathol*. 139:1119–1129.

Vittori E, Marini M, Fasoli A, De Franchis R, Mattoli S. (1992) **Increased expression of endothelin in bronchial epithelial cells of asthmatic patients and effect of corticosteroids.** *Am Rev Respir Dis.* 146(5 Pt 1):1320-5.

Wagner OF, Vierhapper H, Gasic S, Nowotny P, Waldhäusl W. (1992**) Regional effects and clearance of endothelin-1 across pulmonary and splanchnic circulation.** *Eur J Clin Invest.* 22(4):277-82.

Warner TD. and Klemm P. (1996) **What turns on the endothelins?** *Inflamm Res.* 45(2):51-3.

Wawra S. and Fischer G. (2006) **Amide *cis-trans* Isomerisation in Peptides and Proteins**. In: Dugave EC. ed., Cis-Trans Isomerization in Biochemistry, Weinheim, Germany, Wiley-VCH. page 241.

Waxman L, Doshi KP, Gaul SL, Wang S, Bednar RA, Stern AM. (1994) **Identification and characterization of endothelin converting activity from EAHY 926 cells: evidence for the physiologically relevant human enzyme.** *Arch Biochem Biophys.* 308(1):240-53.

Webb DJ, Monge JC, Rabelink TJ, Yanagisawa M. (1998) **Endothelin: new discoveries and rapid progress in the clinic.** *Trend Pharmacol Sci.* 19:5-8.

Weber C, Schmitt R, Birnboeck H, Hopfgartner G, van Marle SP, Peeters PA, Jonkman JH, Jones CR. (1996) **Pharmacokinetics and pharmacodynamics of the endothelin-receptor antagonist bosentan in healthy human subjects.** *Clin Pharmacol Ther.* 60(2):124-37.

Weber MA, Black H, Bakris G, Krum H, Linas S, Weiss R, Linseman JV, Wiens BL, Warren MS, Lindholm LH. (2009) **A selective endothelin-receptor antagonist to reduce blood pressure in patients with treatment-resistant hypertension: a randomised, double-blind, placebo-controlled trial.** *Lancet.* 374(9699):1423-31.

Weitzberg E, Ahlborg G, Lundberg JM. (1991) **Long-lasting vasoconstriction and efficient regional extraction of endothelin-1 in human splanchnic and renal tissues.** *Biochem Biophys Res Commun.* 180(3):1298-303.

Westby CM, Weil BR, Greiner JJ, Stauffer BL, DeSouza CA. (2011) **Endothelin-1 vasoconstriction and the age-related decline in endothelium-dependent vasodilatation in men.** *Clin Sci (Lond).* 120(11):485-91.

Whyteside AR. and Turner AJ. (2013) **Endothelin-Converting Enzyme-1**. In: Rawlings ND. and Salvesen G. eds., Handbook of Proteolytic Enzymes. London, Elsevier, pp. 624-631.

Wilkinson IB. and Webb DJ. (2001) **Venous occlusion plethysmography in cardiovascular research: methodology and clinical applications.** *Br J Clin Pharmacol.* 52(6):631-46.

Winkles JA, Alberts GF, Brogi E, Libby P. (1993) **Endothelin-1 and endothelin receptor mRNA expression in normal and atherosclerotic human arteries.** *Biochem Biophys Res Commun.* 191(3):1081-8.

Woessner JF Jr. (1998) **The matrix metalloproteinase family**. In: Parks WC. and Mecham RP. eds., Matrix Metalloproteinases. San Diego, California, Academic Press. 151:1-23.

Woods M, Mitchell JA, Wood EG, Barker S, Walcot NR, Rees GM, Warner TD. (1999) **Endothelin-1 is induced by cytokines in human vascular smooth muscle cells: evidence for intracellular endothelin-converting enzyme.** *Mol Pharmacol.* 55(5):902-9.

Wort SJ, Mitchell JA, Woods M, Evans TW, Warner TD. (2000) **The prostacyclin-mimetic cicaprost inhibits endogenous endothelin-1 release from human pulmonary artery smooth muscle cells.** *J Cardiovasc Pharmacol*. 36(5 Suppl 1):S410-3.

Wort SJ, Woods M, Warner TD, Evans TW, Mitchell JA. (2001) **Endogenously released endothelin-1 from human pulmonary artery smooth muscle promotes cellular proliferation: relevance to pathogenesis of pulmonary hypertension and vascular remodeling.** *Am J Respir Cell Mol Biol.* 25(1):104-10.

Wu FX, Gagné P, Droit A, Poirier GG. (2008) **Quality assessment of peptide tandem mass spectra.** *BMC Bioinformatics*. 9 Suppl 6:S13.

Xu D, Emoto N, Giaid A, Slaughter C, Kaw S, deWit D, Yanagisawa M (1994) **ECE-1: a membrane-bound metalloprotease that catalyzes the proteolytic activation of big endothelin-1**. *Cell.* 78: 473-485.

Yanagisawa H, Hammer RE, Richardson JA, Emoto N, Williams SC, Takeda S, Clouthier DE, Yanagisawa M. (2000) **Disruption of ECE-1 and ECE-2 reveals a role for endothelin-converting enzyme-2 in murine cardiac development.** *J Clin Invest.* 105(10):1373-82.

Yanagisawa H, Yanagisawa M, Kapur RP, Richardson JA, Williams SC, Clouthier DE, de Wit D, Emoto N, Hammer RE. (1998) **Dual genetic pathways of endothelin-**

mediated intercellular signaling revealed by targeted disruption of endothelin converting enzyme-1 gene. *Development.* 125(5):825-36.

Yanagisawa M, Kurihara H, Kimura S, Tomobe Y, Kobayishi Y, Mitsui Y, Yazaki Y, Goto K, Masaki T (1988) **A novel potent, vasoconstrictor peptide produced by vascular endothelial cells.** *Nature.* 332:411–4.

Yang LL, Gros R, Kabir MG, Sadi A, Gotlieb AI, Husain M, Stewart DJ. (2004) **Conditional cardiac overexpression of endothelin-1 induces inflammation and dilated cardiomyopathy in mice**. *Circulation.* 109: 255-261.

Yang Q, Laporte J, Battistini B, Sirois P. (1997) **Effects of dexamethasone on the basal and cytokine-stimulated release of endothelin-1 from guinea-pig cultured tracheal epithelial cells.** *Can J Physiol Pharmacol.* 75(6):576-81.

Yang Z, Krasnici N, Lüscher TF. (1999) **Endothelin-1 potentiates human smooth muscle cell growth to PDGF: effects of ETA and ETB receptor blockade.** *Circulation.* 100(1):5-8.

Yang ZH, Richard V, von Segesser L, Bauer E, Stulz P, Turina M, Lüscher TF. (1990) **Threshold concentrations of endothelin-1 potentiate contractions to norepinephrine and serotonin in human arteries. A new mechanism of vasospasm?** *Circulation.* 82(1):188-95.

Yoshizumi M, Kurihara H, Sugiyama T, Takaku F, Yanagisawa M, Masaki T, Yazaki Y. (1989) **Hemodynamic shear stress stimulates endothelin production by cultured endothelial cells.** *Biochem Biophys Res Commun.* 161:859-64.

Yu JC. and Davenport AP. (1995) **Secretion of endothelin-1 and endothelin-3 by human cultured vascular smooth muscle cells.** *Br J Pharmacol.* 114(2):551-7.

Zeballos GA, An SJ, Wu JM. (1991) **Endothelin-1 secretion by human fibroblasts in culture: effects of cell density and IFN-beta.** *Biochem Int.* 25(5):845-52.

Zeiher AM, Goebel H, Schachinger V, Ihling C. (1995) **Tissue endothelin-1 immunoreactivity in the active coronary atherosclerotic plaque: a clue to the mechanism of increased vasoreactivity of the culprit lesion in unstable angina.** *Circulation.* 91:941-947.

Zhang L, Chou CP, Moo-Young M. (2011) **Disulfide bond formation and its impact on the biological activity and stability of recombinant therapeutic proteins produced by Escherichia coli expression system.** *Biotechnol Adv.* 29(6):923-9.

Zolk O, Quattek J, Sitzler G, Schrader T, Nickenig G, Schnabel P, Shimada K, Takahashi M, Böhm M. (1999) **Expression of endothelin-1, endothelin-converting enzyme, and endothelin receptors in chronic heart failure.** *Circulation.* 99(16):2118-23.

Web links for database programs:

Delta Mass − http://www.abrf.org/index.cfm/dm.home

Expasy – http://www.expasy.org/proteomics

FindMod – http://www.expasy.ch/tools/findmod/findmod_masses.html

MASCOT − http://www.matrixscience.com

ProteinProspector − http://prospector.ucsf.edu/prospector/mshome.htm

Uniprot − http://www.uniprot.org/